University of Sheffield

Department of Civil and Structural Engineering

Soil-Structure Interaction in Masonry Arch Bridges

By

P A Callaway

MEng

A thesis submitted in partial fulfilment of the requirements for the

Degree of Doctor of Philosophy

October, 2007

Abstract

More onerous axle spacing and an increase in vehicle traffic, brought by the transport policy around the turn of the century has begun to adversely affect some of the UK's masonry arch bridges. The aim of hauling freight more efficiently to deliver environmental and economic benefits, together with engineers inexperienced in how arch bridges work, has meant that industry has been forced to rely on 'black box' computational analysis tools rather than engineering judgement and classical mechanisms.

Research published last century to predict live load capacity of masonry arch structures has started to examine the influence of backfill surrounding an arch. This thesis proposes alternatives to the current codes of practice by using backfill to justify an increase in the live load capacity of a masonry arch bridge. By means of small scale tests, visual imaging techniques were employed to gain insight into the interaction between the arch barrel and the surrounding backfill material. These tests were parametrically studied using the commonly used computational software RING, to ascertain how the current generation of simplistic Rankine based soil models, used in such packages, cope with the complex interaction effects.

This study proved that current soil models in both the existing codes of practice and the computational packages do not represent the distribution or the passive behaviour exhibited by the experiments. However, the current model is sufficiently robust to predict peak loads near to those obtained experimentally when the value for the passive pressure was reduced to one third of its full mobilisation and when the distribution angle was reduced to zero. The assumption of fixed abutments in experimental and computational models was found to be insignificant.

Contents

List of Figures

Chapter 3

Chapter 4

Chapter 5

List of Tables

Chapter 5

Notation

c	Cohesion
δ	Soil-solid interface friction angle
E	Young's Modulus
e	Coefficient of mobilised passive pressure
ε, γ	Shear strain
f	Soil depth ratio at which bilinear pressure starts
F, H, N, P, R, V, W, X, Y	Forces
g	Gravitational constant
γ	Bulk density
H, L, a, b, c, d, h, l, s, x, y, z	Lengths
I	Second moment of area
K_p, K_a, K_o, K_e	Earth pressure coefficients
λ	Load factor
M	Moments
μ	Friction coefficient
ν	Poisson's ratio
P_a, P_p	Soil pressures
q	Live load
Θ, Ω, α, β, η, ρ	Angles
ρ	Settlement
σ	Stresses

s	Sector length
S	Radial shear
T	Thrust
τ	Shear Stresses
U	Energy
V	Velocities
ω	Rotations
ψ	Angle of dilation
ϕ	Internal soil friction angle

Acknowledgement

There are many people I'd like to thank for their invaluable help throughout my study. First, and foremost, I would like to thank my supervisors, Dr. Matthew Gilbert and Dr Colin Smith, for providing me with the opportunity to study this PhD and for their excellent supervision and guidance. Without their support and understanding, this research would not have been completed on time.

My special thanks go to my wife Ru, for everything she has done and my mother, whose tragic untimely death part way through this research gave me the resolve to continue at my nadir.

I would like to thank the technicians at the Department for their kind and professional help.

I am also grateful to Essex County Council for sponsoring this research as part of a wider study concerned with establishing the influence of backfill on the load carrying capacity of masonry arch bridges.

Lastly I would like to acknowledge that I was a recipient of an EPSRC studentship which allowed me to undertake this research.

Declaration

This thesis is based upon research carried out at the Department of Civil and Structural Engineering, the University of Sheffield, UK. Except where specific reference has been made to the work of others, this thesis is the result of my own work. No part of this thesis has been submitted elsewhere for any other degree or qualification.

Phillip Arthur Callaway
October 2007

Chapter 1

Introduction

1.1 Introduction

Masonry arch bridges form a central part of the transportation system in Britain and in many overseas countries. However, most of these bridges were designed and built in the last century for traffic loadings which were much lighter than today. As part of routine assessment work undertaken by the bridge owners, the strength of many of these bridges must be reassessed to determine whether heavy modern loads can be permitted to cross them safely. Figure 1-1 shows how freight traffic has increased upon both the road and rail network in the UK between 1953 and 2005.

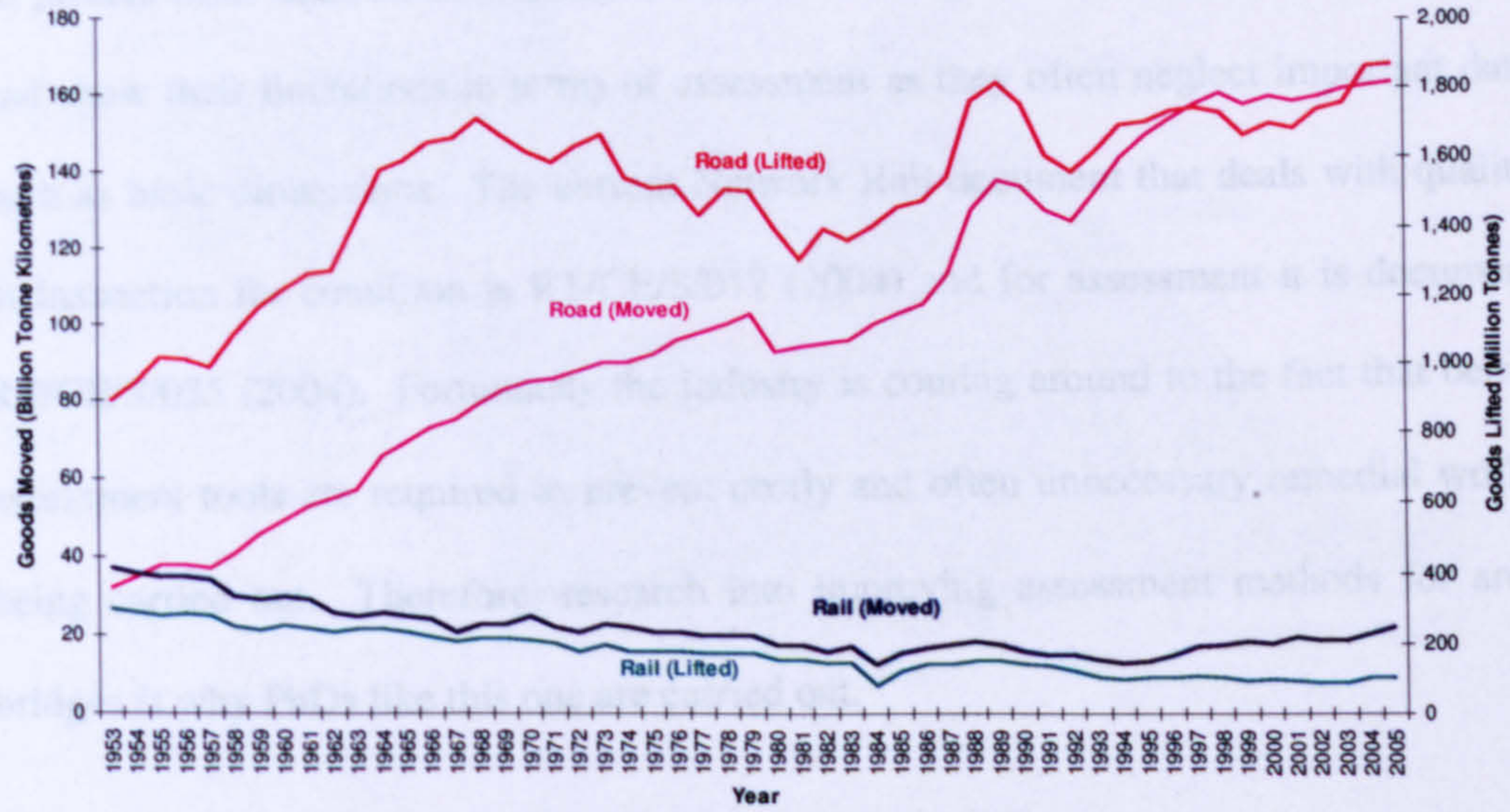

Figure 1-1 A history of increasing traffic loading
(Source: Office National Statistics, Department for Transport[1])

The primary way in which engineers assess arch bridges is by combining a visual detailed examination of the structure with calculations based upon the structure's geometry and characteristics. Up until recently masonry arch bridge assessment had been given a low priority by bridge owners as normally it is not profitable given that the bridge usually was in fair condition and could carry the loads required, and this was reflected in the fees paid to consultants. A visual examination of bridges has to be undertaken every six months, this determines any immediate concerns or damage to the bridge that needs repairing or monitoring. A detailed examination is undertaken every seven to eighteen years depending on the importance and loading of the structure. It is when these detailed examinations are done that calculations are a requirement. The approved and usual method of assessing arch bridges (MEXE) is basic and as such as little as £500 can be the fee for the entire 'detailed' assessment of a short single span masonry arch bridge.

[1] http://www.dft.gov.uk/pgr/statistics/datatablespublications/freight/tsgbchapter4datatablesa Accessed 01/05/2007

At present these detailed examinations concentrate on general condition of the structure and show their limitations in terms of assessment as they often neglect important data such as basic dimensions. The current Network Rail document that deals with quality of inspection for condition is RT/CE/S/017 (2004) and for assessment it is document RT/CE/S/035 (2004). Fortunately the industry is coming around to the fact that better assessment tools are required to prevent costly and often unnecessary remedial works being carried out. Therefore, research into improving assessment methods for arch bridges is why PhDs like this one are carried out.

Until recently analysis methods concentrated on determining the strength provided primarily by the arch barrel. However, the author of this PhD looked at several areas of the arch bridge which thus far have been rarely investigated with a view to identifying additional reserves of strength. The backfill and surrounding soil have recently become the focus of many workers in this research area, and it is one that this study looks at too. In this case, the areas under the microscope are: the dispersion of the live load through the backfill, the second is the effect of the passive restraint provided by the backfill, and finally the effect of having fixed or free abutment skewbacks.

Figure 1-2 below shows the main parts that make up an arch bridge.

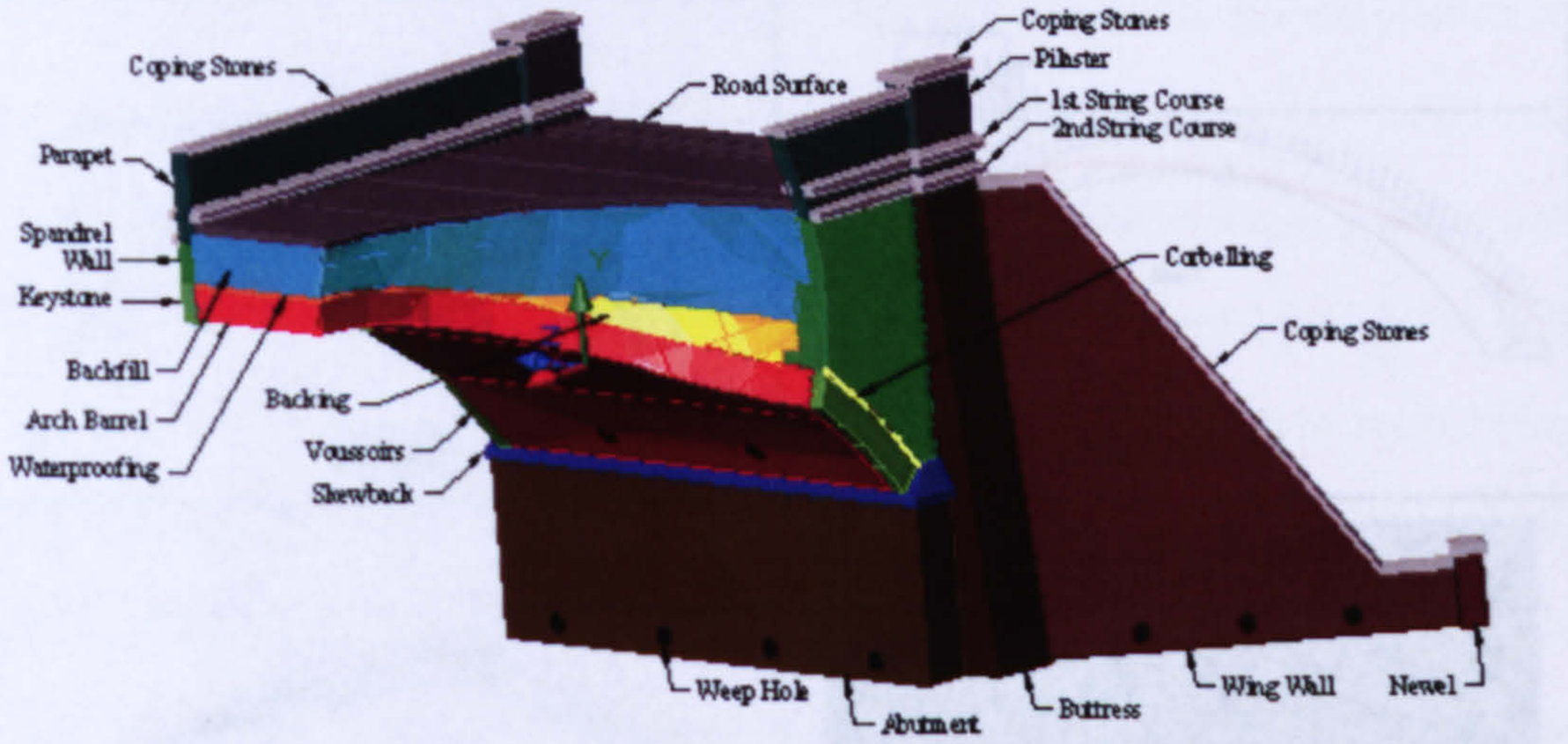

Figure 1-2 A typical arch bridge

It is well known that the quality and type of fill above the arch barrel can contribute significantly to the overall stability and strength of an arch bridge. There are six types of commonly used computational software analysis packages. These include a computerised version of MEXE, Heyman's limit analysis (ARCHIE M), rigid block methods (RING), Castigliano's non-linear analysis (CTAP), finite element (MAFEA) and discrete element (ELFEN). All six include consideration of the backfill as providing dead weight, the later five include the backfill as having deformational properties too (MacFarlane & Ricketts 2001). Figure 1-3 shows a simplistic representation of each model.

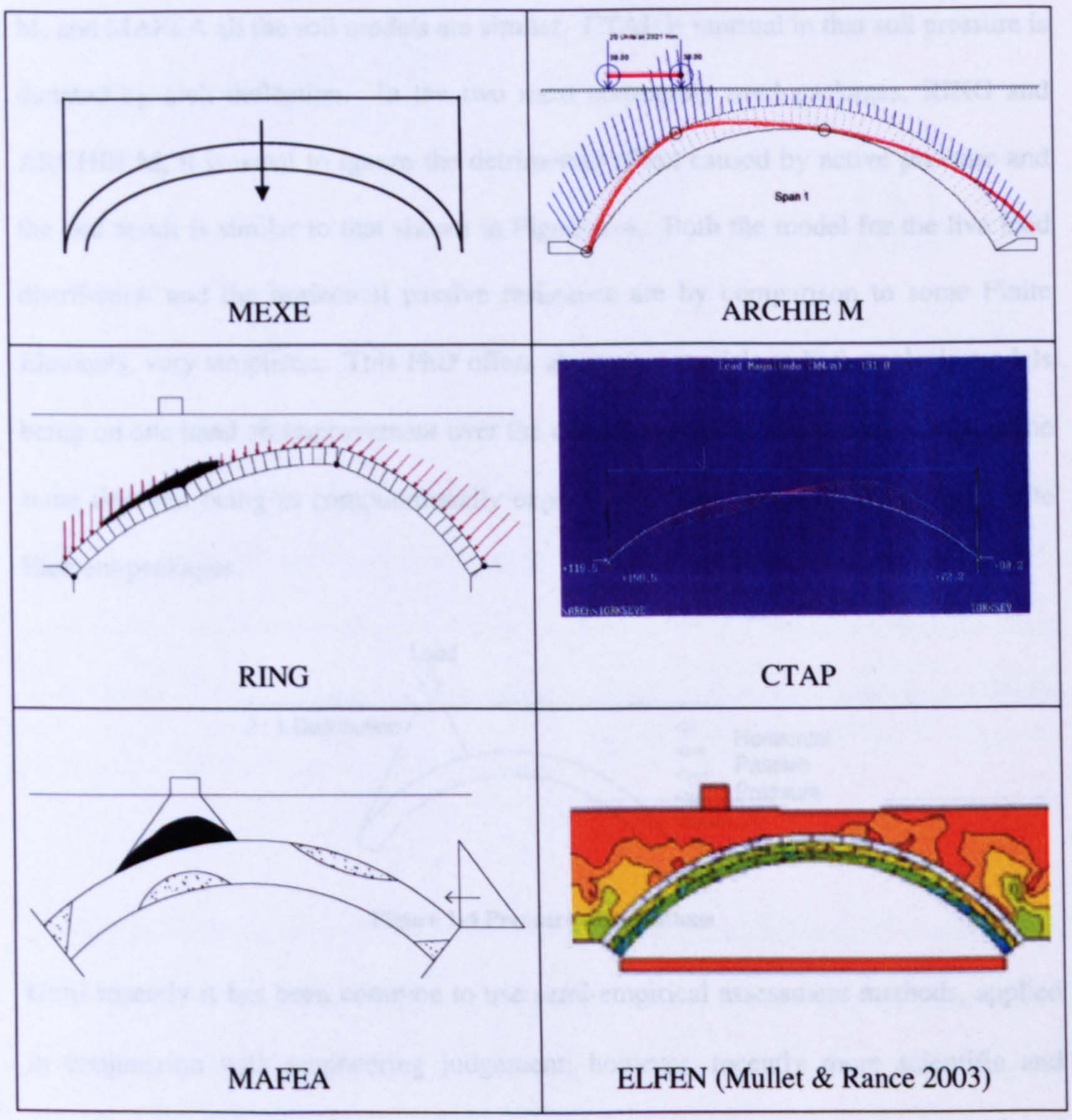

Figure 1-3 Soil models for various masonry arch computer analysis packages

For all packages, except the computerised version of MEXE, the backfill material acts a means of dispersing the applied live load between the road surface and the arch barrel by means of a simple uniform triangular distribution. Also, initially the soil under dead load exhibits at rest earth pressures, which as the arch sways away from the fill under the load this is reduced to an active pressure, and as the arch sways into the fill this becomes a passive earth pressure. It is perhaps unsurprising that for RING, ARCHIE-

M, and MAFEA all the soil models are similar. CTAP is unusual in that soil pressure is dictated by arch deflection. In the two most commonly used packages, RING and ARCHIE M, it is usual to ignore the detrimental effect caused by active pressure and the end result is similar to that shown in Figure 1-4. Both the model for the live load distribution and the horizontal passive resistance are by comparison to some Finite Elements, very simplistic. This PhD offers alternative models to both analysis models being on one hand an improvement over the current simplistic soil models whilst at the same time not being as computationally expensive as those employed by some Finite Element packages.

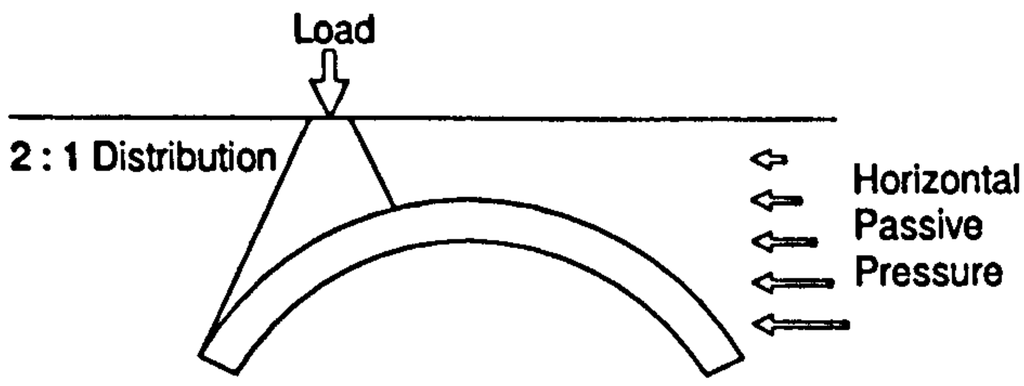

Figure 1-4 Pressure distributions

Until recently it has been common to use semi-empirical assessment methods, applied in conjunction with engineering judgement; however, recently more scientific and arguably rational approaches have been used to determine the load carrying capacity of masonry arch bridges. The need for research in this area stems primarily from government legislation which raised the maximum overall weight for heavy goods vehicles to 44 tonnes in 1999 (CfIT 2000). Although 44 tonne trucks were no bigger than the 40 tonne vehicles used at the time they operated on six axles as opposed to five, (see Figure 1-5).

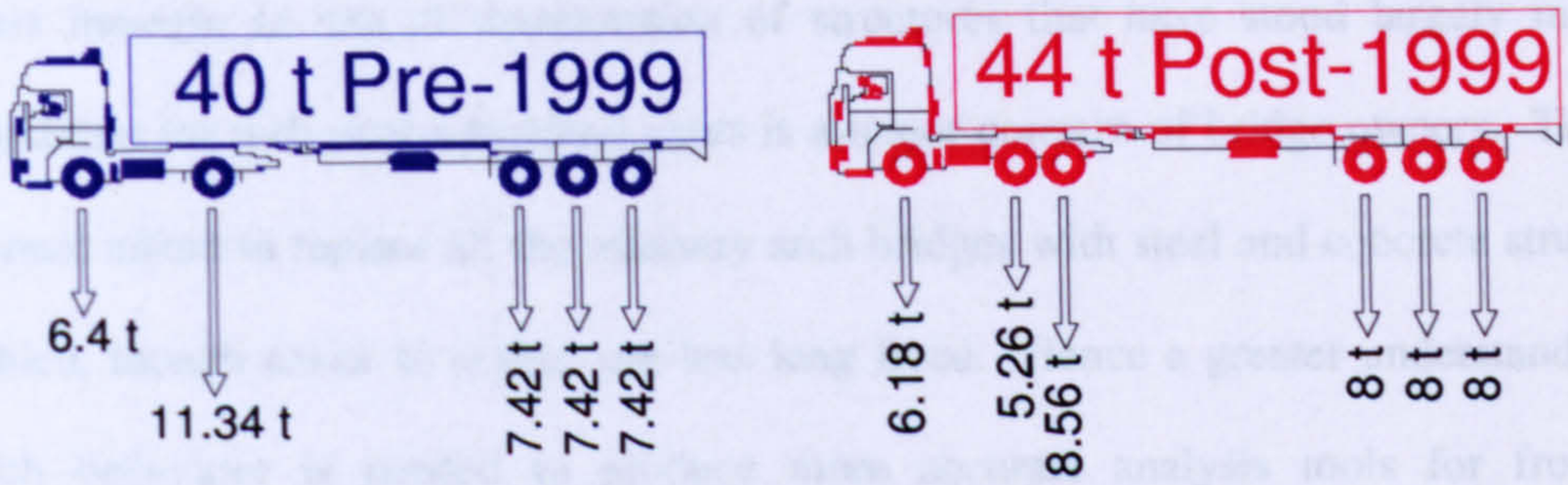

Figure 1-5 Permitted vehicles 40 tonne versus 44 tonne

At first glance running such 44 t vehicles appears to be beneficial due to the better distribution of the live load on existing masonry arch bridges. However, it is the case that most arches can take very heavy loads well in excess of their calculated capacity with little or no detrimental effect maybe as often as once a week, but there are many arch bridges that have proven to be 'weaker', so much so that they cannot cope with the current increase in frequency of such loading.

For the railways the introduction of HTA freight wagons, which have 25 t axles though at a significant smaller spacing than previous similarly loaded wagons, have caused serious concerns where bridges are literally being shaken apart on several heavily trafficked major freight lines in the UK. Both in the railways and the highways experienced inspection and assessment engineers have noticed an increase in the rate of deterioration of masonry arch bridges since the new vehicles were introduced and more often than not monitoring of structures on specific defects (especially cracking) has increased.

This increase in rate of deterioration of structures that have stood largely in good condition for well over a hundred years is a major concern of bridge owners. The UK cannot afford to replace all the masonry arch bridges with steel and concrete structures which, though easier to assess, are less long lived. Hence a greater understanding of arch behaviour is needed to produce more accurate analysis tools for front-line engineers.

To this end this research focuses on shedding some light on areas of masonry arch bridges that will lead to improving current assessment methods. More specifically this PhD focuses on the contribution of live load distribution through the backfill in relation to the passive pressure resistance provided and determining the effect of abutment-skewback interaction on soil movement in a masonry arch bridge.

1.2 Objectives and Method

Three questions are posed in this PhD:

Q1: What effect does the fill between the live load applied at the road surface and the extrados of a single span masonry arch barrel have on the load carrying capacity of the bridge, and why?

Q2: What contribution does the passive restraint of the backfill have on the load carrying capacity of the masonry arch bridge, and why?

Q3: Does having the skewbacks securely fixed to the abutments in a single span masonry arch bridge, affect bridge load carrying capacity? If so, what is the most likely reason for this?

This PhD aims to find out the answers to these three questions utilising state of the art theory, computer modelling and experimental laboratory tests together with field data obtained from real masonry arch bridges. By understanding these issues, existing analysis methods may be enhanced to take account of these three factors.

Arch bridges come in many shapes and sizes and in this study a circular segmental 1:4 (rise:span) geometry has been used throughout. This profile was chosen as it is common on Britain's road and rail network and also has been considered in the past by other research workers in this field. Table 1-1 shows the break down of arch numbers and types as audited by the UIC, the International Union of Railways (2004). (More details can be found in Section 2.1 and Appendix A of this thesis.)

Arch Type	Percentage
Masonry arch spans < 2m	59.6 %
Spans between 2m and 5m	20.6 %
Spans between 5m and 10m	11.3 %
Spans > 10m	8.5 %

Table 1-1 Railway arch bridges as determined by the UIC

1.3 Thesis Layout

Chapter 1 Introduction: This chapter gives a brief outline of the contents of this thesis together with stating the issues investigated.

Chapter 2 Literature Review: This chapter reviews historical lessons and considers the research that has already been undertaken in the field of masonry arch bridge research. Design guidelines, current assessment methods and technical codes of practice are examined and reviewed.

Chapter 3 Test Rig Design: This chapter discusses the issues and considerations when designing, constructing and using scale models as well as giving a comparison of the merits of each.

Chapter 4: This is a self-contained chapter which focuses on identifying the relative importance of load dispersion versus passive restraint on the load carrying capacity of masonry arch bridges.

Chapter 5: This is another self-contained chapter that has been prepared in a form suitable for submission to an academic journal. This chapter focuses on identifying the influence of abutment movement on the strength of masonry arch bridges.

Chapter 6 Discussion: The main discussion points raised by Chapters 3, 4 and 5 are further explored within this section.

Chapter 7 Conclusions and Recommendations: The main conclusions are drawn together and recommendations for future work are given.

Chapter 2

Literature Review

2.1 Introduction

Masonry arch bridges can be considered the backbone of the UK's transport infrastructure. Backbone because almost everywhere you look you will find an arch bridge supporting a road, railway or canal. The pre-industrialised world viewed arch bridge constructions as the province of organised religion and even now it is not clear how they do their job so effectively. This section examines a bit of the background as to how and why this research came about before going into detail on arch bridges themselves.

2.1.1 How the Bridges were Built

Whilst road bridges were often built one at a time as the need arose, on the turnpikes and especially on the railways whole lines of bridges would have been built in quick succession. Due to the way the earthen embankments were formed at the time, utilising horse and cart, it was not uncommon for an entire stretch of line to feature free standing, self supporting arch bridges, whilst awaiting earthworks. This explains why it is common that many railway lines have similar geometry, materials,

and as a result exhibit similar defects and deterioration rate. This is because they would utilise the same wooden formwork centring, the materials would be from the same source, and the same contractor would be responsible for building them.

2.1.2 Types of Arch Bridges

Table 2-1 shows the frequency of different arch bridge configurations included in the literature for both real bridges and laboratory experiments, (Appendix A includes further details).

Bridge Occurrence	Profile	Population	Percentage
Laboratory Tests	Parabolic	1	4% (1/27)
	Elliptical	1	4% (1/27)
	Semi-circular	5	19% (5/27)
	Segmental	18	67% (18/27)
	Not given	2	7% (2/27)
Real	Parabolic	1	2% (1/63)
	Elliptical	20	32% (20/63)
	Semi-circular	8	13% (8/63)
	Segmental	31	49% (31/63)
	Not given	3	5% (3/63)

Table 2-1 A summary of arch types explicitly stated in the literature

It is interesting to note that whilst segmental are the most common form of construction in both the literature and in practice, no details about three-centred arches were found in the literature despite them being the second most common type of arch bridge found in the UK. It should also be noted that whilst semi-circular (1 in 2) arch profiles are segmental, they behave slightly differently to the other

segmental profiles because they have a much reduced horizontal thrust component, (this is why they have been separated here). The main difference is that segmental arches tend to have a critical load position at or near the quarter point, whereas for a semicircular arch it lies nearer the crown. Table 2-2 shows the frequency of the most common rise:span profiles.

Bridge Occurrence	Profile (Rise:Span)	Population	Percentage
Laboratory Tests	1:3	2	11% (2/18)
	1:4	13	72% (13/18)
	1:5	1	6% (1/18)
	1:6	2	11% (2/18)
Real	1:3	8	26% (8/31)
	1:4	12	39% (12/31)
	1:5	7	23% (7/31)
	1:6	3	10% (3/31)
	1:7	1	3% (1/31)

Table 2-2 A summary of segmental arch profiles explicitly stated in the literature

A full summary of arches within the literature broken down by span, span/rise (S/R), profile and type is shown in Table 2-3, and a full list of references pertaining to these can be found in Appendix A.

S/R	Elliptical		Parabolic		Segmental		Not Given	
	Lab Test	Real	Lab Test	Real	Lab Test	Real	Lab Test	Real
Less than 2.00m Span								
2					2	1		
3								
4	1				3		1	
5								
6			1		1			
2.00m to 4.99m Span								
2					3	4		
3		1			2			
4					6	1		
5								
6								
5.00m to 9.99m Span								
2								
3		6				6		2
4		3			4	7		1
5						5		
6					1	3		
Greater than 10.00m Span								
2						3		
3		6				2		
4		3				4		
5		1			1	2		
6				1				
7						1		
8								1

Table 2-3 Bridge type frequency

2.1.3 Extending the Working Life of an Arch Bridge

There are several ways in which the life of an arch bridge can be extended without doing any physical works. The first is to reduce the lane width bringing the loads down the centre of the bridge away from the spandrel walls, and the second is to impose a speed or weight restriction.

The AA[1] state that there are 1700 bridges in the UK with such a restriction on them but they do not keep the data on how many apply specifically to masonry arch bridges. On the railways it is a different matter. As of December 2006 there was just one temporary speed restriction (TSR) in the London North East Territory of Network Rail (LNE) which operates on Froddingham Viaduct in Scunthorpe. This is due to the current state of the structure and the demands placed upon it for freight (mainly coal running from the docks to Yorkshire power stations). However, the railway network utilises operating speed restrictions for Heavy Axle Weights (HAW 2006) which relates to freight traffic above the current assessed capacity.

The Route Availability (RA) of a line represents the heaviest axle weight that can operate on a given railway line without being subject to HAW restrictions. Most railway lines in LNE are RA8. Normally a HAW restriction takes the form of a TSR related to a certain schedule (or group) of vehicles with Schedule 1 wagons being the least onerous and Schedule 4, which includes the heaviest, closely spaced axle HTA wagon (Figure 2-1) being the most onerous. Most Schedule 1 to 4 vehicles are RA10.

[1] Private communication from Carole Enefer, The AA, to the author dated 20th June 2007.

Figure 2-1 A photograph of an HTA wagon (Courtesy of Steve Jones & Wagons on the Web)

The HTA is the most onerous vehicle currently in regular use on the railway network; however this is not the heaviest vehicle that railway arch bridges are assessed for. The Kirow crane used for permanent way ('pway') renewal work can generate wheel loads up to 35 t with groups of four closely spaced axles at 1.1 m. The Kirow crane (Figure 2-2) is not covered by the HAW or normal operating procedures and special assessments are carried out on a bridge by bridge basis to permit its use for working on track.

Figure 2-2 A photograph of a Kirow 1200 crane wagon (Courtesy of Grant Rail)

In addition to coping with these heavy loads many arch bridges in LNE are grade listed structures meaning they form a link to the past in terms of English Heritage. As of December 2006 LNE has seventy six Grade II arch bridge structures and one Grade I listed arch bridge, that being Royal Border Bridge in Berwick upon Tweed.

2.1.4 Historical Loading of Bridges

The Ministry of Transport (MOT) introduced the first standard loading for highway bridges in the form of a load train in 1922, which included a 50% impact allowance (Chatterjee 1985). In 1925, the British Standard 153 included a unit load train where 15 units plus a 50% impact factor was equivalent to the 1922 MOT load train, albeit with different axle spacings. In 1931 the MOT Standard Vehicle Train from 1922, was revised into a series of Knife Edge Loads (KELs) and Equivalent Uniformly Distributed Loading curves (EUDLs). BS153 Part 3A in 1954 adopted this KEL and EUDL vehicle and produced the familiar HA and HB loadings updating the loadings specified for the real vehicle population prevalent during the 1950s, namely 22 ton, 10 ton and 5 ton vehicles. These load models were kept in the 1972 version of BS153, but revised and mentioned in BE1/77, BS5400 Part 2 and BD37/88. The allowable permitted axle weights were 10 tonne axles and a 32 tonne gross vehicle weight in 1973, which then increased to 38 tonnes over 5 or 6 axles in 1983 (Shave *et al.* 2003). In 1999, EC directive 85/3 allowed 40 and 44 tonnes over 5 or 6 axles respectively and a maximum axle weight limit of 11.5 tonnes. However, it must be noted that better vehicle suspensions and less onerous axle spacings were incorporated into the 1999 change.

Whilst it is undisputed that both frequency and weight of individual axles has increased upon the roads during the last 100 years, there is some dispute over whether axle weights for rail vehicles have gone up. There is no doubt that since the 1960s when rail, road and water became integrated for freight it has steadily increased in volume for both road and rail. Likewise at the turn of 1900s railway axle weights were around 8, 10, 15 tons depending on which line was being considered as some were heavy freight routes and others were not. During the First World War these axles increased to 20, 25 and 30 tons with the 30 tons being a 120 ton wagon with a rail mounted gun on four axles (Atkins *et al.* 1998). However, it is reasonable to conclude that only a small percentage of the national railway lines could accommodate such loading. The dispute itself arises over how different statisticians calculate the weights; one method is by taking annual freight tonnage and dividing by annual mileage, whereas another is to look at the actual trains and wagons in use during specific periods.

Another complication is that originally there were hundred of railway companies, then it became the 'Big Four' (LNER, GWR, LMS, SR). Next it was British Railways which became British Rail before being privatised into Railtrack and subsequently into today's Network Rail. This means that what information is available is not easily extracted into a comparable form. The National Railway Museum at York has an extensive library and holds many records for this period, however, due to building works at the time of this PhD these records were in deep storage and unavailable.

When rail freight became relatively expensive when compared to road haulage the traffic intensity dropped off on the railways and increased on the roads in the form of lorries with heavier individual axles. Today one of the heaviest axles is that of the HTA wagon with four axles at 25.5 tonnes. This being the case, individual axle weights have not significantly risen, what is clear is that a higher percentage of the network accommodates such loads than previously, primarily due to Dr Beeching's cuts of the typically non-profitable routes in the 1960s, making the network smaller whilst at the same time cherry picking the best routes. This together with improvements in 'pway' (permanent way- tracks, ballast, signals, etc.) design, materials, maintenance and bogie suspensions, has produced an increased network capacity. However, what is also clear is that axle spacing has become more onerous on the railways, whereas for freight operators on the roads this was identified earlier due to the generally weaker bridges being historically on the highways. Current lorries use modular and easy to adapt trailers to better distribute their loads.

Following privatisation, many of the experienced and knowledgeable engineers left the railway industry and were replaced with generally less railway familiar contractors. The ethos of running a railway based upon safety was replaced by one that runs on a target driven efficiency based upon a monetary unit cost. This has lead to many structures not being adequately maintained despite the greater pressures placed upon the routes which has lead to many of the problems exhibited particularly by arch bridges today. The situation at the minute is that the government's current policy of opening up new freight routes for longer, heavier trains is at odds with operating an aging network on which many routes were originally designed for the 15 ton loadings of the 1900s. This is why the industry is

looking at better understanding how arch bridges work, to ascertain whether these 15 ton axle bridges had a safety factor included that could safely be reduced to allow 25 tonne axles.

2.1.5 Commission for Integrated Transport

Masonry arch bridges are back in the spotlight for research due to the Commission for Integrated Transport (CfIT 2000, CfIT 2002) who in 2002 announced proposals designed to maximise the efficiency of the UK lorry fleet while delivering key environmental benefits. The bridge engineers consulted didn't identify that a significant number of masonry arch bridges, most of which have stood uncomplaining for over one hundred and fifty years would begin to deteriorate at an unprecedented rate with the new loading. Most arch bridges could cope with one or two heavy vehicles well in excess of its assessed live load capacity each year but not the significant increase in the frequency at which heavier vehicles were crossing the structures.

Fortunately the railways studied the effect of increasing the loads for its freight trains before introducing the 25 t axle HTAs to the network in 2000, details of which can be found in Packham (1989). However, in this case rather than just imposing a weight limit the need for a higher standard of maintenance of the wagons was identified as a key requirement of allowing these heavier vehicles to operate.

2.1.6 Assessed Capacities

There are two factors which affect the assessed live load capacity of a masonry arch bridge which by design, using a safety factor, lies below the actual collapse load of the structure. The two critical factors are weight and speed. Weight includes not just how heavy the applied load is but how often the structure has to bear it and in what direction the load is applied. All arch assessment tools currently take the applied live load as vertically downwards even though static loading on a structure of this type is not as onerous as that produced by a vehicle moving across it at speed or even worse if the vehicle decides to brake hard or, in some instances, change gear which means that the live load has both a horizontal and vertical component. Add to this the cyclic frequency generated by successive axle loadings and it soon becomes apparent as to why this type of structure is particularly sensitive to the current load increases.

The research into the area of dynamic effects is very much in its infancy and to the author's knowledge nothing has been published which includes the influence of the backfill on this, although 'hearsay' rumours that several universities in Europe are currently conducting research into this. As it stands dynamic effects tend to affect bridges which have low cover and a steep profile (1 in 2), this is particularly bad on older railway freight to routes where two entire routes are in the process of having their affected bridges replaced such has been the damaged caused (Settle to Carlise and South West Scotland. This is the main route for coal which comes by ship into the country at Hunterstone and is then transported to the Yorkshire power stations).

The cost of bridge replacement of this type means that in the longer term and throughout the railway network it becomes an unsustainable option.

Because of these issues it was identified by industry that there was a need for better assessment techniques for masonry arch bridges (at present the most widely used method is the MEXE method, developed in World War II for use with tanks, which is empirically based and also requires an engineer's sound judgement).

2.1.7 Literature Review

This chapter of the thesis is given over to explaining where arch bridges stem from and what part they have had in history as well as how they were made and what procedures and what was considered prior and during construction. The key word with masonry arch bridges is 'assessment' because the UK does not tend to design or build modern ones so it can be considered as something of a lost art. This is useful because many engineers who deal with arches were taught about concrete and steel and to a lesser extent masonry but for most the first time they deal with assessing a masonry arch bridge is when they actually do it as part of their job.

This section briefly covers their introduction by the Egyptians and the Chinese, and their mass production by the Romans, the artful designs at the renaissance, through the industrial revolution and into the modern day; the arch bridge has truly been an integral part of human history. It is often said that transport links forge countries and that success and failure of a country depends largely on its infrastructure

(DEFRA 1998), therefore it is high time that these 'taken for granted' structures are given the respect they so truly deserve.

This chapter presents an overview of the literature that contributes to our understanding of the behaviour of masonry arch bridges. The related main subject areas are:

- The importance of masonry arch bridges in history.
- Previous research conducted in this area
- Methods to assess the load carrying capacity of masonry arch bridges.
- Design and assessment guidelines in the UK.

2.2 Historical Information

It is important to look at the methods of construction for masonry arch bridges as it is becoming more common that many of these structures are being repaired or replaced using modern methods.

2.2.1 Pre-Industrial

Egypt and Mesopotamia

Masonry arches are thought to have developed from mud plaster covered, bent over reed bundles placed in the ground and tied together at the top to form a roof, in Egypt and Mesopotamia around 3000BC (Page 1993). It is thought that sun dried

mud bricks would have replaced the reeds as it is a more durable material to form the first vaults.

In this instance the arches appear to be a by product of forming columns of bundled reeds which naturally curve over under their own self weight once a sufficient height is reached, the reeds themselves grow up to 6m (Milwich *et al.* 2006). This enabled huts to be built before being reinforced with mud which was then allowed to bake dry and harden in the sun. Such arches are thought to have been able to produce a 3 m rise for a 6 m span.

Mycenae

Slightly later than this is the corbelling present in ancient Mycenae temples and tombs in around 1325BC. Formed of stone, it is thought that at some point 'flat arches' evolved from taking this technique that bit further in construction (Zekkos *et al.* 2005). The reed structures, although possessing outstanding structural properties, would be limited to the amount of both dead load and live load that they could take without severe deformation and this may have been the 'cheap' option in terms of building materials hence the use in housing, whereas stone has the ability to carry much more significant loads.

China

The Chinese appear to have been the first to use the arch in bridge construction shortly afterwards and it is noted that they preferred segmental profiles over the

semi circular design beloved of the Romans, (Figure 2-3). One thing to note is that in modern times, Chinese arches tend to be largely ornate rather than functional, and this difference is a key factor in how the arches in the Far East have developed over time to those produced in Europe[1].

Figure 2-3 An arch bridge, Che Spring Reservation, Ye Chang, China

The Romans

The vast road and aqueduct network spread throughout the Roman Empire, the road bridges built by their impressive military and the aqueducts by city government departments. Bridge building was seen as a very worthwhile task and the emperor himself eventually took the title Pontifex Maximus (Master of Bridges) himself. An interesting side note is that this title is now held by the Pope in the Vatican (Smith 1993) to signify that the head of the Roman Catholic Church is in effect a bridge to God.

[1] Private communication from Professor Wei Lian Qu, Wuhan University of Technology to the author dated 27th December 2006.

It is thought by many that the Romans adopted very conservative construction techniques when it came to building bridges: semicircular arches with thick piers were the norm. However, Romans also built some segmental arch bridges and an assessment of the Pont Du Gard (Hauck 1986) illustrated that their understanding of arches satisfied analysis methods that were in common use during the industrial revolution.

The Romans are known to have built stone arch bridges during a period of over 400 years around 2000 years ago (O'Connor 1993). It is most likely they had rules of thumb for arch bridge design based upon observations gained from repeated construction experience. The construction order for the bridges started first with the abutments which tended to sit directly on the ground, then the foundations and the piers, before the arch ribs were finally constructed. Roman bridges have many traits, including: always having closed spandrels; the voussoirs of the arch pointed towards a circular centre so that outward movement was prevented; the large thick piers tended to give rise to scour problems on river crossings. Whereas later bridges used mainly soil as backing, it is known that the Romans favoured the use of concrete, which helps to explain why a common defect in later bridges, that of separation between spandrels and barrel, did not frequently occur.

Most Roman bridges used a minimum spandrel depth with the depth above the crown often thinner than ring thickness itself and the large soil pressures on the back of the abutments often caused them to move inwards. Romans are known to have left writings detailing knowledge about span to rib thickness ratios and it is evident

that due to their crane technology at the time spans longer than 15 m were problematical due to moving large blocks of stone at distance. They also used different coursing methods in their brickwork; some of the methods used in later times helped prevent the defect of ring separation in arches comprising several brick courses. Roman bridges were often constructed as an upgrade to existing timber bridges which enabled the original wooden crossing to be used to aid in the assembly of the new arch bridge. It is known that they also used formwork and centring and that they tended to build one span of the bridge at a time.

The Churches

During mediaeval times the bridges constructed were done so with the blessing of the churches. In England there are examples where knights would provide funds via the bishops who would grant 'indulgences' for local stone masons to construct bridges, as in one case involving Walter De Grey, Bishop of York in the 13th century[1]. Two examples of bridges in sponsored by the Bishops of Durham, (Ralph Flambard: 1099-1128, and Hugh Puiset: 1153-1195), are shown in Figure 2-4 and 2-5 respectively.

Figure 2-4 Framwelgate Bridge, Durham

Figure 2-5 Elvet Bridge, Durham

[1] Private communication from Christopher Webb, York Archives dated 15th May 2007.

Bridge Building Brotherhoods

The *Frères pontiffs* of the Middle Ages have a much inflated reputation, being given credit for many of the most prominent medieval bridges in France and England (Boyer 1964). However, evidence suggests that given how so little is known of them in France, particularly given their relationship to the bridge at Avignon, and their absence from historical literature at the time, such groups appear to be largely localised rather than being a fraternity. One reason given for the myth of such a brotherhood stems from local bridge building groups gaining merit by association with the beatification of St Bénézet who initiated the bridge across the Rhone at Avignon. What is agreed upon is that these local groups generally looked after and protected travellers in the local area, and provided and maintained both the local infrastructure and its commerce.

Figure 2-6 The bridge at Avignon (Courtesy of Hans Zumstein at www.bastide-midi.com)

Two historically confirmed *fraters pontis* were at Avignon and Lyon, with strong ties to the local church. However, there is a stark contrast between the two. The brotherhood at Avignon dealt with fundraising and administration of property with actually no record of being involved in bridge construction. It also had both male and female members. The Lyon brotherhood by contrast comprised men only and was in charge of bridge construction. A third supposed brotherhood at Pont-Saint-Espirit was revealed to comprise of local people who were paid and did not belong to any particular group. What is clear from the literature is that the 'Bridge Building Brotherhood' has been romanticised by previous historians.

The Renaissance

During the renaissance (1300-1650) parabolic profiles were used (Figure 2-7), and larger span arches became possible, allowing the design of masonry arch bridges to be streamlined (Hauck 1986).

Figure 2-7 The 1388 bridge at Newton Cap, Bishop Auckland, Co. Durham

2.2.2 Industrial Revolution

Between 1750 and 1850, the time known as the industrial revolution, Britain was transformed from a largely agricultural rural population to a factory/manufacturing town-centred society. This period saw a great leap forward in masonry arch bridge construction. The information recorded as a matter of course during the industrial revolution included specifics as to what the engineers at the time considered to be important. In the case of railway viaducts records of construction costs, building times, defects and methods used to remedy them can be found.

The Reconstruction of the English Bridge over the River Severn at Shrewsbury (Ward 1928) gives a good example of how inconsistent the understanding of arch bridges was at the start of the industrial revolution. An examination of the structure found that cracking in the old bridge was due to the joints between successive bricks being too wide. Given the quality of brick foundations and the fact that it was backed with cemented rubble of ample proportions and waterproofed with puddle clay it is hard to see why it was then backfilled with local earth and gravel. In one bridge there are examples of both apparently 'good' and 'bad' techniques.

The almost comical account of the masonry arch bridge over the Pont y tu Prydd (Smith 1838) illustrates that some bridge designs were not always fully thought through prior to construction. The first bridge constructed was washed away shortly after completion and during the building of the replacement bridge there was an unforeseen problem with the geometry. This was caused by the large dead weight of the fill over the haunches, required to obtain the necessary road level, being too

great in relation to the slender crown. The result was that the arch in effect snapped upwards. Nevertheless perseverance prevailed and this time after consultation with the eminent engineer of the time, John Smeaton, holes were made through spandrels that were elsewhere backfilled with lightweight charcoal. Needless to say this bridge had fewer troubles and stands to this day.

Since at the time English engineers were in demand throughout the world, a novel approach to identifying the load carrying capacity of a masonry arch bridge was demonstrated on Vevey Bridge, in Switzerland (Gaudard 1879). It was load tested upon completion to prove it could carry the load required; fortunately it performed very well although it highlights the fact that designs were not always trusted by clients and that the risk of destroying a new bridge was seen to be preferable than having a perfectly functional bridge of uncertain capacity.

In the memoirs of the eminent Victorian engineer John Fowler (Mackay 1900), the case for a very flat arch at Maidenhead is given. Much to the dismay of many of the engineers of the time a bridge was built which stood with one of the spans severely distorted. The reason for the perfectly functional yet worrying profile was deemed to have been caused by the removal of the formwork prior to the being cement sufficiently set. The case in point demonstrated the use of superior materials in bricks and mortar which had greater uniformity than that of previously used lime and Roman types.

It is clear in the work on the Dora Riparia (Albano 1836) that great pains were undertaken to ensure the structural integrity of a bridge during and after construction. In this case prior to the building of the arches the structure was left for a whole season to allow enough curing time for the masonry abutments so that they would have sufficient strength to resist the thrust forces of the arch once constructed. Also caution was exercised to prevent damage to the arch during the striking of the centring as it was known that accidentally knocking a corner off of a voussoir or allowing the abutment to spread too far would cause problems later on in the life of the bridge. In addition Albano indicates that maintaining the arch profile and the individual positioning of the blocks during construction is of the utmost importance.

In the description of the bridge across the River Hoogly (Laurie 1904) it is noted that considerable movement and hairline cracks within the barrel and abutments were observed just after completion. The engineer concluded that scour was undermining the foundations and the remedial measures undertaken were discussed. Scouring of the piers was also the problem identified in the case of Waterloo Bridge, London; however, the engineers noted that the arch barrels and the interior spandrels, longitudinal walls backfilled with clay, were sound.

Not all defects are noticeable or significant. The case of Stockport Viaduct (Morris 1948), which was built in 1840, for a long time showed no significant signs of distress. However, for some unknown reason it began to fail in 1917. The bridge was closely monitored and over the next decade the sixteenth arch span began to develop transverse cracks. Eventually these hinge formations were put down to the

natural 'breathing' of arches whereby temperature variations over the year from being hot in the summer to cold in the winter affected the masonry. Nevertheless this span had to be replaced.

Not all defects are real either. In the case of the Jubilee Bridge (Laurie 1904) scour and foundation problems appear to have been over exaggerated so that a new replacement would be built.

Figure 2-8 Royal Border Bridge (Courtesy of Network Rail)

It is a sobering thought that engineers of this time had more confidence in masonry arches than in soil embankments. Problems at the Royal Border Bridge (Bruce 1851) highlights that embankment failures, due to slope stability failures, was seen as a common problem, such that in this case part of the approach embankments were replaced with masonry arches (Figure 2-8). Once again mortar type and quality was seen as the lynchpin of a structure's success. Since this was a working bridge temporary timber arches were constructed for traffic whilst the main arches were built. Another bridge that saw the replacement of its embankments was the case of St Pinnock's Viaduct (Margary 1882) in Cornwall.

To obtain an indication of just how good the quality of masonry used at this time could be it is worth examining the viaduct at Brighton (Toms 1945). This bridge was struck by a bomb which destroyed two middle spans and a pier. However, the remainder of the bridge remained standing for long enough so that repairs could be made. Engineers doing the repairs put the fact that the bridge did not immediately collapse down to the excellent quality of the materials used in the original bridge construction.

In the literature about Chapple Viaduct (Bruff 1850), it is documented that the engineer in charge of the project could not locally obtain suitably hard enough bricks for arch construction; therefore he had his own bricks made especially in the fields nearby. He also employed concrete backing.

At Lockwood Viaduct (Hawkshaw 1851) efficient new construction techniques replaced traditional methods. In this case carefully selected and placed rubble masonry was used in the construction (as opposed to the more traditional uniform or ashlar masonry). Another innovation was the use of internal spandrel walls with flagstones spanning the gaps and the ballast placed on top in an effort to reduce dead weight. The old notion that coarse sharp sand was better than fine sand for the mortar was also disproved. The plan of works shows that in this case material quality for the bricks and the use of fine sand mortar with sufficient setting time was of paramount importance at all stages of the building works.

The construction of Hownes Gill viaduct (Cudworth 1862) is a testament to the development of bridge construction during this time. The use of fire brick and hydraulic mortar were the very best materials available. The bridge was water proofed with puddle clay and still stands to this day near Consett in County Durham.

It is clear that the engineers working near the end of the industrial revolution had considerably improved construction practises and developed better materials in terms of standardising bricks and mortars. They also showed that engineering judgement was important when selecting the type of bridge to use in a certain location as well as using different span to rise geometries and varying the number of spans (Figure 2-9).

Figure 2-9 The 1848 bridge at Newton Cap, Bishop Auckland, Co. Durham

Originally large span viaducts were built by village stone masons with experience mainly gained on building workshops and mills. Over time these masons could be elevated to greater standing in society upon successful completion of a railway bridge of significance. The engineers showed that variations or changes in arch conditions led them to fail more quickly and also that asymmetric or distorted profiled arches tended to fail sooner.

The problems engineers identified in large masonry arches were the massive construction costs, the enormous self-weight of the structure and the problems with erecting scaffolding around these bridges. However, at this time a large number of frequently maintained timber viaducts were replaced with iron or steel and masonry depending on the local conditions, and although timber bridges were common it was not long before longer lasting arches were preferred as they also required less maintenance than iron or steel bridges. Materials were studied for economy and fitness for purpose which meant over time reduced cost for viaducts as designs improved. Iron and steel were not as durable as masonry but led to cheaper bridges in most cases. However, masonry arches were preferred as they demonstrated more durability, solidity and rigidity and were better at absorbing vibration if properly founded. The downside was that arches tended to increase the vertical level of highways which was not always ideal, whereas iron/steel beam bridges could remain at low level.

The paper by Gaudard (1879) also highlights three calculation methods developed and used by engineers at the time. The methods given are the monolithic elastic with tensional strain method, put forward by Perrodil, the principle of least resistance, given by Williot and an equilibrium based approach which uses the point at which the centring is removed, suggested by Dupuit. None of the methods predict where hinges will form but do enable simple statics to be used to analyse the arch. Each method assumes friction is sufficient to prevent sliding between blocks (rather than the cohesion provided by the mortar) and Perrodil, Williot and Dupuit all knew that the setting time of an arch was important. Perhaps the most intriguing point is the fact that engineers knew crushing of the masonry could occur where the hinges

formed and that they used a line of thrust analysis to determine potential weak parts of structure before putting in harder materials to help prevent crushing.

2.2.3 Modern Arch Bridges

It is thought that there are nearly forty thousand highway bridges and thirty three thousand railway spans of masonry arch construction in Britain today (Page 1993), most of which have spans less than ten metres and were built during the industrial revolution. Masonry arch bridges are not often built today since concrete and steel are now the predominant bridge construction materials (although Kimbolton Butts (Ponniah *et al.* 1997) stands as one real exception). In 2004 the Highways Agency issued a new design guide for masonry arch bridges (BD91/04) in the hope that masonry can once again become mainstream for bridge design alongside steel and concrete.

One example of using modern techniques to assess old bridges is that of Stanwell Park viaduct (Yan *et al.* 1988) which after opening in 1920 suffered subsidence from local mine workings and as a precaution one of the arch spans was replaced by steel and pre-cast concrete at the time. However, problems continued over time before becoming more significant and in 1985 repair work made use of a two dimensional finite element model in planning the remedial works.

Another example is that of Egton Bridge (Smith 1994) which was built in 1758. In 1931 two spans of the bridge were destroyed and at the time replaced by a steel deck;

however, in 1993 the main arches were restored to their original state not just for aesthetic reasons but also as the local council realised that the long term maintenance costs would be less than that of a steel deck bridge.

Like Egton Bridge, old masonry arch bridges are being renovated and repaired as local authorities are made aware of how comparatively low their whole-life costs are compared to other structures. Furthermore, anecdotal evidence indicates that local people prefer the aesthetics of masonry arches to concrete and steel alternatives.

It should be pointed out here that rather than designing new bridges, a large amount of work done is on the assessment and remedial works of existing masonry arch bridges due to the cost and inconvenience caused by having to replace them. Schemes such as those shown in Figure 2-10, where a disused railway viaduct has been converted for highway use, are becoming commonplace as congestion on alternative routes leads to local political pressure.

Figure 2-10 The 1848 bridge at Newton Cap, Bishop Auckland, Co. Durham which has been adapted for modern day traffic

2.2.4 Review of Backfill Material

Many civil engineers would assume that backfill material used in arch bridges at the time of their construction would be material that would be lying around or easily accessible at site, because this is logical and makes sense and it is what they would do. However, apart from vague references to this being the case it is quite difficult to prove or disprove this statement. To see what actually was recorded in the literature a survey of all recorded backfill material from the records were correlated and can be seen in Table 2-4.

Backfill Material	Occurrences	References
Asphalte	1	Bruff (1850)
Carrstone	2	Mann & Gunn (1995), Ponniah *et al.* (1997)
Cement	2	Albano (1836), Page (1989)
Charcoal	1	Smith (1846)
Clay	10	Buckton & Fereday (1936), Chettoe & Henderson (1957), Cudworth (1862), Hawkshaw (1851), Heyman & Padfield (1972), Heyman (1980), Page (1987), Page (1989),Ward (1928), Harvey (1992)
Concrete	3	Bruff (1850), Ward (1928), Harvey (1992)
Gravel	7	Albano (1836), Ward (1928), Bruce (1851), Heyman (1980), Mann & Gunn (1995), Page (1987), Page (1988)
Rubble	6	Bruce (1851), Cudworth (1862), Hawkshaw (1851), Heyman & Padfield (1972), Page (1989), Ward (1928),
Sand	11	Albano (1836), Heyman & Padfield (1972), Heyman (1980), Laurie (1904), Mann & Gunn (1995), Page (1987), Page (1988), Harvey (1992), Royles & Hendry (1991)

Table 2-4 A summary of backfill material explicitly stated in the literature

It must be borne in mind that not every bridge is in the records and quite a large proportion of what is tends to be for viaducts, nevertheless an attempt has been made. It was initially thought to expand the survey into currently used highway and railway bridges but due to the way assessments have been done (with it not being common practice to dig trial pits for soil samples on the majority of arches) no comparable data was available.

As can be seen there is definitely no standard type of backfill used and actually rubble which is what is likely to be easily accessible and readily available at a worksite is the fourth most common with sand being top, then clay, followed by gravel before it. Also of note is the lack of references where backfill has been explicitly stated. Not shown in the above table, but utilising the records for underbridges at Network Rail revealed that in many cases there exists 'low' cover over the crown of arches meaning that most of the backfill is track ballast.

The reason information about backfill is patchy comes down to two key issues, the first being that most engineers simply do not understand why it is important and, beyond obtaining the depth of cover for a bridge or proving the existence of backing for MEXE assessment purposes, do not consider that a waterlogged clay will have a different effect to well compacted limestone on the behaviour of the arch structure. The second issue is the difficulties associated with carrying out cores or trial pits (Figure 2-11 and 2-12).

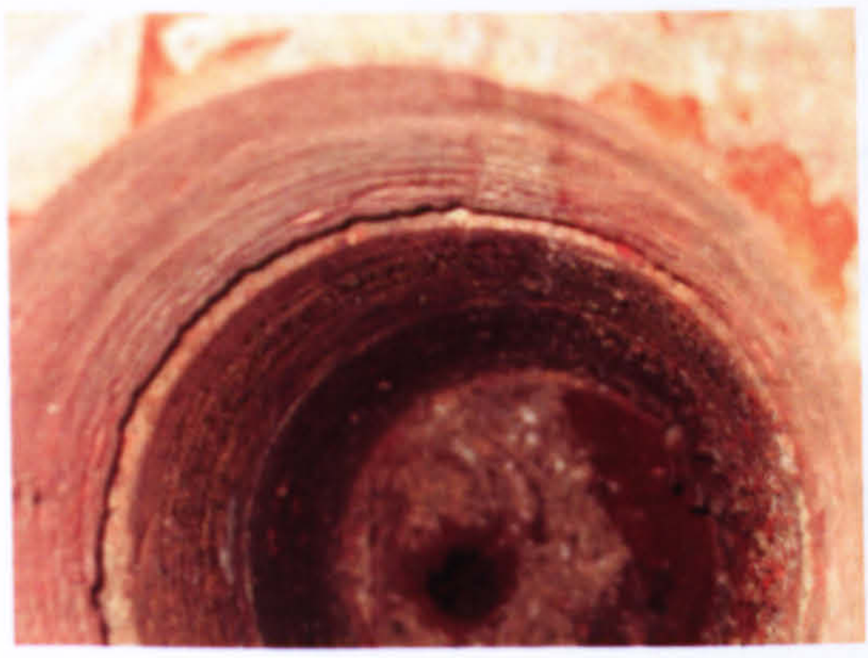

Figure 2-11 Core hole in Patience Bridge, Essex (Courtesy of Essex County Council)

Figure 2-12 Trial pit in bridge TCC/20 (Courtesy of Network Rail)

The problem with taking core samples from beneath or digging trial pits on the top presents an engineer with two challenges, the first being there is likely to be an operational road or railway over the top and the same or more likely a water course underneath, which makes setting up a safe environment to do the necessary work difficult at the best of times. (Approximately half of all LNE arches span over water, there are also other issues with tenancies but that is not covered here.) The second problem faced by the engineer is politics, in that whilst the engineer does his pits or cores, the normal traffic flow is interrupted costing the local, and sometimes national, economy money. This means that closing even part of a road, railway or watercourse for even a short period of time is very expensive.

2.2.5 Summary

Masonry arch bridges have been around since the dawn of civilization in Europe and were pioneered in three distinctive eras. The Romans mass produced great bridges that still survive to this day (though alas not in the UK). The mathematics brought by the renaissance streamlined bridges enabling magnificent designs to be constructed and the powerhouse of the industrial revolution brought in new material

standardisations as well as empirical and analytical methods to be used for bridge design. It is clear that great lengths were gone to in order to ensure that the arch bridges built were of high quality and of good design as well as being suited to the location in which they were built. However, what was apparent was that specifying the backfill type/properties to be used during construction was the exception and not normal practice. What is also apparent is that in the drive for concrete and steel bridges the art of how these bridges were designed and built by rule of thumb has been lost.

2.3 Review of Previous Experimental Work on Masonry Arch Bridges

Following the renewed interest in masonry arch bridges many reports have been published and much has been written about how masonry arches should be assessed and what parameters and defects should be taken into account both during a site inspection and when calculating strength. Work done as part of assessment investigations are given in detail in the references by Sowden (1990) and in work done by the Wolfson Bridge Research Unit (Harvey 1992). The reader should remember that some research published in 2004 and later was too late to change the direction of the reported work, particularly work done by Harvey (2006). It is interesting to note that some of the recommendations in the current research work were addressed by this PhD.

The implications of Harvey (2006) have little bearing upon the research conducted within this PhD. It does, however, provide additional support to the fact that live load spreading through the backfill down to the extrados for shallow depths of fill is less than current guidelines state. The main thrust of Harvey's paper is the fact that the arch itself distributes the stresses applied to it from a point directly under the applied load in a fan shaped pattern to both abutments. This presents difficulties in existing 2D analytical models as all rely on a strip analysis, based upon an effective width.

2.3.1 Field Tests on Arches

In the 1950s, the Ministry of Transport continued its pre-war work on load testing of the nation's bridges (Davey 1953). Although many different types of bridges were examined only the masonry arch bridges are of interest here. On these, Davey looked at the dispersal of the load through the fill, the strength contribution of the fill and the effect of abutment movement on the arch. Three masonry arch bridges were tested to destruction by means of hydraulic jacks (as shown in Figure 2-13) and many more were loaded whilst being monitored.

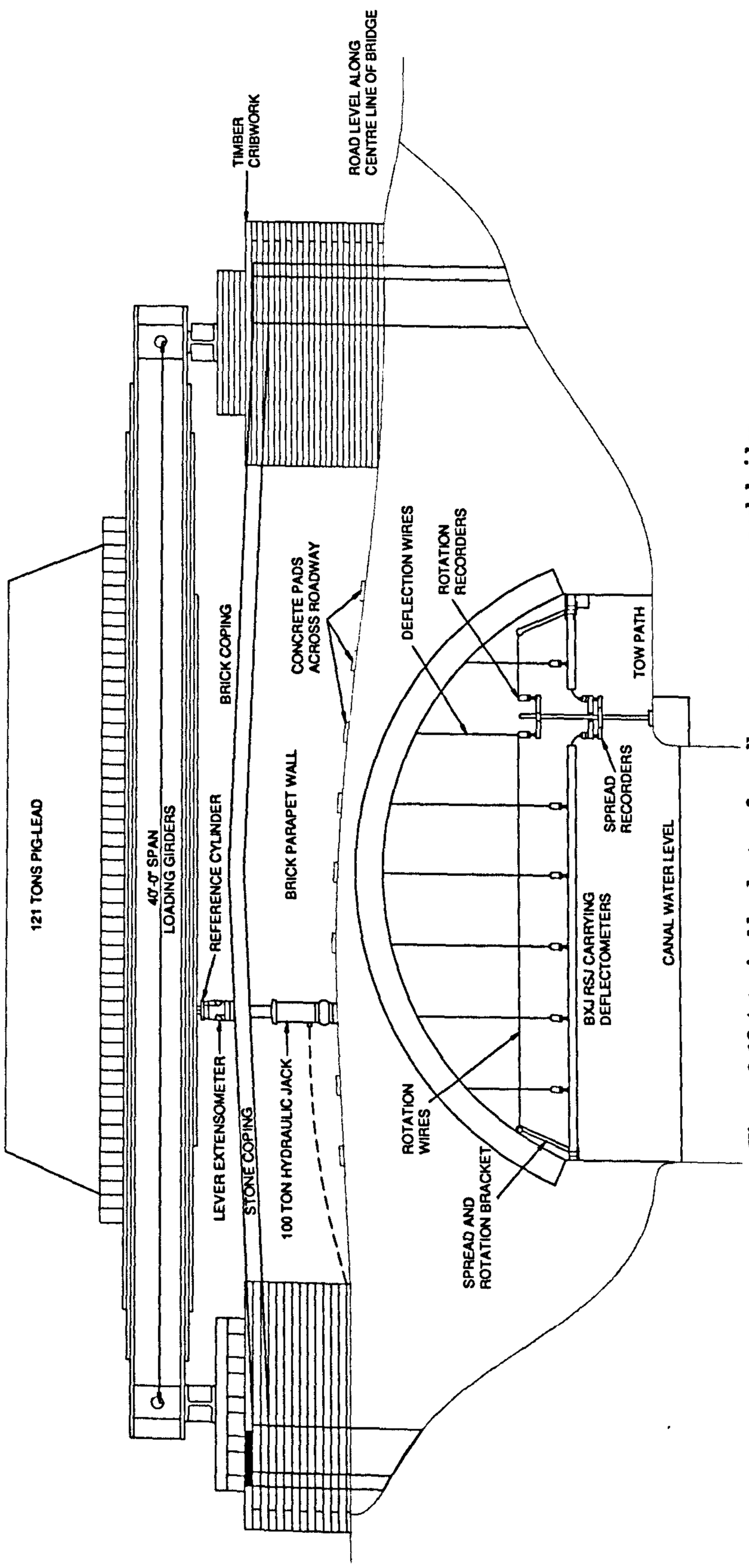

Figure 2-13 A typical load set up for collapse on a masonry arch bridge

It should be noted that depending on the nature and type of the backfill at the bridges the positioning of the cribwork is likely to have influenced the failure. However, in spite of reservations surrounding the loading arrangement, three important conclusions can be taken from this work, the first being that when an arch was loaded the abutments in every case moved outward, secondly that the spandrel and abutment fill should be assumed to act as one uniform unit and that consolidated backfill contributes greatly to structural strength.

The work of the Ministry of Transport was continued by Chettoe & Henderson (1957). This work comprised load tests on masonry arch bridges whilst measuring both deflection and abutment spread. It appears that the basis of the load spreading clauses of the current UK assessment codes is based upon this work, which although the tests were slightly flawed as many bridges were not loaded to collapse and only crude instrumentation was used, is useful to see where they come from. The main findings and recommendations from the series of tests were that arches should be considered to behave elastically, and that a live load dispersal of 45° should be adopted for assessment purposes. However, no direct account of fill was to be taken and no spandrel restraint should be considered, somewhat predictable given that no details of the backfill over the arch was included in the published document. Also, a permissible stress method was recommended for general use as can be seen in the old assessment code used by the railways in RT/CE/C/015 (1995). Whilst on one hand Chettoe and Henderson produced much needed data, with hindsight the actual quality of the instruments and the setup and nature of the tests limits their usefulness.

Much of what was concluded and recommended at the time has over the years been proved inaccurate.

Most people involved in masonry arch bridge assessment are aware of the tests conducted by the Transport Road Research Laboratory in the 1980s (Page 1993). Rather than reproduce them in detail here, Page provides brief details of them in his State of the Art Review. A summary of eight of the tests are given in Table 2-5.

Name	Profile	Span (mm)	Rise (mm)	Width (mm)	Depth of Fill above Crown (mm)	Ring Thickness (mm)	Collapse Load (kN)
Preston	Elliptical	5180	1640	5700	380	600	2110
Prestwood	Segmental	6550	1430	3800	165	340	228
Torksey	Segmental	4900	1150	7800	246	380	1080
Shinafoot	Segmental	6160	1180	7020	215	365	2524
Strathmashie	Segmental	9420	2990	5810	410	Varies	1325
Barlae	Segmental	9860	1690	9800	295	400	2900
Bridgemill	Parabolic	18300	2850	8300	125	711	3100
Bargower	Segmental	10000	5180	8680	160	558	5600

Table 2-5 Bridges tested to destruction by the TRRL during the 1980s

Suffice to say that these tests were not as useful as initially expected as they seemed to be directed at proving that the current assessment method (MEXE) was adequate (many material properties necessary for more advanced analysis techniques were not sought). The bridges were also in various conditions and the loading arrangement also varied making direct comparisons between structures difficult.

2.3.2 Full Scale Laboratory Tests

The main series of full scale laboratory tests to be looked at here comprise those done at the Bolton Institute during the 1990s. This is because these tests informed some of the decisions taken as part of this PhD.

The first series of tests to be looked at are described in a paper by Melbourne & Gilbert (1995). These tests involved examining the failure mechanisms of multi-ring brickwork arch bridges of 3 m and 5 m span, 1:4 (rise:span), segmental arches. Details of the two bridges are shown in Figure 2-14 and 2-15 respectively.

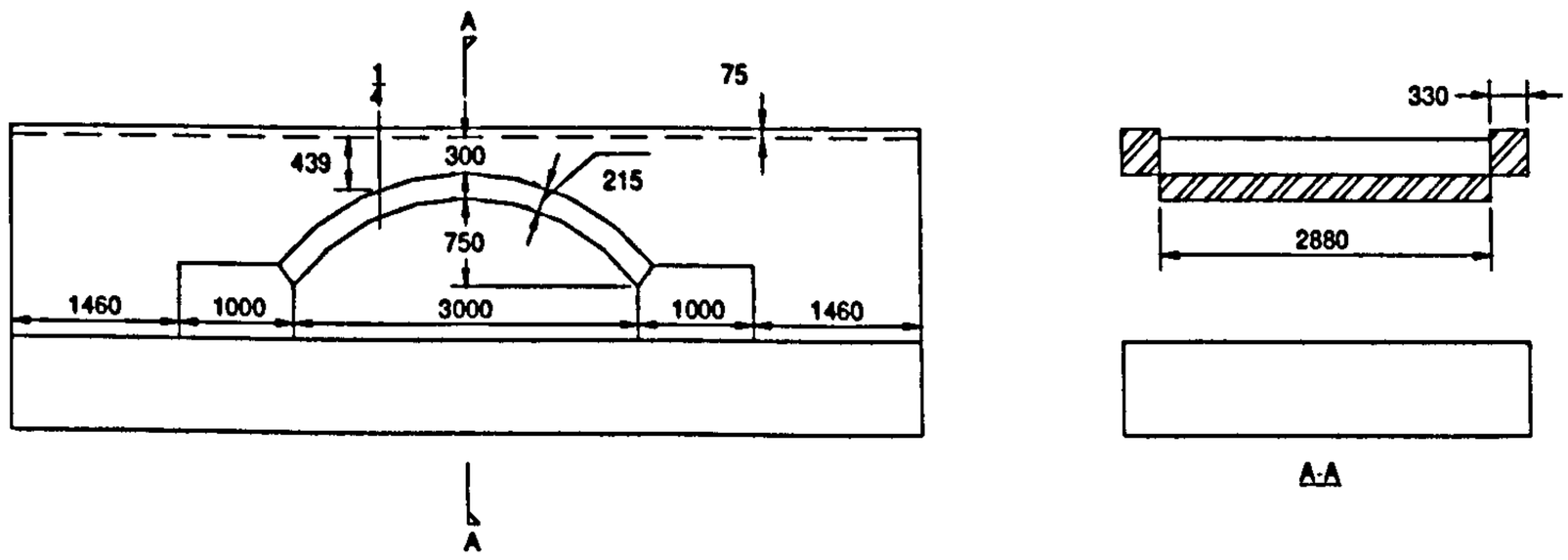

Figure 2-14 Bolton Institute tests: 3 m span bridge dimensions

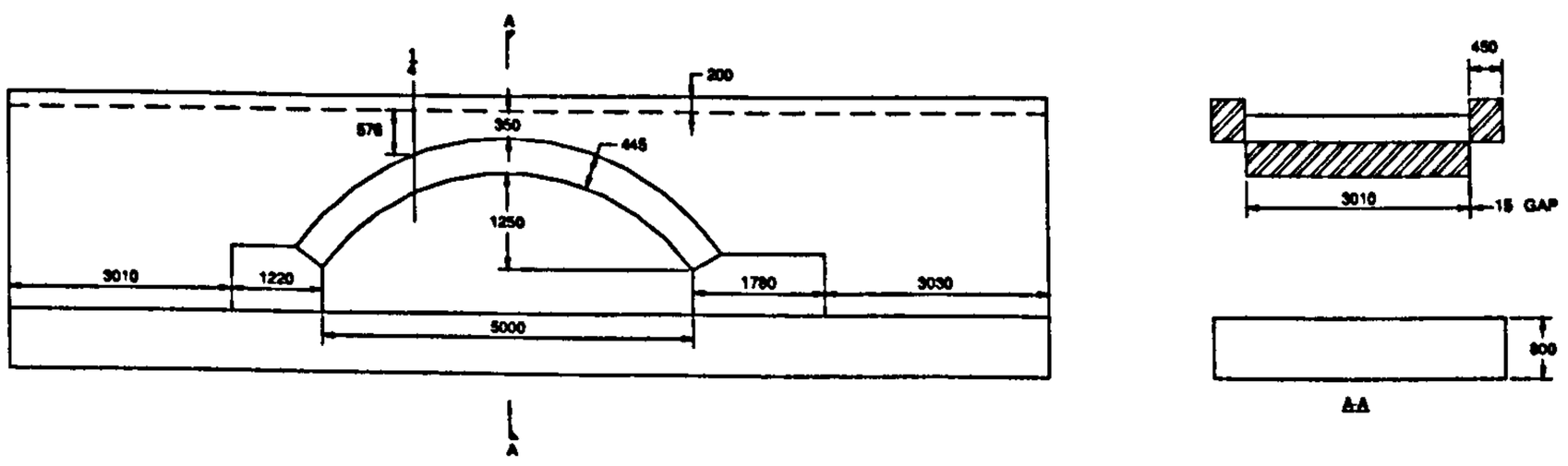

Figure 2-15 Bolton Institute tests: 5 m span bridge dimensions

The backfill comprised graded crushed limestone and the arches were constructed using stretcher bond which is susceptible to ring separation failure. Loading was applied at the quarter point via two hydraulic jacks bearing on a loading beam.

What was found during the tests was that all the arches failed by a four hinge mechanism and that horizontal backfill pressures increased after gross deformation. The presence of ring separation reduced load carrying capacity in an unpredictable way when ring separation occurred. The failure loads had been estimated prior to testing using the rigid block mechanism method (Gilbert & Melbourne 1994).

A second series of tests focussed on the behaviour of multi-span bridges and the influence of spandrel walls, Melbourne *et al.* (1997). This time three bridges of three spans each comprising a 3 m span by 0.75 m rise barrel were tested in a similar manner to before. Once again all the bridges tested failed by formation of a mechanism and the bridges failed at lower loads than corresponding single span bridges. It was also found that the critical loading position was nearer to the arch crown for multi-span rather than the quarter point for single span segmental arches. The experiments also provided evidence to support the theory that spandrel walls have a strengthening effect. Once again backfill horizontal pressures were found to be beneficial, but less so than in the case of single span bridges.

Full scale tests on segmental and semi circular arches were conducted in 2004 by Roca & Molins (2004). What was surprising was that in both cases the arch was loaded at the quarter point. It is generally accepted that for a segmental arch indeed the critical position is at the quarter point; however, for a semicircular arch the critical loading position is likely to lie nearer the crown. The tests used compacted sand and in both cases a four hinge failure mechanism developed. The bridges included spandrel walls whose stiffening effects were lost at 60-75% of peak load as they separated from the main arch barrel. Upon the separation of the spandrels hinges immediately formed in the arch barrel directly beneath the load and at the loaded side springing. At 80-90% of the peak load the third hinge formed on the unloaded side prior to the fourth hinge forming at the unloaded side springing.

2.3.3 Small Scale Tests on Arches

Hughes & Kitching (2000) investigated the use of small scale models to predict the behaviour of large scale prototypes. Valid concerns were raised about the differences between the prototype and the small scale models. It was concluded that small scale models were suitable for qualitatively examining structural behaviour and that they were also useful for calibrating emerging numerical models. This section looks at some of the more influential tests done at scale on arch bridges.

One of the first modern pioneers in this field was Alexander Pippard who undertook an experimental and analytical study of the voussoir arch in 1936 at the behest of the Building Research board (Pippard *et al.* 1936). A segmental arch made of steel

voussoirs was used in the tests (see Figure 2-16). The span was four feet with a rise of one foot, and the ring thickness was three inches, and the width of each voussoir was one and a half inches. The arch was made such that it could be mounted on pins or on skewbacks at each abutment. One end was always kept fixed and the other was attached to a rolling saddle arrangement that permitted horizontal movement. The force in the arch (thrust) was measured by an extensometer. The span was controlled by the use of a turnbuckle. The centre of each voussoir carried a weighted spindle to represent the backfill load and an extra weight was hung to represent the live load. The only restraint that the voussoirs had was slots and pins to prevent rotation. Following calibration, a series of tests to determine arch behaviour was carried out using the apparatus.

In experiments where no movement of the abutments occurred, the arch behaved for small loads in the manner of an elastic arch rib whilst for larger loads it was found to behave as a three pinned arch. In experiments where the abutments did move, the arch behaved as a three pinned arch.

Melbourne (1988) described tests on concrete arches with hinge inducers both with and without spandrel walls. It was concluded that as the hinges formed stress redistribution occurred within the structure and the passive soil pressures on the non-loaded side did not change significantly, proving that long term consolidation of the backfill increased the soil pressures. This indicates that engineers have known for many years about the positive effect of backfill within arch bridges.

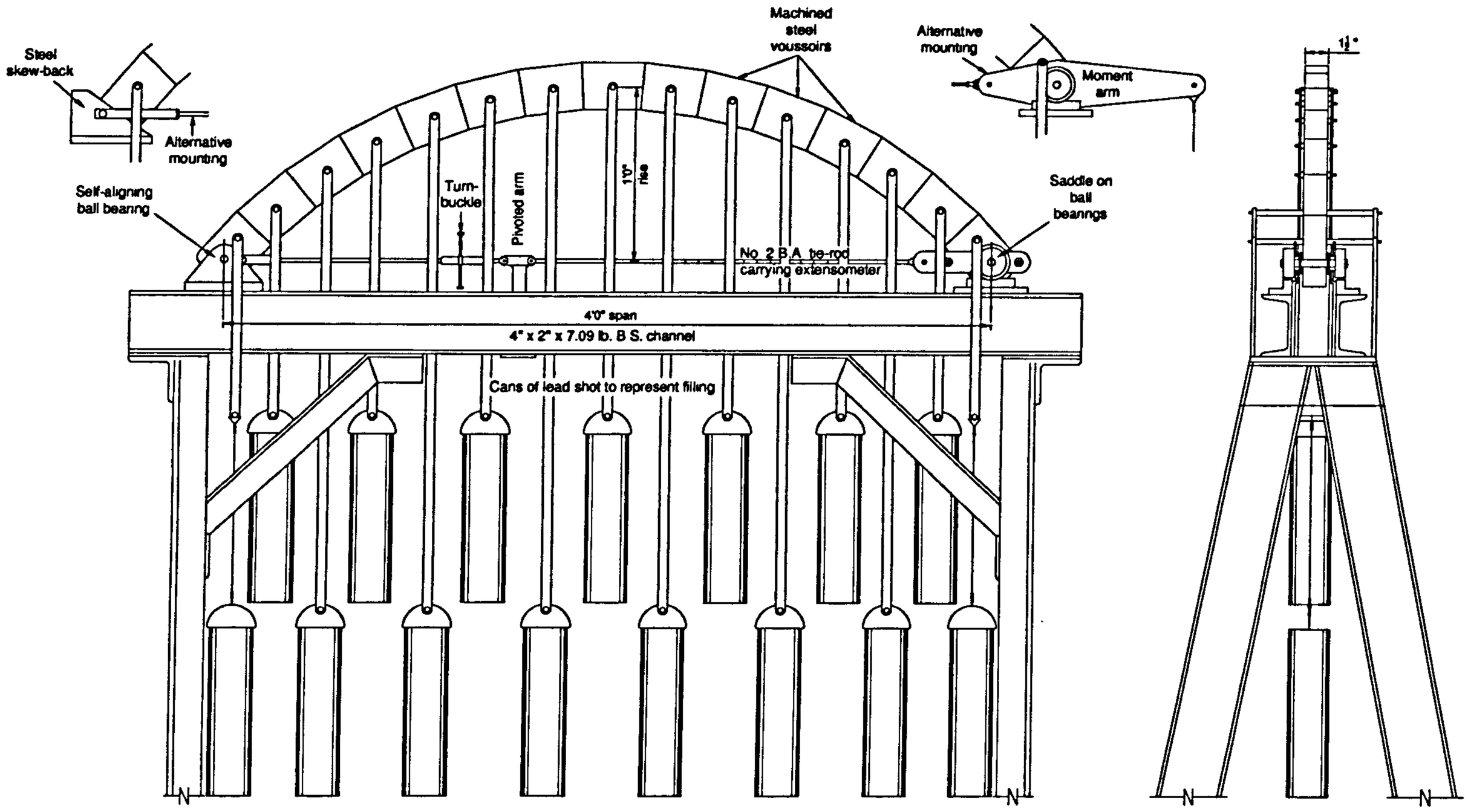

Figure 2-16 Pippard's apparatus

Another piece of corroborating evidence for the beneficial effects of the backfill comes from the conclusions reached by Royles & Hendry (1991) when they tested twenty four model arches of three different spans and two different span:rise ratios. They mention that the fill contributes to the strength and stiffness of the arch and that a small horizontal restraining force was also likely due to the restraining effect of masonry components such as the spandrels.

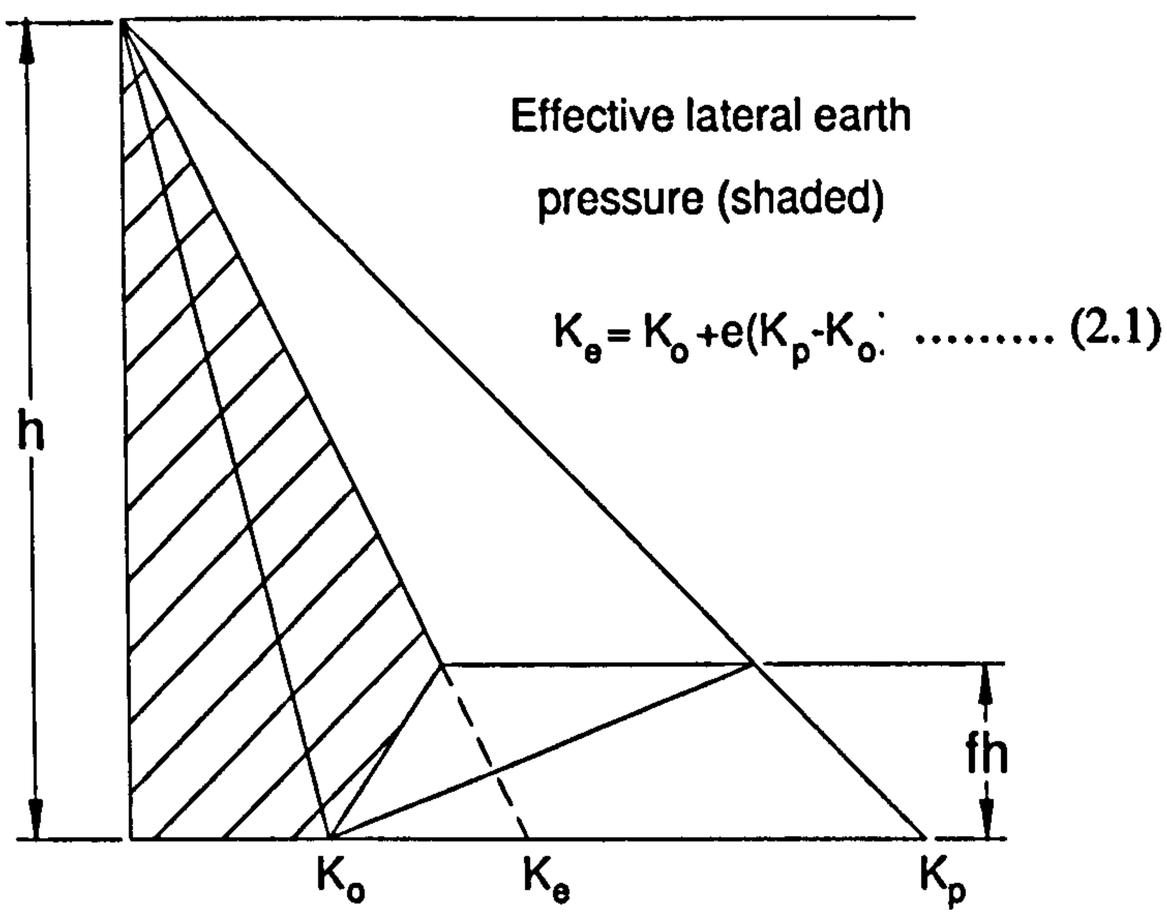

Figure 2-17 Burroughs' modified Rankine model

Burroughs *et al.* (2000) used a 1/12th scale arch backfilled with sand in centrifuge whilst studying the effects of an applied dynamic load. In 2002, Burroughs *et al.* studied the lateral pressures generated at the point of failure in masonry arch bridges using the same model. It was concluded that full passive pressures were never reached and that what did develop was approximately one third of the full passive pressure. A modified classic Rankine soil model was postulated as shown in Figure 2-17, refer to the reference Burroughs *et al.* (2002) for more details of this bilinear model.

Some of the work contained within this PhD runs in tandem with work carried out and published by Hulet *et al.* (2005). The effect of flooding was examined in a small scale test rig on an acrylic segmental arch with sand backfill. Although not dealing with dynamic effects of water inundation, the paper gives useful insight into the effect of flooding on masonry arch bridges and the likely reduction in live load carrying capacity. These small scale experiments were successfully computationally modelled using the arch bridge analysis software RING 1.5.

2.3.4 The Benefits of Backfill

It is generally agreed that buried structures usually cannot resist concentrated loads without utilising the strength of the surrounding soil in a complex interaction. Soil structure interaction is affected by material, size, stiffness, construction method, type and placement of backfill and external loading. The same can be said for arch bridges. Two other points of interest relating to the backfill are the effects of consolidation and compaction. Compaction is used to reduce air voids in the backfill (at constant moisture content) which is important in maintaining a stiff media on which to allow the passage of loads. Consolidation is a reduction in the pore water pressure over time due to the loading placed upon it. Compaction is normally an issue when voids are detected in the backfill possibly as a result of rain and drainage problems resulting in the washing out of the finer soil particles. One solution is to go back and re-compact the fill. Consolidation is an issue for cohesive fills or even fills with poor drainage as water logged fills utilise a buoyant component which has an effect on the stability of an arch. A coincidental issue relating to this can be seen on many railway arch bridges spanning

over water; two lines, yellow and red, telling trains when to slow down or even to stop due to the level of the water flowing underneath. Often these scour guidelines are at a sufficient level to have the side effect of preventing trains 'pumping' the fines out of the backfill, and make sure that the backfill is not so buoyant as to affect structural carrying capacity. One often overlooked result of pore water is the effect it has on pushing out spandrel walls when in liquid or frozen form.

In an overview of current UK research Melbourne (2001), states that a large number of model tests of varying spans have been undertaken in recent times, and also that many parameters have been studied using two dimensional 2D models, most not including the spandrel walls and modelling the backfill as dead weight alone. He also comments that centrifuge models help alleviate some of the problems associated with using small-scale models.

Discussion of a paper by Ponniah & Prentice (1998) by Hughes (2002) makes for interesting reading. It states that the depth of fill over multi-span arch bridges is generally less than that of a single span. Also the fill tends to be less varied than that in a single span. It goes on to say that single span arches are generally founded at ground level and then use an appropriate rise:span to allow the passage of traffic beneath whereas in the case of a multi-span arch it was more common to raise the tops of the piers and keep the arch geometry intact in order to reach the required road level.

2.3.5 New Instrumentation Techniques

The use of test models to help better understand the behaviour of masonry arch bridges has led in the course of this PhD to the consideration of techniques from other fields. One such technique is that of 'GeoPIV' which was developed by White *et al.* (2001). This method uses image processing techniques, which were developed for use with liquids, being adapted to work with soils. Using Particle Image Velocimetry (PIV) had several distinct advantages over the targeting techniques previously used to measure soil kinematics. Many of these standard techniques introduced foreign bodies into the observed fill and the use of real time low resolution video cameras. PIV allows for high resolution accuracy of soil movements, without the use of introducing contamination into the observed fill, that when used along side other information gathered can be used to quickly validate the working theories being tested.

One of the few actually published documents using GeoPIV on soils is by Gachet *et al.* (2003). They used the technique on an unsaturated soil in order to measure plane displacements with different boundary conditions (i.e. glass/acrylic side walls with sand fill). This piece of research highlighted the need for side wall transparency to enable good digital images.

Mallinson (1989), Fairfield (1994) and Fairfield & Ponniah (1994) used particle image analysis for kinematics of a loaded soil-arch system which was supplemented by work done by Hughes (1997). Tests conducted on a wooden voussoir arch with sand backfill are detailed together with comparisons of computational software available at the time,

ARCHIE, MAFEA, CTAP and a computerised version of MEXE. A point of interest is the effect of soil-arch action above the barrel affecting the soil-structure interaction. Rather than repeat the details here the reader is directed towards these aforementioned texts.

2.3.6 Summary

Backfill is reputed to fulfil four distinctive functions. The first and most obvious is that of maintaining the highway vertical alignment. The second is that of adding, through increased dead load, extra stability and thirdly it enables the live load to be distributed onto the main part of the structure. Finally it helps the arch to resist deformation by the mobilisation of passive and active soil pressures. Using previously under utilised techniques it is now possible to map how the backfill does this under laboratory conditions. The next section briefly reviews research which has been conducted to determine the mechanics of the arch itself.

2.4 Overview of Methods for the Assessment of Load Carrying Capacity

'The Riddle of the Arch, ut pendet continuum flexile, sic stabit grund rigidum" (Hopkins 1970). A rough translation of Robert Hooke could be, "As hangs a weighted chain, so an arch stands but inverted". The original quotation was in anagrammatical form to obscure its meaning and can be found in Hooke (1676).

At present there are several different approaches used by industry to assess the carrying capacity of masonry arch bridges. Most are automated for use with computers whilst the most frequently used method has been found to be inappropriate and often inaccurate. Over the years various research studies have been carried out into elastic and plastic methods varying from two dimensional mechanism and thrust line analyses to attempts to model arch bridges using finite elements. Some of these methods are considered here to facilitate comparison. Initially the focus was on the arch barrel but to a large extent the arch barrel has been exploited for strength as far as it can be by the various analytical techniques. Now focus is turning to the backfill material to find additional capacity as it is well known that the quality and type of fill above the arch barrel can contribute significantly to the overall stability and strength of the arch bridge. The majority of existing arch analyses packages model the backfill material as possessing dead weight and as being capable of dispersing the applied live load between the road surface to the arch barrel. In some cases basic horizontal soil pressures acting on the arch are also included; these tend to be assumed to increase

linearly with depth. One known exception is that Ng & Fairfield (2004) provided a method by which passive pressure varied with arch displacement using a bilinear backfill lateral pressure integrated with a mechanism method for the arch barrel.

2.4.1 Action of the Arch

Before reviewing the literature surrounding analysis of the arch several methods for consideration are briefly outlined as to how (according to the experiments conducted by Pippard) arches were assessed prior to the 1970s. This is used to illustrate what sort of design calculations might have been expected for arch construction in the latter period of the industrial revolution. Each method increases in complexity due to the number of hinges considered in a curved beam scenario.

It is well know that the critical reactive forces for the equilibrium of any system of loads acting upon a plane frame are provided if the structure is supported on a pin at one point and on a frictionless bearing at the other. Using static equilibrium the reactive forces can be calculated for the now determinate structure. Considering an arch as a curved beam (see Figure 2-18).

The resultant actions at a section of the beam normal to its centre line are as follows:

- A thrust equal to the algebraic sum of the forces to the right of X resolved in a direction normal to the section.
- A shearing force equal to the algebraic sum of the forces to the right of X resolved in a direction parallel to the section.
- A bending moment $M=Wc-V_BX$

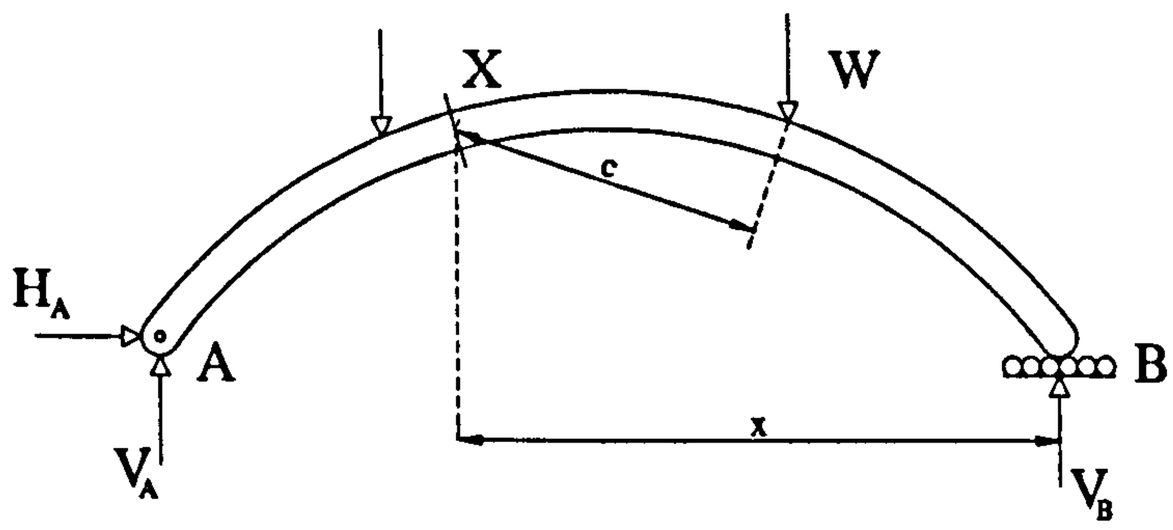

Figure 2-18 A statically determinate curved homogeneous beam

The first method to be looked at is known as Pippard's Elastic Method (Pippard *et al* 1936). This method assumes that a small induced spread of the abutments makes the arch barrel (which is pinned at the abutments) form three hinges between certain voussoirs transforming it into a statically determinate structure. However, the calculation assumes pins on the centre line of a parabolic arch with a concentrated load placed at the crown. Using virtual work it is possible to calculate expressions for the horizontal thrust at the abutments, the bending moment and the strain energy, which can be used to determine the maximum value of concentrated load required to produce failure. The limitation of this approach is that commonly accepted arch theory dictates

that an arch is weakest under the action of a point load at the quarter-span rather than at the crown.

It should be noted at this point that whilst it is generally accepted that for a 1:4 rise:span segmental arch the quarter point is the critical location, and for a semi-circular it is nearer the crown, Ng & Fairfield (2004) observed that due to the inclusion of backfill, the resulting soil stress distribution, caused the migration of the hinge to nearer the crown rather than at the centre of the loaded area above the quarter point.

Returning to a bare arch, an alternative and more generally applicable approach for a three pinned arch is given in Figure 2-19. (Note that this is based upon calculations common at the time, (see Morley 1950)

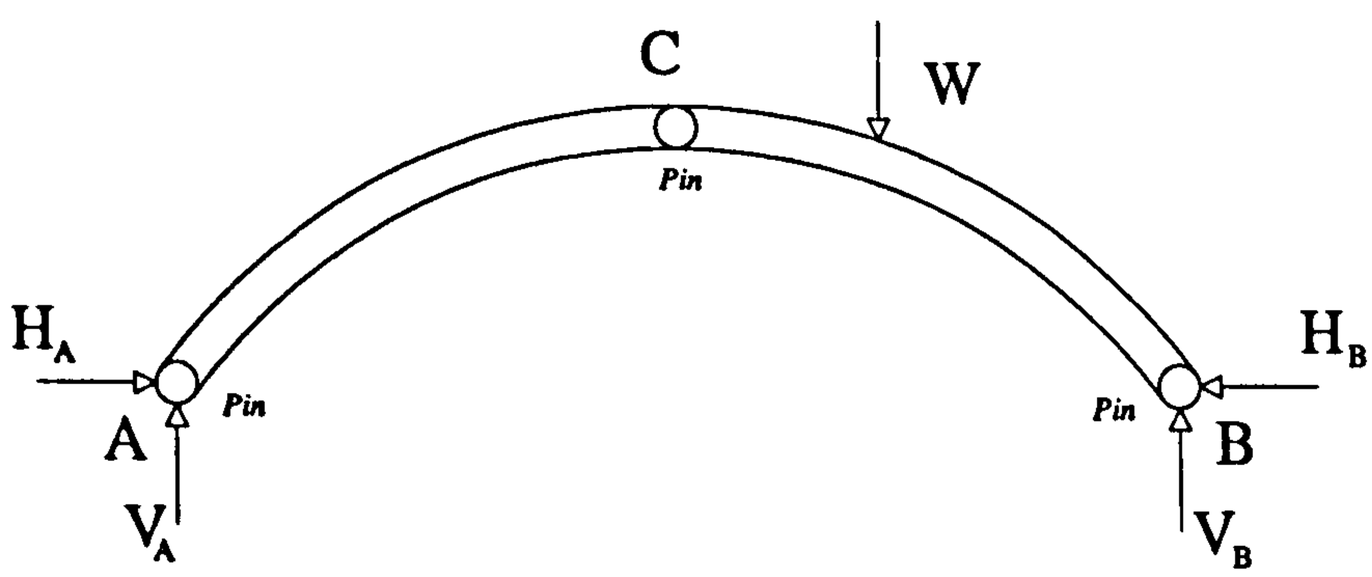

Figure 2-19 A segmental three-pinned arch

AB and BC are taken to be the same as two bars connecting point C to A and B. Assuming that the frame is of sufficient stiffness the arch becomes statically determinate and resolving horizontally and vertically gives the following equations:

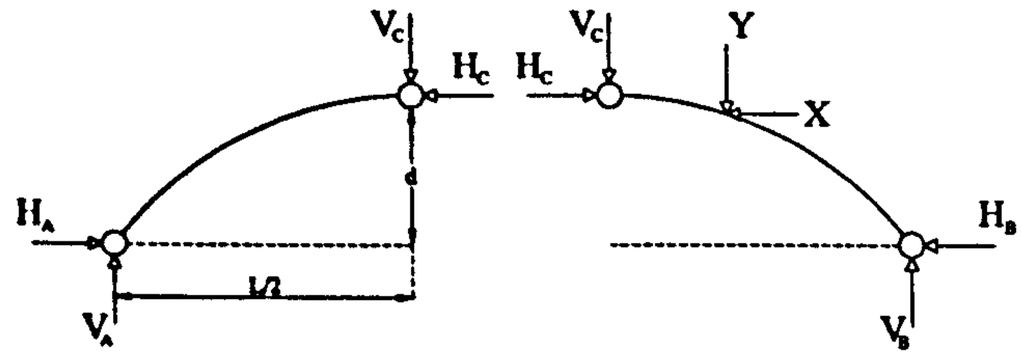

$$V_A + V_B - Y = 0 \qquad (2\text{-}2)$$

$$H_A - H_B - X = 0 \qquad (2\text{-}3)$$

$$Y(L/2 + x) - Xy - V_B L = 0 \qquad (2\text{-}4)$$

Figure 2-20 Half of a segmental three-pinned arch

Splitting the arch into two halves, (see Figure 2-20) separated by the pin at the crown and solving for equilibrium gives the following for the left hand side:

$$V_A - V_C = 0 \qquad \text{.....(2-5)}$$

$$H_A - H_C = 0 \qquad \text{.....(2-6)}$$

$$H_C d - V_C L/2 = 0 \qquad \text{.....(2-7)}$$

Equations (1) to (6) enable the values H_A, H_B, H_C, V_A, V_B, V_C to be found for any particular case, (see Figure 2-21).

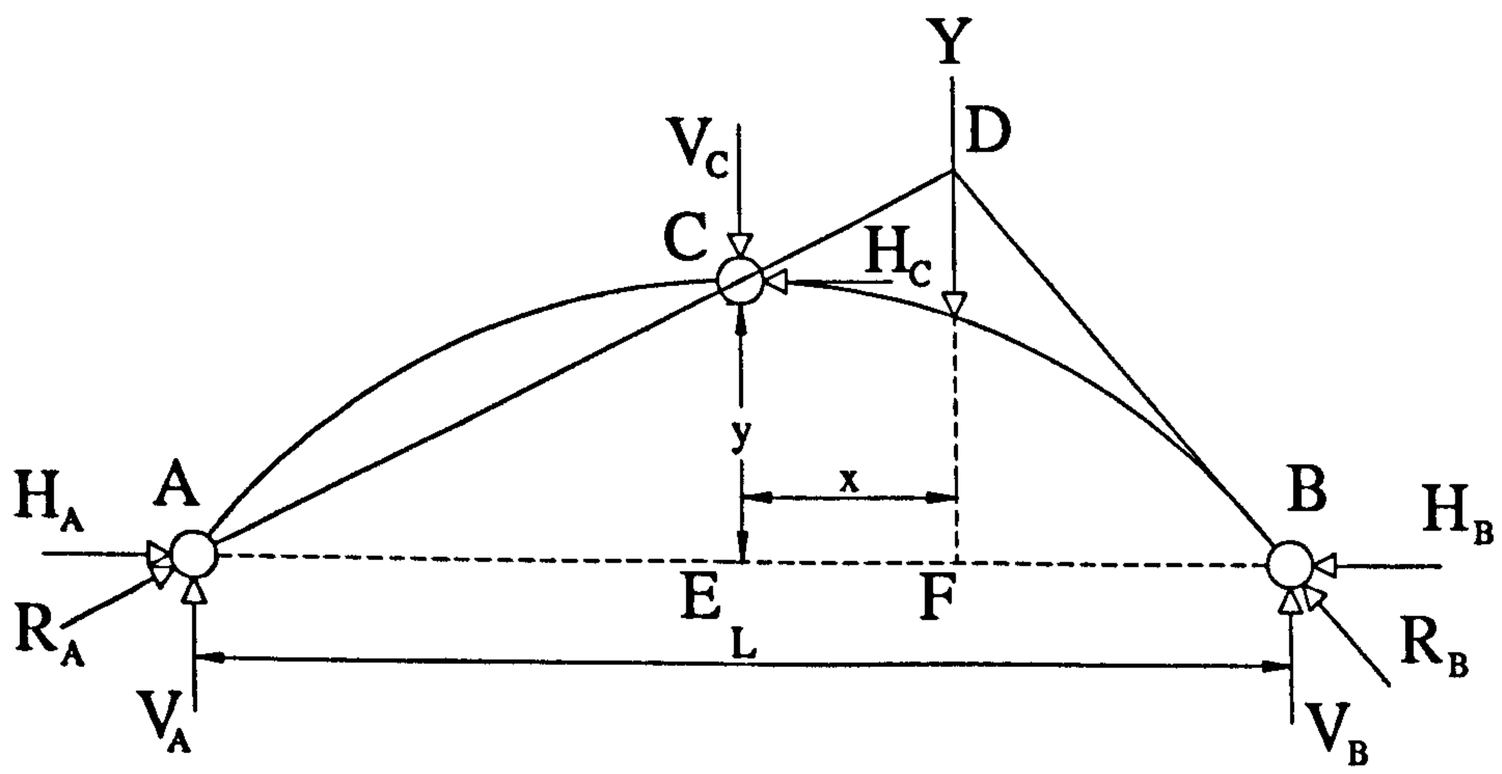

Figure 2-21 Three-pinned arch

In order to determine the bending moments in a three pinned arch it is necessary to calculate the thrust as shown in Figure 2-22.

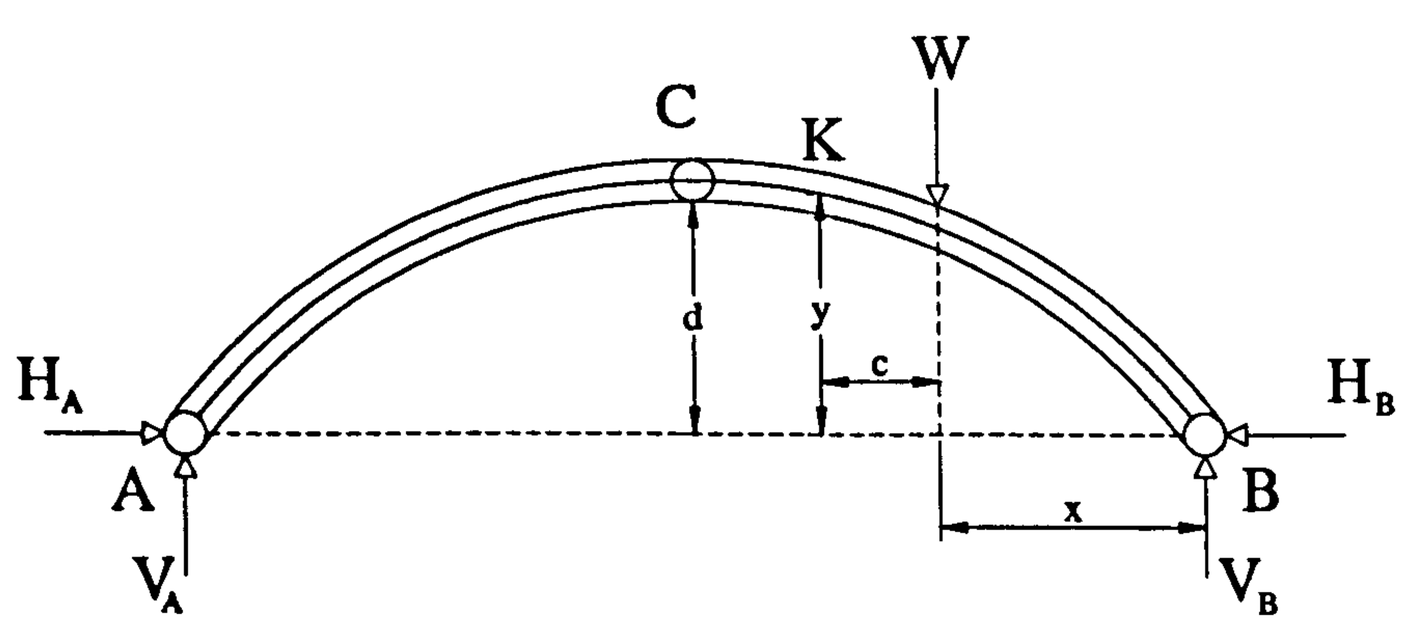

Figure 2-22 Three-pinned arch under load

Once the thrusts are found the moment at K is given by:

$$M_K = 3W_C - V_B x + H_B y \quad \text{.....(2-8)}$$

Where, W_C is a summation of the loads to the right of section. Figure 2-23 shows the bending moment diagram for the 3 pinned curved beam.

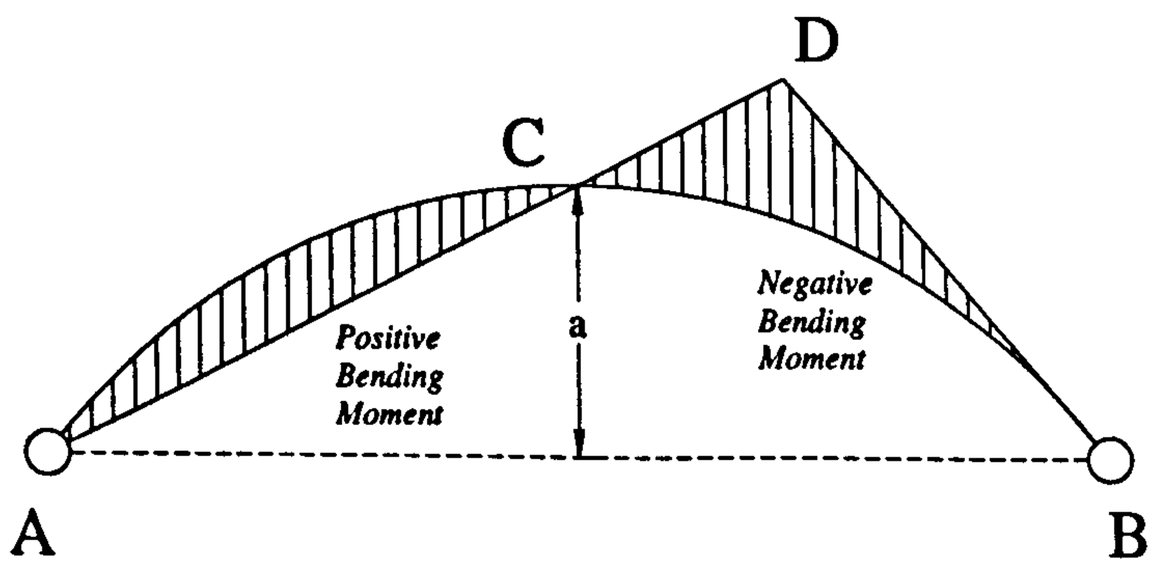

Figure 2-23 Bending moment diagram of the curved beam

Taking the beam analogy one step further, similar analyses for computing the strength of an arch can be found for two pinned and fixed ended conditions.

Two Pinned Arch

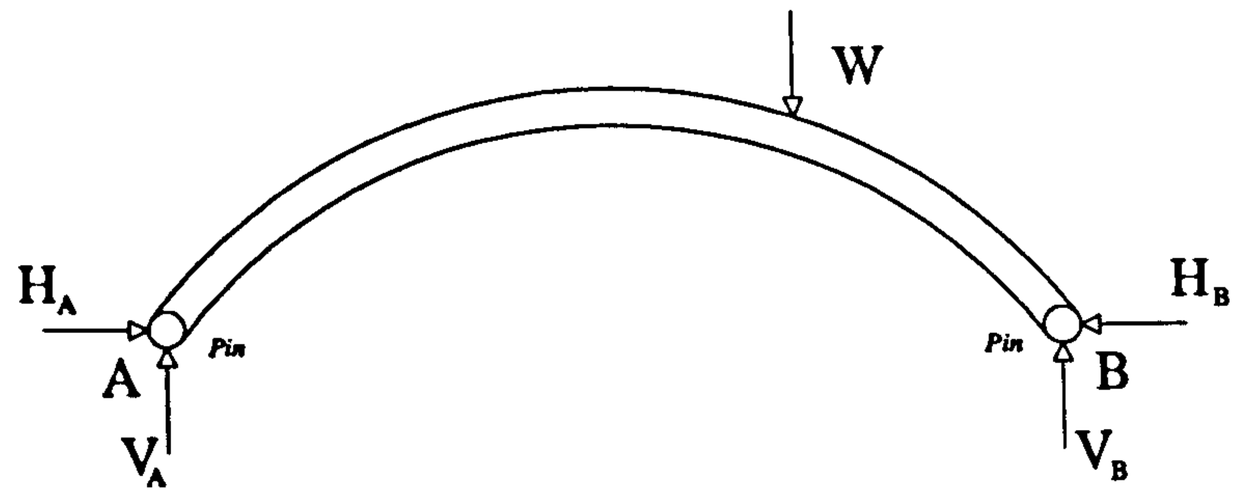

Figure 2-24 Two-pinned arch

Using a strain energy analysis the two pinned curved beam shown in Figure 2-24 can be considered as a segmental two pinned arch as shown by Figure 2-25.

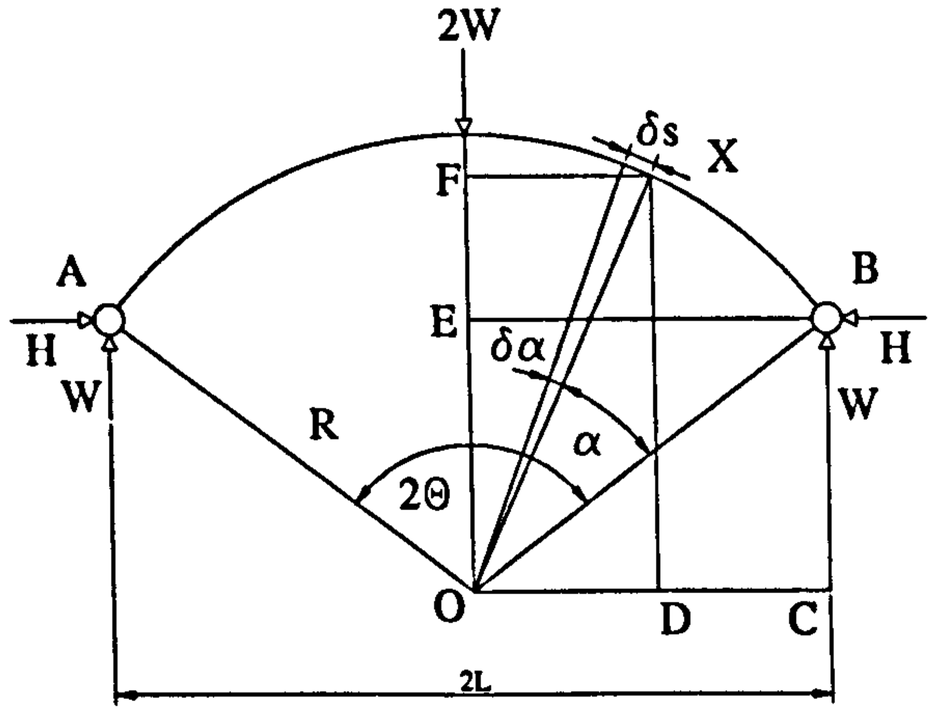

Figure 2-25 Two-pinned arch diagram

At any point X on the arch rib at an angular distance α from B the resultant actions are a thrust normal to the section, a shearing force tangential to the section and a bending moment. The effects of the first two are negligible when compared to the third. Taking U as the total strain energy due to bending in the arch rib then the value of H will be such as to make U a minimum.

i.e.

$$\frac{dU}{dH}=0 \qquad \text{or} \qquad \frac{2}{EI}\int_{\alpha=0}^{\alpha=\theta} M_x \frac{dM_x}{dH} ds = 0 \quad \text{.....(2-9)}$$

Since $ds = R d\alpha$

$$\Rightarrow \int_0^{\theta} M_x \frac{dM_x}{dH} d\alpha = 0 \quad \text{.....(2-10)}$$

Now,

$$M_x = -W.CD + H.EF = -W(OC- OD) + H\,(FO-EO) \quad \text{....(2-11)}$$

$$= -WR\{\sin\theta - \sin(\theta-\alpha)\} + HR\{\cos(\theta-\alpha) - \cos\theta\} \quad \text{.....(2-12)}$$

and,

$$\frac{dM_x}{dH} = R\{\cos(0-\alpha) - \cos 0 \quad \text{.....(2-13)}$$

$$\Rightarrow \int_0^{\theta} [H\{\cos(0-\alpha) - \cos 0\}^2 + W\{\sin 0 - \sin(0-\alpha)\}\{\cos 0 - \cos(0-\alpha)\}] d\alpha = 0$$

.....(2-14)

Upon integrating,

$$\Rightarrow H\left[\frac{\alpha}{2} - \frac{1}{4}\sin 2(0-\alpha) + 2\cos 0 \sin(0-\alpha) + \alpha\cos^2 0\right]_0^{\theta}$$

.....(2-15)

Which equates to:

$$H\,[2\theta - 3\sin 2\theta + 4\theta\cos^2\theta] = -W\,[2\theta\sin 2\theta + 3\cos 2\theta + 1 - 4\cos\theta]$$

.....(2-16)

So when Q=90°

$$H = \frac{2W}{P} \quad \text{.....(2-17)}$$

Having calculated the value of horizontal thrust the normal thrust, the bending moment and the transverse shearing force can be found for any point on the arch. Considering Figure 2-26 in which the bending moment at X is given by:

$$Mx = Hy - \{V_A x - W_1(x-a) - W_2(x-b)\} \quad \text{.....(2-18)}$$

Terms (x-a) and (x-b) are only included when x>a and x>b respectively.

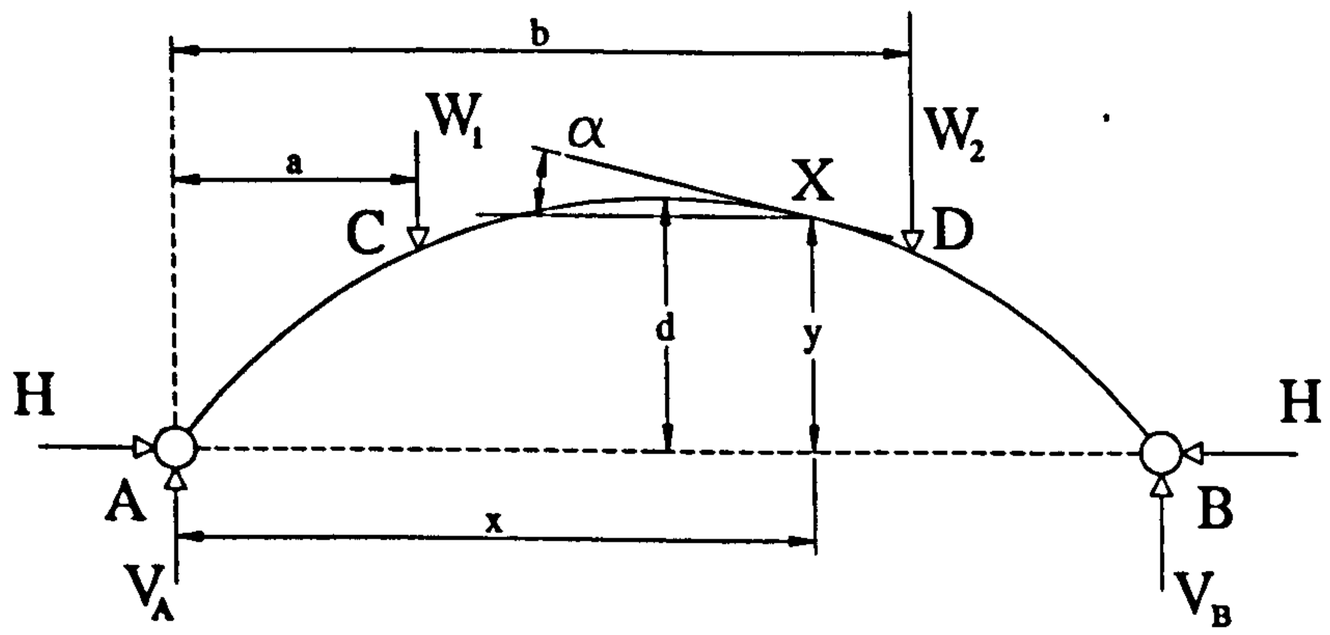

Figure 2-26 Two-pinned arch

Thus at x if the tangent makes an angle α to the horizontal the resultant forces at x are:

$$\text{Vertical Shearing Force} = V_B - W_2 \quad \text{.....(2-19)}$$

$$\text{Resultant Horizontal Force} = H \quad \text{.....(2-20)}$$

Resolving parallel and normal to the tangent yields:

$$\text{Normal Thrust at X} = (V_B - W_2)\sin\alpha + H\cos\alpha \quad \text{.....(2-21)}$$

$$\text{Transverse Shear Force} = (V_B - W_2)\cos\alpha - H\sin\alpha \quad \text{.....(2-22)}$$

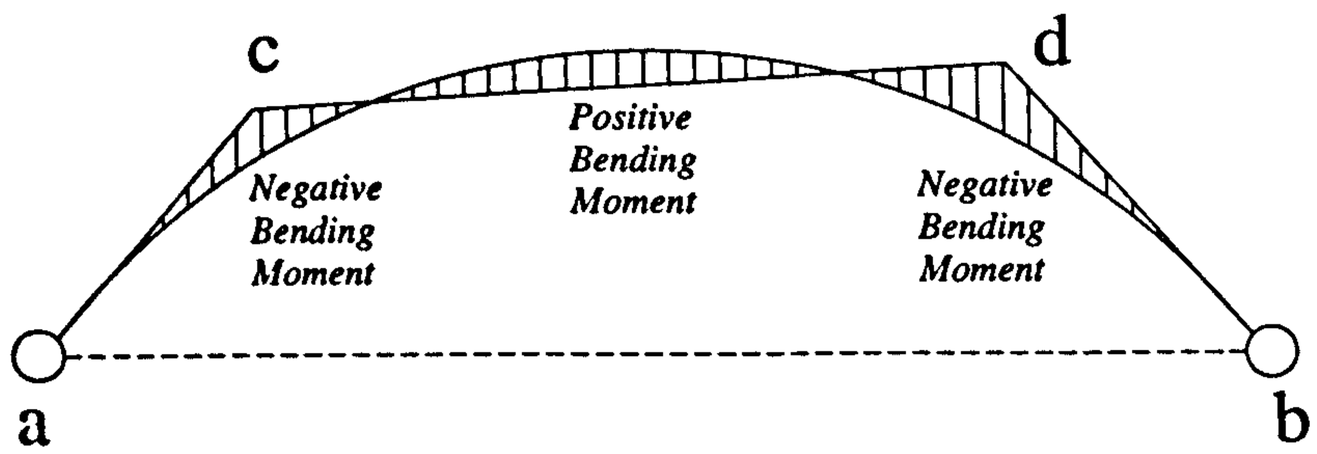

Figure 2-27 The linear arch

Figure 2-27 shows the linear bending moment diagram for a two pinned curved beam.

Fixed Ended Arch

The last beam analogy to be looked at here is the consideration of the arch as a fixed ended curved beam, see Figure 2-28.

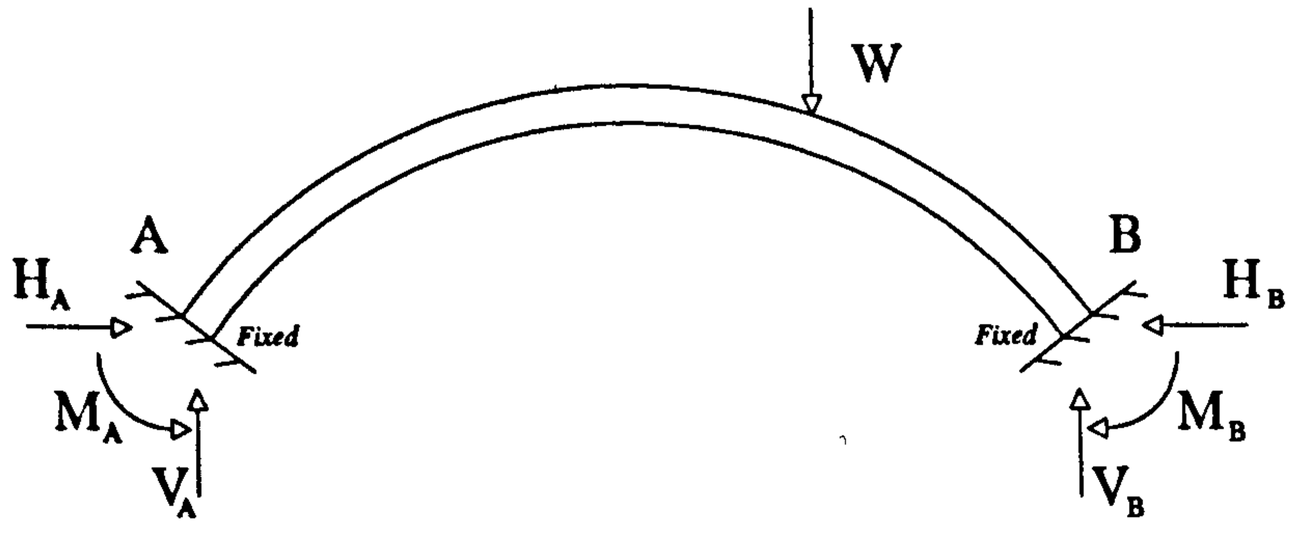

Figure 2-28 Fixed-ended arch

Considering an arch rib with both ends fixed and assuming it acts like that shown in Figure 2-29 and that the end actions at B are sufficient to keep B in a constant position which is in effect treating it as fixed.

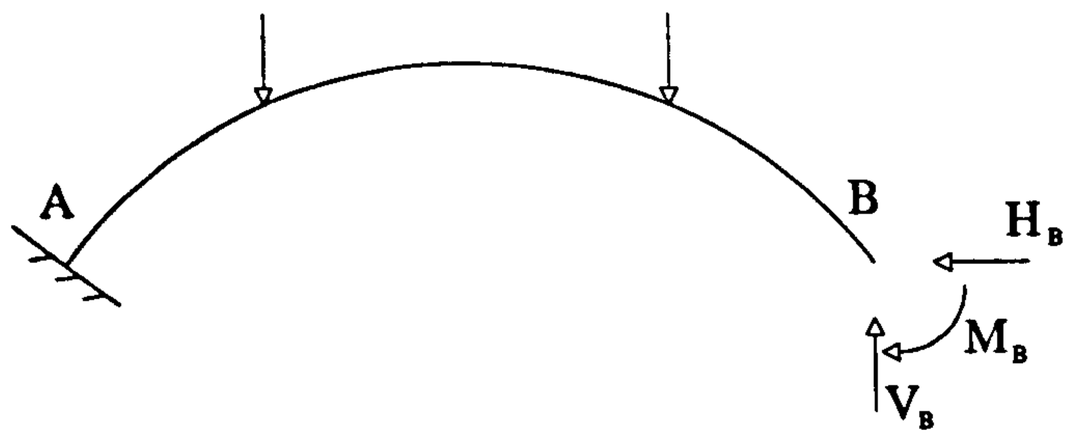

Figure 2-29 Fixed-ended arch

The bending moment at X on the arch shown in Figure 2-30 is as follows:

$$Mx = M_B + H_B y - V_B x + W_1(x-a) + W_2(x-b) + W_3(x-c) \text{ .....(2-23)}$$

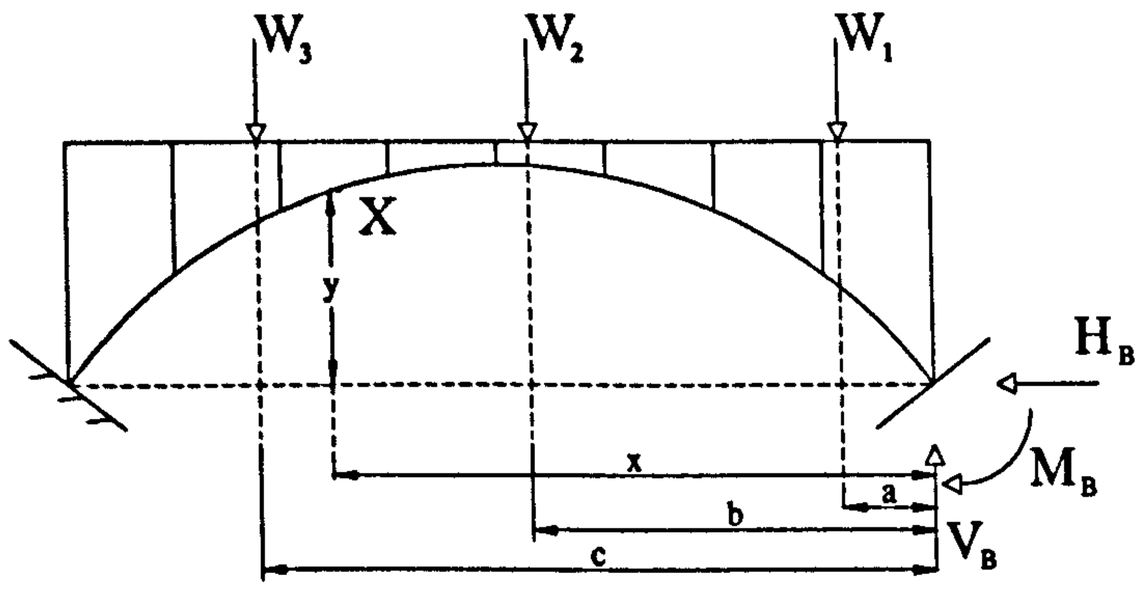

Figure 2-30 Fixed-ended arch

The unknown reactions may be found by the principle of minimum strain energy with the conditions that:

$$\frac{\partial U}{\partial H_B} = 0, \qquad \frac{\partial U}{\partial V_B} = 0, \qquad \frac{\partial U}{\partial M_B} = 0, \text{ .....(2-24)}$$

Again since the transverse shear force and normal thrust is negligible compared to the bending strain energy.

$$\int \frac{M_x}{I_x} y ds = 0, \qquad \int \frac{M_x}{I_x} x ds = 0, \qquad \int \frac{M_x}{I_x} ds = 0, \text{ .....(2-25)}$$

Once again the equations can be solved by integration.

This section has briefly looked at the way the arch barrel was considered by engineers as behaving like a curved beam and whilst not based upon catenary profiling as published previously (Alexander & Thomson 1927) it shows that understanding of the arch barrel at that time was largely based upon beam theory rather than being treated as an element in its own right.

2.4.2 Empirical Based Methods

In 1927, Alexander and Thomson produced mathematical design guidance based upon their experiences of masonry arch bridges. This was one of the first post-industrial revolution text books on how to choose the profile of an arch based upon equilibrium and stress calculations together with material quality. It should be noted that this guide includes the examination of backfill stresses, which it treats as an additional load to which the arch rib is subjected. Additionally, allowances are made for the stresses of the road surface bedding into the backfill, and the book also covers the use of compacted granular media around the arch barrel itself. (Current modern theory indicates that the backfill also has a strengthening effect on the arch barrel.)

During the early 1950s a military load classification was introduced by the Military Engineering Experimental Establishment (MEXE). As a result of empirical experiments and elastic theory devised by Pippard, a nomograph relating bridge dimensions to permissible loads was produced. Factors based on geometry, materials and bridge condition can then be used to modify this permissible load to establish likely load carrying capacity. Over the years this method has been widely used but it is

becoming accepted by both academics and industry that it is just a very crude tool, over predicting strength in some cases and under predicting in others. The method is not outlined here but BA16/97 (2001) provides details of a modified MEXE method.

2.4.3 Mechanism Methods

Mechanism methods analyse the structure at the point of collapse. Three methods are covered here though more can be found in the references by Harvey (1991), Bridle & Hughes (1990) and Orduna & Lourenco (2001).

Perhaps one of the first applications of a modern approach to arch assessment can be found in Heyman's classical plastic analysis. This upper bound method uses the theory of plasticity to consider the modes of arch barrel deformation which can lead to collapse. In other words enough hinges must form within the barrel to turn the structure into a mechanism. Hinges pose no danger until there are sufficient releases to transform the structure into a mechanism, (normally four hinges must form but in a theoretically perfect model loaded directly at the crown a five hinge formation is possible). Heyman's original model works only if the masonry is assumed to have negligible tensile strength, no crushing of the materials and provided no sliding occurs. Heyman observes in his remarks about Clare College Bridge (Heyman & Padfield 1972) that the upper bound theorem of plasticity considers the mode of deformation leading to collapse whilst the lower bound theory deals with a thrust line analysis. His plastic method was developed specifically for relatively narrow small span mediaeval bridges and utilises a geometric factor of safety.

The lower bound theorem indicates that an arch is stable if a line of thrust can be found which is in equilibrium with the given dead and live loading and it lies entirely within the masonry. It should be noted that the thrust line being considered need not be the actual thrust line, but can be any line that satisfies equilibrium. The basic method can be modified so that a zone of thrust based on the strength of the materials is considered instead of a thrust line. Also the soil between the back of the arch and the road surface provides horizontal restraint as well as dead weight and acting as a means of distributing live loads.

For example, Crisfield & Packham (1987) put forward a modified mechanism method which took into account an allowance for material damage based upon the compressive strength of the materials. An accurate profile survey of the arch was also used which could include the effect of minor distortions to the barrel and together with a visual output showing the hinge locations at the collapse load obtained by iteration, allowed this powerful analytical tool to output a predicted minimum load that would cause the bridge to collapse.

Based upon a combination of Heyman's and Crisfield's work, Gilbert & Melbourne (1994) put forward an upper bound, plasticity, limit analysis package allowed crushing and sliding failures to be modelled. The current version of what became RING was used during this PhD and relies upon a joint equilibrium formulation similar to that proposed by Livesley (1978), and a very basic outline of the method is given here.

Consider the arch bridge given in Figure 2-31.

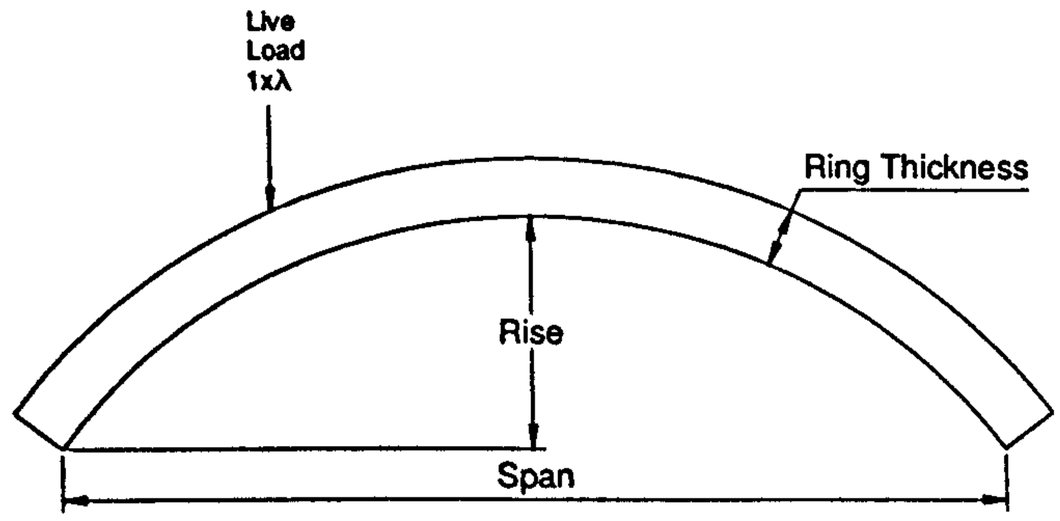

Figure 2-31 An arch under loading

Considering the forces acting on a given block (in Figure 2-32):

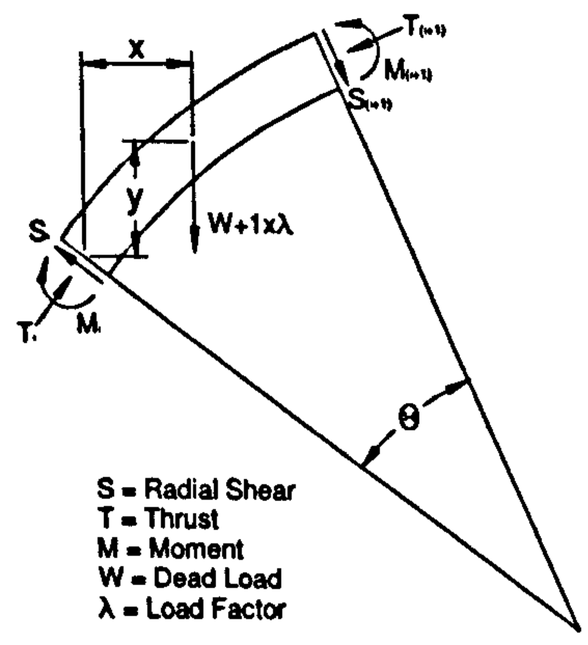

Figure 2-32 A system of forces

The first step is to establish equilibrium constraints by resolving the forces horizontally, vertically and rotationally:

Resolving parallel to the line of action of S_i: $S_{(i+1)} \sin\Theta = T_{(i+1)} \cos\Theta + S_i$

.....(2-26)

Resolving parallel to the line of action of T_i: $T_i = S_{(i+1)} \cos\Theta + T_{(i+1)} \sin\Theta + \lambda + W$

.....(2-27)

Taking moments about the centroid: $yS_i + xT_i + M_i + yS_{(i+1)} = xT_{(i+1)} + M_{(i+1)}$

.....(2-28)

After establishing equilibrium constraints for each block, in order to work out the maximum load carrying capacity it is necessary to maximise λ subject to yield constraints which enforce no tension, and sliding conditions. By using a linear programming solver a solution to the posed problem can be obtained. In addition, RING also includes an option to model the finite strength of masonry. It should be noted that two important assumptions are made, the first being that any elastic strains are negligible and that the masonry blocks initially fit together perfectly.

2.4.4 Finite Element Methods

Finite Element (FE) is a powerful numerical analysis tool that has many potential applications. Many attempts have been made to predict the failure load of masonry arch bridges and it is not the intention of the author to cover them all here. Interested readers are referred to papers by Brencich *et al.* (2001), Mann & Gunn (1995), and Sicilia *et al.* (2001).

The first FE technique to be looked at was developed by Choo *et al.* (1990). The arch was discretised using elastic tapered beams, which were assumed to have no tensile strength. It was assumed that any cracking of the arch due to an applied load resulted in zones of negligible structural stiffness. In addition, where compressive stresses within the arch exceeded the crushing strength of the material, regions of no structural stiffness were formed, which were still considered to contribute to the overall strength of the arch. Also un-cracked and un-crushed portions of the arch at adjacent blocks may be different from each other. This means that the resulting profile resembled that of a tapered beam. And using an iterative solution process for each applied load, a convergent solution can be found that satisfied equilibrium.

The mixed finite-discrete element program ELFEN has been applied by Cintec/Giffords to masonry arch bridges (Mullet & Rance 2003). A feature of this technique is the ability to model each part of the bridge separately and the deformation and contact between these parts to be automatically calculated. This process is analogous to modelling each brick or stone unit, the mortar, the fill; backing, road surfacing and vehicle loading.

Cavicchi *et al.* (2004) have published work regarding FE limit analysis for masonry structures including arch fill interaction. Although using a limited no tensile resistant beam with just two nodes as the arch barrel, the fill is modelled using triangular constant strain rate elements. The authors themselves have discussed the limits on their

proposed models particularly regarding problems encountered modelling velocity discontinuities, but their endeavours are encouraging.

Another FE method to be looked at here is that developed by Fairfield (1994). This research used small scale and in-situ testing of field bridges to observe the interaction between the soil and the structure under loading. Tests to destruction on 0.75m and 2m span masonry arches were used as a base for development of a finite element analysis model. The conclusions of this research confirmed that the soil-structure interaction effects could contribute significantly to load capacity both from live load dispersal and lateral earth pressure distribution. Also of note is the fact that modelling of partial mobilisation of the passive pressure was theoretically difficult.

Issues that limit the effectiveness of carrying out elasto-plastic FE on masonry arch bridges include the fact that there are many input parameters, which include the initial stress state and often numerical parameters are included to adjust the results to force a fit a theory. Also, obtaining a solution can be problematic, such as premature failure of a single element, perhaps just because it was a strange aspect ratio, can trigger loss of convergence and hence implied failure of the bridge, which isn't necessarily realistic. Another issue is mesh sensitivity when modelling quasi-brittle failure especially when dealing with unit-mortar de-bonding.

Masonry bridges are complex and obtaining the many necessary parameters from site is both difficult and costly. Furthermore the constituent masonry and fill materials are inherently variable. Over-simplification or misrepresentation of parameters in FE models can lead to erroneous results, which in turn can lead to unlikely predicted arch behaviour. Many experts in the field of arch bridges suggest that not enough is known about the inner workings of an arch bridge to the extent that a comprehensive and accurate three dimensional model cannot be produced.

2.4.5 Conclusion

For the work described in this PhD, the two dimensional rigid block method used by the computer program RING was chosen (simple static methods were considered too crude and FEM were considered over-complicated). Advantages of RING over other methods included the fact that it could be used to relatively rapidly carry out parametric studies of chosen variables and also that backfill pressures could be manually modified providing great flexibility. Also since the original RING code was developed by Gilbert of the University of Sheffield a unique opportunity to work with RING was too good to be dismissed. A further and perhaps more unusual benefit is that as RING is now widely used in industry, the studies carried out would be understandable to a wider than usual audience.

2.5 Review of Current Practice for the Assessment of Load Carrying Capacity

2.5.1 Introduction

Hayes's (1938) paper on the Traffic Act gives a unique insight into various laws and politics up to and including the 1933 Act on bridge maintenance. Needless to say that due to the lessons learned from the First World War Britain was concerned by the state of its railway and canal infrastructure should war break out at some point in the future. A general document detailing how substandard masonry arches should be strengthened or replaced by arches as well as detailing remedial works for other bridge forms is given. This paper shows the transfer of responsibility for bridge assessment and maintenance from private bridge owners to the public, most likely as they were deemed to be of national importance.

Things seemed to have remained this way even during the reconstruction after the Second World War, until in the 1970s when Operation Bridgeguard (Harvey 1990) was instigated to assess the nation's old bridges to see if they complied with current legislation. Since that time vehicle weights have increased and the frequency of these heavier vehicles has also significantly increased. However, whereas concrete and steel bridges were assessed using modern methods, as pointed out by Chatterjee (1985), by their very nature masonry arch bridges were still to be assessed primarily on the basis of physical inspection and sound engineering judgement, with secondary numerical

calculations for added peace of mind. The following section reviews the design requirements of the current UK codes of practice.

2.5.2 UK Codes of Practice

Several assessment codes are examined here for the highways and for the railways.

RT/CE/C/025 (2001) is the code of practice for the structural assessment of underbridges used by Network Rail, (a typical rail bridge is shown on Figure 2-33). Section six deals specifically with the assessment of masonry arch bridges which includes three levels of assessment: Level One involves using conservative assumptions (MEXE), Level Two involves using a more refined analysis and better structural idealisation (2D analysis) and Level Three involves using test data from site and known traffic levels to produce the most comprehensive analysis of the three levels (3D Finite Element). The now widely mistrusted and potentially unsafe modified MEXE method is covered in great detail. Also given is some guidance on the use of alternative mechanism and elastic methods as well as plane strain two dimensional and three dimensional finite element approaches where the 'Professional Head of Structures Engineering' deems it appropriate. Multi-span bridges are covered briefly together with allowances for spandrel walls, foundations and haunching. In Appendix F, the code states that some of the railway assessment approach and assumptions for masonry arch bridges are based on the Highways code BD21/01 (2001).

Figure 2-33 Attercliffe Road, Sheffield

Given the overlap with the railway code, the Design Manual for Roads and Bridges BD21/01 will now be considered. Beginning at Section 6.15, MEXE is once again covered this time referring to the method given in BA16/97 (2001). The most relevant parts of the code to this research are Clause 6.22 which states:

"In the longitudinal direction, any applied wheel load shall be deemed to have a dispersal of 2 vertical to 1 horizontal through the fill material. Transversely, the effective width of the arch barrel carrying a wheel load applied at any position along the span can be derived...from the following formula:

$w=h+1.5$

Where h is the fill depth at the point under consideration and both w and h are in metres."

And Annex H2.2 which gives the background to the requirements for masonry arch bridges, which adds:

"The effective width for a wheel load has two components – the dispersal through the fill material and the transverse structural action of the barrel itself."

These are the two most important things gleaned from this code of practice dealing with the partial safety factor for live loads and the concept of the effective width based upon recommendations given by Chettoe & Henderson (1957). It is not apparently clear in the literature where this 2 in 1 spread came from though it is inferred from the surrounding text in the code that it is based upon the tests conducted by Chettoe & Henderson (1957). The earliest reference to 2 in 1 was found in BE3 (1978) where it was used for live load distribution through sand behind retaining walls and bridge abutments though even in this code no reference is given to its origin.

The final code of practice to be looked at for assessment purposes is BA16/97 which is specifically designed for the assessment of highway bridges (such as that shown in Figure 2-34) and is to be used in conjunction with BD21/01. Section 3 of this code gives a most comprehensive account of the modified MEXE method whilst Section 4 examines a comparison between MEXE, an alternative elastic method (CTAP), and a mechanism method (ARCHIE) with the TRRL full scale tests (detailed in this thesis in Section 2.3) which is detailed in more depth in Annex E.

Figure 2-34 Blonk Street Bridge, Sheffield

Unlike many other aspects of Civil Engineering the current assessment codes for arch bridges are not going to be upgraded with an equivalent Eurocode (in this case Eurocode 6: Masonry), although the author is aware that a new masonry arch bridge design code has been issued, BD91/04 (Highways Agency 2004).

BD91/04 was produced for three different reasons. The first being that masonry arch bridges require very little maintenance when compared to other types of bridges, second they are to be considered as viable options now that the selection process to determine new structures are to be based upon whole lifecycle costs, and thirdly there has never been a previous standard to guide designers in producing effective and robust arch bridges based upon ultimate limit state. This standard states that new bridges should be designed to last 125 years and utilise the 2 in 1 live load distribution factor as seen in BD21/01. One surprise is that they have to be designed for SV vehicles rather than the normal HA and HB type loading. It is clear that BD91/04 is a totally new code as it is quite short and very vague, this perhaps reflects the uncertainty of how these

structure actually work and leaves the design engineer almost a free rein to produce an appropriate solution.

2.5.3 Load Distribution Methods

This section looks at the current live loading dispersal methods. Displacements in soil occur from stresses applied by loading forces. These stresses can be obtained from displacements caused by the applied load on the supporting soil. The distribution of stress in soil depends on the contact pressure between the buried structure and the surrounding soil.

A uniformly loaded flexible foundation causes a uniform contact pressure whilst a uniformly loaded rigid foundation causes a highly non uniform contact pressure distribution. Contact pressures are limited to maximum pressure known as bearing capacity, and contact pressure distribution is affected by load magnitude depth of applied loads, size, shape, method of application of load (dynamic or static).

2 in 1

A 2:1 distribution assumes soil distributes applied load over an area the same shape as on the surface but increased by amount directly proportional to depth. A uniform load at surface is assumed to be distributed uniformly at depth, (Figure 2-35).

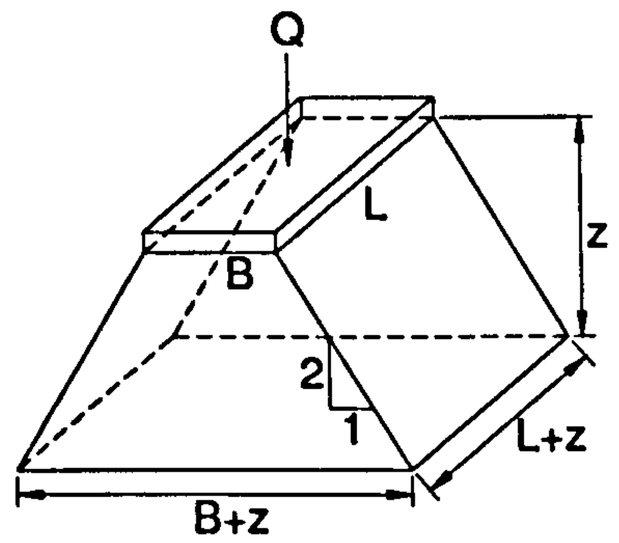

Figure 2-35 2 in 1 distribution

The increase in vertical stress with depth can be determined from the formula:

$$\Delta\sigma_z = \frac{Q}{(B+z).(L+z)} \quad \text{.....(2-29)}$$

Boussinesq

A Boussinesq (1883) solution assumes a weightless half space free of initial stress and deformation with a constant elastic modulus and valid principle of linear superposition within an isotropic soil, (Figures 2-36 & 2-37) for that of a 2D strip footing used in RING 1.5.

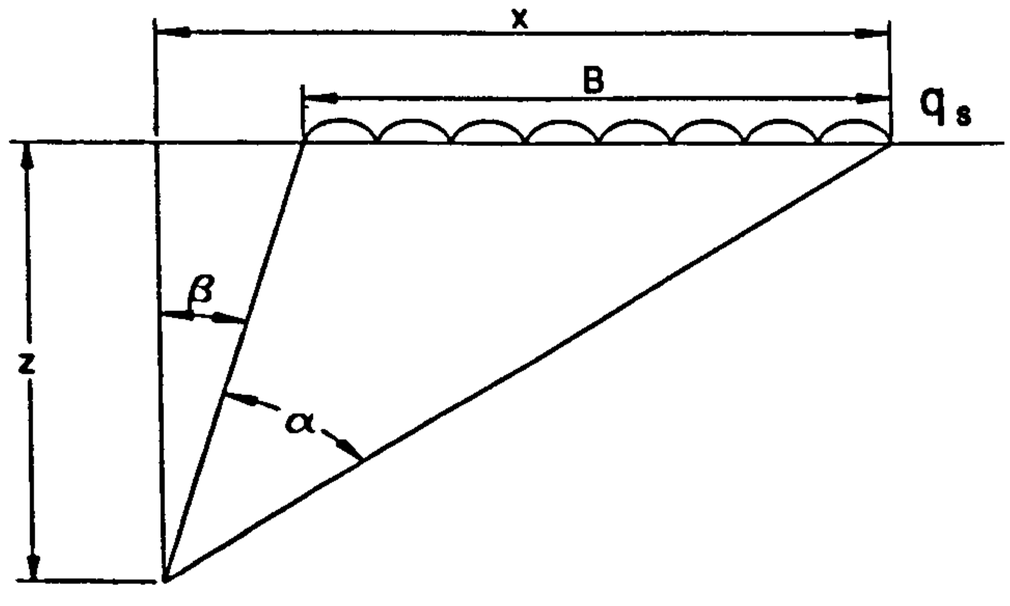

Figure 2-36 Boussinesq distribution for a strip footing

The equations for changes in stresses are as follows:

$$\Delta\sigma_z = \frac{q_s}{\pi}[\alpha + \sin\alpha.\cos(\alpha + 2\beta)] \quad \text{.....(2-30)}$$

$$\Delta\sigma_z = \frac{q_s}{\pi}[\alpha - \sin\alpha.\cos(\alpha + 2\beta)] \quad \text{.....(2-31)}$$

$$\Delta\tau_{zx} = \frac{q_s}{\pi}[\sin\alpha.\sin(\alpha + 2\beta)] \quad \text{.....(2-32)}$$

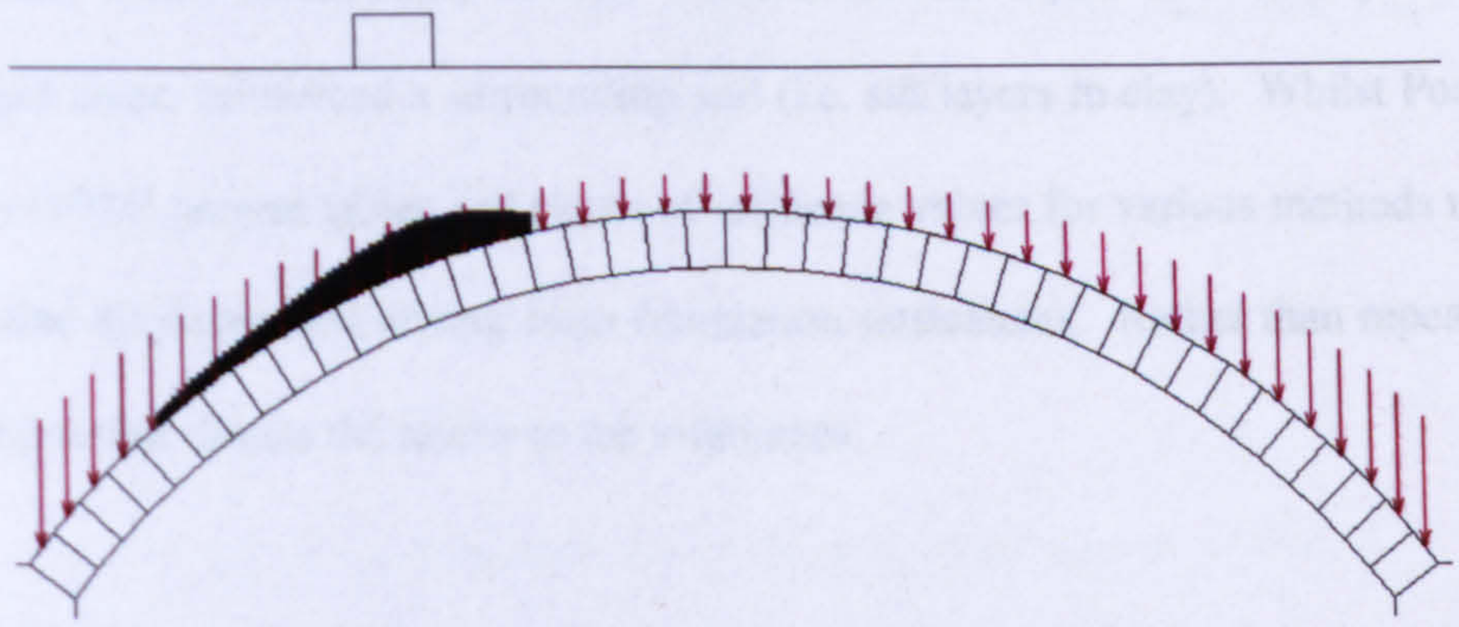

Figure 2-37 Arch with a truncated Boussinesq distribution

Limit of Theories

These two theoretical solutions have their limitations and these are noted as the following:

i. Boundary conditions may be far from idealised and therefore this invalidates the elastic theory.

ii. Boussinesq assumes no initial stress of a weightless material. This is unlikely as initial stress is always present in situ due to past activity. The effect of Poisson's ratio causes initial stresses significantly influence in situ stress and strain that occur through additionally applied loads.

iii. Errors in stress distribution – actual stresses beneath shallow footings can exceed Boussinesq values by 15-30% for clays and 20-30% for sand.

iv. Critical depth errors in settlement caused by non-linear heterogeneous soil beneath the depth where increase in stresses is significant are negligible.

Other Methods

Westergaard (1938) developed solutions for the stress distribution in soils with lateral constraint, which would apply in soils where horizontal layers of infinitely thin, stiff and rigid layers reinforced a surrounding soil (i.e. silt layers in clay). Whilst Poulos & Davies (1974) present tables and charts of influence values for various methods used to determine displacements arising from foundation settlements. Rather than repeat them here the author directs the reader to the references.

Comparison

It is useful to note that vertical stresses calculated using 2:1 distribution are close to those given by the Boussinesq method for depths between B and 4B below the loaded plate.

A comparison of the different distribution methods is shown in Figure 2-38. The Boussinesq equations apply for any value of Poisson's Ratio whereas the standard geotechnical practice for the Westergaard Method is to use a Poisson's Ratio equal to zero although the value of Possion's Ratio appears to have negligible effect.

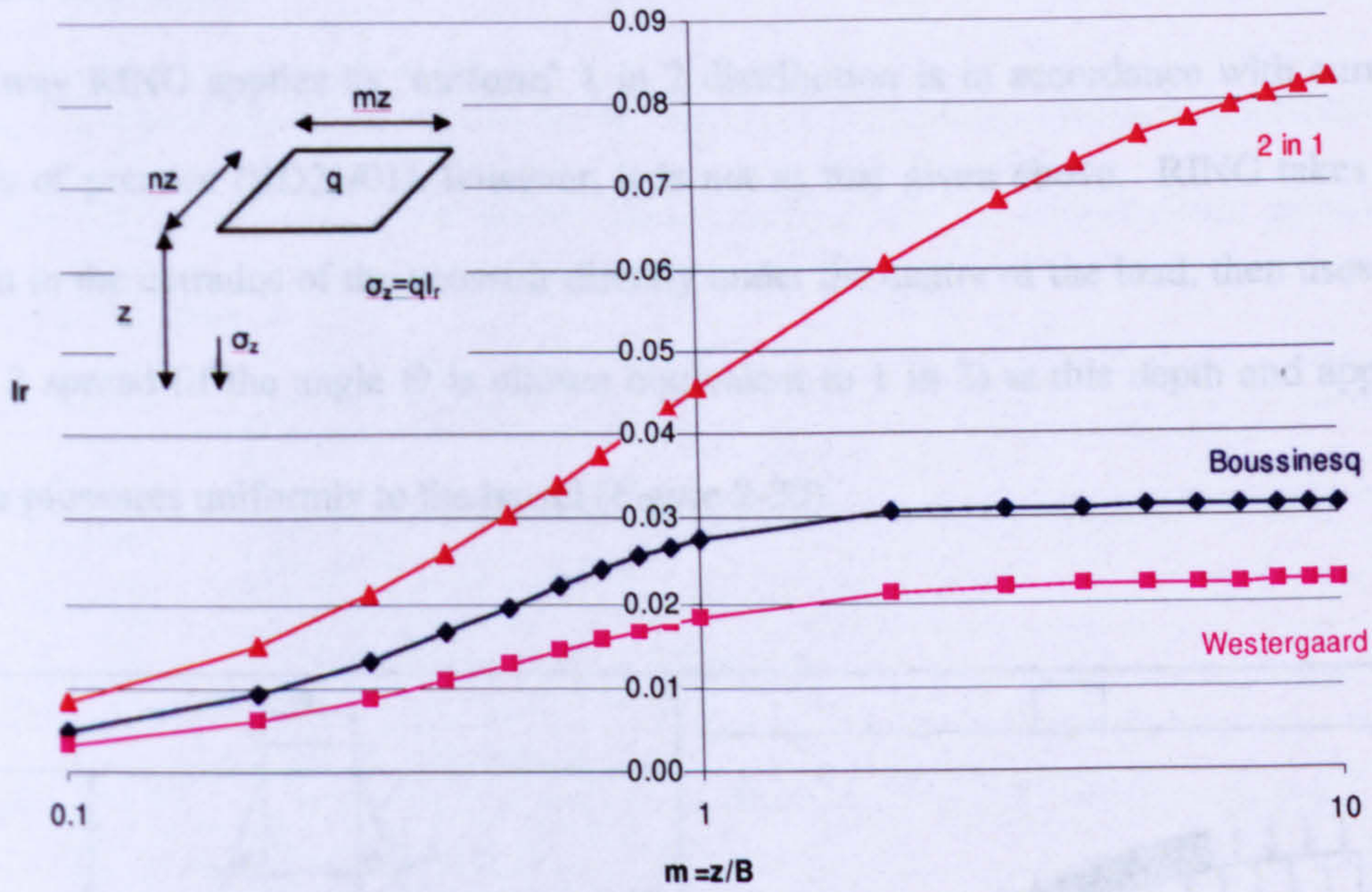

Figure 2-38 A comparison of the Boussinesq, Westergaard and 2 in 1

distribution methods for the influence value n = 0.1

The Boussinesq method provides results from a 2D stress field of which certain parts have no influence on the arch (only radial and shear stresses actually affect the arch). The current analysis methods then truncate and scale the vertical pressures and whilst this is effective, it is necessary to calculate the corresponding horizontal effects. Thus by using the full two dimensional values of horizontal and vertical stresses together with the shear stresses, the radial and tangential stresses along with the corresponding shear stresses can be calculated. It has been found that when the Boussinesq distribution is used in RING and ARCHIE-M analysis packages it produces a closer agreement to experimental results than the 2 in 1 distribution1[4].

[4] (Private communication between the author and Bill Harvey and Matthew Gilbert dated 01/08/07)

RING 2 in 1

The way RING applies its 'uniform' 1 in 2 distribution is in accordance with current codes of practice (BD21/01), however, it is not as that given above. RING takes the depth to the extrados of the voussoir directly under the centre of the load, then uses the 1 in 2 spread (if the angle Θ is chosen equivalent to 1 in 2) at this depth and applies these pressures uniformly to the barrel (Figure 2-39).

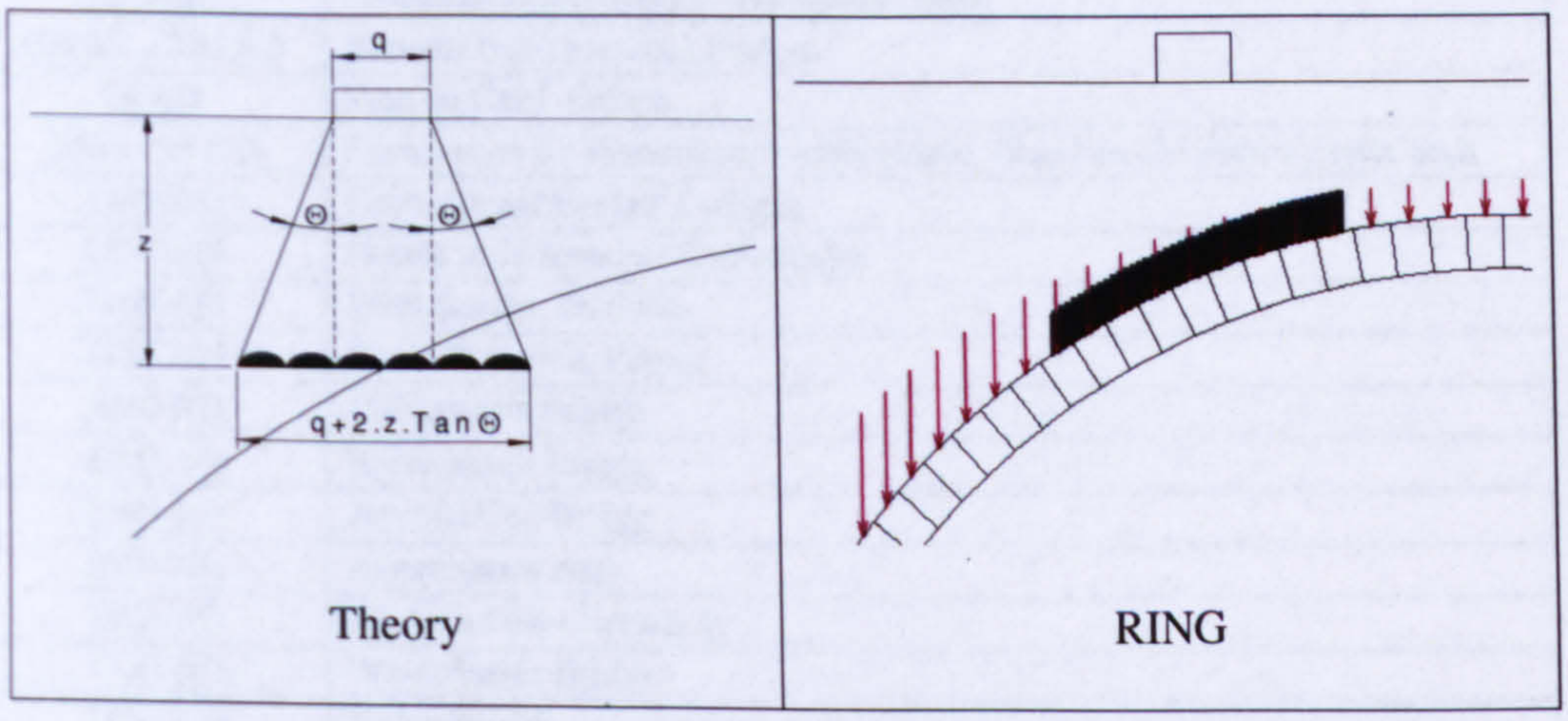

Figure 2-39 RING's 'uniform' distribution

2.5.4 Summary

Table 2-2 shows a brief history of the development of masonry arches in construction, analysis and assessment with approximate dates given for construction, published articles and events.

Year	Event
3000 BC	Arch construction techniques used in Mesopotamia, Egypt and elsewhere, but not in bridge-building
2000 BC	Chinese begin building masonry arch bridges
1325 BC	Corbelled arches used in Mycenean tombs
100 BC - 300 AD	Romans build masonry bridges
14 AD	Pont du Gard, France
900-1100 AD	Domination by Romanesque architecture, based on the semi-circular arch
1100 AD	Framwelgate Bridge, Durham
1150 AD	Gothic style replaces Romanesque
1160 AD	Elvet Bridge, Durham
1188 AD	Pont d'Avignon, France
1210 AD	Old London Bridge
1300 AD	Renaissance begins
1388 AD	Newton Cap Bridge
1650 AD	Rennaisance ends
1660 AD	Hooke's Law of elasticty
1750 AD	Westminster Bridge
1758 AD	Egton Bridge
1773 AD	Coulomb's 'some statical problems' is presented
1777 AD	Maindenhead Bridge
1780 AD	Industrial Revolution begins in the UK
1817 AD	Waterloo Bridge
1828 AD	New London Bridge
1820-50 AD	Masonry arch bridges begin to be built en masse by the newly formed railway companies
1840 AD	Stockport Viaduct
1846 AD	Pont y tu Prydd
1848 AD	Brighton Viaduct
	Newton Cap Viaduct
1850 AD	Second Industrial Revolution in the UK
1850-1930 AD	Majority of UK railway arches constructed
1850 AD	Royal Border Bridge
	Chapple Viaduct
1851 AD	Lockwood Viaduct
1862 AD	Hownes Gill Viaduct
1879 AD	Gaudard's paper on Perrodil, Williot and Dupuit calculation methods
1882 AD	St Pinnock's Viaduct
1904 AD	River Hoogly Bridge

	Jubilee Bridge
1920 AD	Stanwell Park Viaduct
1922 AD	First vehicle load train produced for assessment by Ministry of Transport (MOT)
1925 AD	British Standard 153
1927 AD	Publication by Alexander & Thompson
1928 AD	English Bridge
1933 AD	Traffic Act regarding maintanence of bridges
1936 AD	Pippard conducts tests which would lead to the MEXE method
1953 AD	Load tests by Davey for MOT
1957 AD	Load tests by Chettoe & Henderson (form basis of current assessment codes)
1970s AD	Operation Bridgeguard examines the condition of Britain's bridges.
1972 AD	Heyman puts forth a plastic mechanism method for assement purposes
1980-1989AD	TRL load tests
1987 AD	Crisfield et al. put forward a modified mechanism method
1990 AD	Maintenance of Masonry Structures by Sowden is published
	Choo et al. put forward an Finite Element analysis method
1990-1995 AD	Bolton Institute tests
1997 AD	Kimbolton Butts Bridge
2000 AD	Cardiff University centrifuge tests
2004 AD	BD91 is the first Standard to use Ultimate Limit State for the design of new masonry arch bridges
2006 AD	CIRIA c656 "Masonry arch bridges: condition appraisal and remedial treatment" is published

2.6 Discussion

In this chapter it has been shown that why research from a few arch bridges, normally 1:4 (rise:span) segmental, can be applied to a wider range of structures due to how and who they were built by. Assessment methods are a powerful tool to help determine mitigation and remedial works to extend the working life of a bridge given that it is increased frequency of the heaviest axle weights that has begun to adversely affect the condition of the UK bridge stock rather than the usually cited heavier axle weights. Whilst it is true that many arches were designed to 15 t axle loadings on the railways, they now carry 25.5 t axles, and as such have developed a reputation for having hidden strengths and requiring minimum maintenance. Unfortunately this lack of minimum

maintenance, usually on cost grounds, has not been carried out and this lack of care is beginning to show in increased rates of deterioration. A knee-jerk reaction culture (predominantly in the railways) has meant that where repairs are now necessary to keep the bridges open, these defects could have been prevented for minimum cost if treated sooner, and the now proposed significant repairs are often generic and change the way the arch works. Couple this together with the often sub-standard work practices used by contractors, again on a cost basis, this has often meant that rather than 'strengthening' they have often proved to be 'weakening' schemes. What is clear is that engineers experienced of how arches work are few and far between, and the judgement required by all arch assessment methods has not and is not being done due to a lack of skills. Figure 2-40 shows the legacy of a poor understanding of an arch; the structure is now due to be 'infilled' as the repairs have caused too much damage for the arch to be saved.

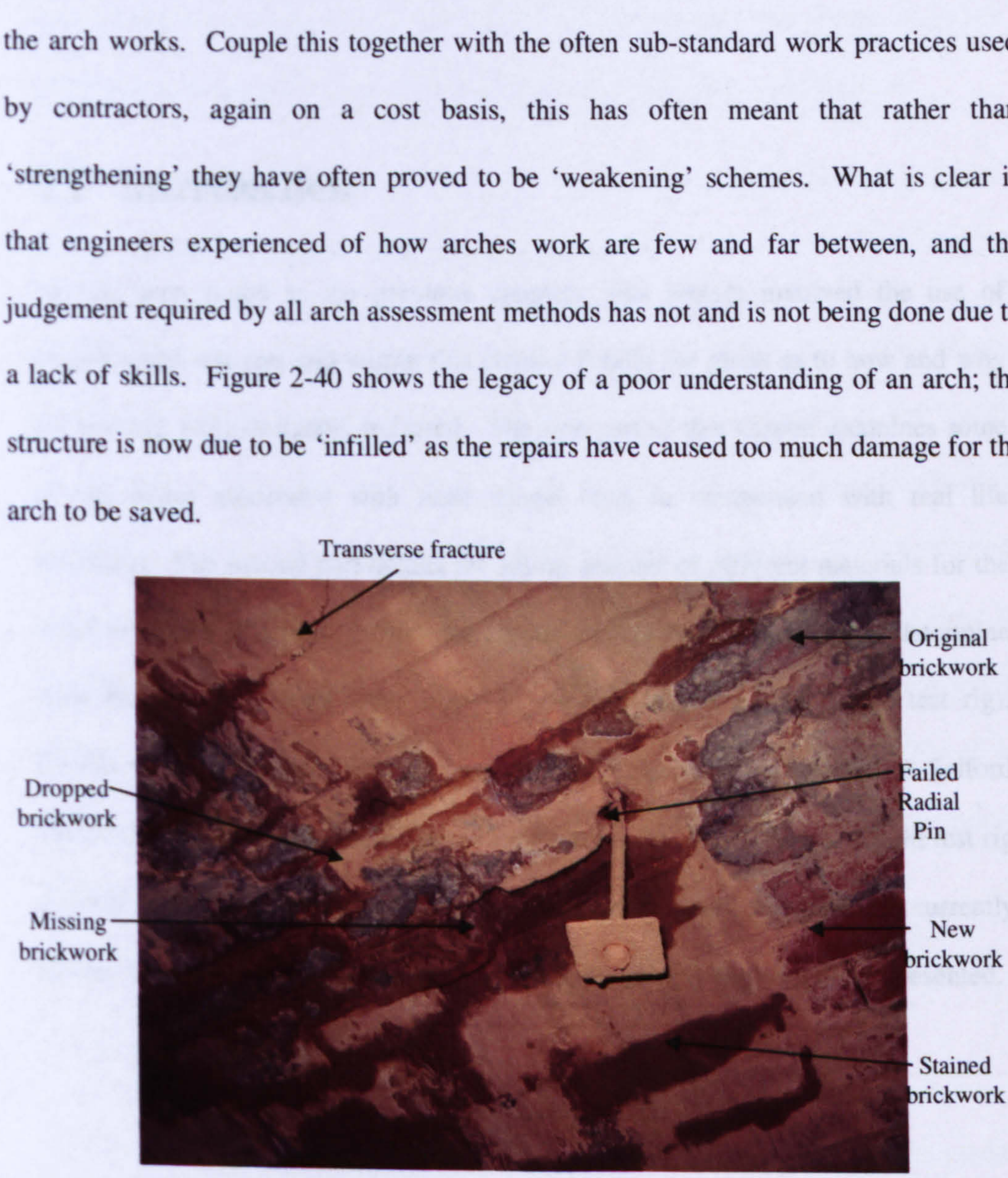

Figure 2-40 Inappropriate choice and poor installation of repairs on an arch bridge

Chapter 3

Test Rig Design

3.1 Introduction

As has been stated in the previous chapters, this project involved the use of experimental test rigs and within this chapter details are given as to how and why the test rigs were designed and used. The first part of this chapter examines some of the issues associated with scale model tests in comparison with real life structures. The second part details the set-up and use of different materials for the small test rig at Sheffield, (which the author used as part of this PhD to determine what behavioural effects were likely to be encountered on the larger test rig). Details of the large test rig, designed by the author and constructed at Salford University, are briefly included for completeness. Next the case for a third test rig is made in order to act as a stepping stone between the small and large rigs currently in use. Finally a comparison of the pros and cons of each test rig type is presented.

3.2 Scale Model Issues

Both the small-scale model and the full-scale model test setups were designed. It was important that during the design and experimental stages that experience of similar work carried out in the field be taken into account to ensure that a useful model capable of producing realistic results was developed. This section describes what texts were looked at and what measures were undertaken to this effect.

3.2.1 Model and Prototype Relationship

The use of small scale models related to prototypes is not new; however, caution must be taken so as to accurately replicate model phenomena in a test rig that would be observed at full scale. Ketcham & Black (1995) examine this use of physical modelling at small scale to test the response of a prototype. From this it is gathered that it is important to ensure that the scale model relationship to the prototype is both dimensionally similar and that any significant factor is also quantifiably similar so that kinematic and geometric similarity can be obtained. Also it is important to observe the fact that any scale factors are governed by both physical and modelling laws.

3.2.2 Scaling Issues

When it comes to understanding soil-structure interaction and the ability to predict behaviour using numerical methods, it depends almost solely upon test data and observations obtained from physical models to calibrate them. Generally the

important factors are the soil stress-strain response (usually non linear), pore water pressure generation and dissipation and the effects of creep. Another benefit of small scale models is that although full scale prototypes are useful to observe specific details, it is hard to get a general understanding of any phenomenon due to the natural variability of the fill and boundary conditions at this scale.

The appearance and magnitude of the response of a soil in an arch bridge is often largely dependent on effective stresses generated by live load and its relationship to the soil self weight. If the soil in the model and the soil in the prototype are the same then the modelling laws of soil mechanics and the requirements for geometric and kinematic similarity, must lead to the scale factors used for the model.

Many of the scale factors listed in Table 3-1 are basic structural modelling scale factors and have been derived from mechanical considerations. This table was derived by the author based upon that given for centrifuge models in Taylor (1995).

Quantity	Prototype	Model (N=Scale Factor)
Linear dimension and displacement	1	1/N
Area	1	$1/N^2$
Volume	1	$1/N^3$
Mass	1	$1/N^3$
Mass density	1	1
Force	1	$1/N^3$
Stress	1	1/N
Strain	1	1
Temperature	1	1

Table 3-1 Model – prototype scale factor relationships for 1g models

As can be seen in the table the relationship of stress to strain is 1:N rather than 1:1 which is potentially problematical in circumstances where soil stress-strain response is linear. This is the primary reason for utilising centrifuge models. However, this does not mean that 1g models are not useful as most soils are modelled analytically or numerically as having a linear response. Also these analytical models are normally calibrated with such interpreted data.

If as soil is described using parameters c and ϕ (apparent cohesion and internal soil friction angle), the soil response is implicitly assumed to follow a linear Mohr-Coulomb failure criterion.

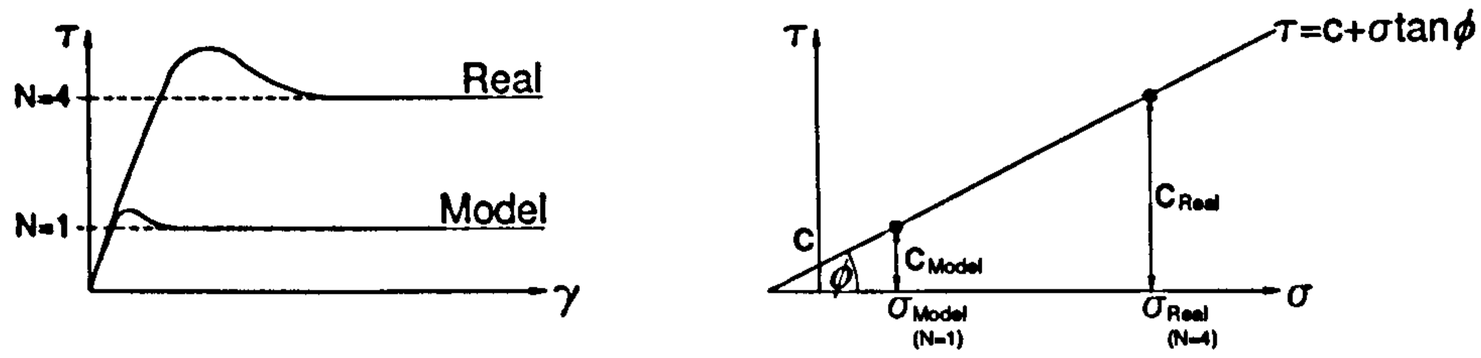

Figure 3-1 Stress/strain response of a linear soil

However, as can be seen in the Figure 3-1 at high stresses of real life situations, cohesion has much more of an influence than the low stresses where the 1g model operates. However, since the tests in this PhD are primarily using dry sand which is non-cohesive the effect of cohesion has been taken out of the area of consideration. For sands real cohesion is not expected.

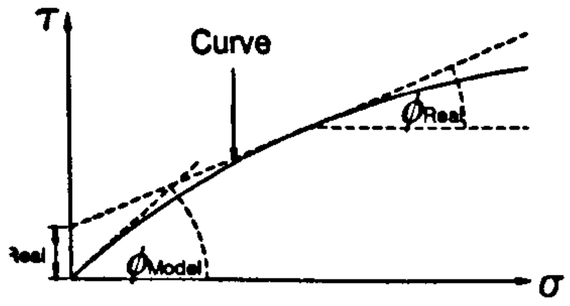

Figure 3-2 Stress/strain response of a sand

In reality the stress-strain response of soil is non-linear, for high stresses the true ϕ value differs from the low stress value since the line is generally curved (see Figure 3-2). However, considering the curve at a local level it can be taken as being linear and because of this assumption, locally the ϕ value can be taken as a constant. This means that the model results are representative for a soil with the local ϕ value and that as long as ϕ is measured in the stress range, the stress strain response of a 1g model can be used to calibrate simple analytical and numerical models based on the value of ϕ' and c'.

3.2.3 Contact Friction

Contact friction plays a big part in masonry arch bridges and replicating such frictional behaviour at small scales can be difficult. However, proof that masonry can exhibit a constant friction coefficient was illustrated by Bernardini *et al.* (1998) when experimental tests were performed on cracks in clay bricks. These tests showed that a brick on brick surface had an almost constant value for both static and dynamic friction. This is important when it comes to representing masonry behaviour both physically and analytically.

3.2.4 Soil – Structure Idealisation

Within the realm of soil structure interaction modelling it is necessary to make some idealisations about the soil and about the structure purely for analytical reasons. It is necessary to distinguish between two broad objectives in carrying out soil-structure interaction analyses. The first is the need to estimate the form and magnitudes of relative movement so that damage assessment can be made. The second and much more complex part is to quantify force distribution and internal stresses within the structure. Any physical model designed must take these into account since the whole point of scale model tests will be to provide a greater understanding of the behaviour of the backfill-arch interaction.

It is difficult to obtain real life data during a bridge inspection though on the basis of the limited data obtained, from desk study and site investigation, judgements and assumptions have to be made about the continuity of the backfill thickness, extent

and composition. Also, appropriate values for permeability, undrained stiffness, compressibility, and real behaviour such as local pressure distributions and relative displacements are dependent on local variation and the history of the soil.

The resultant loads acting on a static structure at any one time can be defined with some precision and the final geometry of a structure can usually be defined accurately. However, changes in the geometry can have a significant effect on the distribution of forces and the connections between various parts. This isn't helped by the fact that the structural loading cannot be accurately determined as each element withstands both the magnitude and distribution of the applied loads. Some comfort can be drawn from the fact that the materials comprising the structure are usually easier to model than the backfill. However, actual as-built properties tend to differ from those idealised for analyses.

Another problem with modelling the backfill is that the existence of varying stiffness has a very important influence on the form and extent of the soil behaviour around loaded areas. Underlying rigid strata concentrate surface loads and also stiffness increases with depth. Conversely overlying stiff upper strata disperse the loads further. The sensitivity of surface load dispersal and non-homogeneity together with lateral variations of compressibility are clearly significant, however, little work has been done on these areas and it was one of the aims of the current research investigation to examine this area in more detail.

Whilst soils are shown not to behave elastically, it is sometimes useful to use elastic theory with heterogeneous soils (Gibson 1967). Thus as the soil stiffness increases with depth, the effects on the settlements and stresses are calculated using elastic theory, which assumes that:

$$E_z = E_0 + Z\frac{\partial E}{\partial Z} \quad \text{.....(3-1)}$$

Where E_z = Young's modulus for the soil.

Whereas in a homogenous soil the stiffness does not increase with depth and the settlements can extend well beyond the loaded area, in heterogeneous soils as the heterogeneity increases the extent of this settlement zone is reduced. Gibson shows that for an incompressible soil, when Poisson's ratio, $\nu = 0.5$, surface settlement is infinite when E_0=0, and that for any given uniformly loaded shape the settlement, ρ is calculated by the expression:

$$\rho = \frac{3q}{2\lambda} \quad \text{.....(3-2)}$$

Where q is the applied surface load.

3.3 Small-Scale Test Rig

Since full-scale tests are comparatively time-consuming and expensive to set up, simple small-scale tests were undertaken as part of this study. A small scale test rig allowed tests to be performed relatively rapidly, enabling parametric studies to be

performed which would be used to guide the full-scale test programme. Additionally, investigations into the influence of test variables which can be difficult to investigate at full-scale can be undertaken. (This small-scale test rig has been used in tests by Hulet *et al.* (2005) at Sheffield University.)

3.3.1 Test Apparatus

The small scale test rig in use at Sheffield University is shown diagrammatically in Figure 3-3.

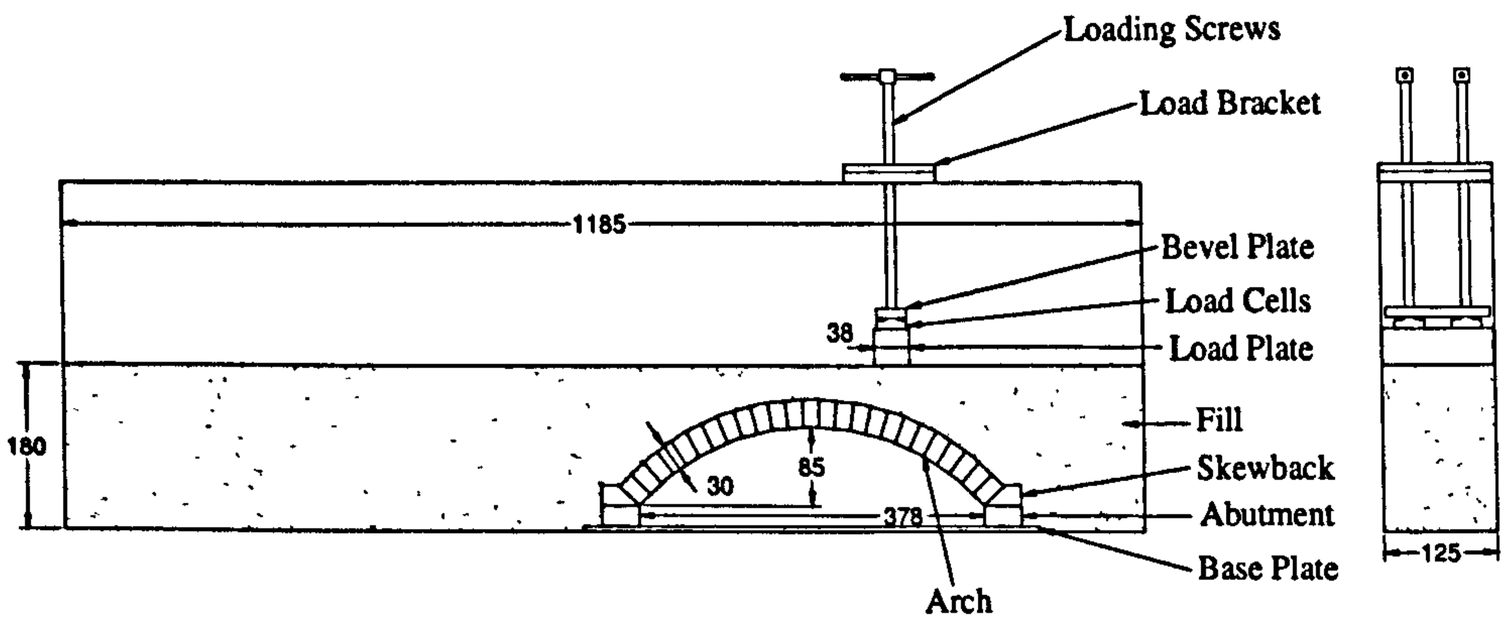

Figure 3-3 Small-scale test apparatus

A rigorous test method has been developed for use with this rig, with both the arch tests and subsidiary materials characterisation tests (shear box, Proctor density, sieve analyses etc.) enabling a better understanding of soil-arch behaviour to be developed.

3.3.2 Boundary Conditions

One of the most important issues to quantify is the effect of the boundary conditions, in this case the transparent side walls. In 2004, Fang *et al.* conducted experiments

on models under plane strain conditions. By using a sliding block test as opposed to the more normally used direct shear test (shear box test), it was found that the commonly used 'grease method' (Rowe *et al.* 1964) was not so good at achieving a constant and low friction value at low stress (<10kN/m^2) situations. The grease method involves a layer of rubber membrane lubricated by silicon grease in order to minimise friction with an acrylic wall. However, alternative approaches using both thick and thin plastic polythene sheets were also examined by Rowe *et al.* and it was found that in some arrangements these were useful for low normal strains with a low constant friction angle obtained.

These experiments highlight that current techniques for measuring boundary friction in model test rigs are flawed and that quantification by alternative methods to the direct shear apparatus and sliding block method must be considered when quantifying test condition variables. This PhD. conducted a set of specially designed in-situ friction tests specific to the experimental situation (more details are given in Section 3.3.6) to obtain a more accurate value for the side wall friction.

3.3.3 Material Properties

Although three backfill materials were initially used, only sand was taken forward with the small test rig due to the problems highlighted in Section 3.3.5 when using limestone and clay. The material properties of the sand can be found in Chapters 4 and 5 of this thesis. What was important in each test was to ensure that the fill

possessed the same characteristics at the start of each test; normally this required new fill to be graded and re-selected for each test.

3.3.4 Test Procedure

It was envisaged that the small test rig be able to investigate the behaviour of sand (see Figure 3-4), limestone and clay backfill. Therefore the first task before using the provided small test rig was to explore its limitations with each material and possible minor modifications as well as developing a robust, comparable and scientific test method which would enable repeatable and consistent results. (Due to the small statistical sample arising from the limited number of tests conducted as part of this PhD, it was not possible to apply the statistical methods of trueness and precision covered by BS ISO 5725:1994.)

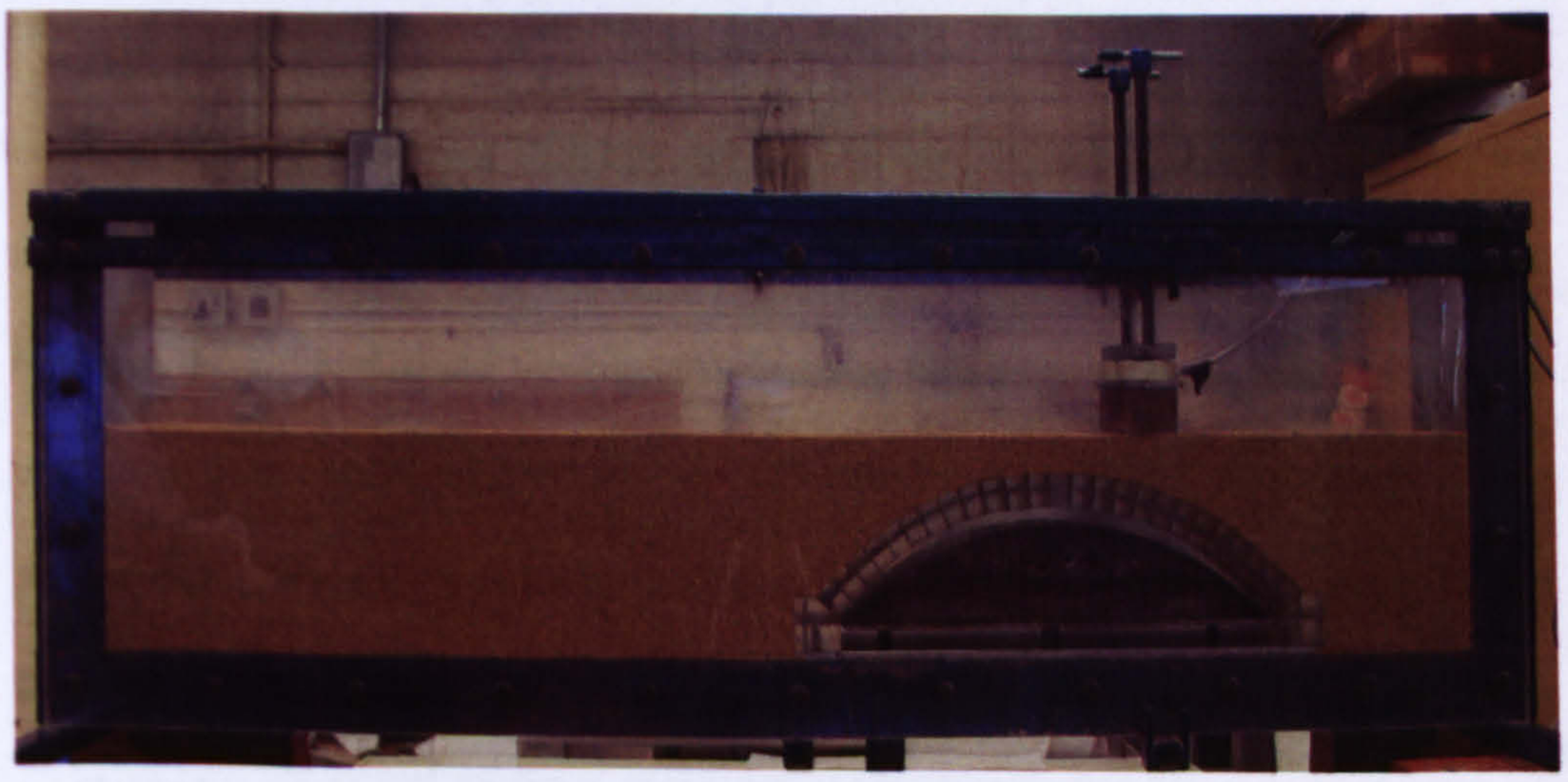

Figure 3-4 Small-scale test apparatus filled with sand

Visual Imaging

Distortion within the visual imaging due to reflection and refraction had to be taken account of during both the test procedure and analyses. The reflection was minimised by the use of a thick black curtain placed behind the camera and by blanking out the background within the field of vision within the rig with white paper. The refraction distortion caused by the different distances between the camera lens and the rig at different points were corrected manually within the GeoPIV data files.

Clear Cast Acrylic

The first technical obstacle encountered was the fact that acrylic has a very low coefficient of friction on a polished side and quite a high level of friction on a machined surface ($\mu_{machined} = 0.4$, $\mu_{polished} = 0.2$)[1]. So whilst almost ideal for the issue of side wall friction, slippage between voussoirs was complicated by the use of silicon grease which was being used to prevent particles of backfill migrating between the sidewalls and the voussoir faces to under the arch. It was found that a complete disassembly of the test rig followed by a complete de-greasing of the acrylic and contact elements with sufficient drying time was required after each test to maintain repeatability of the experimental results. Each of the individual tests conducted were repeated three times to confirm that the results obtained were consistent. There were also some other slight modifications to both the developed

[1] Values for static friction for 'acrylic on acrylic' are taken from information provided by the manufacturer.

test procedure (given in Chapters 4 and 5 of this thesis) and the rig before experimental testing began where the results would be used.

Latex

Another material examined was the use of a layer of silicon greased latex on the sidewalls. It was found that at this small scale the chosen latex actually hindered the effectiveness of the visual imaging as it was difficult to generate sufficient lateral pressures in the low stress areas during the test to prevent the latex from migrating (wrinkling) into the fill. Therefore the latex was removed from the test procedure.

3.3.5 Preparation of Soil Beds

The small test rig was developed to test three materials: sand, limestone and clay. Each material was subjected to testing within the rig to determine its suitability.

Sand

Sand tests are very useful as a test material as it is comparatively well understood and easy to work with. Also the nature of the coarse colourful sand adopted to investigate meant that there was sufficient texture to work with visual imaging techniques (see Figure 3-5) and that the likely backfill movements could be quickly established.

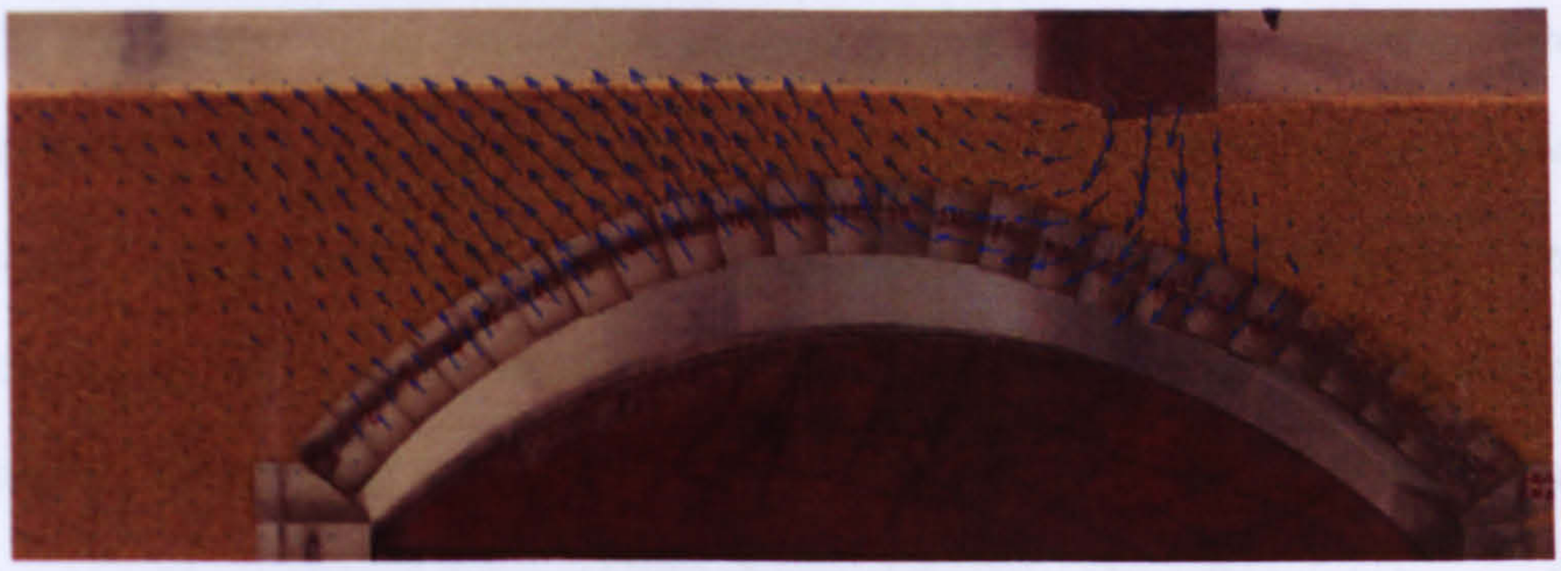

Figure 3-5 Sample GeoPIV image: sand test (Arrow magnification = 25)

Much more detail of the sand tests carried out together is given in Chapters 4 and 5 of this thesis. Needless to say that the basic test method was developed mainly using sand.

Limestone

The Series 800 Specification for Highway Works (2004) gives for SHW Type 1 sub-base a sieve grading for unbound crushed rock. However, these values equate to those to be used with a full sized prototype. Part of producing a scale model is scaling the fill which in the case of crushed limestone results in a great deal of fine graded powder as well as the larger fragments. The image shown in Figure 3-6 shows one of the many tests carried out with compacted limestone.

Figure 3-6 Sample GeoPIV image: limestone test (Arrow magnification = 25)

The grey bands were originally thin layers of graphite shavings used to enhance the surface for visual imaging purposes since white limestone is of insufficient visual texture. Compaction of the layers of limestone was done using a vibrating plate and resulted in two negative outcomes. The first being that the amount of scratch damage done to the acrylic side walls by the larger limestone particles was considerable, such that repeated replacement of the two side walls would have to be undertaken at fairly frequent and regular intervals in any potential test programme.

The second was the unexpected problems associated with the dust. Given that the location of these experiments was the Geotechnical Basement at Sheffield University, (the only place available), it quickly became apparent that it lacked adequate ventilation should the limestone be compacted dry. Since the proposed tests utilised oven dried limestone, filling of the rig was done very carefully allowing sufficient time for the dust to completely settle upon completion of the compacting of each layer. Nevertheless future work with limestone would require better ventilation and the incorporation of a sacrificial layer of acrylic on each interior side wall of the test rig itself.

Clay

A single clay test was carried out utilising the small test rig to ensure that potential future tests with this type of material were viable. Small changes to the test rig proved to be necessary at an early stage in the proceedings. Not only to enhance the surface texture using markers for digital imaging, but also to enable the long

term over consolidation of the clay layers, as dynamic compaction methods do not work with cohesive soils (because it is not possible to remove moisture from the voids by compaction) and were envisaged to be too damaging to the fragile acrylic side walls. The downside was that to obtain the required void ratio (eliminating 90% of voids) consolidation of the clay layers had to be done by applying a heavy load for a set period of time.

For the first test a soft to firm clay was used, capped with a thin sand layer. PTFE (Teflon) spray was applied to the acrylic to reduce wall adhesion and 5 mm limestone particles were inserted into the clay in a grid at one side to enhance contrast for image processing. As can be see in Figure 3-7 the GeoPIV analysis works well even in areas without markers.

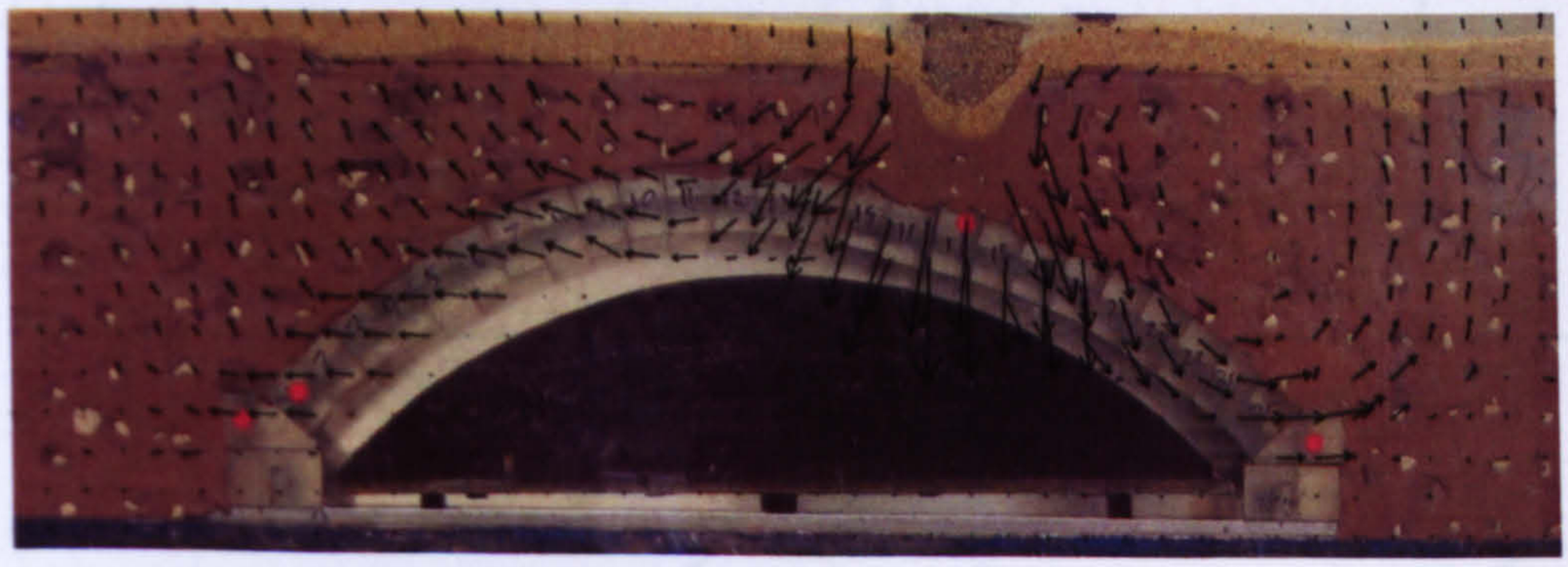

Figure 3-7 Sample GeoPIV image: clay test (Arrow magnification = 25)

The sand in the picture was used for distribution purposes although it transpired that the layer was of insufficient thickness to work as anticipated to prevent local shearing of the clay. Another problem discovered during the carrying out of this clay test was the evidence for variability. For example there was difficulty in maintaining constant moisture content throughout. The strength of clay is

dependent on its moisture content; however, as this test was neither fully saturated nor fully dry and the use of damp towels and water sprays resulted in a severe lack of consistency. It was determined that significant changes to the adopted test procedure and possibly the test rig itself must be investigated before carrying out more tests with clay.

Particle size distribution curves

Figure 3-8 shows the soil particle size distributions for the sand and limestone fills.

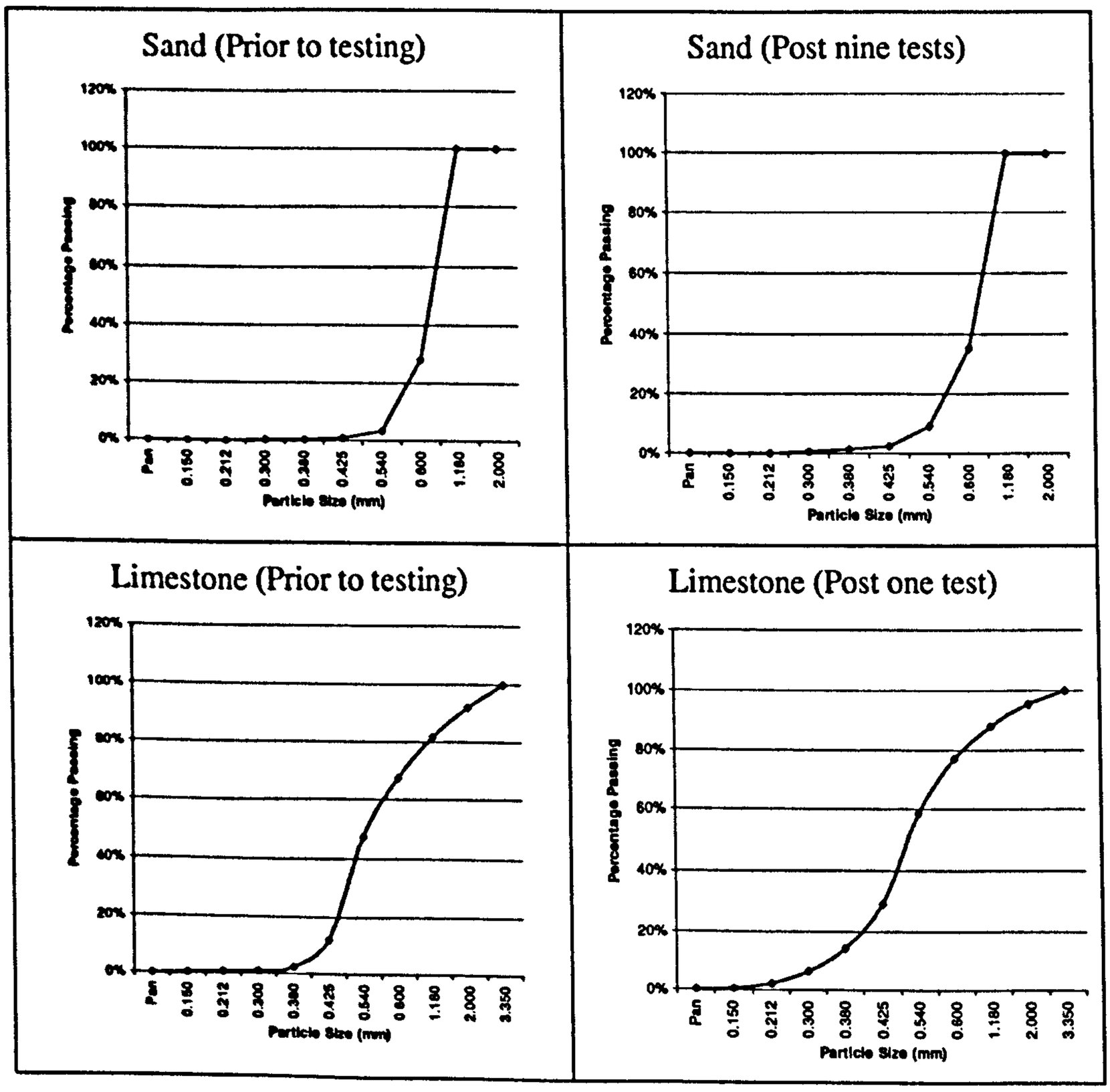

Figure 3-8 Soil distribution curves for sand and limestone fills

It is interesting to note that, whilst for the sand prior to and post experiments little change in the particle distribution was observed, the limestone showed a much greater change to smaller particles due to the compaction process. This was mitigated by completely replacing the fill with newly graded limestone, so that each limestone test conducted would have the same particle size distribution as the other limestone tests. Also of note is that the particles of limestone tend to be smaller than those in the sand and it is important to remember that the limestone is a scaled fill to represent that of SHW Type 1 sub-base.

3.3.6 Additional Testing

An additional test was devised and developed which reproduced the fill's contact with the wall under test conditions as shown in Figure 3-9.

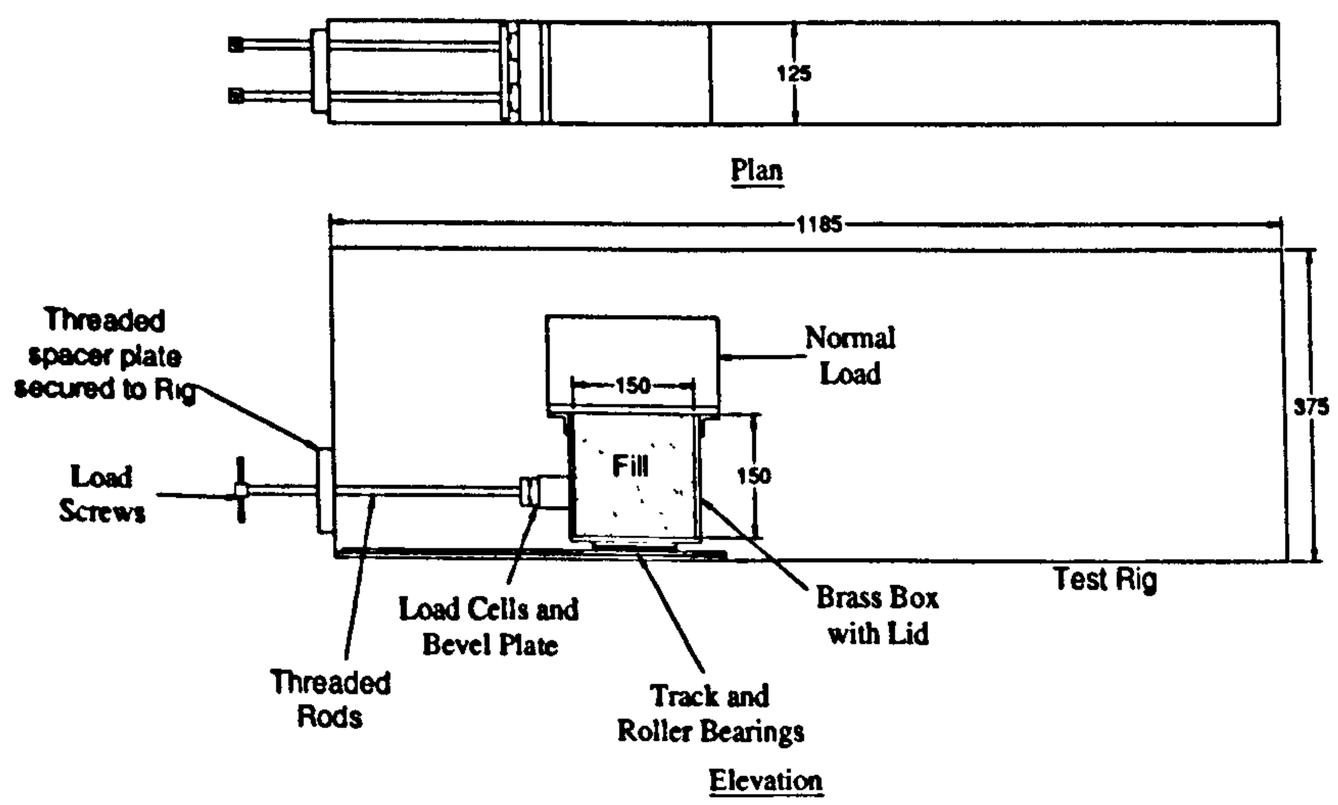

Figure 3-9 Wall friction test apparatus and set-up

Using a brass box on roller bearings within the test rig it was possible to simulate the movement of backfill within the rig under experimental conditions. Prior to

filling the box, silicon grease was used at the interface between the edges of the box and the side walls of the rig to prevent sand particles becoming lodged. The weighed fill was placed by pluviation from the desired height to achieve the properties of the particular arch bridge experiments and the box top then secured and a normal load placed on top. Horizontal loading was applied via the bevel plate connected to a simple hand screw arrangement and its intensity recorded by two electrical resistance-strain-gauge type load cells. Each full turn of a load screw corresponded with a horizontal displacement of 1.6mm. So by mimicking the arch test set up for fill placement the fill within the box in this experiment would be under similar conditions in an arch test. By comparing an empty box test and a full box test under different normal loads, an estimation of the friction between the sand within the box and the acrylic side walls could be made using the equation $F=\mu R$ where R is based upon the area of sand in contact with the side wall and the lateral pressure given by $\sigma_h=K_0\gamma z$, where $K_0 \approx (1-\sin\phi')$ (Jâky 1944).

3.4 Large-Scale Test Rig

A full scale (1:1) test rig was designed and procured by the author at the University of Sheffield in relation to this PhD (Figure 3-10).

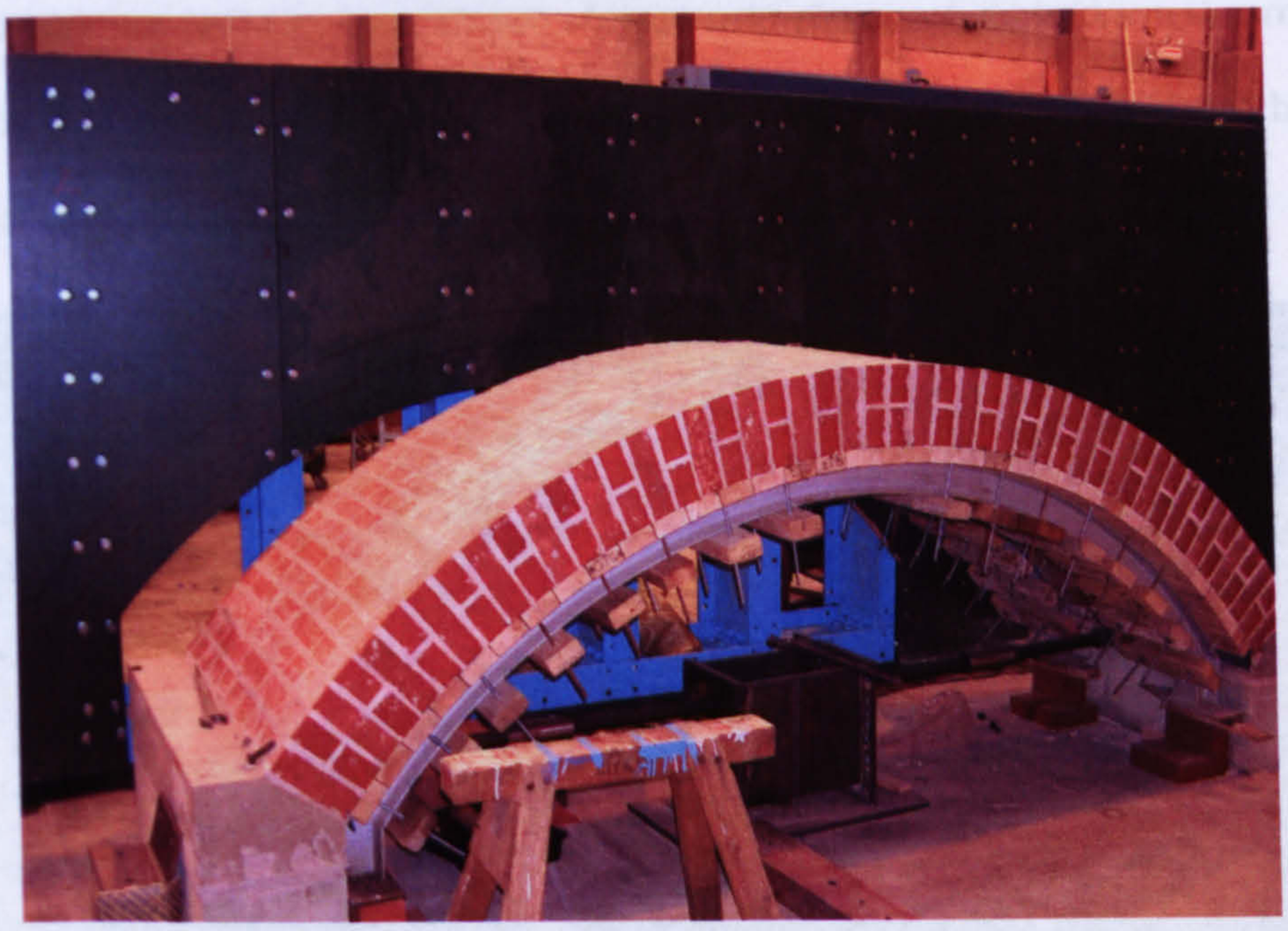

Figure 3-10 The brickwork arch for use with the large-scale test rig at Salford University

This large test rig was constructed in partnership with Salford University who would carry out the test programme under guidance from Sheffield. This rig was built at Salford University and was funded by Essex Country Council. Unfortunately due to logistical difficulties no test data were available for use within this PhD. The aim of the large test rig was to act as a stepping stone to relate the results from the small scale rig to real life bridges. More details of this rig can be found in Appendix B.

3.5 Field Tests

As stated at the start of this chapter it is important to relate laboratory experiments to those conducted in the field and although rare, experimental field tests do take place today on masonry arch bridges. Figure 3-11 shows a field bridge test carried out by Professor Bill Harvey in Barcelona 2005. (The photograph is included here by his kind permission.)

Figure 3-11 Field bridge test Barcelona 2005

3.6 Medium-Scale Test Rig

From the experience and lessons learned from the small and large test rig it has become obvious that the next logical step to be taken is to design and construct an intermediate sized test rig. This would enable the tests carried out thus far on the small test rig to be better related to the tests carried out on the full scale test rig.

The medium rig would have a likely scale of 1:4 and would use machined clay brick voussoirs constructed on centring for the arch barrel, most likely built directly off the laboratory floor. A simple set-up could be designed so that the use of better and more extensive monitoring instruments such as deflectometers and pressure cells together with a fixed position camera attached to a sub frame of the main rig could be made to get real time data analyses during the tests with output sent directly to a laptop enabling real time analyses to be plotted. The test rig could also be further enhanced by having a computer controlled constant rate of loading which would also allow simple dynamic tests to be undertaken. The location of the medium rig could also take account of ventilation and compaction issues that have arisen from the carrying out of tests thus far as well as being in effect constructed in a photographic 'dark room' to minimise visual imagery interference. It is envisaged that such a set up would take a similar method to the large scale test rig in terms of design and construction yet from a test point of view the small scale test rig would provide better basis for the adopted test procedures.

3.7 Comparison between the Models

Table 3-2 shows a comparison of the three different test rigs and a real life bridge. It is clear from the table why small scale rig tests are preferred for research purposes, whilst also showing why it is inadvisable to compare results from small scale test rig experiments with bridges in real life without keeping the tests in context. Perhaps the most significant fact from this table is that for the same cost as replacing one masonry arch bridge on Britain's road network, quite a lot of research that could save many arch bridges from renewal could be carried out.

Parameter	Small (1:8) [Sheffield]	Medium (1:4) [Proposed]	Full Size (1:1) [Salford]	Real Life[1]
Initial cost to construct (excluding labour)	£260	£2000 (Estimate)	£14k	£200k[2]
Cost per test to failure	Negligible	Negligible	£3k (original) £6k (current)	N/A
Labour cost for construction	Small	Medium	High	Very High
Storage of material	Negligible	Small	Significant	Small
Ability to model kinematics	Good	Good to Reasonable	Reasonable	Very Difficult
Ability to represent real structure	Poor	Poor but better than small	Reasonable	Perfect
Test preparation and duration	1 day	3 days	2-3 Weeks	N/A

1 Private communication from Bill Harvey to the author dated 16 June 2006.

2 Private communication from Tony Bagchi (Mouchel Parkman) to the author dated 09th June 06.

Table 3-2 A comparison of different test rigs

3.8 Summary

This chapter has investigated the issues associated with producing scale models for problems involving soil-structure interaction. As well as physical scaling laws of geometric and kinematic similarities considerations of the prototype's relationship with the smaller scale model has been examined.

Determination of the suitability of the small test rig with the use of clay, sand and limestone backfill together with the development of an appropriate robust and effective test method has also been detailed.

A comparison between the small scale model, the full scale model and a real life bridge has been given and a third medium sized test rig has been proposed to address some of the concerns related to the danger of applying results and trends found at small scale to the full scale prototype. The medium rig also gives some details as to address some of the lessons learned from designing and building the large test rig and the operation of the small test rig.

The next two chapters look at the main studies with which the small test rig has been used.

Chapter 4

Influence of Passive Pressure and Live Load Distribution

This chapter is in the form of a self contained paper. It should be noted that this was originally proposed as a joint paper and as such some of the work covered on the sliding block model was contributed by Dr Colin Smith.

An experimental investigation of the influence of passive restraint and live load distribution within the backfill of masonry arch bridges

4.1 Abstract

The influence of backfill on the load carrying capacity of a masonry arch bridge can be considerable; the backfill is responsible for transmitting the live load from the surface through to the arch barrel as well as having a lateral stabilising effect on the arch itself. A general live load distribution of one horizontal to two vertical is currently recommended for use by the UK codes of practice, however, evidence suggests that in some cases this assumption could be conservative or over conservative. This paper reports a series of experiments which aimed to separate the contribution by live load distribution and passive restraint provided by the backfill in an effort to determine theoretical approaches that would better represent these in current arch assessment tools. Details of twenty seven small scale bridge tests are given together with conventional analyses of the soil-structure interaction and novel approaches involving the use of digital imaging techniques. The model test results indicate that the contribution of passive restraint can be significant whereas the actual benefits from live load distribution appear to be negligible for certain depths of backfill.

4.2 Introduction

This research work comes about due to the current effort to re-examine soil-structure interaction in masonry arch bridges in order to better assess bridges in the field. A programme of joint research between The University of Sheffield, Salford University and Essex County Council is investigating masonry arch bridges at scale in the laboratory and in the field in order to produce a greater understanding of how real bridges behave and how best to improve assessment techniques used at site and in the consultancy office.

Current UK codes of practice recommend the assumption that live load distributes laterally with depth to the extent of one horizontal to two vertical (BD21/01, RT/CE/C/025), though it is not transparently clear where this is derived from. In any case, this live load distribution cannot be guaranteed, as it may be expected that the angle of distribution would depend to some extent upon the type and consistency of the backfill present. Passive restraint is another action that is assumed to exist but determining the magnitude and distribution is less clear. In this case the only passive restraint to be currently taken on board during assessment is as dead load or a simple horizontal uniform or Rankine style pressure restraint, (see Figure 4-1 and 4-2).

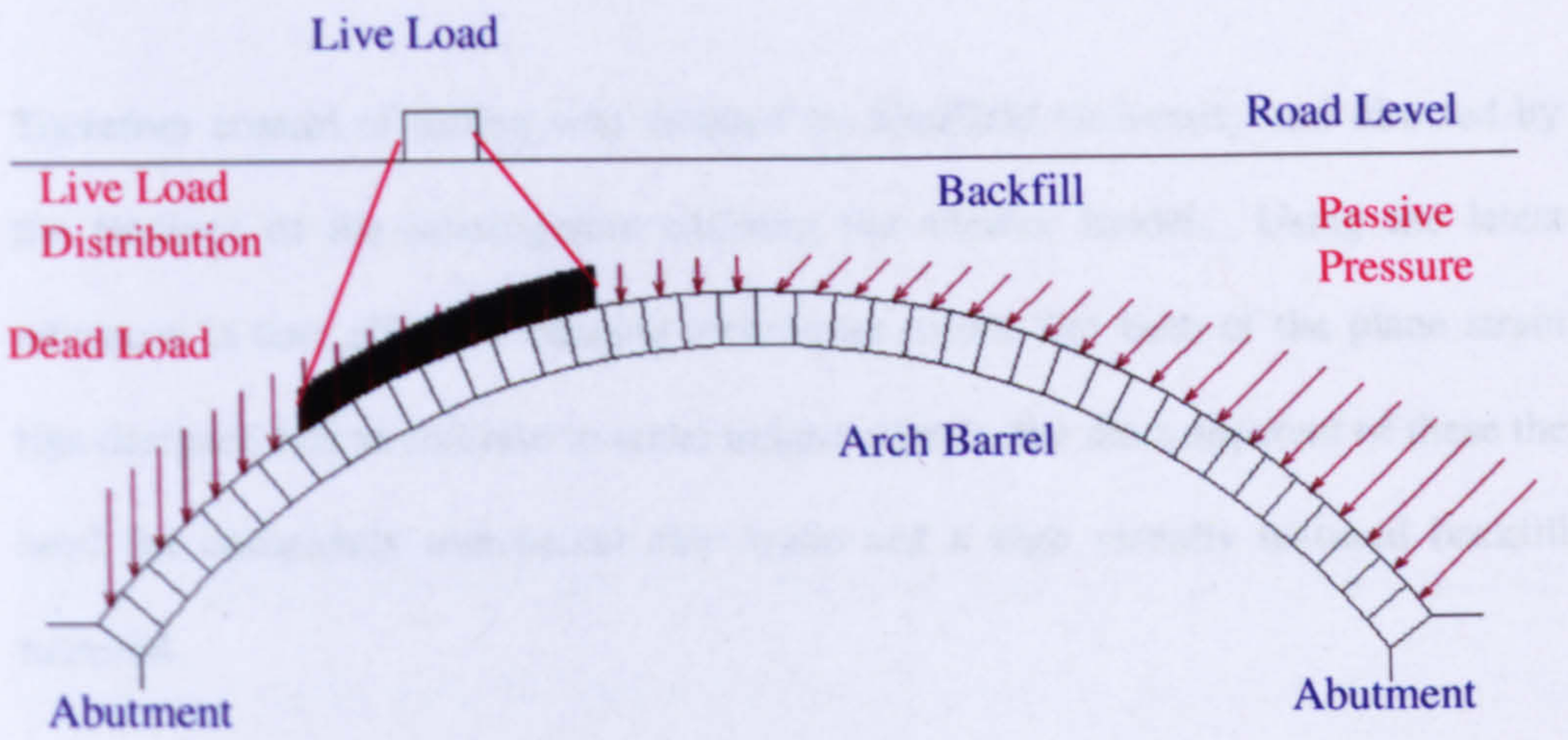

Figure 4-1 Areas where passive restraint and live load distribution currently dominates an arch bridge assessment

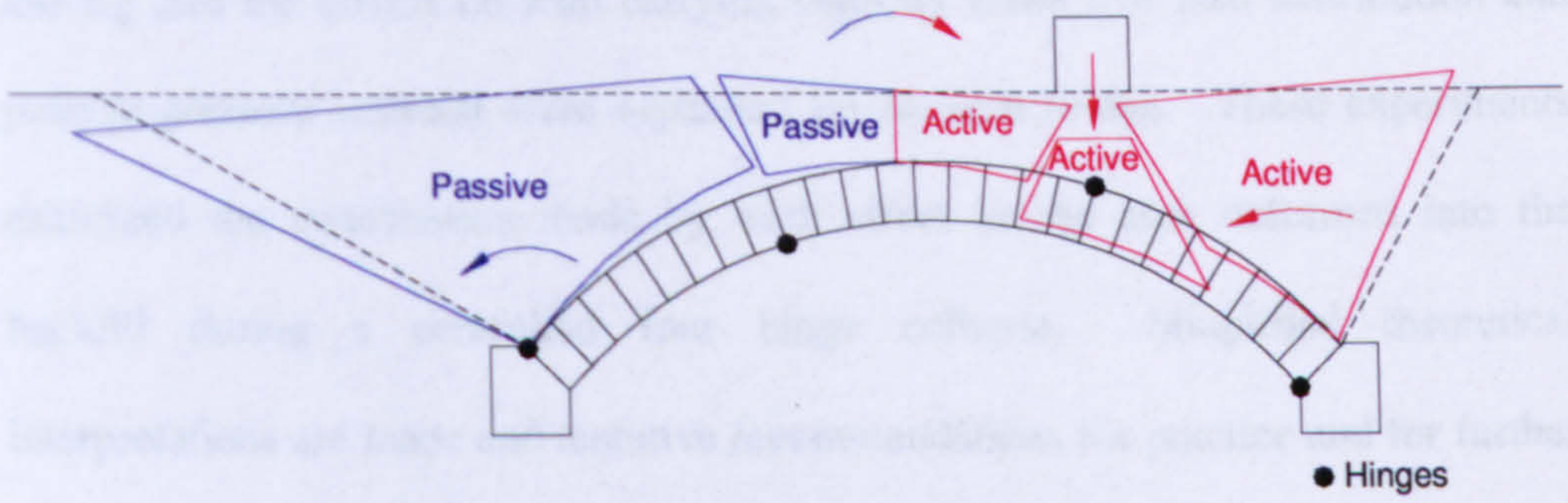

Figure 4-2 Areas where active and passive soil pressures dominate an arch bridge during failure

To give an insight to these phenomena and to try to ascertain a general understanding of the issues involved, a series of tests on small and large scale models was commissioned by Essex County Council to be undertaken at the University of Sheffield. Two test rigs were commissioned, the first being a 1/8th scale model constructed at the University of Sheffield and the second being a full scale model designed by the University of Sheffield but built at the University of Salford. The idea behind the two models was that issues could be examined quite rapidly on the smaller test rig and then corroborated and studied on the larger rig.

Therefore control of testing was dictated by Sheffield University and directed by the findings of the investigation utilising the smaller model. Using the latest advances in cost effective imaging techniques meant that both of the plane strain rigs designed had to conform to some unique criteria, the most apparent of these the need for completely transparent side walls and a high visually textured backfill material.

This paper reports the results of a large parametric study undertaken using the small test rig into the effects on load carrying capacity when live load distribution and passive pressure restraint were separated on an arch bridge. These experiments examined the contribution made by each effect as the arch deformed into the backfill during a controlled four hinge collapse. Simplified theoretical interpretations are made and tentative recommendations for practice and for further large scale tests are made.

4.2.1 Background

The experimental tests conducted by Davey (1953) and Chettoe & Henderson (1957) during the fifties provide some indication that some types of backfill on real life masonry arch bridge distribute the live load better than others. Bearing capacity problems in the field of geotechnics also indicate that this should logically be the case, (see BS8004: Section 3). It is somewhat surprising therefore that current UK codes (BD21/01, RT/CE/C/025) use a one size fits all blanket approach. Very little research to date has been done on examining the backfill contribution to arch

capacity, hence its current renaissance, but one article by Harvey *et al.* (2005) shows that it is one area of bridge assessment for which the time has come for it to be re-evaluated.

Passive restraint has typically been modelled employing a modified pressure distribution model used for frictionless vertical retaining walls. Recent work by Burroughs *et al.* (2002) for example, suggests the adoption of a passive pressure model as shown in Figure 4-3, to represent the passive pressures mobilised within a masonry arch assessment. This model acknowledges the effect of strength mobilisation, though neglects the stress rotations likely to be associated with a curved frictional arch extrados.

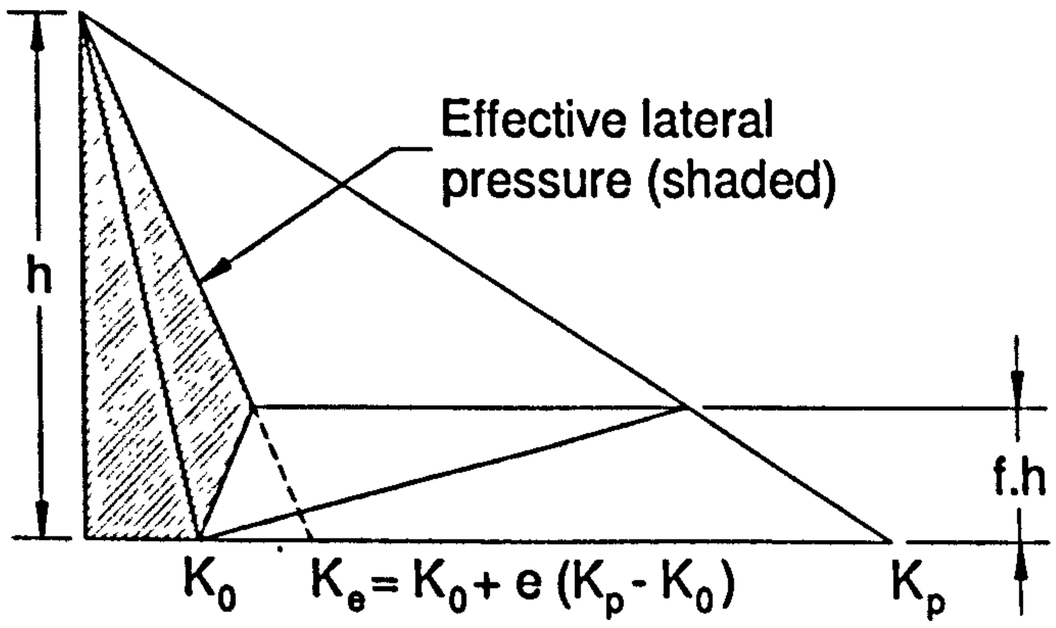

Where:

e = coefficient defining portion of full passive pressure mobilised.

f = ratio of soil depth at which bilinear pressure starts.

K_0= at-rest pressure coefficient.

K_p= passive pressure coefficient equivalent.

K_e= lateral earth pressure coefficient.

Figure 4-3 Burroughs' passive pressure model for masonry arch bridge assessments

Values of e and f depend on soil properties and have only been examined for a few soils types, for which Burroughs et al. give a fairly broad ranges. While the reduction in stress close to the base of the distribution is likely to be realistic, it will only have a second order effect on the overall arch collapse load since displacements at this location are small.

4.3 Experiments

4.3.1 Apparatus

Using a clear cast acrylic tank reinforced with steel, tests were carried out on a twenty five voussoir 4:1 span:rise clear cast acrylic 1/10th scale arch bridge model of a 3 m span bridge as shown in Figure 4-3. The fill comprised coarse dry sand, which had a high visual contrast texture, and the load was applied through loading screws via a load plate onto the fill. This meant that the applied load was controlled by the vertical displacement of the load plate. (Sand was chosen as it is fairly well understood from a theory viewpoint though other materials are to be tested as part of this overall research programme.)

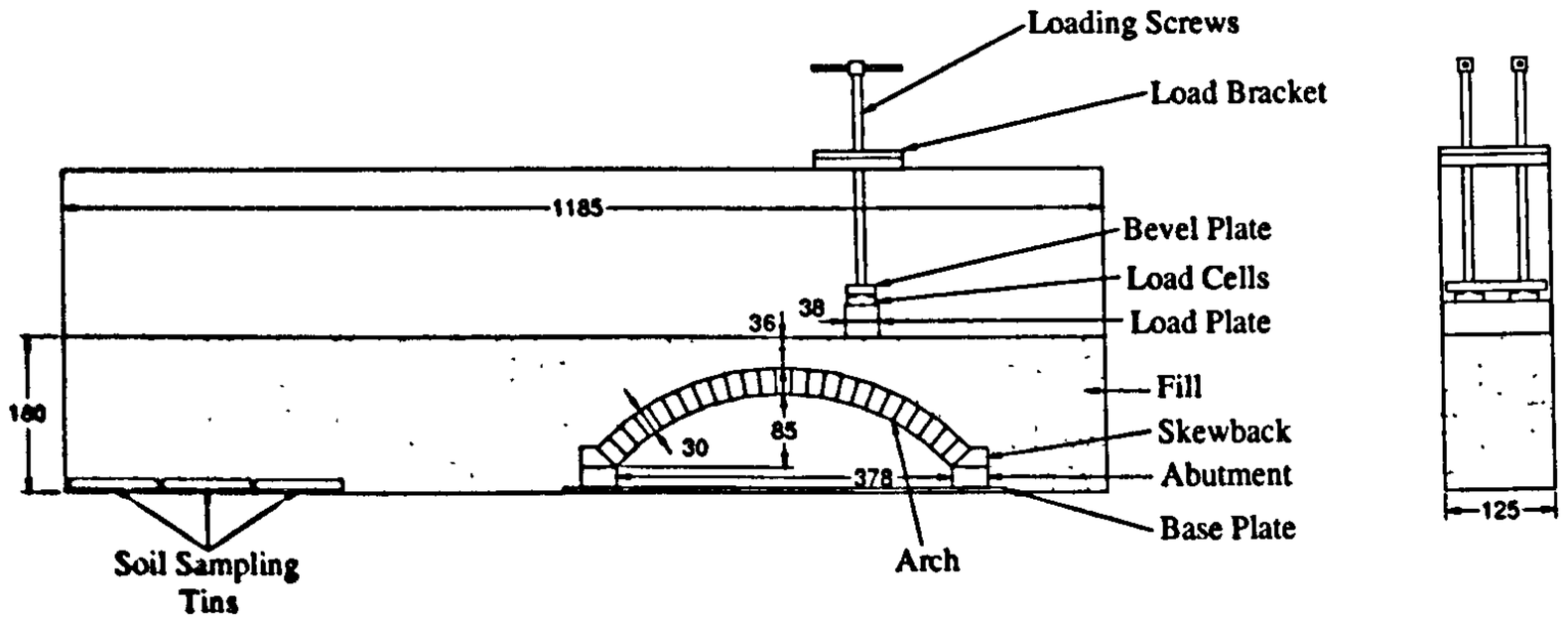

Figure 4-4 Apparatus setup and dimensions (all dimensions in mm)

Prior to filling the test rig as shown in Figure 4-4, silicon grease was used at the interface between the edges of the arch and the side walls of the rig to prevent sand particles becoming lodged there. The weighed fill was placed by pluviation from a height of 422mm to achieve the density given in Table 4-2 and the depth of fill required. Upon removal of the centring, loading was then applied at the quarter point via a load plate connected to a simple hand screw arrangement and its intensity recorded by two electrical resistance-strain-gauge type load cells. Each full turn of a load screw corresponded with a vertical downward displacement of 1.6mm. After each displacement increment a photograph was taken with a digital camera to create a series of images which were then subjected to particle image velocimetry (White et al 2001) to obtain soil displacement vectors which enabled the soil failure mechanism to be visualised. Figures 4-5 and 4-6 show an alternative set up of the test rig and by varying the combination of the two different setups shown, nine scenarios in total were investigated as shown in Table 4-1.

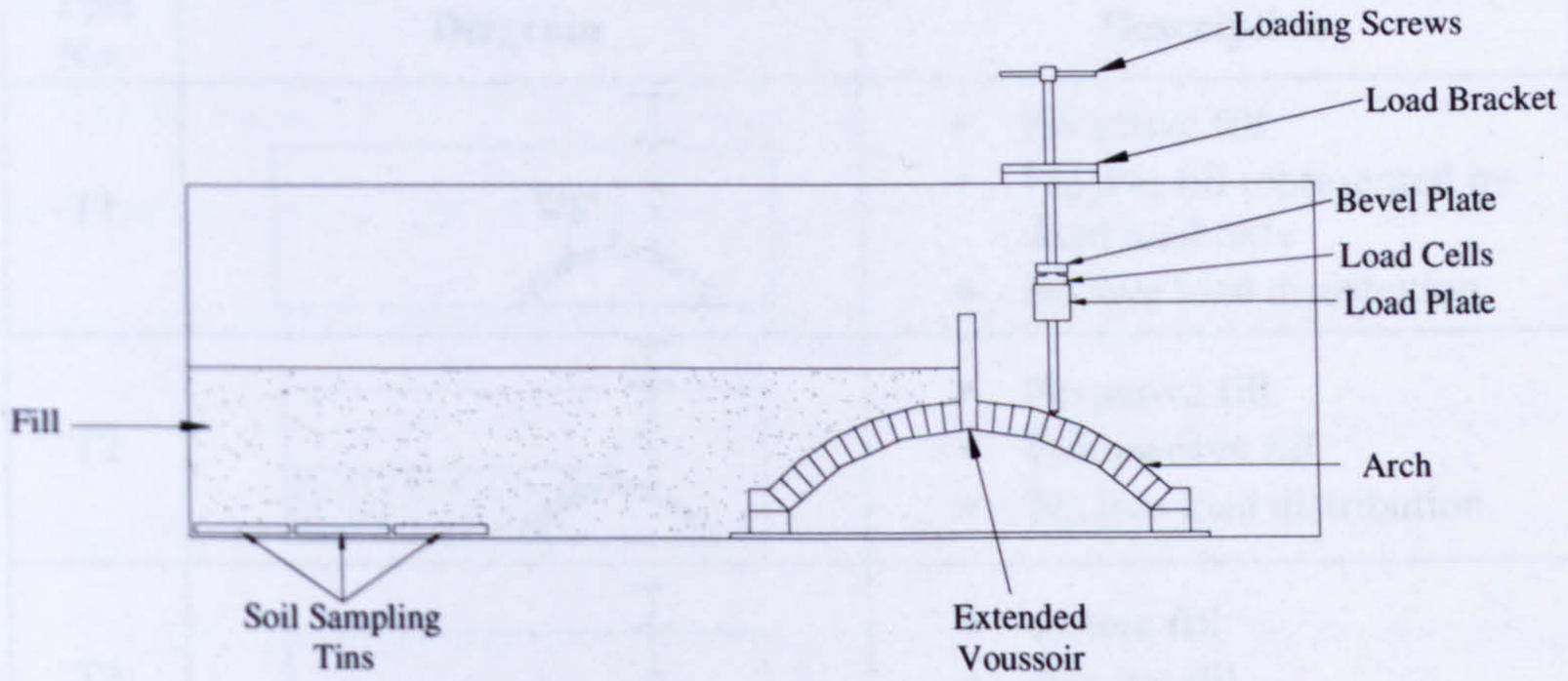

Figure 4-5 Alternative apparatus setup and dimensions

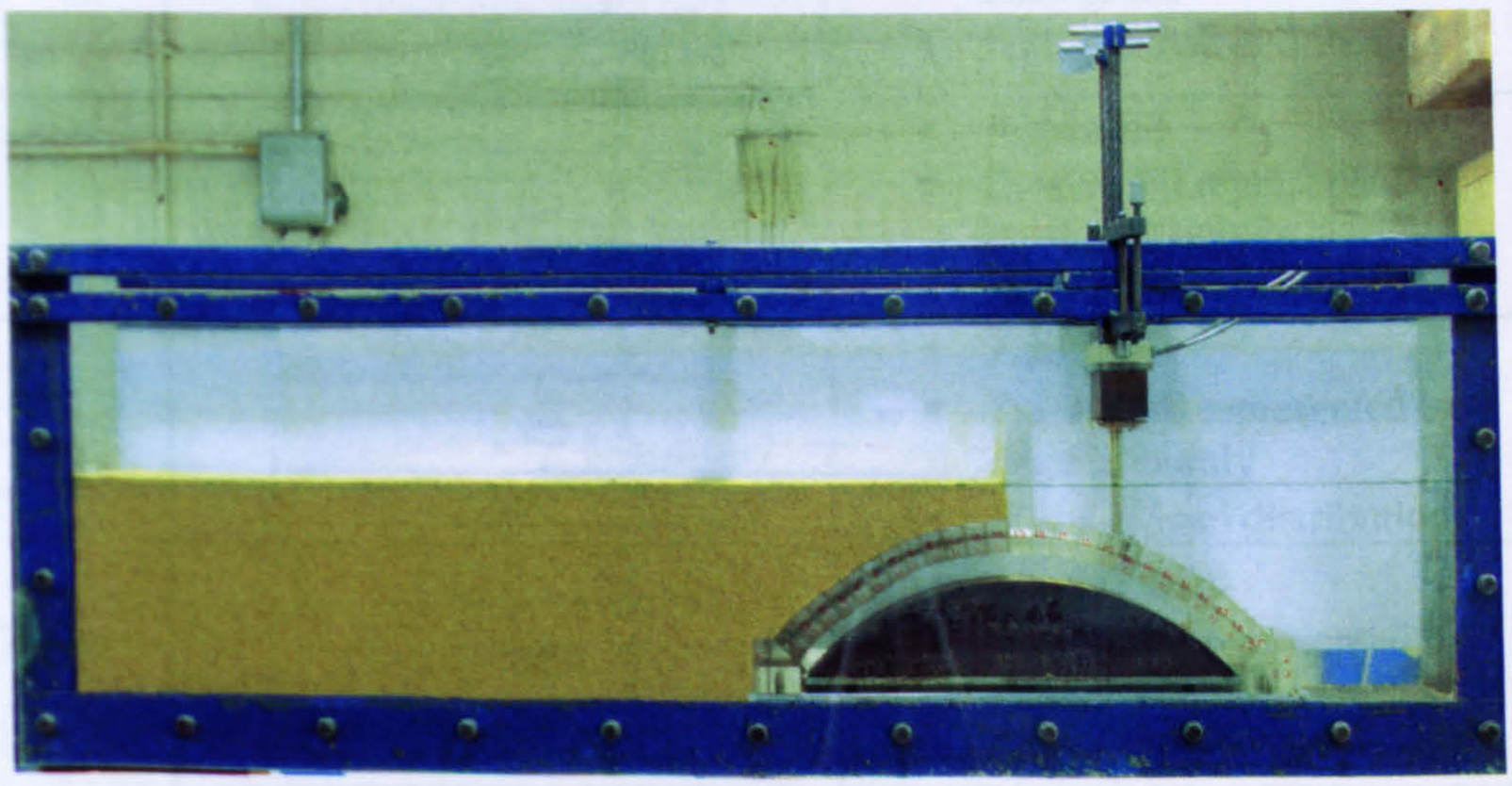

Figure 4-6 Photograph of an arch test (T2)

Each scenario employed a depth of fill above the crown of 38mm and was repeated three times in order to assure repeatability. In total twenty-seven tests were carried out.

Test No.	Diagram	Description
T1	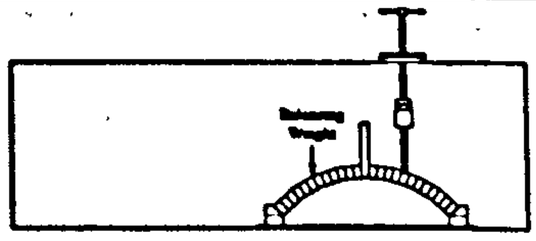	• No active fill • Passive fill represented by dead load only • No live load distribution
T2	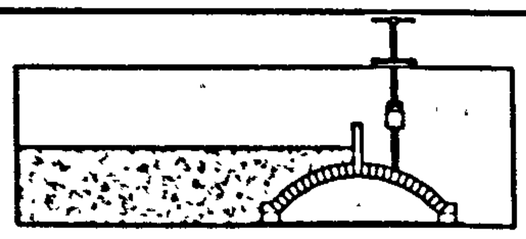	• No active fill • Full passive fill • No live load distribution
T3	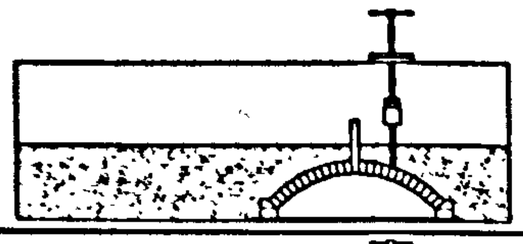	• Active fill • Passive fill • No live load distribution
T4	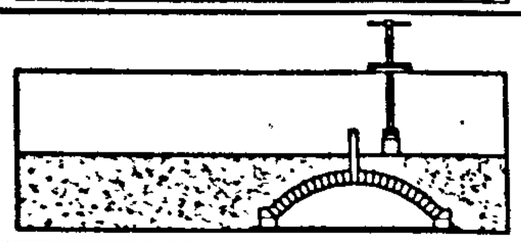	• Active fill • Passive fill • Full live load distribution
T5	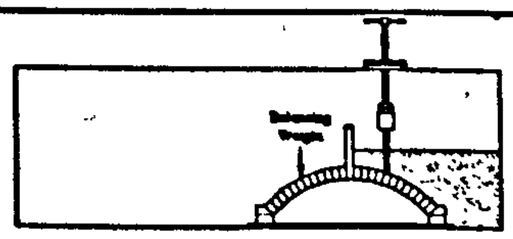	• Active fill • Passive fill represented by dead load only • No live load distribution
T6	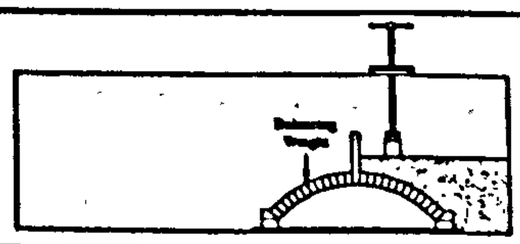	• Active fill • Passive fill represented by dead load only • Full live load distribution
T7	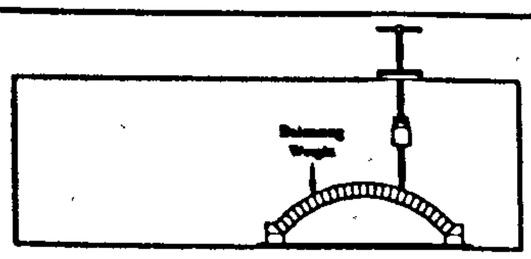	• No active fill • Passive fill represented by dead load only • No live load distribution
T8	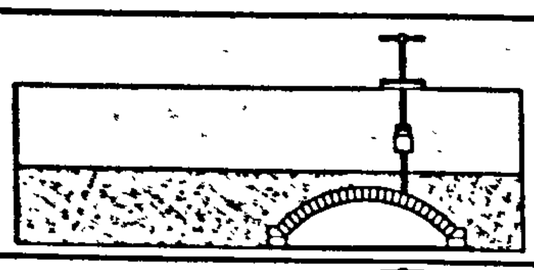	• Active fill • Passive fill • No live load distribution
T9	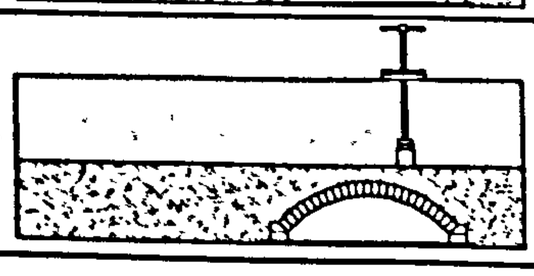	• Active fill • Passive fill • Full live load distribution

Table 4-1 Scenarios to separate passive restraint and live load distribution

In order to maintain maximum transparency of the side walls for the visual imaging technique used, no attempt was made to reduce the boundary friction interface between the sand and the clear cast acrylic side walls though additional experimental work was undertaken to quantify the friction angle at this surface (~ 8°), which is detailed here in the Appendix. Additional tests using deflection gauges on the side walls of the tanks showed deflections of <0.1 mm over a width of 125 mm indicating that plane strain conditions were achieved within the test rig during each experiment. (More details of this test can be found in Chapter 5 of this thesis).

In tests T1, T2, T3, T5, T7 and T8, the load was applied directly to a voussoir by means of applying a pair of 2mm diameter rods to the extrados of the arch as shown in Figure 4-5. This was assumed to be equivalent to the load being applied over an area of a 2mm wide strip running the full width of the arch extrados since the voussoirs are solid.

4.3.2 Material Properties

The properties of the test materials were experimentally determined in accordance with the Manual of Soil Laboratory Testing by Head (1982) and are shown in Table 4-2 and Figure 4-7.

Material	Property	Value	Units	Notes
Sand	Soil friction angle, ϕ'	44	°	(100 mm x100 mm Direct Shearbox Test)
	Cohesion, c'	0	kN/m^2	
	Void ratio	0.58		(Using a textbook value for specific gravity value of 2.65)
	Bulk unit weight, γ_{rig}	16.5	kN/m^3	(in-situ sampling via soil sampling trays)
	Moisture Content	<1	%	(Sand was oven dried before used in testing)
Sand-Acrylic Interface	Interface friction angle, δ	8	°	In rig test
Teflon-Teflon Interface	Interface friction angle, μ	2.3	°	(Manufacturer's Value)
Acrylic	Unit weight	13.7	kN/m^3	(Manufacturer's Value)

Table 4-2 Material properties

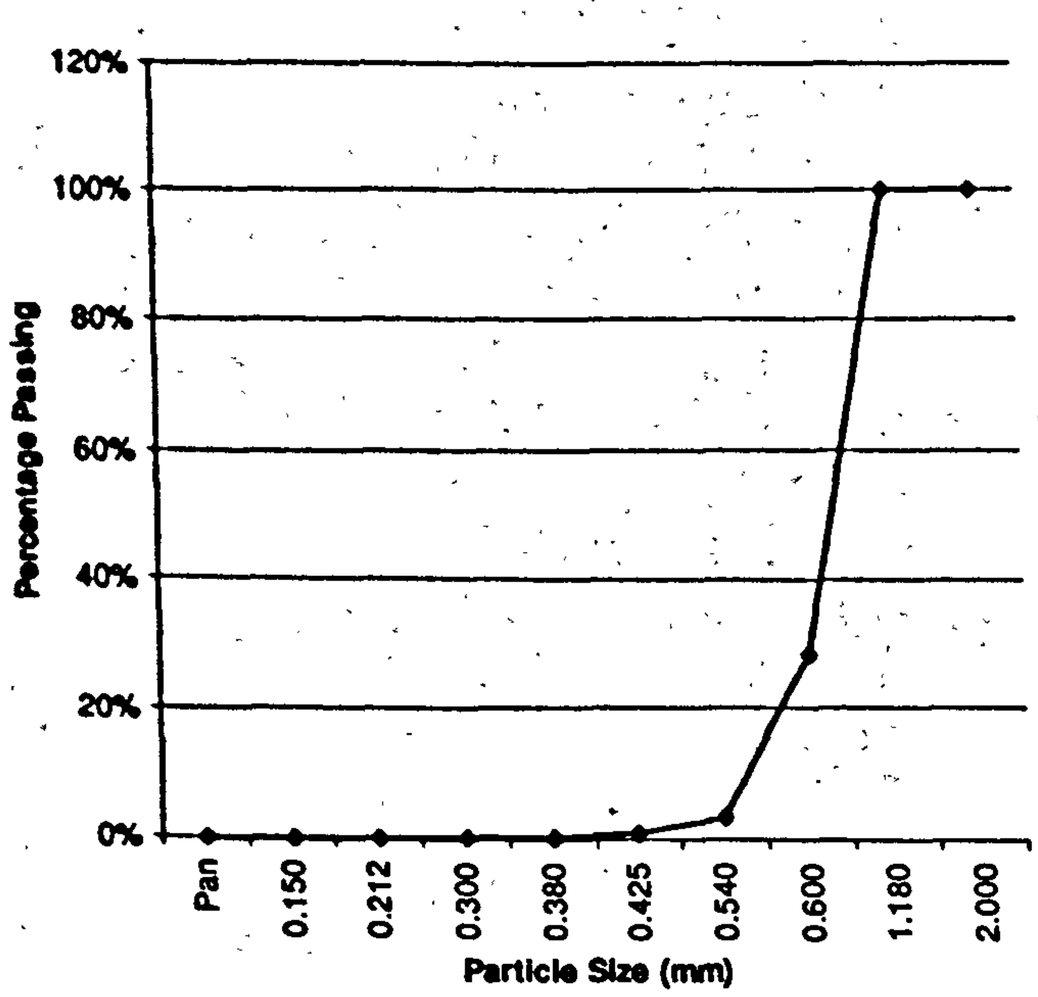

Figure 4-7 Particle size distribution for the sand (prior to testing)

4.3.3 Test Results

The experimental results obtained with the soil-arch test rig for the different scenarios are summarised in Table 4-3.

Test No.	GeoPIV displacements at peak load	Experimental peak load capacity (N)		
T1	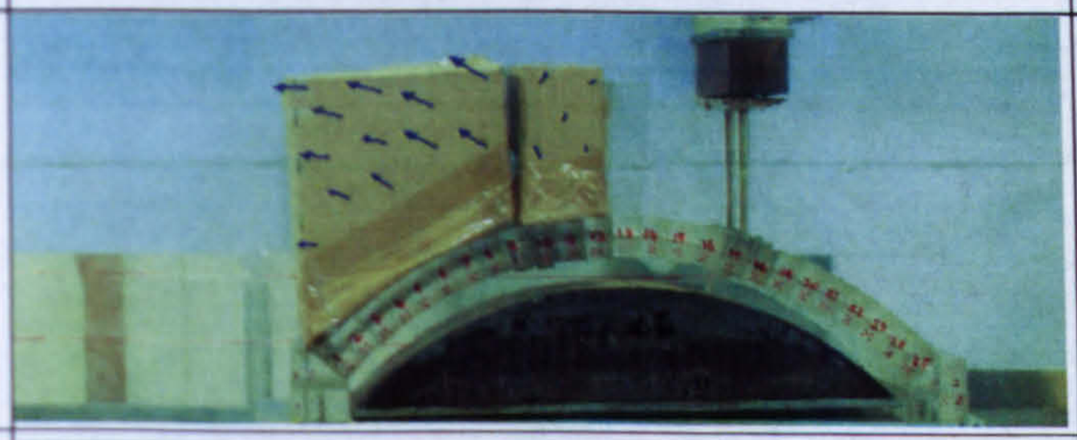	107	108	107
T2	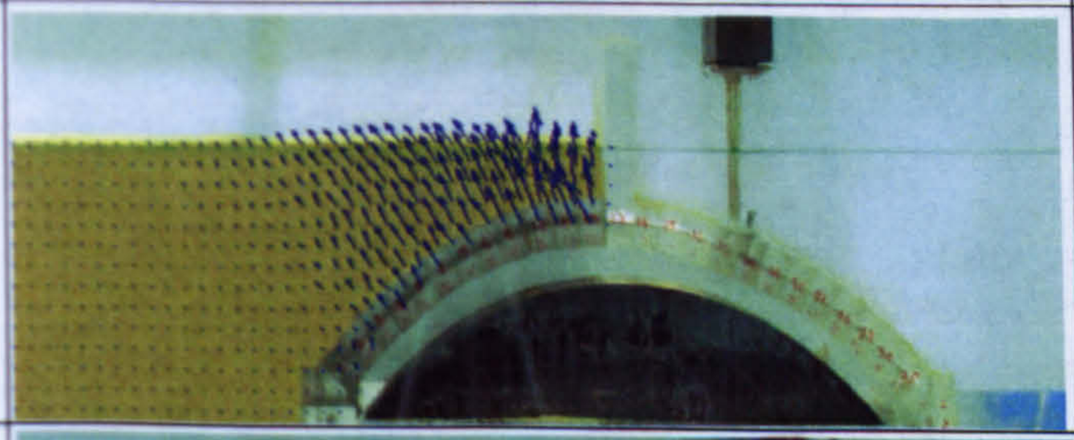	141	142	140
T3	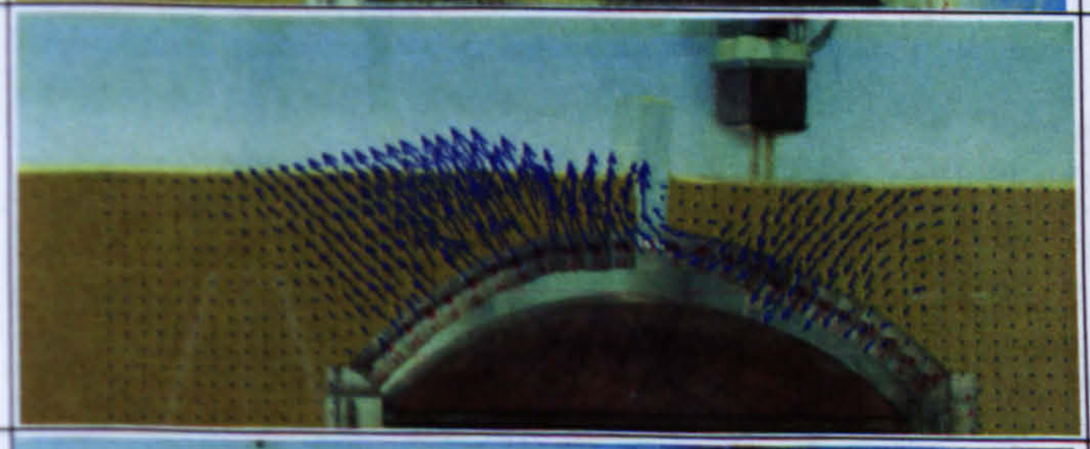	138	137	137
T4	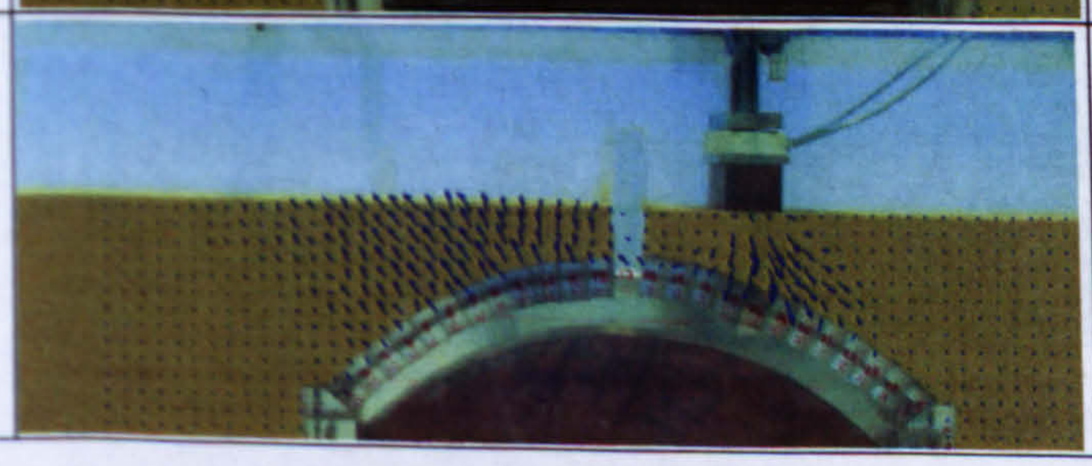	181	183	182

T5	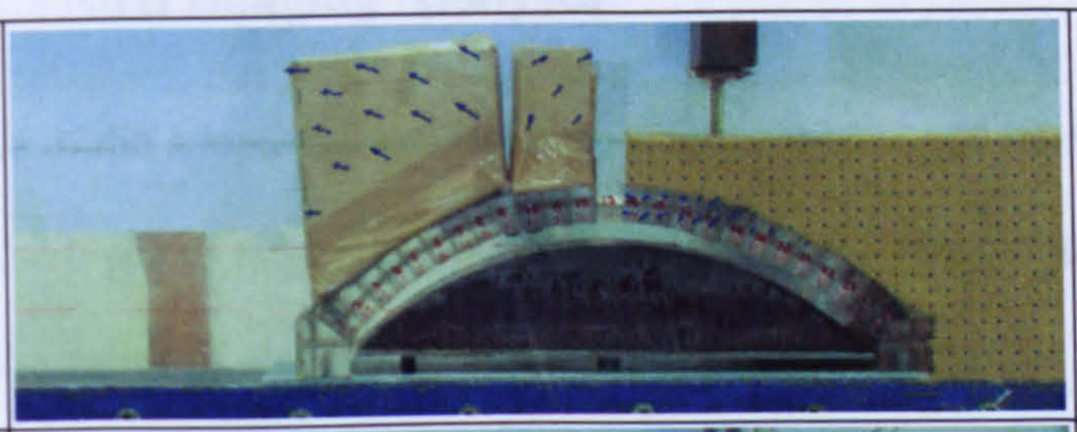	103	104	100
T6	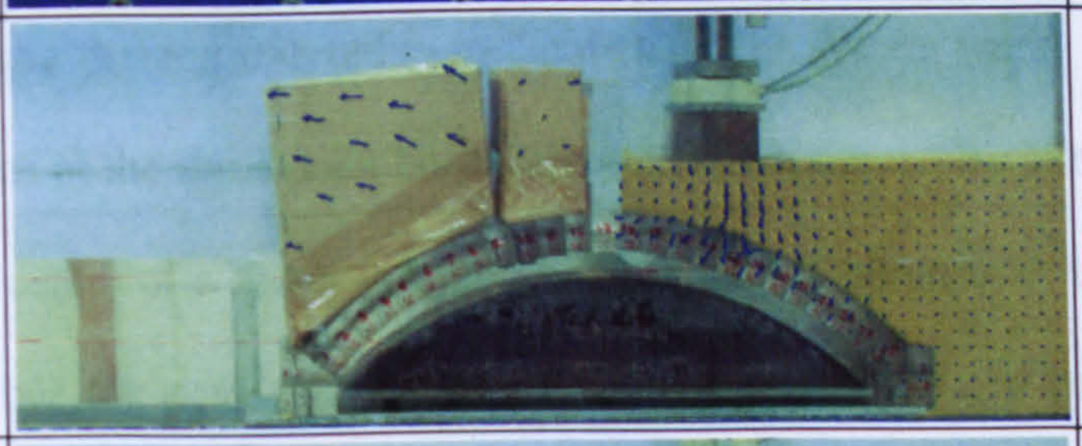	130	131	136
T7		104	104	106
T8		137	135	138
T9	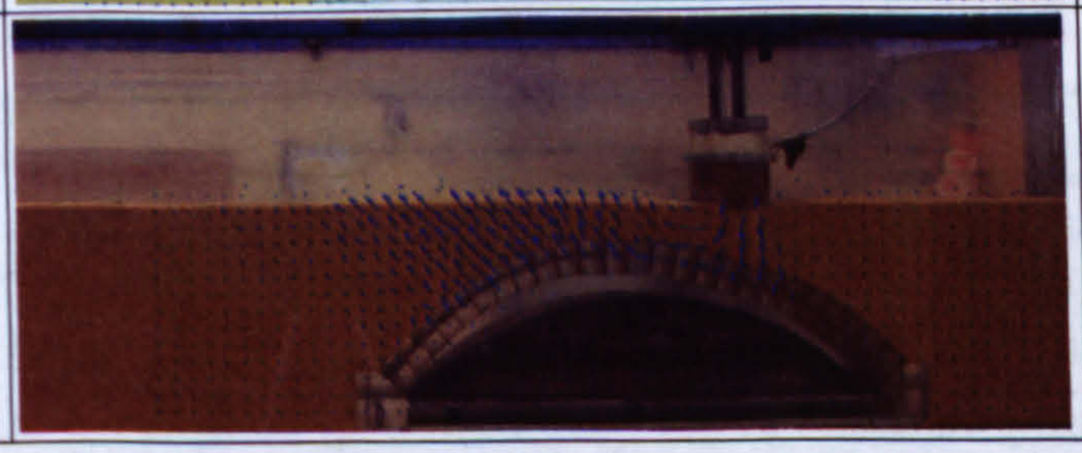	178	177	179

Table 4-3 Peak load of each scenario tested (Arrow magnification factor = 25)

4.3.4 Visual Imaging Analyses

The use of the adopted visual imaging technique has been proven to work very well for these types of tests involving both structure and soil components. Photographs from the series of tests were each analysed using the Particle Imaging Velocimetry technique (hereon referred to as GeoPIV). The system works by comparing image captures of the same point but taken at different times. By allocating a pixel colour to the centre of a sector in a grid and tracking it, plotting of the relative kinematic velocities are possible. Table 4-3 shows GeoPIV images produced for each test showing displacements at peak load.

Extended Voussoir Influence

The influence of the extended voussoir can be examined using the kinematics obtained for T4 and T9 from GeoPIV are shown in Figures 4-8 & 4-9 respectively. As can be seen the difference between having an extended voussoir and a normal voussoir was negligible both from a kinematics and a peak load point of view.

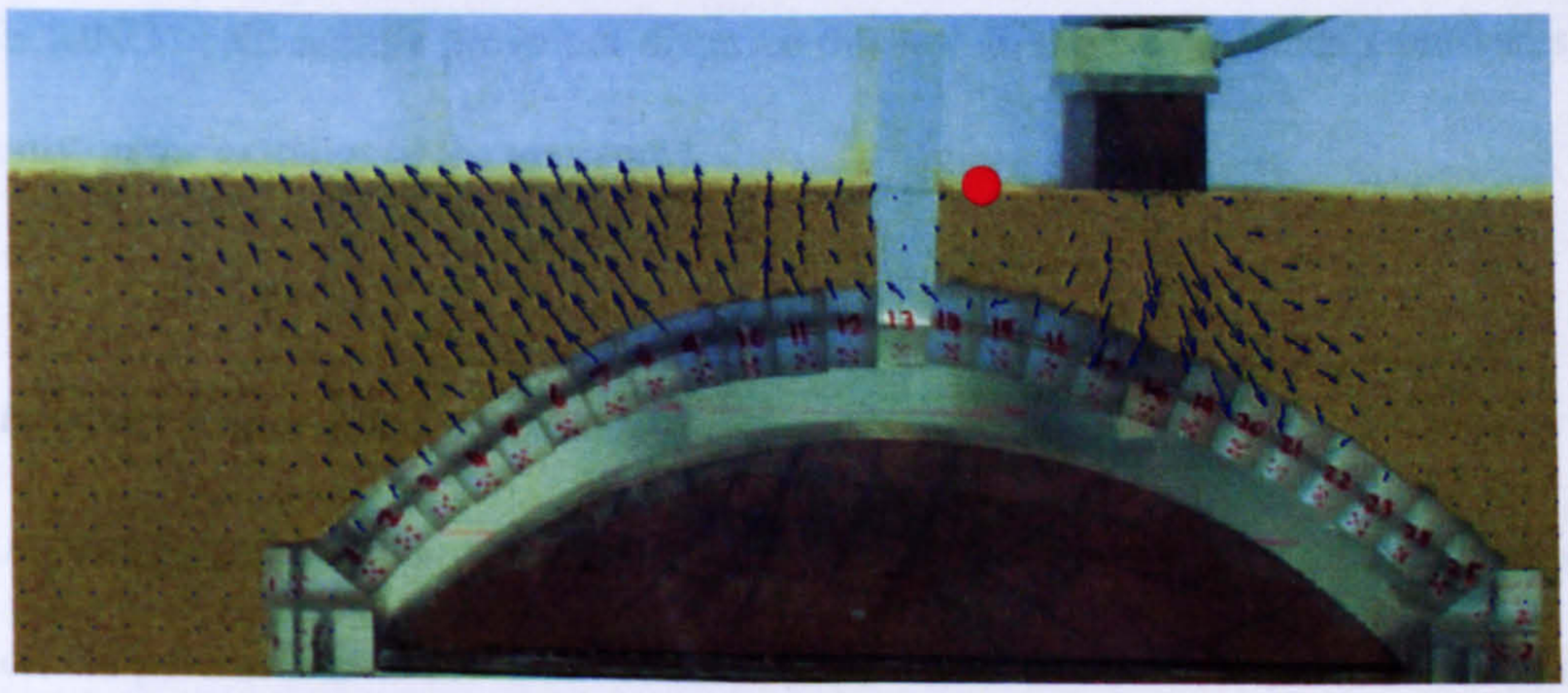

Figure 4-8 T4 Kinematics (Arrow magnification factor = 25)

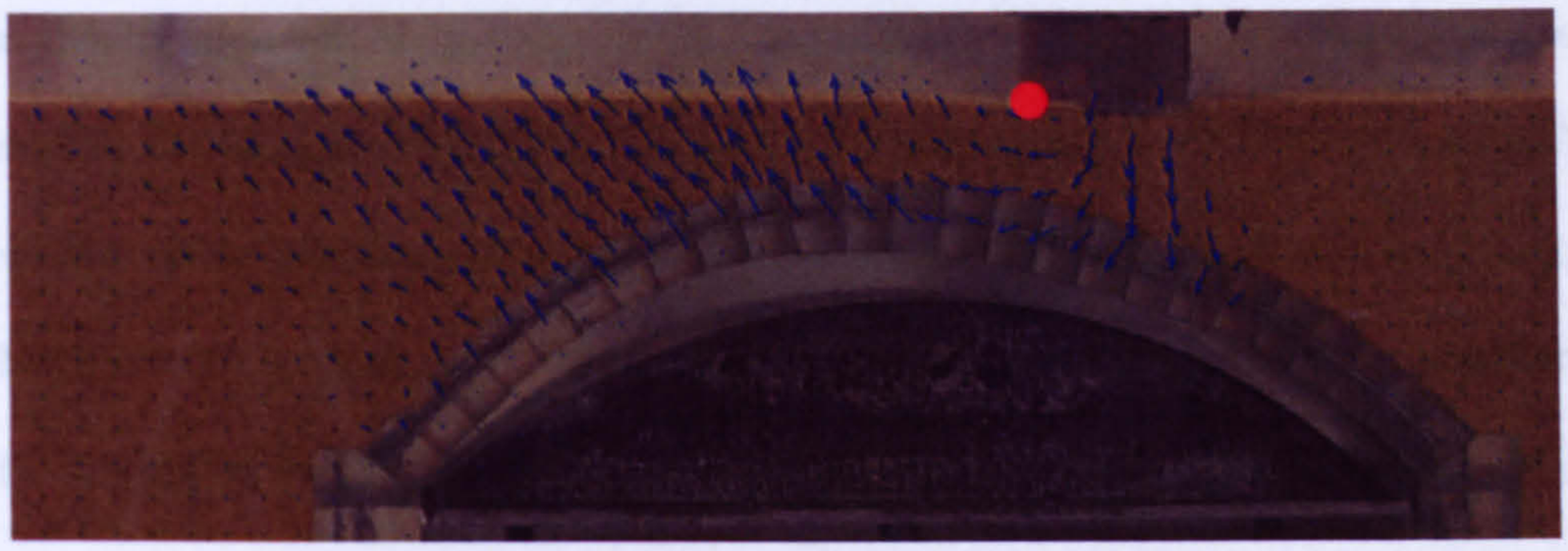

Figure 4-9 T9 Kinematics (Arrow magnification factor = 25)

In the area under the load that in the case of the non-extended voussoir the arrows are all focused pretty much vertically downwards where as in the extended voussoir case they are much more fan like. The other observation of significance is that the centre of rotation (denoted in Figure 4-9 as ●) is nearer to the applied load when the voussoir is not extended. These two features imply that a proportion of the soil failure without an extended voussoir is similar to a bearing failure and that when the extended voussoir is present this bearing part is forced (reflected) to the non-preferred side. However, as the results show this has a negligible effect on the peak load carrying capacity of the model. [The slightly higher load capacities may be attributed to the work required to move the extended voussoir, however, modelling in RING could neither prove not disprove this due to the way it models pressures only on the extrados of the voussoir.]

Influence of Sidewall Friction

An independent test (given in Section 5.4.2) was designed to replicate fill stresses on the passive side of the arch. In these areas lateral strains were much lower than directly under the load. It was therefore asked whether the increase in lateral stress

at this location contributed significantly to the reduction in the load capacity of the models in question. The digital images were fed into AutoCAD 2004 and the soil wedge under the load plate being moved downward was calculated using the MASSPROP command. Together with the experimental data, the equation $F=\sigma_h.\mathrm{Tan}\delta A$ (where $\sigma_h=K_O\gamma z$) was used in each case to work out what the sidewall friction load was. In all instances it came back as having a small effect on the overall carrying capacity (<10%).

4.3.5 Analysis of Results

Figure 4-10 shows the averaged load displacement graphs for the deep and shallow filled arch tests showing vertical displacement of the loading plate and of the voussoir directly below the load plate. This was obtained via the GeoPIV analysis utilising the vertical vector generated by tracking the load plate and the respective voussoir. Because there is some horizontal movement of the load as the arch rotates under the applied force this means that the peak vertical stress is slightly off centre of the loaded area for the cases where fill exists between the load plate and the arch extrados, however, due to the small rotations involved the effect on the value of the peak stress is negligible.

The greatest variability between the three repeat tests was during loading when the backfill compressed under the load plate and near the end of the test when gross deformation of the arch was present. The results for tests T4, T6 and T9 show deviation between the two displacements right from the start. This clearly indicates

localised partial bearing capacity failure on top of the underlying arch movement. For the other tests, displacement deviations occurred post peak due to the load screws sliding on the extrados of the arch as it deformed away from the vertically applied load system.

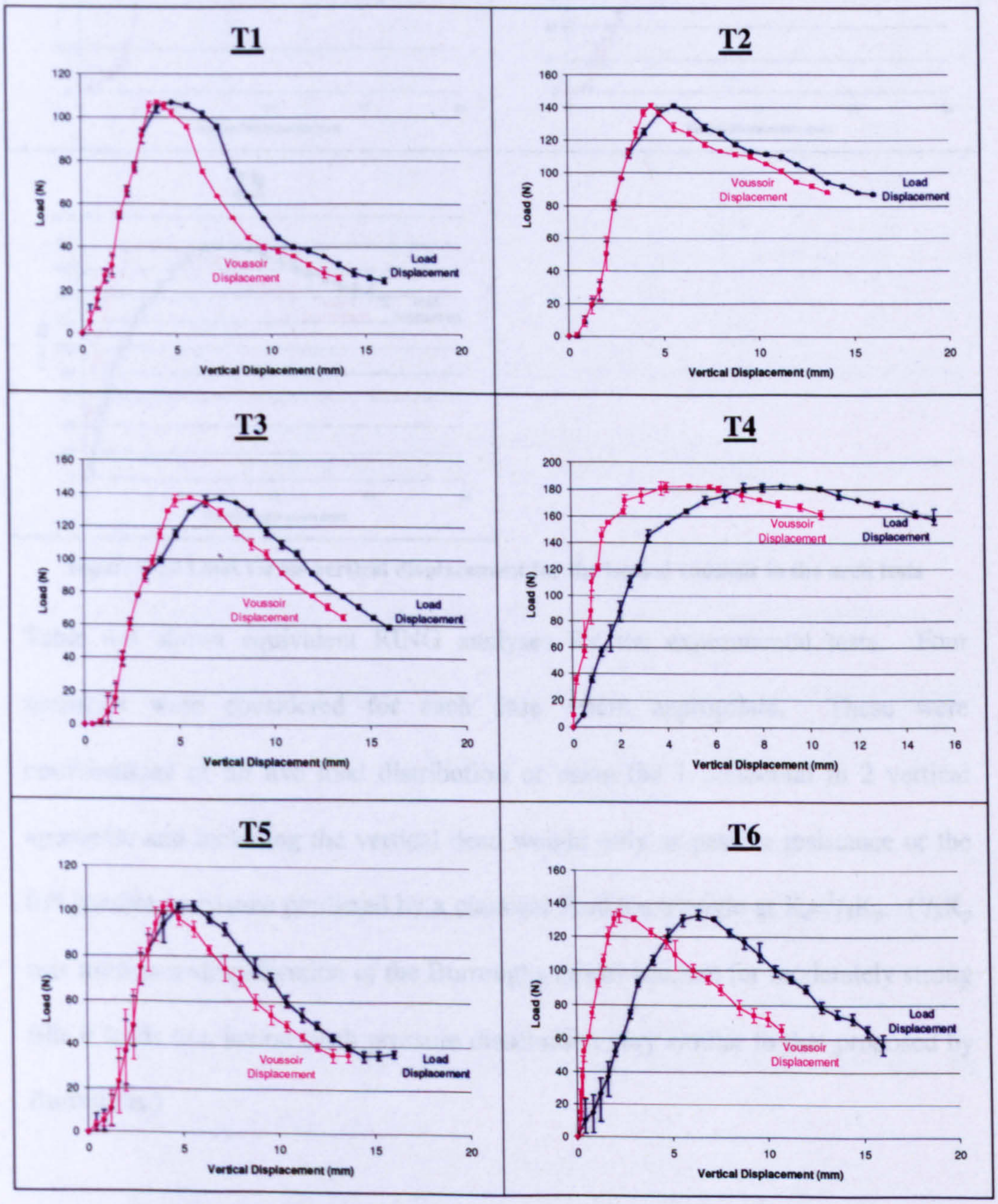

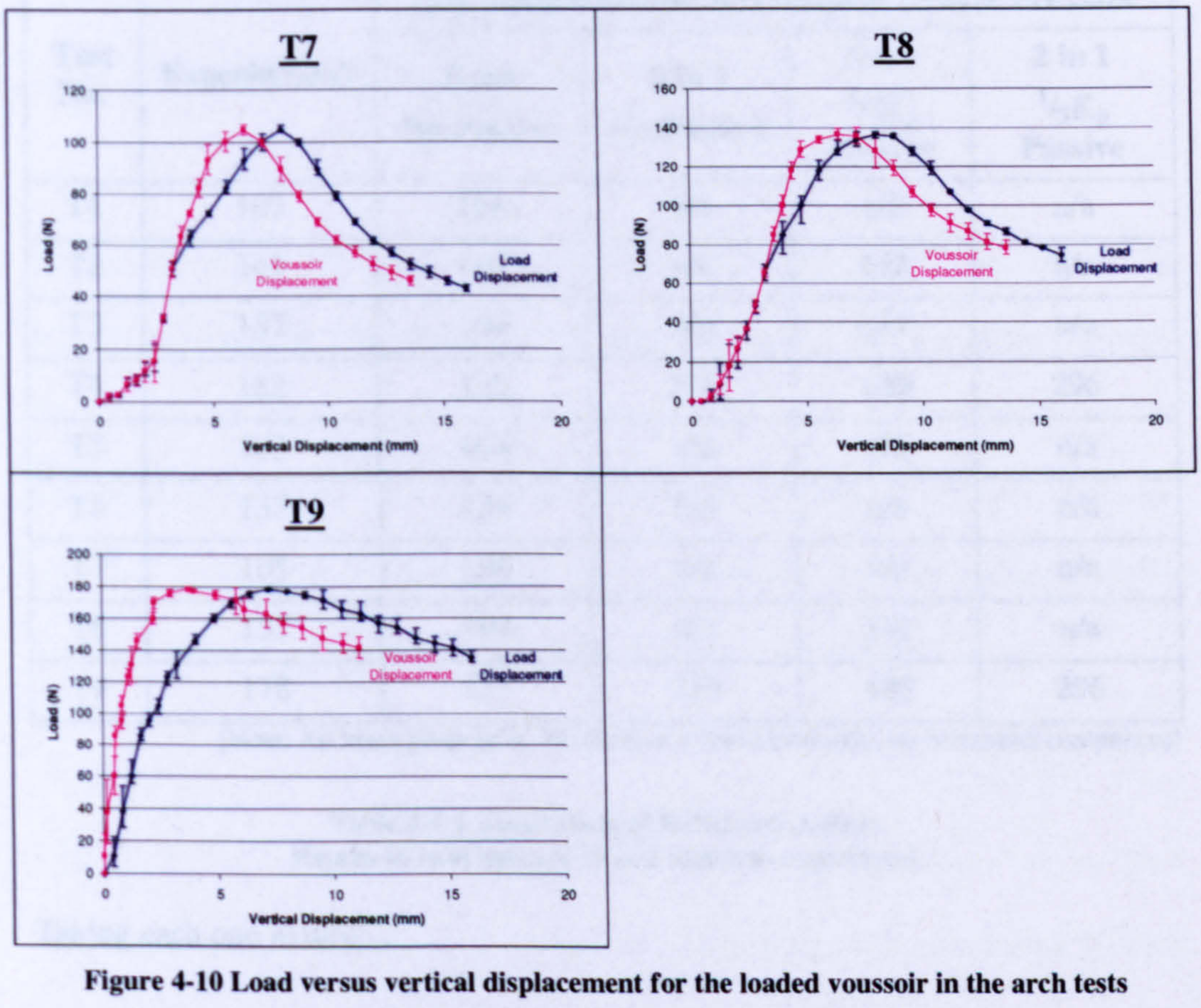

Figure 4-10 Load versus vertical displacement for the loaded voussoir in the arch tests

Table 4-4 shows equivalent RING analyses for the experimental tests. Four scenarios were considered for each case where appropriate. These were combinations of no live load distribution or using the 1 horizontal in 2 vertical approach, and including the vertical dead weight only as passive resistance or the full passive resistance predicted by a classical Rankine triangle at $K_e = {}^1/_3 K_p$. (${}^1/_3 K_p$ was used as a simplification of the Burroughs model because for moderately strong fills it leads to a lateral earth pressure distribution very similar to that proposed by Burroughs.)

Test No.	Experimental	Live Load Distribution / Backfill Passive Pressure			
		None No Passive	2 in 1 No Passive	None $^1/_3K_p$ Passive	2 in 1 $^1/_3K_p$ Passive
T1	107	106	n/a	n/a	n/a
T2	141	106	n/a	**143**	n/a
T3	137	104	n/a	**141**	n/a
T4	182	135	215	**185**	296
T5	103	**104**	n/a	n/a	n/a
T6	133	**135**	215	n/a	n/a
T7	105	**106**	n/a	n/a	n/a
T8	137	104	n/a	**141**	n/a
T9	178	135	215	**185**	296

[Note: All loads given in N. No Passive = Dead load only, no horizontal component]

Table 4-4 A comparison of RING simulations.
Results in bold indicate closest match to experiment.

Taking each one in turn:

- T1 shows that RING agrees well with the experiment for this scenario.
- T2 shows that a triangular pressure distribution using $K_e=0.33K_p$ represents a good correlation between RING and the experimental test.
- T3 shows a slight discrepancy which can be put down to RING not taking any consideration of the active pressure. The error is small at about 3% and can be considered in most cases negligible.
- For T4 the experiment agrees well with no load distribution and the $K_e=0.33K_p$ passive pressure.
- T5 Once again RING shows good agreement with the experimental result.
- T6, the experimental result agrees well with no load distribution.

- T7-T9 are repeats of previous experiments without the extended voussoir and show that the effect of the extended voussoir was negligible.

In all instances the use of the 2 in 1 live load distribution would have produced a higher load capacity than what was in reality available. The use of no live load distribution produced very similar capacities to those demonstrated by the experiments; however, even this was slightly over estimating the true live load capacity. In order to quantify the reasoning behind this small discrepancy further numerical investigations were undertaken: Scenario 1 and Scenario 2.

Scenario 1

The first investigation looked at whether the value for K_e was incorrect and by back calculating, taking $K_e = \alpha K_p$, α was varied to obtain a load capacity identical to the corresponding experimental value. This scenario only applied to the experiments where the horizontal component of passive pressure was present, i.e. T2, T3 and T8 as shown in Table 4-5.

Test No.	Value of K_e Required for Experimental Agreement	Corresponding α Value
T2	1.75	0.32
T3	1.65	0.31
T8	1.65	0.31

Table 4-5 α value required for experimentally determined load capacity

These results indicate that an assumption of $K_e=0.33K_p$ would be a viable semi-empirical model for this scenario.

Scenario 2

In the second scenario the live load distribution angle (β) was varied in order to obtain the exact experimental load, assuming α=0.33. This time only test numbers T4, T6 and T9 were investigated as they were the only tests to have the ability for live load distribution. Since it is not possible to enter negative (i.e. load narrowing) into RING, the live load length was changed and the angle back calculated in order to determine the distribution angle provided by the fill. In all instances the loaded length was reduced from 38mm to 36.5mm before the required result was obtained (i.e. β= -8.77°). This showed that rather than exhibiting the predicted 1 in 2 distribution the live load may have been concentrated on a narrower strip as it passed through the backfill, however, there is insufficient experimental evidence to substantiate this at this time.

4.3.6 Theoretical Indications

While it is beyond the scope of this paper to derive a complete analytical solution to the arch-soil interaction problem, insights can be obtained from the study of analogous problems.

Load Spreading

Smith (2005) presented an investigation of the stress field below a footing undergoing bearing capacity failure. The results at depth B below a footing of width B are given in Figure 4-11 and show that the load is significantly more focused than predicted either by a Boussinesq distribution or a 2:1 spread.

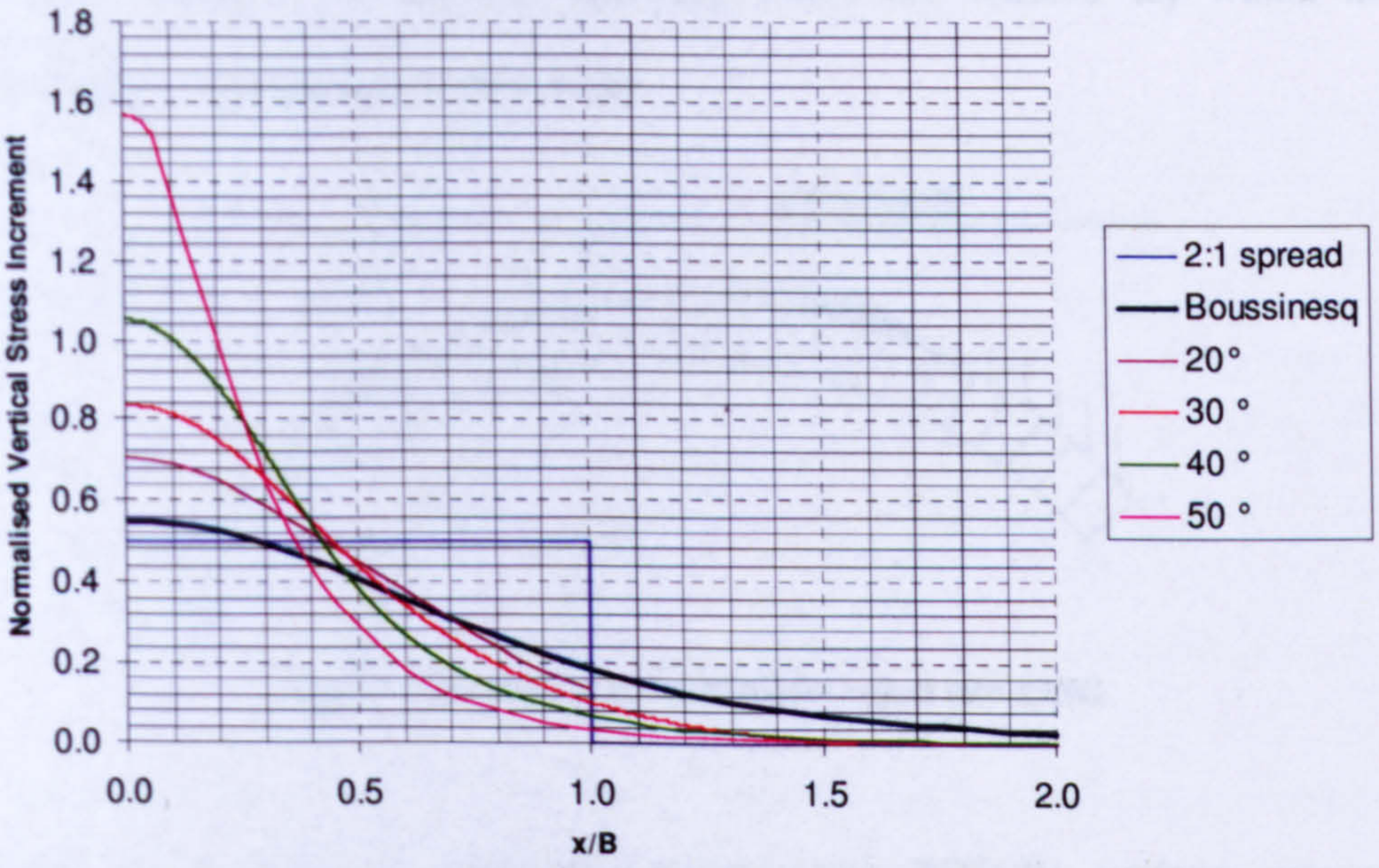

Figure 4-11 Normalised vertical stress increment distributions acting at depth B beneath rough footing, $q/\gamma b=0$,

Table 4-6 compares the results of RING simulations using the stress distributions from Smith (2005), a 2:1 distribution and a truncated Boussinesq distribution (Figure 4-12).

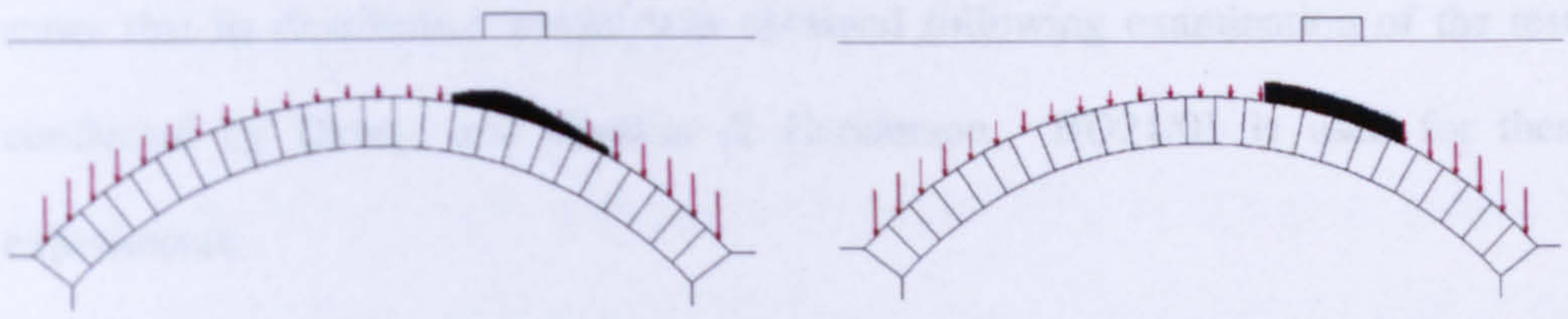

Figure 4-12 Boussinesq distribution (Left) versus 2:1 type distribution (Right)

Since it is currently not possible to use the Smith model in RING the vertical load for each voussoir was adjusted manually where the voussoir lay within the distribution envelope, (see Figure 4-13).

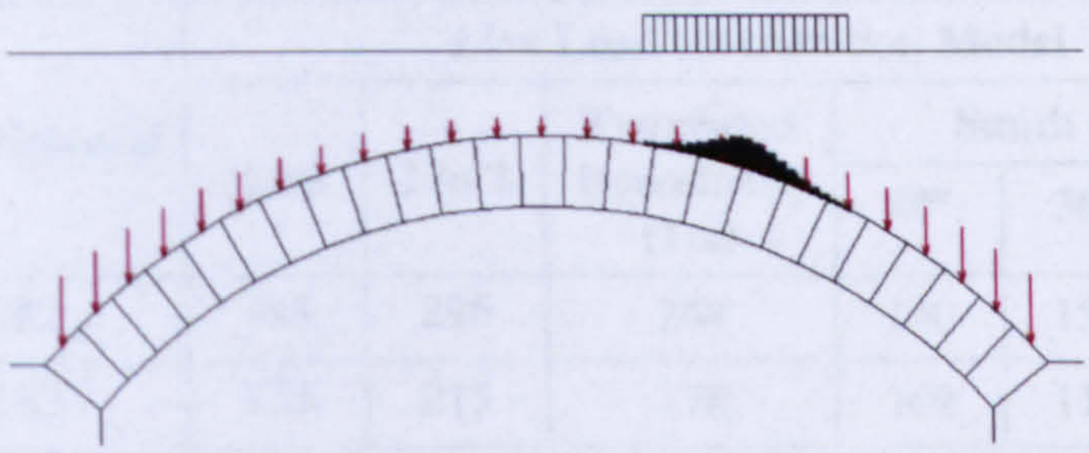

Figure 4-13 Smith distribution model edited into RING

Figures 4-14 shows a comparison between the BD21/01 uniform pressure distribution and an equivalent 2 in 1 obtained from an equivalent pressure bulb.

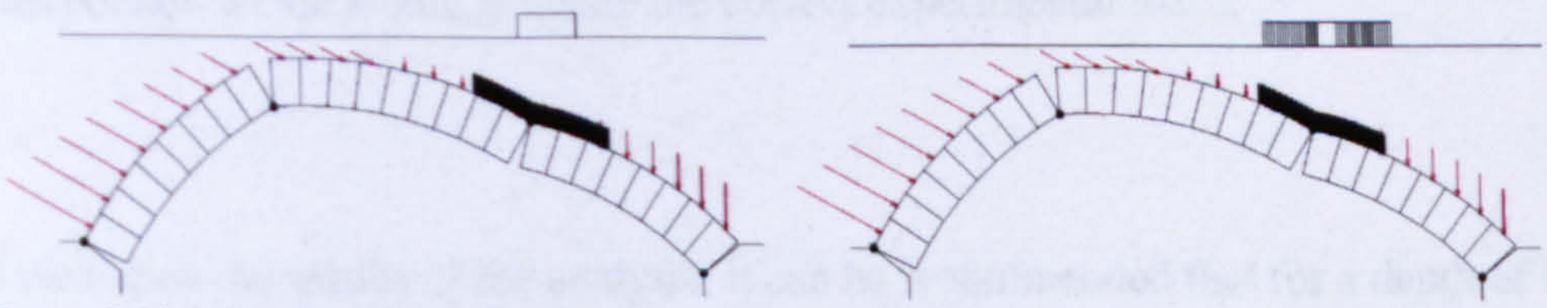

Figure 4-14 A 2 in 1 uniform distribution as given by BD21/01 (Left) versus equivalent bulb of pressure (Right)

The collapse load predicted for the BD21/01 model was 268kN whereas for the equivalent pressure bulb it was predicted at 194kN. The bulb of pressure equivalent is more conservative than the BD21/01 distribution model; however, BD21/01

states that its distribution model was obtained following examination of the tests conducted by Davey, and Chettoe & Henderson. BD21/01 is used for these experiments.

Table 4-6 shows a comparison of the predicted results for load carrying capacity using the four different approaches all using the full passive resistance ($K_e={}^1/_3K_p$, $\phi'=44°$) where applicable.

Test No.	Experimental	Live Load Distribution Model					
		None	1 in 2	Truncated Boussinesq (1:2)	Smith (2005)		
					40°	30°	20°
T4	182	185	296	244	140	151	170
T6	133	134	215	178	102	110	123

Table 4-6 Comparison of live load distribution models for RING simulations

The results show that using the measured peak soil angle of shearing resistance of 44° would significantly underestimate the carrying capacity of the arch, i.e. the live load was focussed too much. However, for both T4 and T6 an angle of 15° can be interpolated which would generate the correct experimental loads.

Based upon the results of the analysis, it can be recommended that for a depth of fill that is the same value as the width of the load plate either a reduced mobilised angle is taken utilising the distribution of Smith (2005) or in the most simplistic case the use of no load spreading should be considered for this type of fill.

4.4 Passive Resistance

It is possible to use the soil kinematic analysis from GeoPIV as a guide in order to model the passive displacements of the arch. When considering the passive side kinematics, an idealised failure mechanism of sliding rigid blocks as shown in Figure 4-15 can be assumed. In Figure 4-14 the displacement vectors are orientated on average at an angle of 49° to the horizontal.

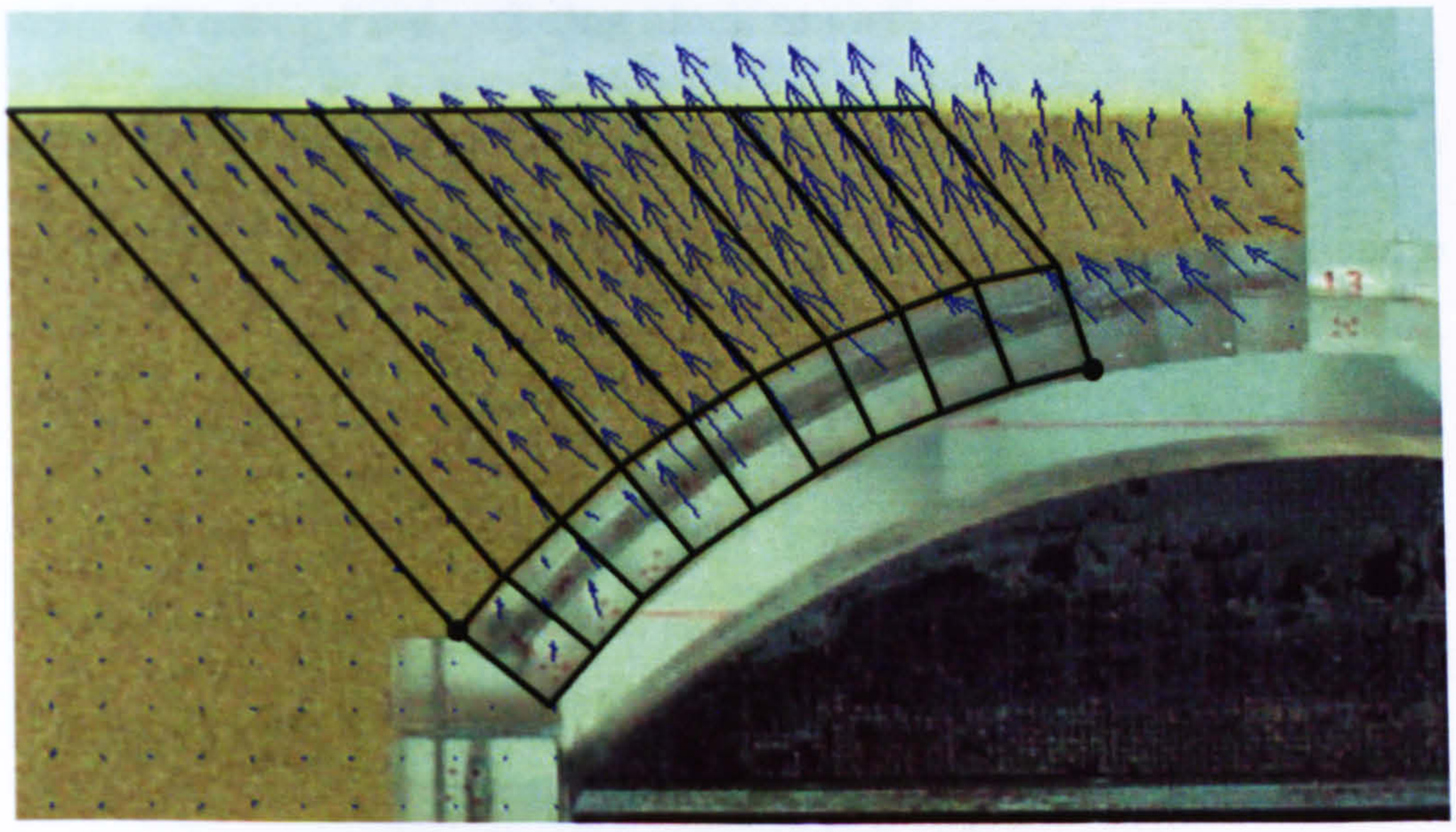

Figure 4-15 Soil wedge representation of failure kinematics (Arrow magnification factor = 25)

Starting with a simple idealisation model as shown in Figure 4-16 a known limit angle numerical model can be established for a cohesionless material based upon external work and internal energy dissipation under equilibrium conditions. This is used to gain theoretical insight into the empirically derived horizontal stress model of 1/3 K_P, rather than model the full arch-soil interaction.

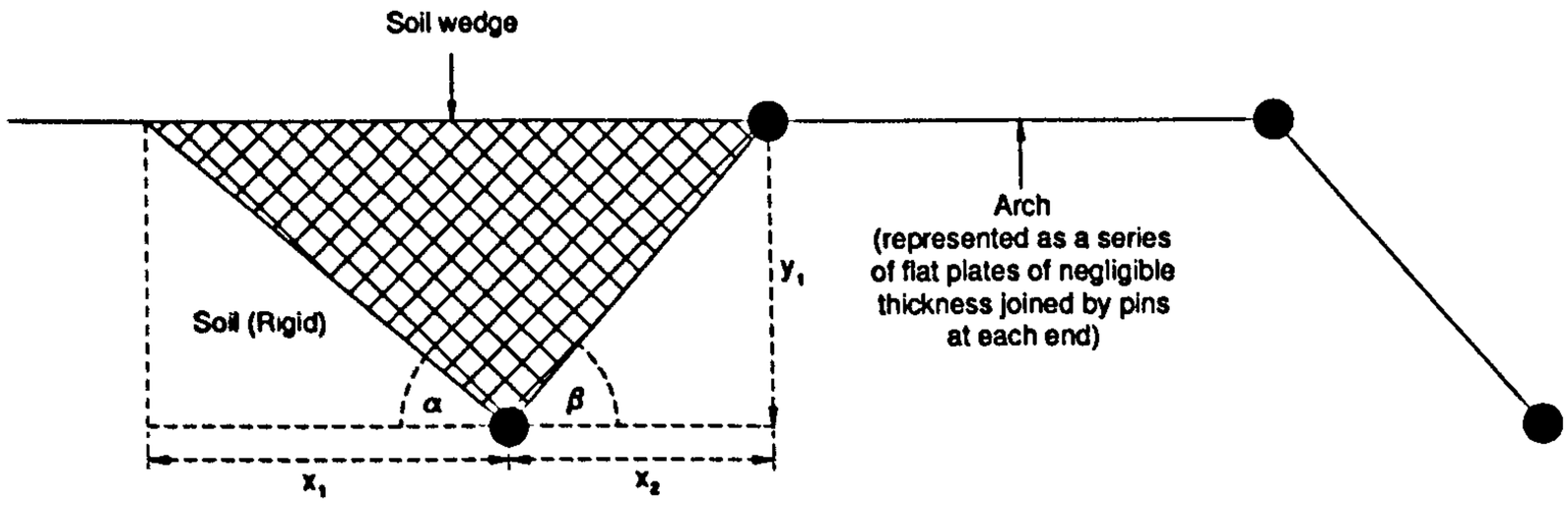

Figure 4-16 Simple wedge analogy

4.4.1 Rotating Plate – sliding block model[1]

Figure 4-17 depicts a uniform horizontal stratum of soil containing a plate hinged at the base O at angle β to the positive x-axis extending to the top of the stratum at point E.

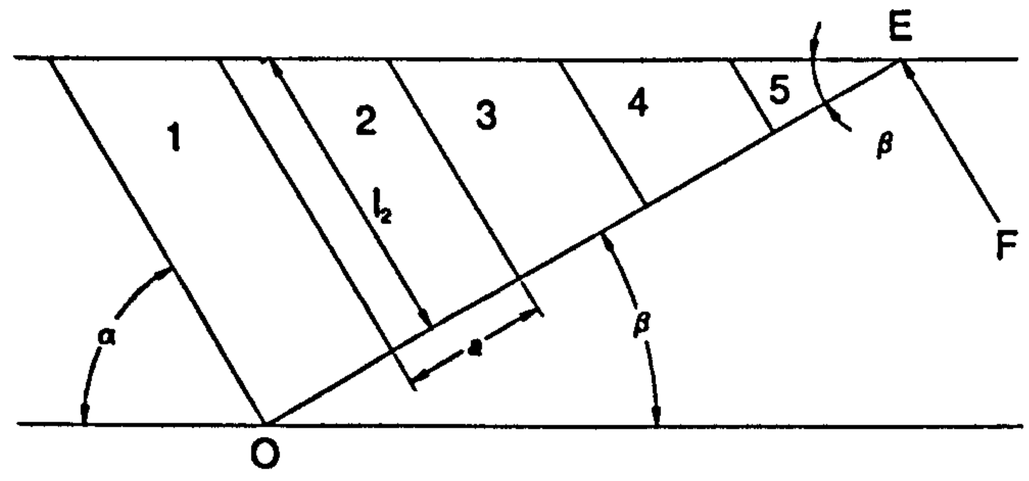

Figure 4-17 Sliding blocks

This plate rotates at an angle $\delta\Theta$ anticlockwise. Assuming that the soil deforms in n equal width sliding blocks, each block of width a measured along the plate, each sliding on a plane oriented at an angle a to the negative x-axis. Assume soil dilation angle ψ and plate interface angle of dilation δ. Figure 4-18 shows the corresponding hodograph.

[1] This model was proposed and developed by C.C. Smith of the University of Sheffield

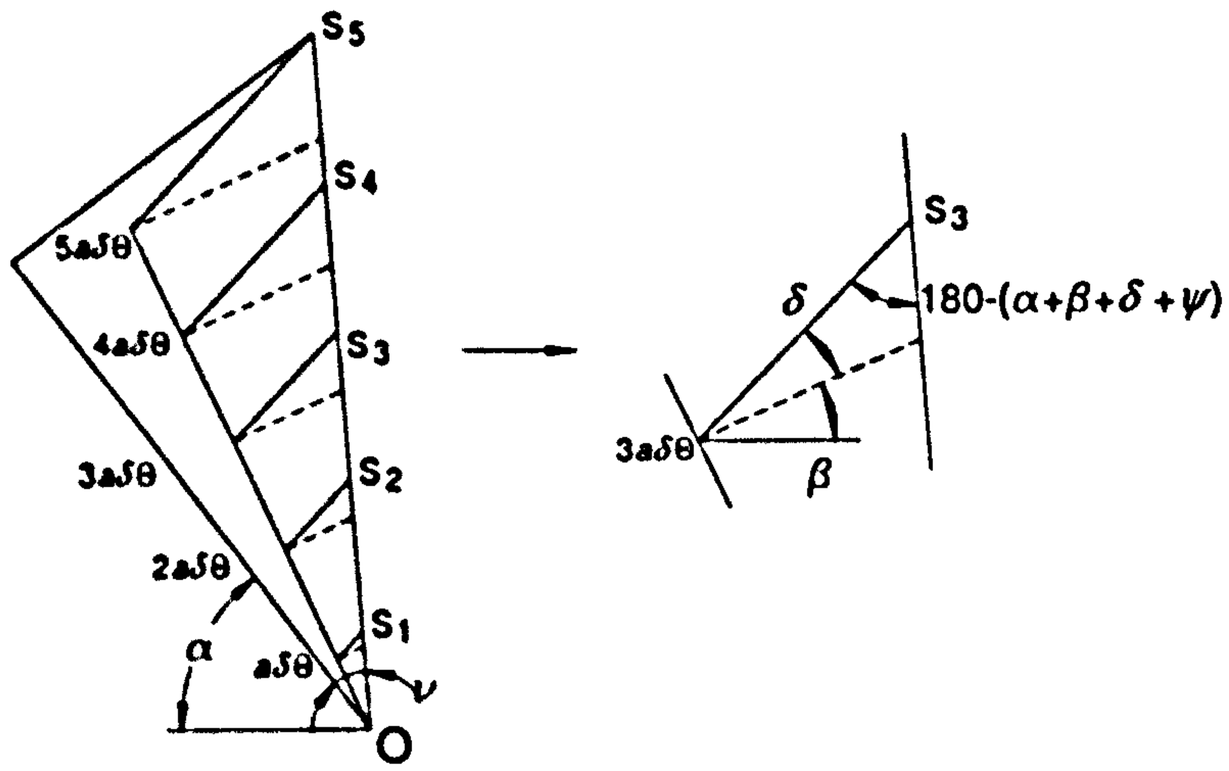

Figure 4-18 Hodograph

Number the blocks 1..*n* from O. Let l_i be average length of block *i* as indicated in Figure 4-16.

$$\frac{\sin\beta}{li} = \frac{\sin\alpha}{(n-i+0.5)a} \tag{4.1}$$

Block *i* has an area:

$$(a\cos(90-(\alpha+\beta)))\left[\frac{\sin\beta}{\sin\alpha}(n-i+0.5)a\right] \tag{4.2}$$

Block *i* moves s_i:

$$\frac{\sin(180-(\alpha+\beta+\delta+\psi))}{ia\delta\theta} = \frac{\sin(90+\delta)}{s_i} \tag{4.3}$$

Rearranging gives:

$$s_i = \frac{ia\delta\theta\cos\delta}{\sin(180-(\alpha+\beta+\delta+\psi))} \tag{4.4}$$

Vertical movement is given by:

$$v_i = s_i \sin(\alpha+\psi) \tag{4.5}$$

Now calculating the work done against gravity, W_i:

$$W_i = \frac{\rho g a^3 i(n-i+0.5)\delta\theta \sin(\alpha+\beta)\sin\beta\cos\delta\sin(\alpha+\psi)}{\sin\alpha\sin(\alpha+\beta+\delta+\psi)} \tag{4.6}$$

Assume normal force on plate at end E is F, thus equating work terms:

$$Fna\delta\theta = \frac{\rho g a^3 \delta\theta \sin(\alpha+\beta)\sin\beta\cos\delta\sin(\alpha+\psi)}{\sin\alpha\sin(\alpha+\beta+\delta+\psi)} \sum_{i=1}^{n}(n-i+0.5)i \tag{4.7}$$

Making $L=na$, as $n\to\infty$ and thus $a\to 0$, the work balance equation can be expressed by the integral:

$$FL\delta\theta = \frac{\rho g \delta\theta \sin(\alpha+\beta)\sin\beta\cos\delta\sin(\alpha+\psi)}{\sin\alpha\sin(\alpha+\beta+\delta+\psi)} \int_0^L (L-x)x\,dx \tag{4.8}$$

$$\Rightarrow FL = \frac{\rho g \sin(\alpha+\beta)\sin\beta\cos\delta\sin(\alpha+\psi)}{\sin\alpha\sin(\alpha+\beta+\delta+\psi)} \left[\frac{Lx^2}{2} - \frac{x^3}{3}\right]_0^L \tag{4.9}$$

$$\Rightarrow F = \frac{\rho L^2 g \sin(\alpha+\beta)\sin\beta\cos\delta\sin(\alpha+\psi)}{6\sin\alpha\sin(\alpha+\beta+\delta+\psi)} \tag{4.10}$$

4.4.2 Rotating plate - empirical model

If it assumed that the stresses acting on the rotating plate are as follows:

$$\sigma_v = \rho g z \tag{4.11}$$

$$\sigma_h = aK_p\sigma_v \tag{4.12}$$

Thus if the plate is orientated at β to the horizontal, the normal stress on the plate will be given by:

$$\sigma_n = \frac{\sigma_v(1-\sin\phi\cos 2\beta)}{1-\sin\phi} \tag{4.13}$$

Taking moments about O gives the equivalent normal force at the end of the plates as:

$$F = \frac{\rho_s L^2 \sin\beta(1-\sin\phi\cos 2\beta)}{6(1-\sin\phi)} \tag{4.14}$$

Equating equation 4.14 to 4.10, allows a value of ϕ to be derived for use in the simple K_p model that will give the same global effect on the plate as the sliding block model.

4.4.3 Analysis

Using MatLAB to calculate and minimise the internal work for the properties given in Table 4-2 and the idealised arch shown in Figure 4-15, a critical angle of α=36° is derived (see Figures 4-19 and 4-20) based on an angle of β=31° for the associative case (i.e. ψ=5.5°, δ=8°). Taking into account dilation, this implies an actual soil displacement vector of 54° to the horizontal. The equivalent angle ϕ for the simple K_p based model is 44°. Neither of these values match the experimental data of soil displacement angle at 49° and equivalent ϕ=16° which gives K_p=1.76 = 0.33K_p when ϕ=44°.

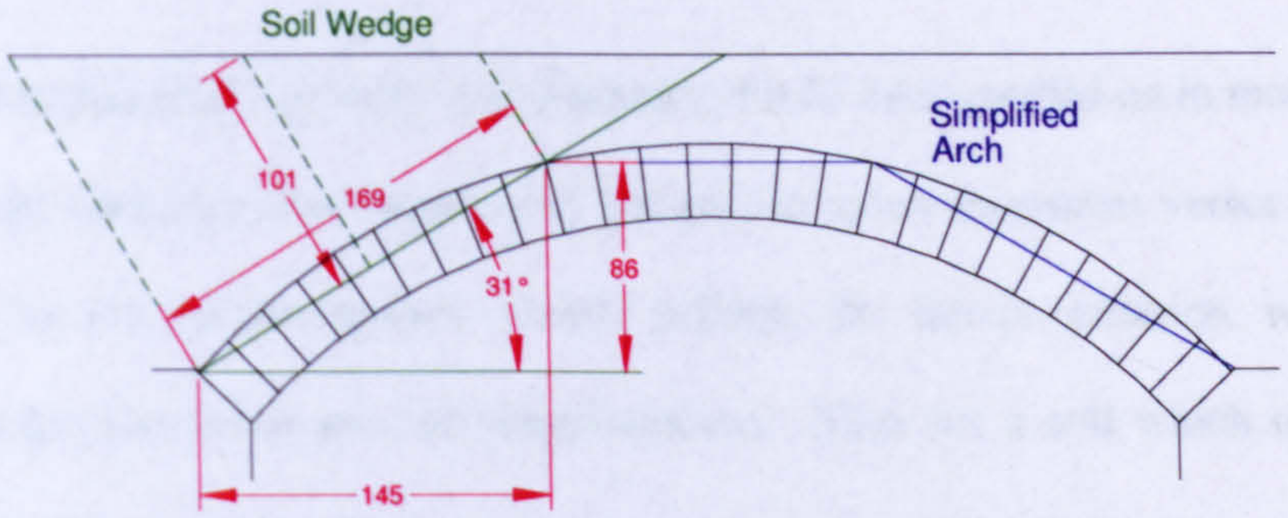

Figure 4-19 Idealised arch

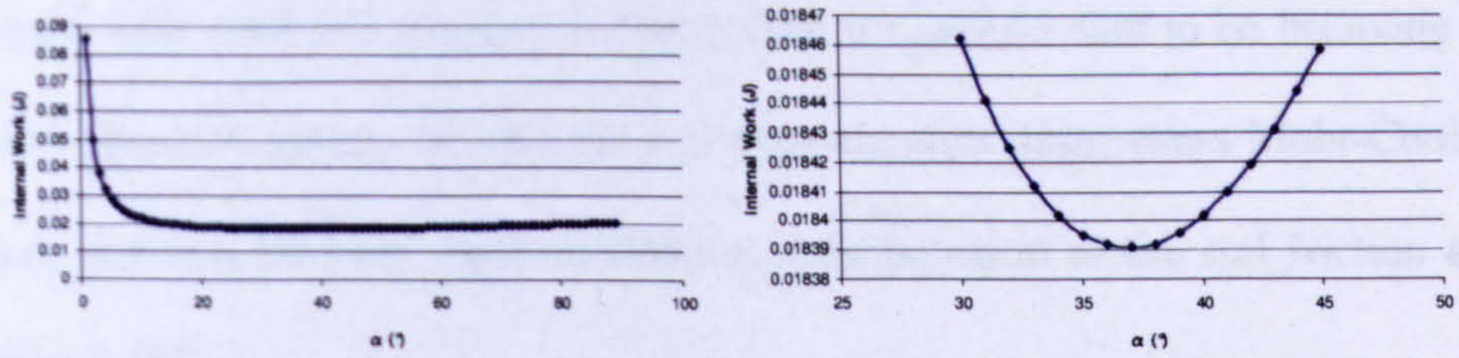

Figure 4-20 Angle α versus internal work

This discrepancy can be attributed to four possible factors:

1. Inadequacy of the sliding block model
2. Incorrect choice of soil-extrados friction angle δ
3. Assumption of associative flow (which is in general incorrect for cohesionless soils)
4. Partial mobilisation of soil strength

Normality

It is at this point that normality and dilatency should be expanded on in more detail. Regarding normality, the direction of the plastic strain increment vector must be normal to the failure surface which defines the failure criterion when the deformation and stress axes are superimposed. Thus for a soil which obeys the maximum shear stress criterion ($\tau_u=\tau_{max}$), the soil volume deforms at a constant rate which is consistent with critical state. Therefore, if the soil is a clay with a constant void ratio and moisture content, then it could be said to be behaving as a perfect plastic material. Should the soil obey the maximum stress Mohr-Coulomb failure criterion then the angle of dilation must be equal to the soil friction angle (Figure 4-21).

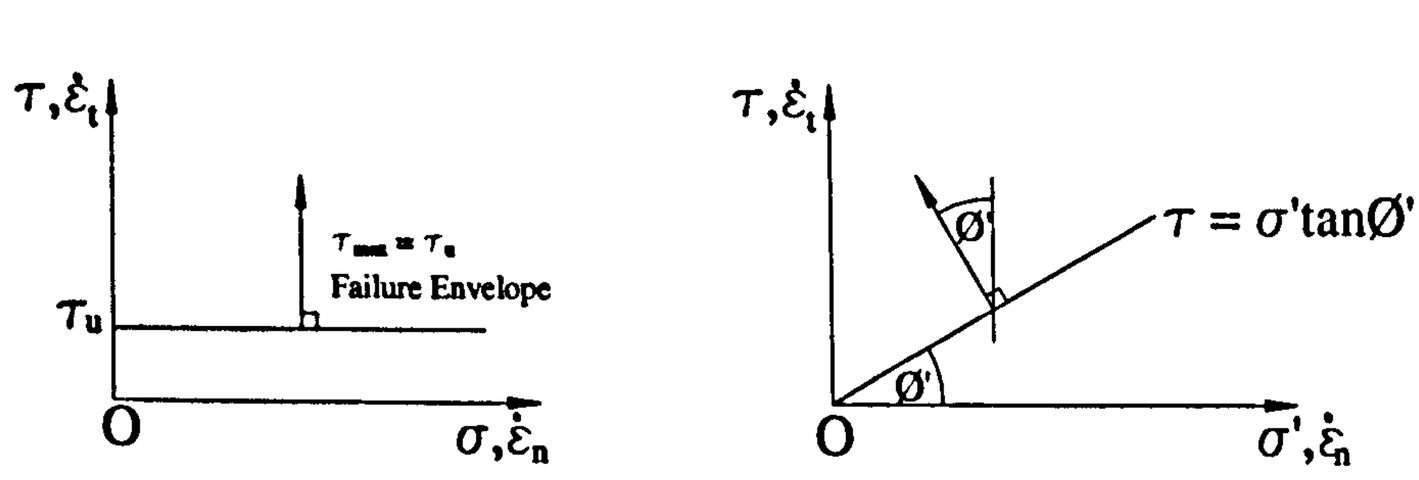

Figure 4-21 Normality

Where ε_t = stain increment tangential to the potential failure plane and ε_n = strain increment normal to the potential failure plane.

Dilation

By considering a direct shear test, when the top half of the shear box moves relative to the bottom, the lid of the shear box rises. This is caused by the shearing particles re-aligning as a result of their movement. This effect is known as dilation and the results obtained from a shear box test can be used to calculate the angle of dilation (Figure 4-22).

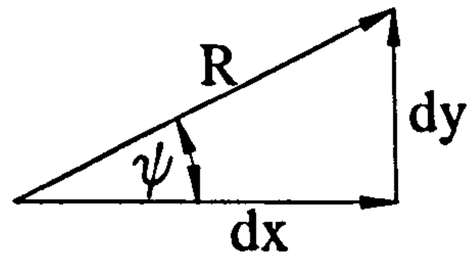

Figure 4-22 Angle of dilation

Where R = actual direction of movement, dx = change in x displacement, dy = change in y displacement, ψ = angle of dilation.

Maximum Dilation

Since there is only a finite amount of soil within the shear box only a finite amount of dilation can occur. Once this peak value has been reached the vertical displacement value begins to reduce, never quite reaching the starting value of dy.

Soil Friction Angle

It is important not to confuse dilation, ψ, with internal soil friction angle, ϕ. Having one block of soil sheared in half creates a failure criterion based upon the horizontal, vertical forces and the angle of friction within the soil (Figures 4-23 and 4-24).

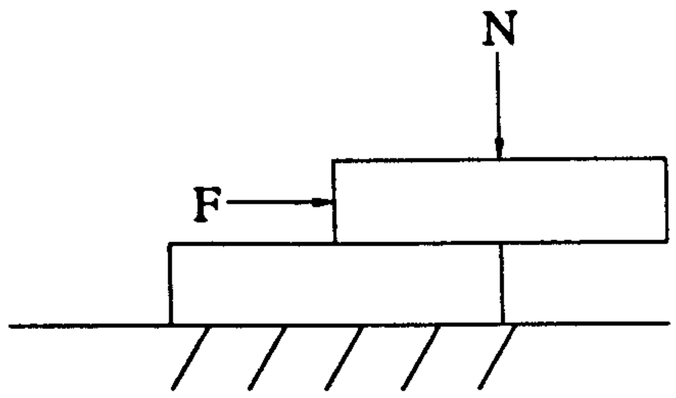

Figure 4-23 Simple illustration of the Direct Shear Test

If: $F < N.\tan\phi$ then the soil will remain stationary.

$F = N.\tan\phi$ then the soil is on the equilibrium limit.

$F > N.\tan\phi$ then the soil will begin to slide.

Where, F = horizontal force, N = vertical force, ϕ = angle of friction.

Graphically illustrated:

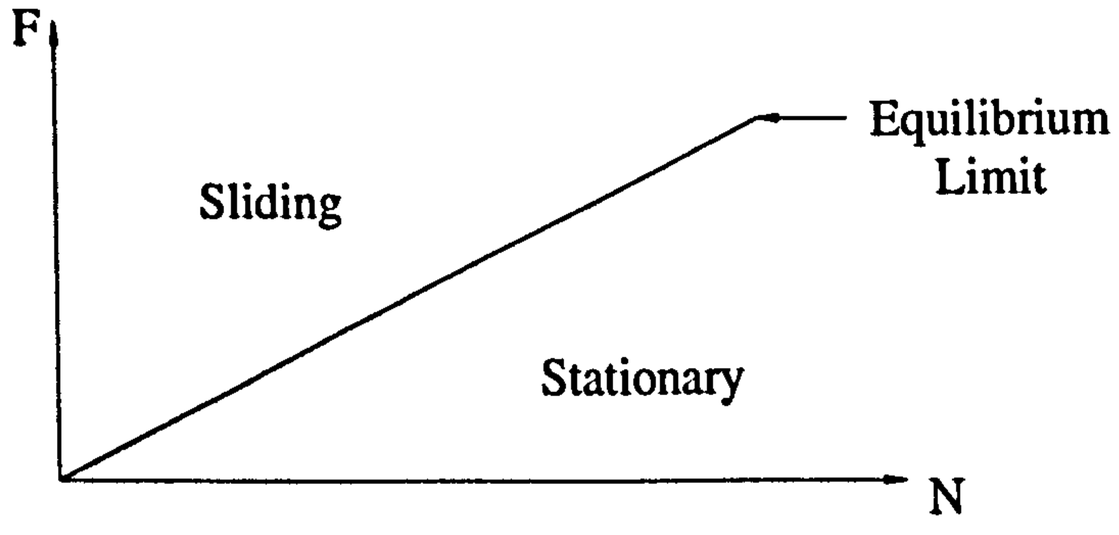

Figure 4-24 Graphical representation of Figure 4-21

In the above example, shear stress can be determined and so can the total normal stress by dividing the respective forces by the cross sectional area (A), i.e.

$\tau = F/A$ and $\sigma = N/A$.

Now by carrying out several shear box tests and varying the vertical load, N, thus incrementally increasing the direct stress and constructing the Mohr's circles of effective stress, a pattern begins to emerge. By drawing a line tangential to the Mohr's Circles a failure envelope for sliding can be found (Figure 4-25).

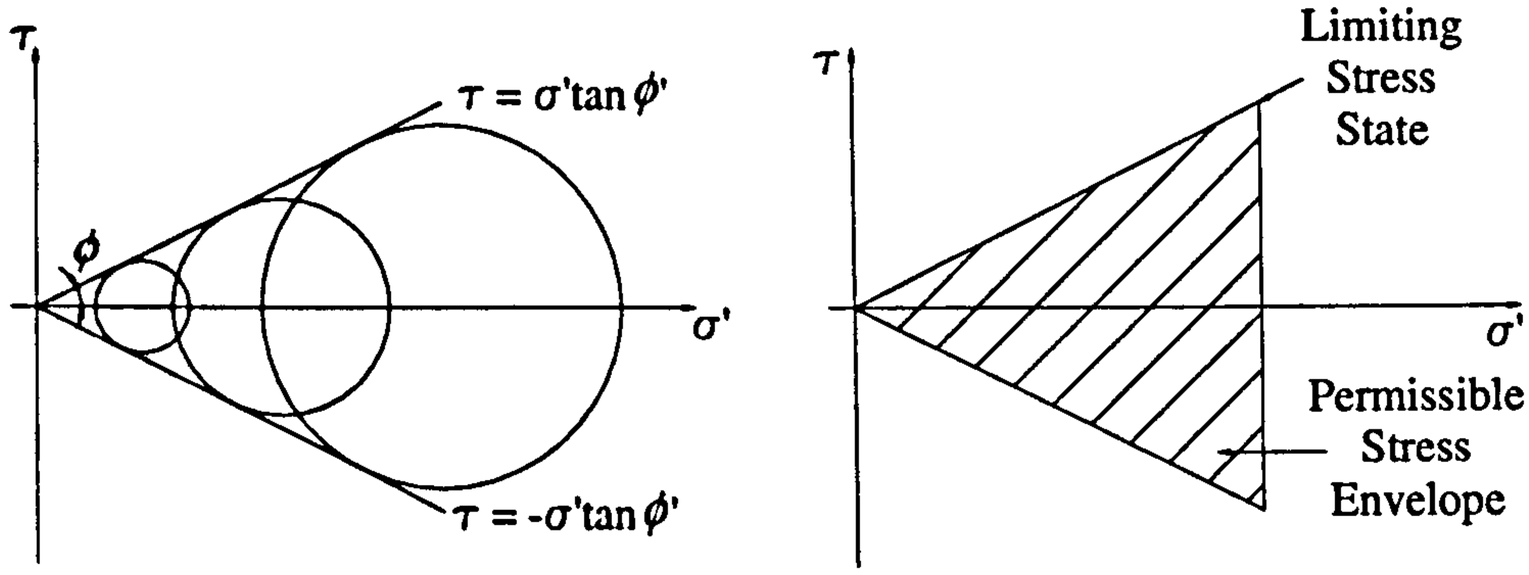

Figure 4-25 Mohr's circles showing the limiting stress envelopes

Sliding Block Model

It will be assumed that the sliding block model is applicable since this is broadly what is observed from the soil kinematics. The soil-extrados interface friction angle is improbable to be equal to ϕ and although it was not directly measured during the tests, it is probable to be higher than interface angle between the soil and the acrylic side walls. This is because the voussoirs had rough machined faces, compared with the float finish of the side walls.

Non-associative flow may be addressed using the theorem of Drescher & Detournay (1993). Both fully associative flow and non-associative flow with zero-dilation will be investigated. According to Drescher & Detournay, the same sliding block mechanism analysis may be used for non-associative flow and associative flow, provided that modified dilation parameters ν_n and δ_n are used for the calculation in the case of the former.

For zero actual dilation:

$$\sin\psi = \tan\psi_{cv} \tag{4.15}$$

$$\sin\delta = \tan\delta_{cv} \tag{4.16}$$

If soil strains are not large enough, then not all the soil strength will have been mobilised. The task is to find the combination of ϕ, δ, and non-associatively that gives a soil displacement angle of 49° and equivalent ϕ=16° for the simple K_P model. This condition can arise at the ultimate limit state for the soil-arch system because the arch, as an isolated structure, is likely to mobilise its peak strength (which then falls with further displacement) much earlier than the soil. Thus the structural arch strength is falling as the soil strength is still rising.

Equation 4.10 was calculated for a range of values of ϕ and different assumptions about interface friction and dilatancy, and the corresponding soil displacement angle and equivalent ϕ for the simple K_P model derived. The results are given in Figures 4-26 and 4-27.

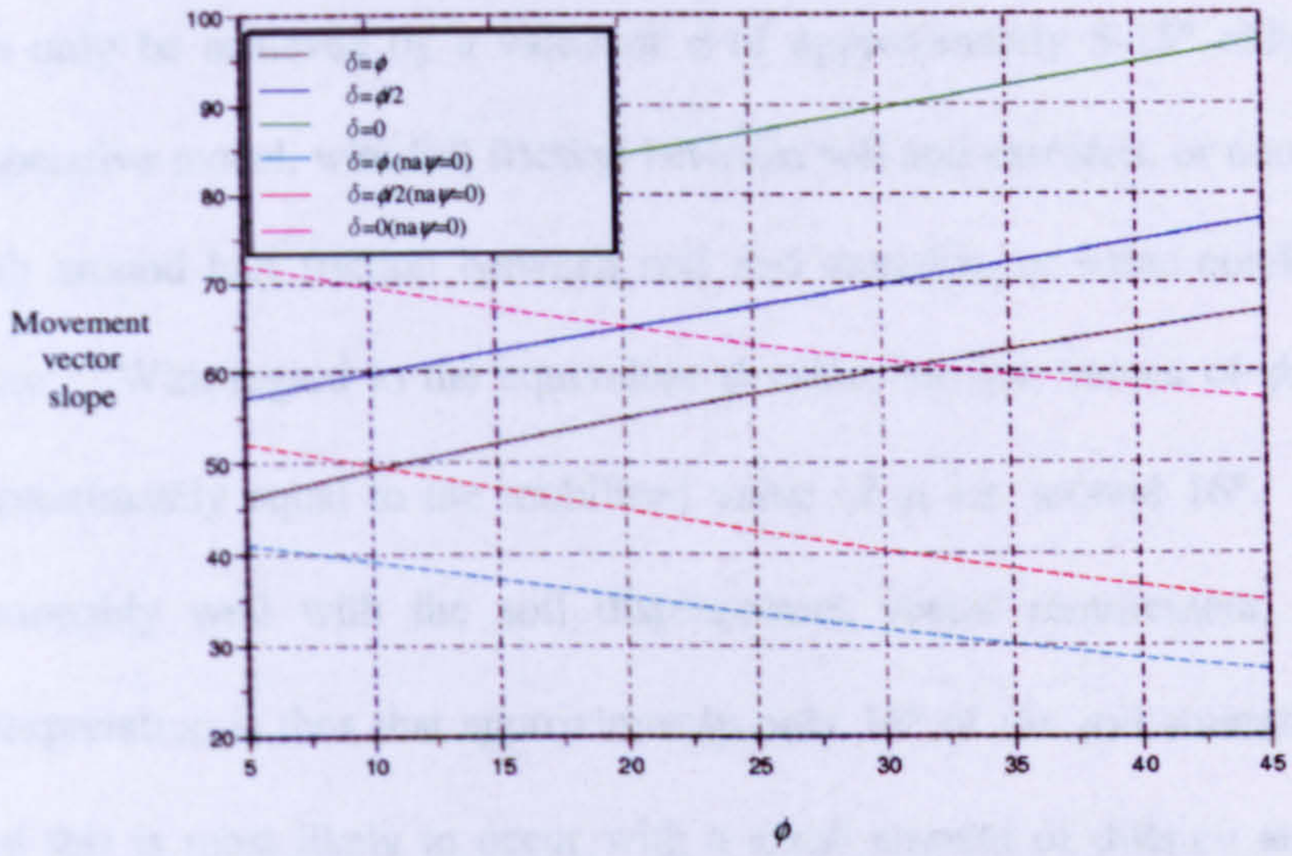

Figure 4-26 Variation of soil displacement angle vs ϕ

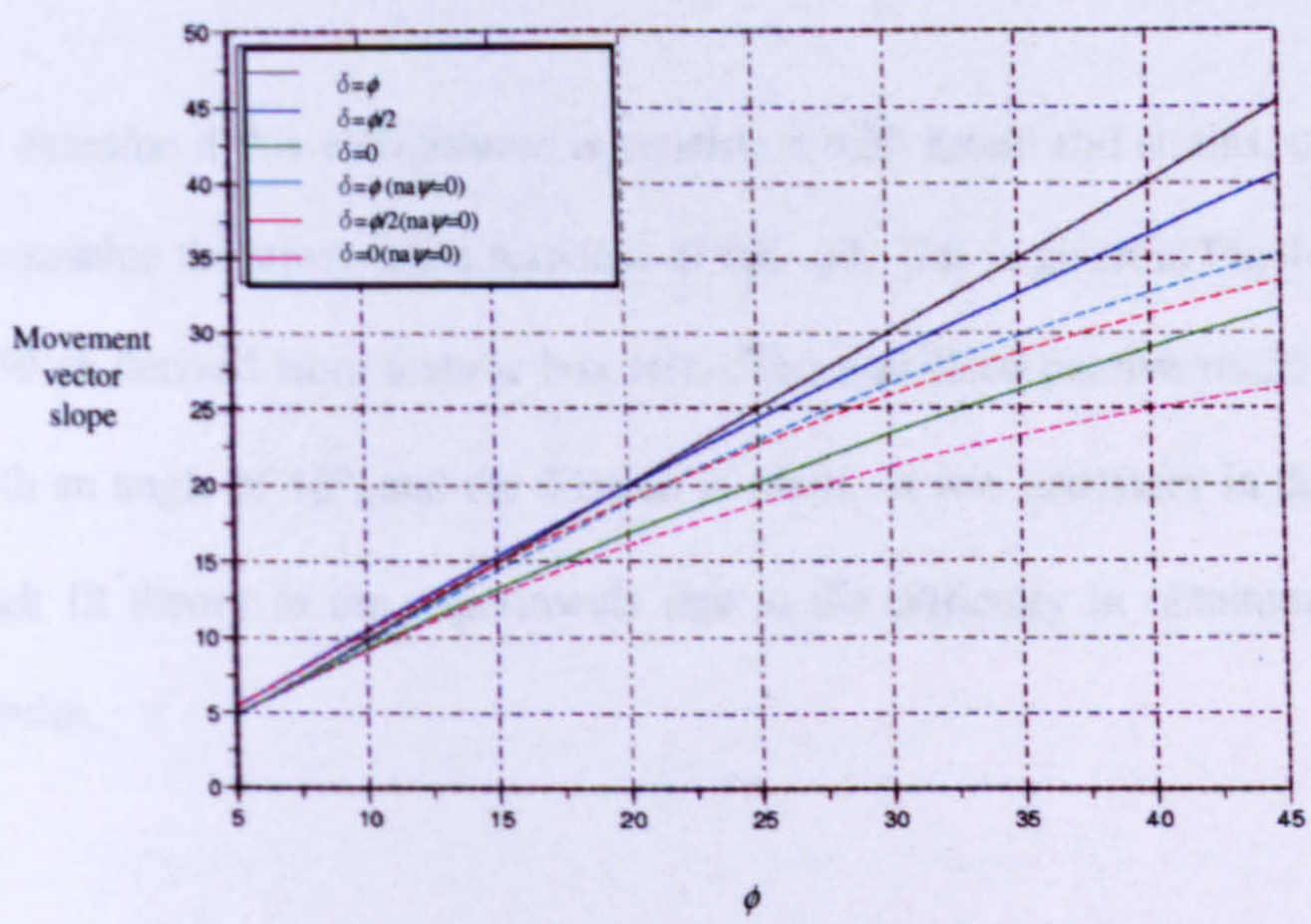

Figure 4-27 Variation of equivalent ϕ for the simple K_P model vs ϕ

Examining these results it can be seen that a soil displacement vector angle of 49° can only be achieved by a value of ϕ of approximately 5-15° either for a fully associative model, with full friction between soil and extrados, or non associatively with around half friction between soil and extrados, or some condition between these. With regard to the equivalent ϕ value, for low values of ϕ, this must be approximately equal to the mobilised value of ϕ, i.e. around 16°. This also fits reasonably well with the soil displacement vector requirement. The overall interpretation is thus that approximately only 16° of the soil strength is mobilised and this is most likely to occur with a small amount of dilation and around half friction between soil and extrados which is reasonable.

To examine if this mobilisation is consistent with actual soil strains, it is necessary to examine the stress-strain response of the soil. This is given in Fig 4-28, 4-29 and 4-30 as derived from a shear box test. The mobilised passive range is consistent with an angle of 16°, and the dilation is small. It was necessary in this instance to back fit theory to the experiments due to the difficulty in obtaining comparable results.

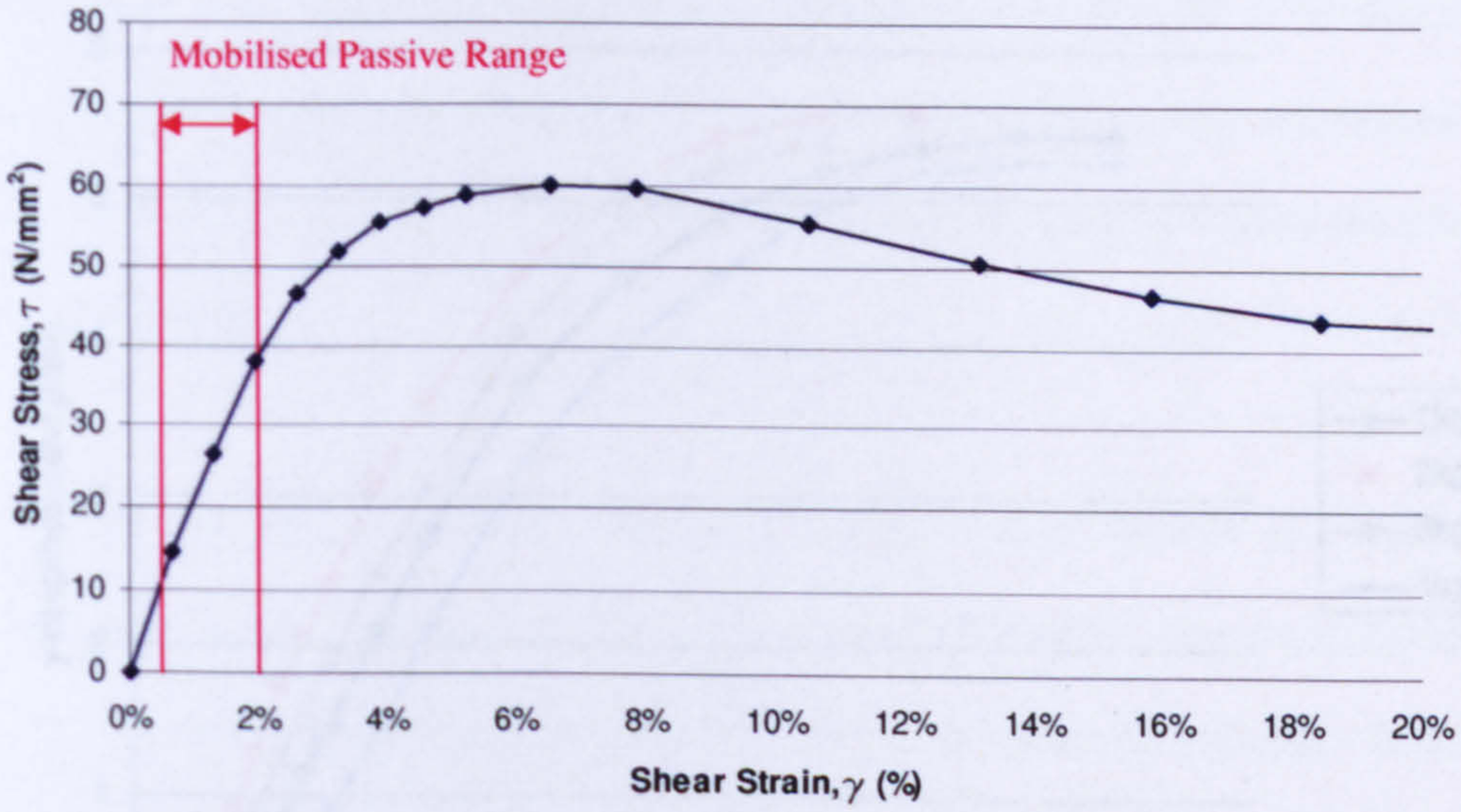

Figure 4-28 Mobilised passive pressures from Direct Shear Box Test (100mm)

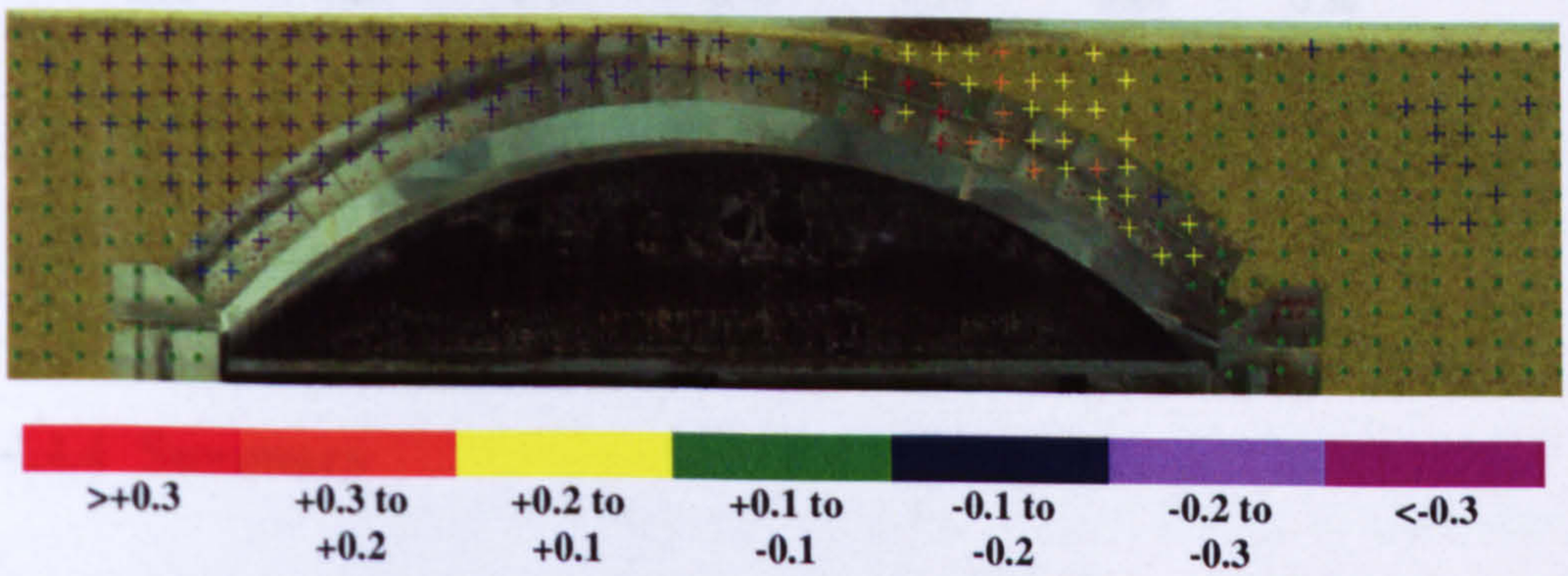

Figure 4-29 GeoPIV strain analysis

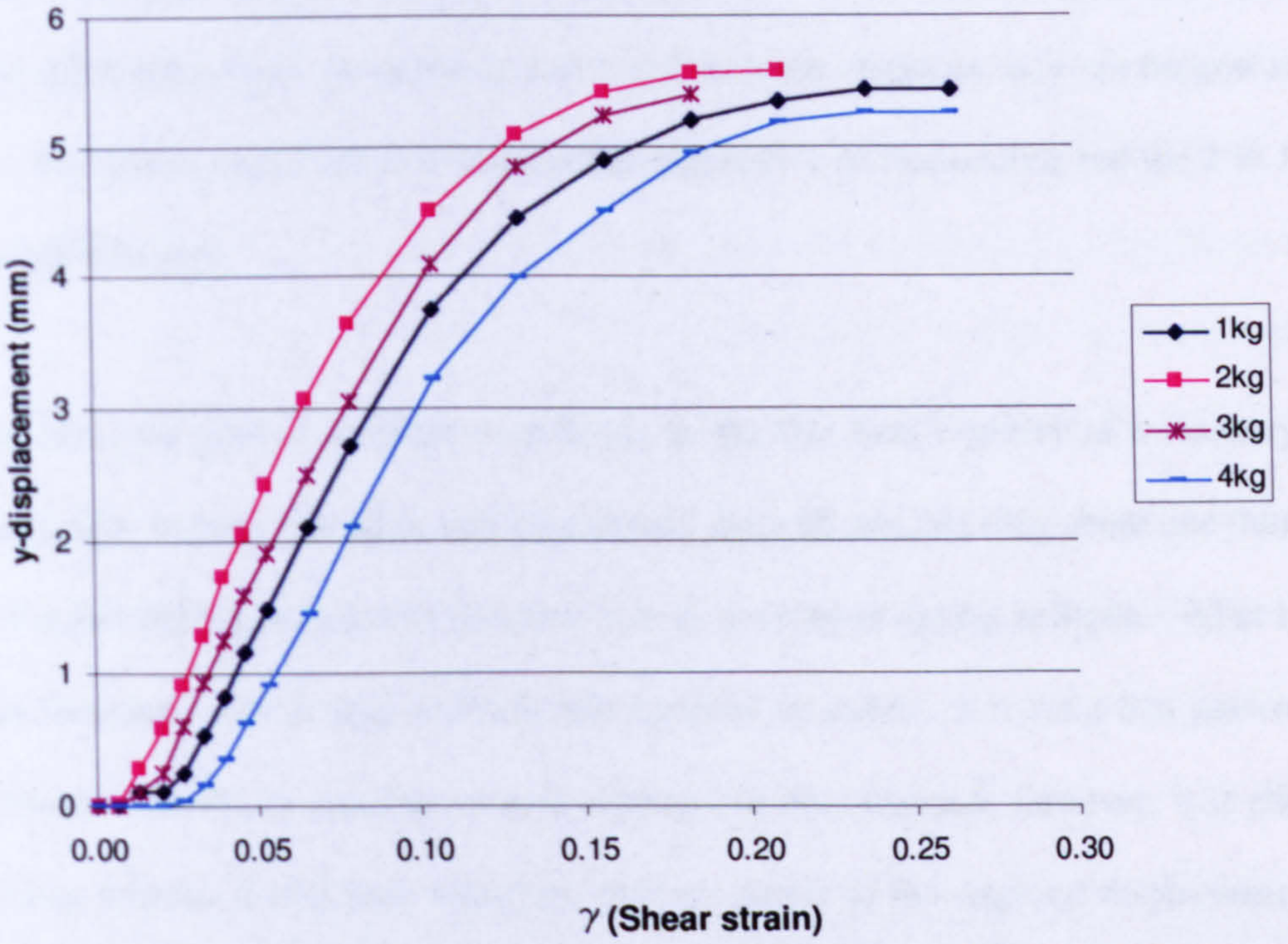

Figure 4-30 Dilation of sand from shearbox tests (100mm)

4.4.4 Summary

The simplistic nature of this model lends itself nicely to an additional step in the soil-structure interaction models in the next generation of computer programs such as RING. Although only the most basic approach is outlined here it is the intention to fully develop this theory into a calibrated workable model for use with assessment of arch bridges.

It has long been held by academics and industry that the vagueness of BD21/01 based upon work by Davey (1957) and Chettoe and Henderson (1953) is misleading.

New work done herein confirms recently discussed works by Harvey (2006) that load distribution does not occur at 2 in 1 and in some instances may not happen at all. The Smith model offers a quantifiable alternative to Boussinesq and the 2 in 1 load distribution.

The idea that passive pressure contributes to the live load capacity of a masonry arch bridge is not a new idea, and experiments have shown that only about one third of the full theoretical passive pressure is ever developed during collapse. What is less clear until now is why and how this happens in arches. It is clear that passive pressure is useful to stabilise an arch undergoing displacement, however, it is still unclear whether a real arch would be deemed unsafe at the required displacement values. The new proposed model offers a real alternative to current methods once it has been corrected.

These tests were all done at a constant depth and constant density to allow direct comparisons to be made. This was particularly important to assess the effect of load dispersal and the effect of passive resistance. (Active pressures were found to have little influence on the arch collapse load.) However, of further interest would be to examine the effect of different depths of fill. Work by Fairfield & Ponniah (1994) examined the influence fill density obtained from changes in the depth of backfill. Their discussion concluded that an increase in fill density affected the live load carrying capacity of the arch for two reasons, the first due to the corresponding increase in dead load that accompanies a greater depth of fill limiting the zone of thrust within the arch. The second was due to a greater dispersion of live load

arising from the higher stiffness backfill as a result of being at a higher density. They concluded that an increase in dead load corresponded to an increase in live load capacity of between 30% and 40% and that the live load dispersal contributed to an increase in capacity of 60%-70%. This was supported by a simple application of Boussinesq theory for a point load showing that the depth for dead load increasing with depth was linear, whereas for the live load dispersal, this increased at a power greater than one. In addition, higher lateral support pressures arising from the greater density at depth restrain the movement of the arch resulting in an increase in live load capacity (Hughes 1997).

Caution should be utilised with modern analytical models using simple soil models when applied to deep arches as they theoretically predict large lateral forces near the springing level particularly in the cases of semi circular arches. Current assessment tools incorporate soil models that include the increased dead load and lateral restraint which vary linearly with density.

4.5 Conclusions

1 The results obtained from the experiments and analytical models indicate that the current code of practice recommendation of using a 2 vertical in 1 horizontal live load distribution through the backfill for all scenarios can be unsafe.

2 The true dispersal angle has shown to be as low as zero in some instances depending upon type of backfill material, internal angle of soil friction, dilatency, void ratio and depth of fill.

3 Back calculating an equivalent distribution angle for theory to match experiments resulted in the perception that the load could focus rather than disperse in some cases. However, further investigation using energy considerations and examining the influence of the side walls are needed to ascertain as to whether focussing actually takes place.

4 Rather than utilising a Boussinesq or a 2 in 1 distribution for live load, the distribution model devised by Smith (2005) for strip footings provided good correlation between theory and experiments.

5 As previous research has shown passive pressure was mobilised during collapse, however, only as the arch rotated and it is unclear whether such a rotation would be classed as "failed" at full scale due to the size of the displacements involved.

6 Similarly to previous research, only about one third of the full theoretical value of passive pressure was ever mobilised during the experiments.

7 By using digital imaging techniques, a sliding block model was back developed using modern geotechnical theory based upon the observed

kinematics during the experiments. This numerical model, although kinematically similar, could not attain numerically agreement with the experimental results within the research time and is currently approximately a factor of 2 away from what is required. However, it is envisioned that further refinement would overcome this shortcoming.

8 It is anticipated for deeper depths of fill the equivalent void ratios involved is likely to mean that a greater degree of live load distribution would take place.

4.6 Future Work

The next step in this research is three fold:

- The first is to repeat the tests on the larger test rig at Salford University to ensure that the results are not a particular quirk of testing at small scale.

- The second part is to investigate different backfill materials within the small rig, soft clay and crushed limestone, to examine what happens with these more commonly occurring and structural materials. In addition, a new test rig is to be designed and built to provide an intermediate step for testing between the small test rig at Sheffield University and the large test rig at Salford University.

- The third part is to fully develop and calibrate the sliding block method outlined herein for incorporation into an existing arch assessment program so that a more robust computational model can be developed.

Chapter 5

The Influence of Abutment Fixity

This chapter is in the form of a self contained paper.

An experimental investigation of the influence of low friction between the skewback and abutments of masonry arch bridges

5.1 Abstract

Abutments are responsible for transmitting the load from an arch barrel into the fill behind. Although an arch relies on firm abutments, investigations of certain bridges in the field have revealed that in practice abutments are often thin and are restrained only by very soft clay with frequent voids in the soil. This paper is concerned with bridge behaviour when the skewbacks are free to slide over the abutment imposts into the fill beyond. Details of twenty-four small scale bridge tests are given together with details of conventional analyses of the soil-structure interaction. Novel digital imaging techniques were employed in the bridge tests. Test results indicate that for certain scenarios involving shallow depths of sand backfill the risk of sliding forming part of a failure mechanism is increased if the joint between the abutment and skewback possesses insufficient shear resistance. Also, in the cases where sliding occurs only a fraction of the full passive resistance attainable is mobilised. Both these mean that the true strength of the arch may be lower than that predicted by current computational tools, because of the simplistic soil models currently employed by the latter.

5.2 Introduction

Over the past few decades many attempts have been made to understand the response of masonry arch bridges. The issue of abutment fixity was raised as a potential area for concern as current UK codes of practice advocate the use of 'rule of thumb' approaches in order to assess abutment adequacy (e.g. BA16/97 2001). Abutments carry the thrust from an arch and transmit this to the surrounding soil. Recent site investigations by Essex County Council undertaken as part of routine assessment of their bridge stock, revealed some surprising findings. In some cases core surveys indicated that the abutments were no thicker than the arch barrel and that what lay beyond in some instances comprised of very soft waterlogged clay fill. In other bridges large voids were present in place of the free draining stiff backfill material anticipated. Without a medium to transfer thrust from the arch into the ground, in cases where the shear resistance at the base of the skewback was clearly insufficient to restrain the skewback, supplementary restraint from the surrounding fill is necessary. However; how much restraint could be expected to be provided was unknown.

To provide guidance and to develop more accurate assessment tools for frontline arch bridge assessment engineers, research in this area has recently been undertaken at the University of Sheffield. This document presents the findings of an investigation of the mode of response of arches where the failure mechanism involves translational sliding of the skewback located on top of the abutment. The situation being modelled is that which occurs when the horizontal thrust in the arch

overcomes the frictional resistance between these two parts of the structure and requires mobilisation of passive restraining pressures in the surrounding soil in order to prevent collapse.

Figure 5-1 A selection of arch bridge skewbacks

5.2.1 Assessment of Abutments

Abutments have for many years been assumed for the purposes of assessment to be separate from the main arch barrel, though it is true, especially for brick arches, that for many masonry arch bridges it is near impossible to state exactly where the arch barrel ends and the abutments begin. However, some masonry arch bridges have skewbacks at the springing neatly separating the barrel from the abutments (see Figure 5-1).

Little research appears to have been carried out on how the abutments, skewbacks and arch interact with each other, although Ochsendorf (2006) has recently investigated the influence of horizontal support movements on the response of semicircular arches in buildings (i.e. with no fill). He found that as the supports move apart the intrados hinge in the arch migrates towards the crown, altering the arch geometry, and also that the collapse of masonry arches on spreading abutments is complex, with precise hinge locations being difficult to ascertain, in turn leading to doubts regarding the exact mode of collapse.

Considering bridges specifically, perhaps the first attempt to determine the mode of response of the abutments was carried out in experimental tests conducted by Davey (1953) and Chettoe & Henderson (1957) during the 1950s. They found that abutments tended to move outwards when a heavy load passed over an arch bridge before gradually returning to their original positions. This flexing of the structure is perhaps the first piece of evidence to suggest that it may not always be appropriate to consider the abutments as rigidly fixed. More recently Smith *et al.* (1990) concluded that abutment movement can significantly affect the load carrying capacity of an arch bridge whilst Harvey (1991) found that this was because small movements of the abutments causes a change in the stress distribution within the structure. This appears to indicate that the commonly made assumption in analysis that abutments are rigidly fixed could be potentially unsafe.

The current UK assessment codes all refer to guidance given in BA16/97, which treats the assessment of the arch barrel separately from the assessment of the

abutments, and which relies on the judgement and skill of the inspecting engineer to assess the latter. This approach has also been followed by many engineers responsible for developing computational and analytical tools, which ignore the abutments and assume that the skewbacks are effectively fixed for assessment purposes (e.g. Gilbert & Melbourne 1994, Smith *et al.* 1990). This has also influenced the design of experimental test apparatus, with many model arches having been tested between rigidly fixed abutments (e.g. Burroughs *et al.* 2002, Melbourne & Gilbert 1995).

Any residual shear-bond strength at the interfaces between masonry units cannot be relied upon once the mortar-brick bond has been broken (i.e. when a joint is visibly cracked), and in this case the actual friction coefficient may be less than the recommended value of 0.6 given in current UK Codes of Practice.

To sum up it is on record that the abutments of real life masonry arch bridges move whereas current assessment tools take the abutments as being rigidly fixed; to date most laboratory tests have also taken them to be fixed. However, the reasonableness of this assumption will now be assessed.

5.2.2 The Problem

Today many computational masonry arch assessment software packages model the arch barrel directly, but only model the expected effects of surrounding fill, rather directly modelling the fill itself. Figure 5-2 shows a conventional four hinge failure

mechanism together with typically assumed soil pressure distributions. Note that it is often forgotten that a four hinge failure mechanism is only one of several potential failure mechanisms for an arch bridge, with other potential mechanisms including those involving formation of three hinges in the barrel plus sliding or rotation of one abutment. However, analysis packages such as RING (Gilbert 2001) permit these and other mechanisms to be computationally modelled.

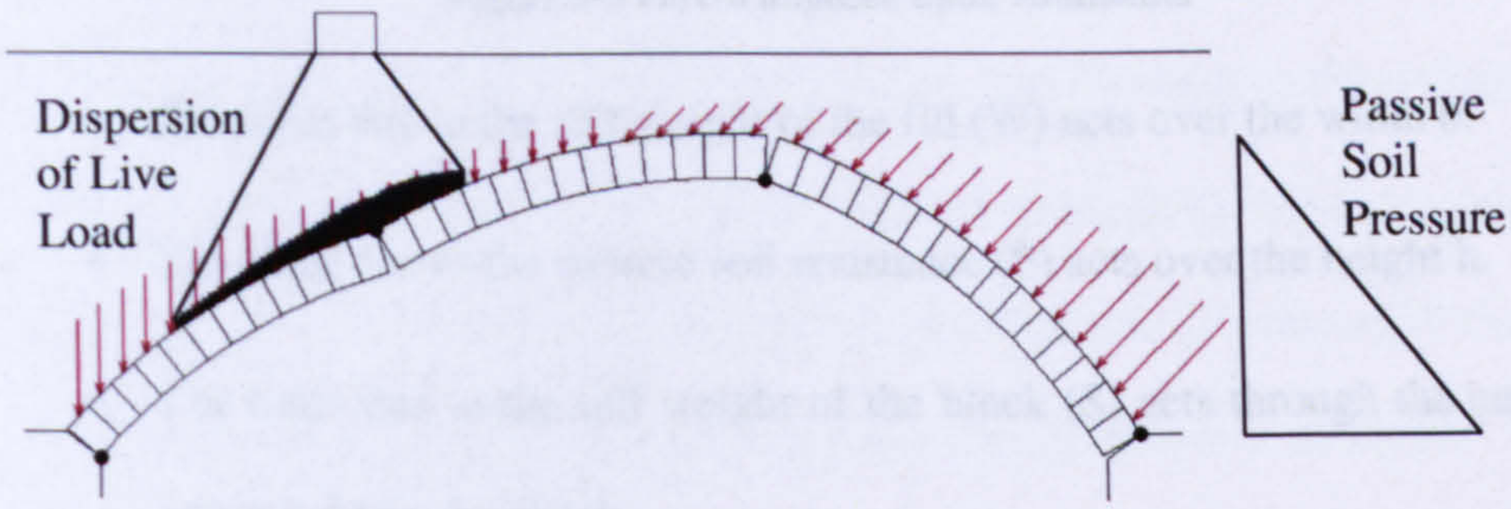

Figure 5-2 Current simple passive pressure soil model in RING

However, it is unclear whether the assumed triangular distribution of passive soil pressure can be extended below the level of the skewbacks and abutments, and whether this is actually representative of what happens in a real bridge.

By considering one of the skewbacks, there are at least three forces of resistances opposing the thrust (T) generated by the arch. These are the passive soil resistance (P), the frictional resistance at the interface between the skewback and the top of the abutment (F), and the clamping load due to the dead weight of the fill above the skewback (W). These forces are shown in Figure 5-3.

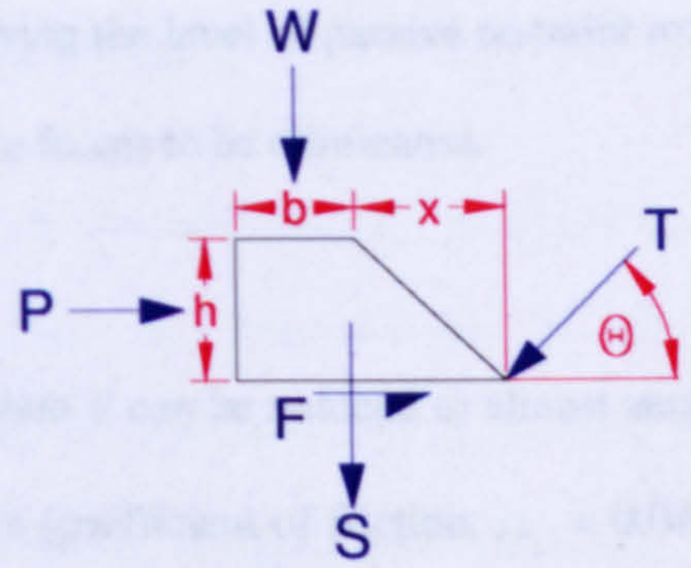

Figure 5-3 Forces imposed upon abutments

- The force due to the self weight of the fill (W) acts over the width b.
- The force due to the passive soil resistance (P) acts over the height h.
- The force due to the self weight of the block (S) acts through the centre of gravity of the skewback.
- The frictional force (F) is independent of area and acts along the base of the block. (Note the adhesion component of friction is area dependent and has not been considered here as it was anticipated that it would be negligible due to the materials and set-up used).
- The thrust from the arch (T) acts at an angle Θ to the horizontal at the springing. (Note that the position of the thrust can vary and the thrust includes the self-weight of the arch voussoirs and backfill.)

Even if the self-weight of the skewback is taken as negligible, it is difficult to examine the influence of forces W, P and F when all these act simultaneously. Therefore, to simplify matters it is convenient to remove (or make negligible) two of these three forces compared to the third. Since this investigation is principally

concerned with quantifying the level of passive restraint required, i.e. P, this means that F and W are the two forces to be eliminated.

In an experimental context F can be reduced to almost zero by using a low friction material, such as Teflon (coefficient of friction, μ = 0.04). The force W per unit width can be calculated by multiplying the width (b) by the overburden height (z) by the bulk unit weight (γ). Thus by reducing the dimensions of b and/or z, the value for W can be reduced (though not entirely eliminated). However, since the surface under the skewback is also nominally frictionless the value of W then does not have any influence. Hence this leaves only one variable to investigate.

Clearly a sliding failure has the potential to be problematic as it results in a larger arch span, a drop in arch rise and can introduce tension into the arch. (This result is similar to that of the crown dropping upon the removal of the wooden centring, with the arch shortening as the masonry takes up the loads. In the small scale experiments GeoPIV was used prior and post removal of the centring to ensure any crown dropping was quantified. As it transpired no crown drop was detected during the tests, which can be attributed to both the quality of the workmanship of the barrel and the centring, and to the care and robustness of the test method used.)

5.3 Parametric Study

To inform the planning of the experimental investigations, parametric studies were carried out to investigate the influence of the skewback-abutment friction coefficient. For this purpose segmental arch bridges with rise:span ratios of 1:4, 1:5, 1:6 were modelled numerically using RING. These rise:span ratios were chosen as the thrust in <1:3 arches is dominated by the vertical component of the thrust at the abutment whilst >1:7 arches are not very common. The additional parameters used in the simulations are shown in Figure 5-4. Three backfill unit weights (γ=14/16/18 kN/m^3), three angles of soil friction (ϕ'=30°/40°/50°), and three abutment widths (300, 500, 700mm) were investigated.

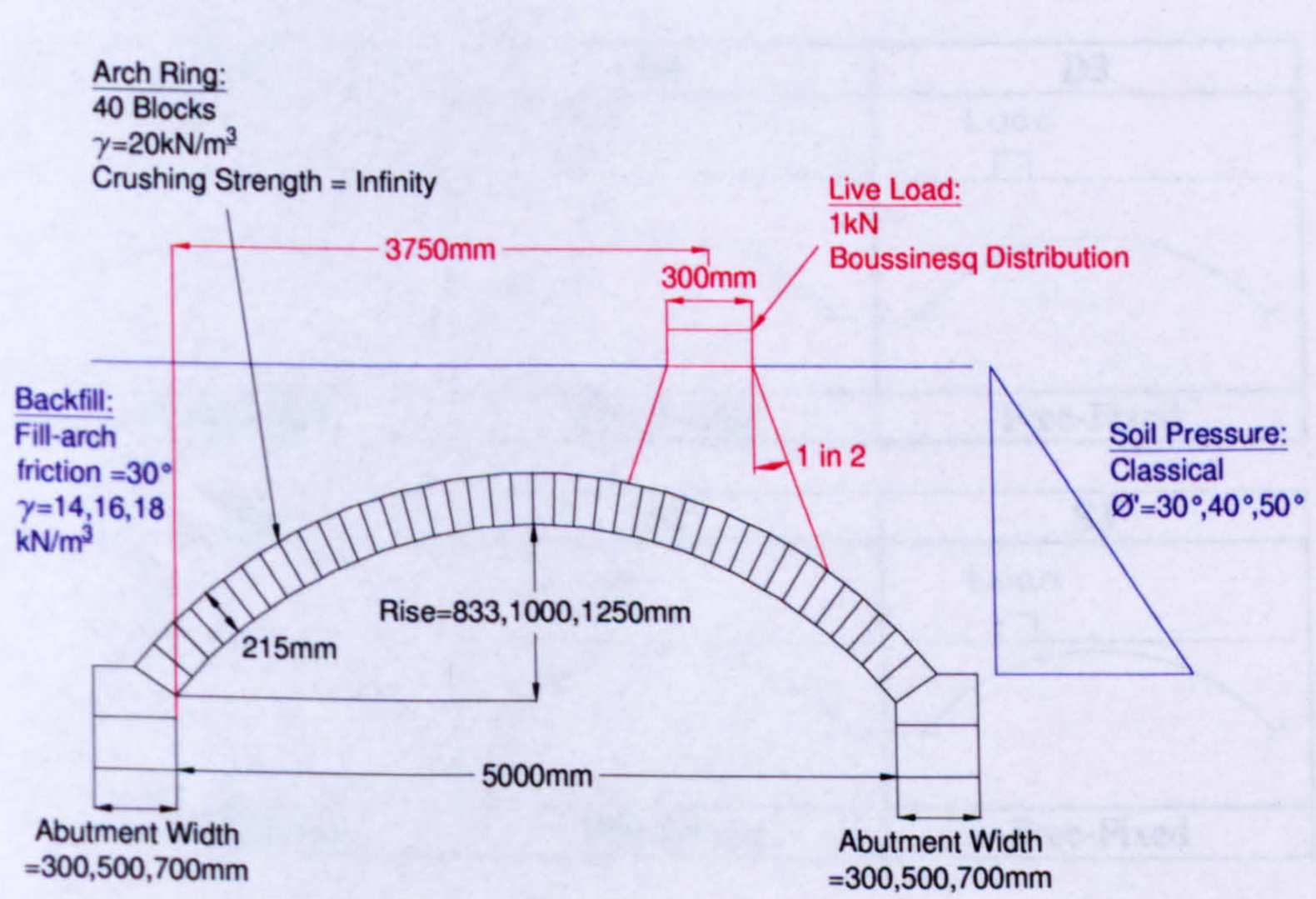

Figure 5-4 RING parameters

Given that this investigation pushed RING beyond its normal everyday operating area, though was not beyond its capabilities, care had to be taken when defining the

models to make sure they could be solved by RING and that they had realistic inter-block contacts.

5.3.1 Details of Study

The main objective of the study was to determine the amount of passive restraint required behind a skewback to obtain a failure load and mechanism similar to one with traditional fixed skewbacks. Two depths of fill were tried; the D (Deep) and S (Shallow) fill bridges had fill depths at the crown of 0mm and 300mm respectively. Six different simulations were performed, details of which are provided in Table 5-1.

D1	D2	D3
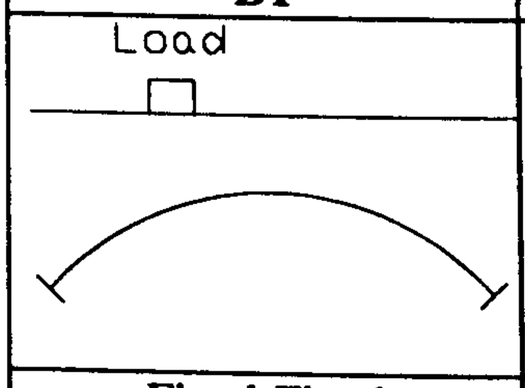	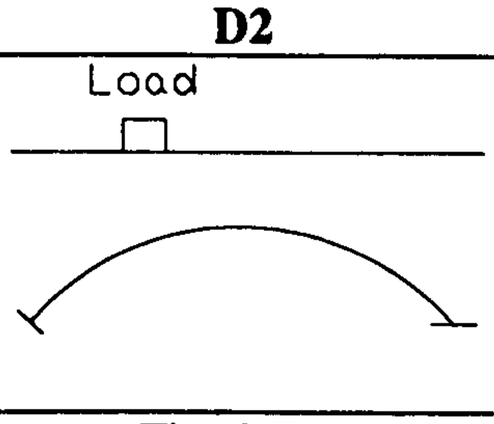	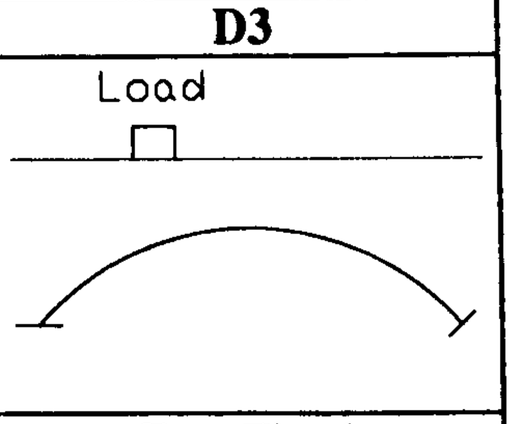
Fixed-Fixed	Fixed-Free	Free-Fixed

S1	S2	S3
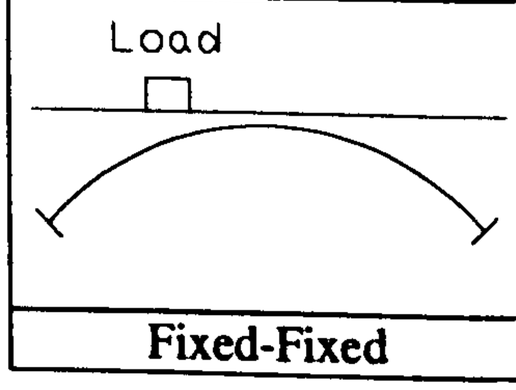	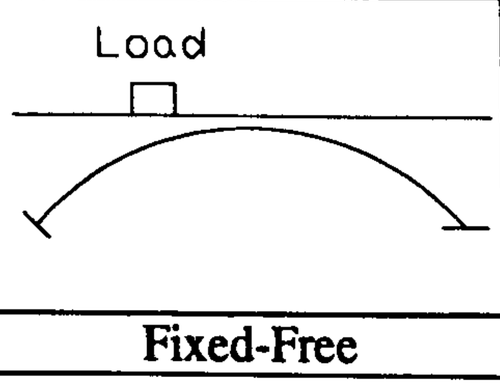	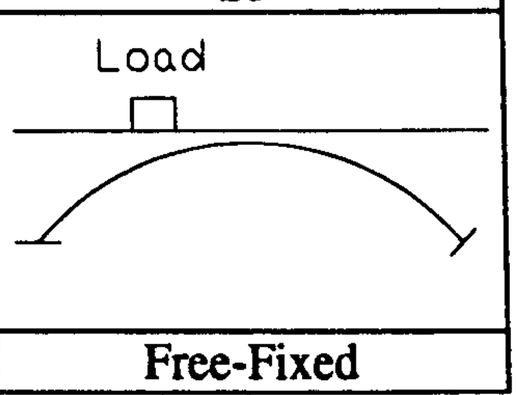
Fixed-Fixed	Fixed-Free	Free-Fixed

Table 5-1 RING simulation models

By setting up RING models as shown in Figures 5-5, 5-6 & 5-7, the restraining pressures A and B can be manually adjusted to obtain failure load values corresponding to those obtainable when fixed abutments are present. This was done

as it felt that this was one way of justifying (or otherwise) the current 'fixed abutment' assumption generally used for assessment purposes. Note no pavement was used for these tests.

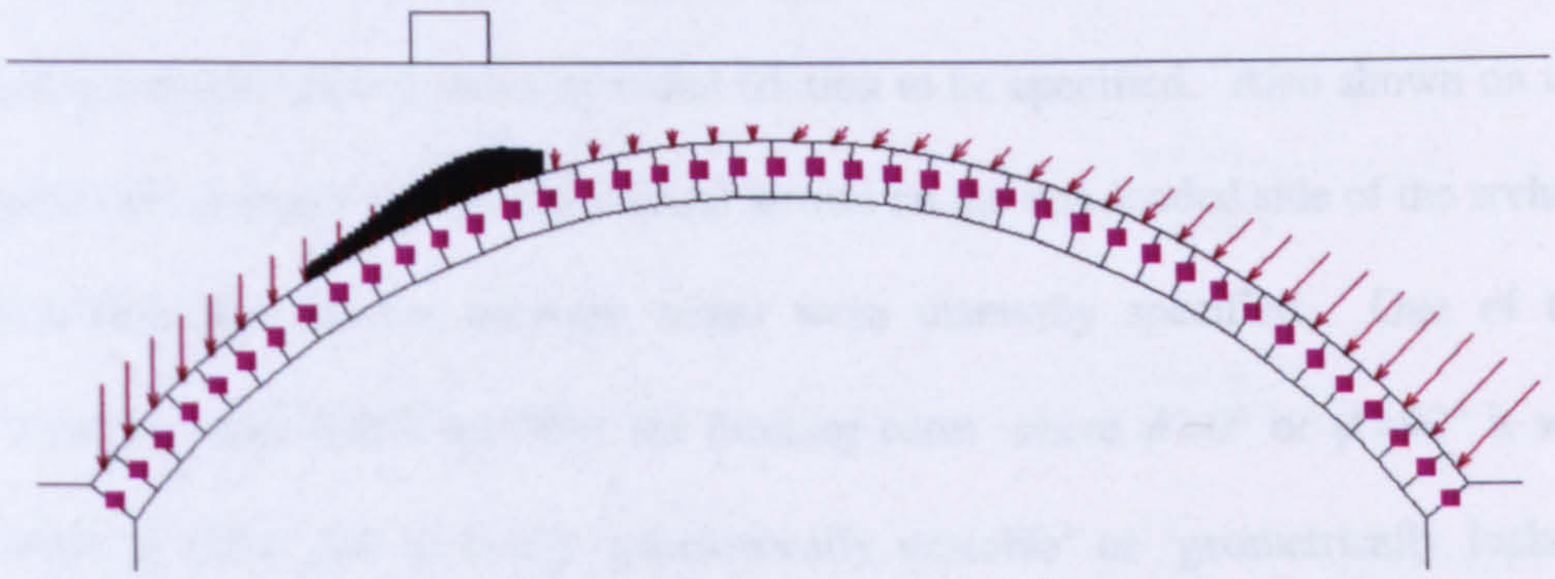

Figure 5-5 RING simulation having fixed abutments

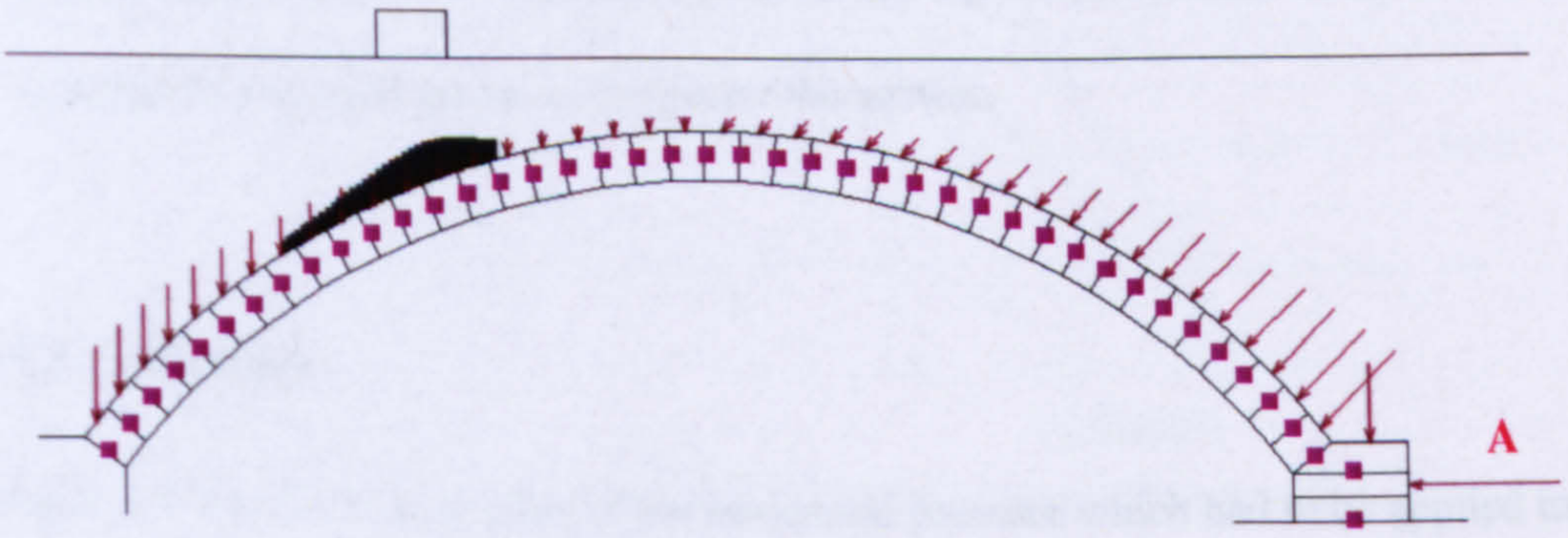

Figure 5-6 RING simulation having fixed, loaded side abutment

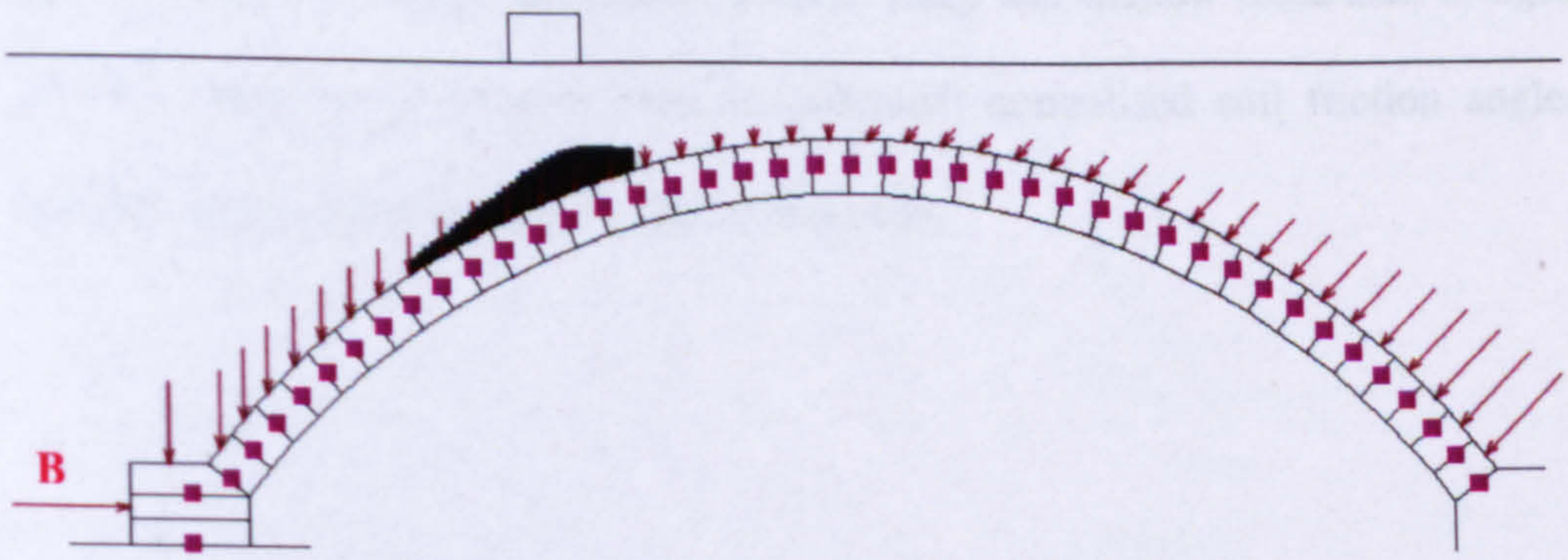

Figure 5-7 RING simulation having fixed, non-loaded side abutment

All the models had so-called 'Advanced' RING properties setup: the purple square at the interface between each block (except at the interface under investigation), shown on Figures 5-5, 5-6 & 5-7, indicates that inter-block sliding is being prevented. This was necessary because the version of RING used (RING 1.5) only allows a single, global, value of radial friction to be specified. Also shown on the figures are diagonal rather than vertical arrows on the non-loaded side of the arches, indicating that passive pressure zones were manually specified. One of the limitations with RING was that for limiting cases where $\phi'=0°$ or $\phi'=90°$ it was unable to solve due to being 'geometrically unstable' or 'geometrically locked' respectfully. This is due to the way it formulates its algorithms requiring the soil response magnitudes to be calculated prior to solving the mechanism in order to use the properties of equilibrium to determine the answer.

5.3.2 Results

Figures 5-8 to 5-11 show plots of the horizontal pressure which had to be applied to the back of skewbacks possessing differing base friction characteristics in order to ensure a classical 4 hinge mechanism formed. Deep and shallow filled arch bridges and the following parameters were investigated: normalised soil friction angle, backfill density, abutment width, and arch profile.

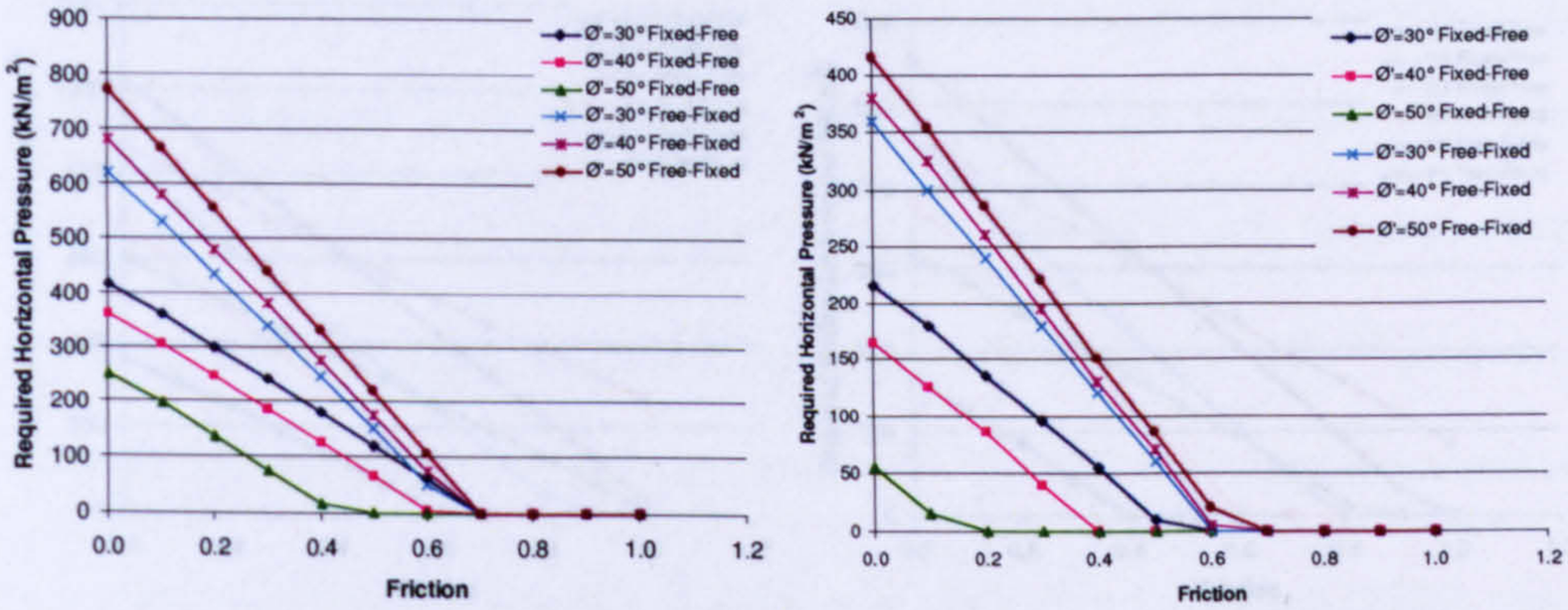

(a) Deep **(b) Shallow**

Figure 5-8 Parametric study showing influence of soil friction angle

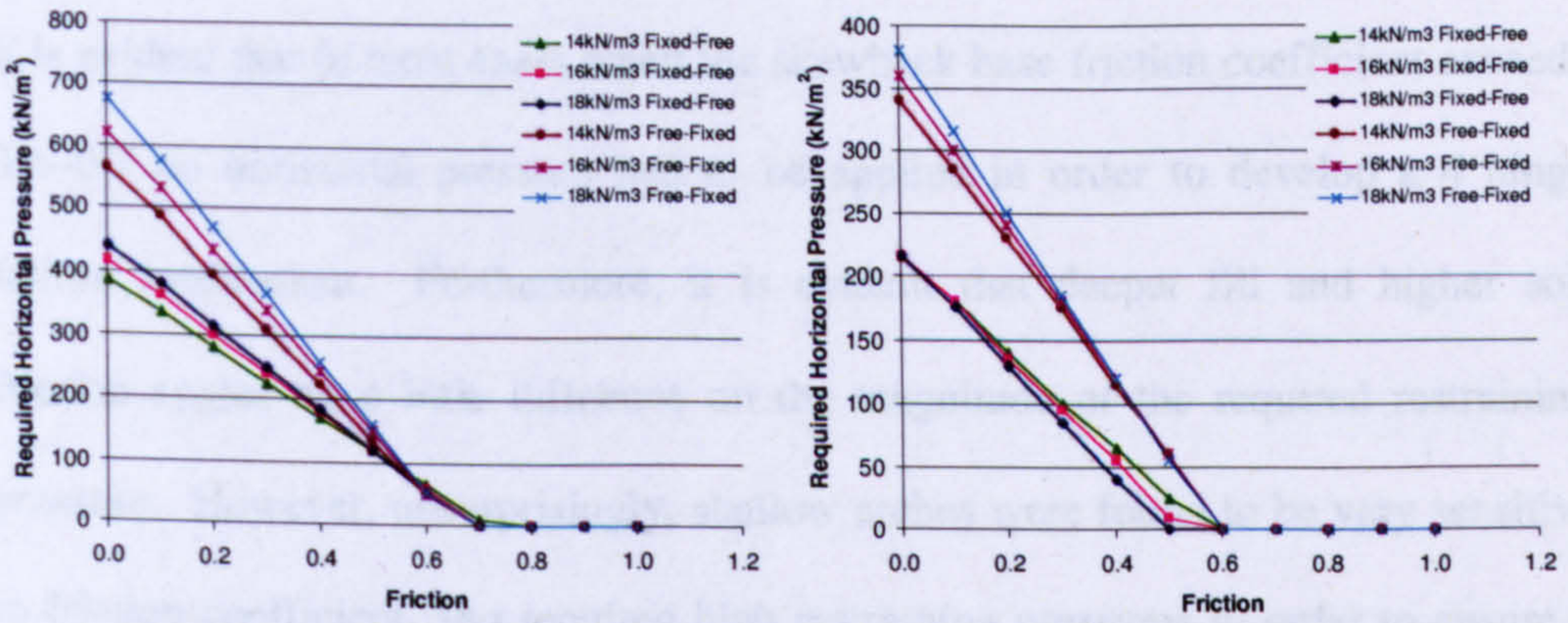

(a) Deep **(b) Shallow**

Figure 5-9 Parametric study showing influence of backfill unit weight

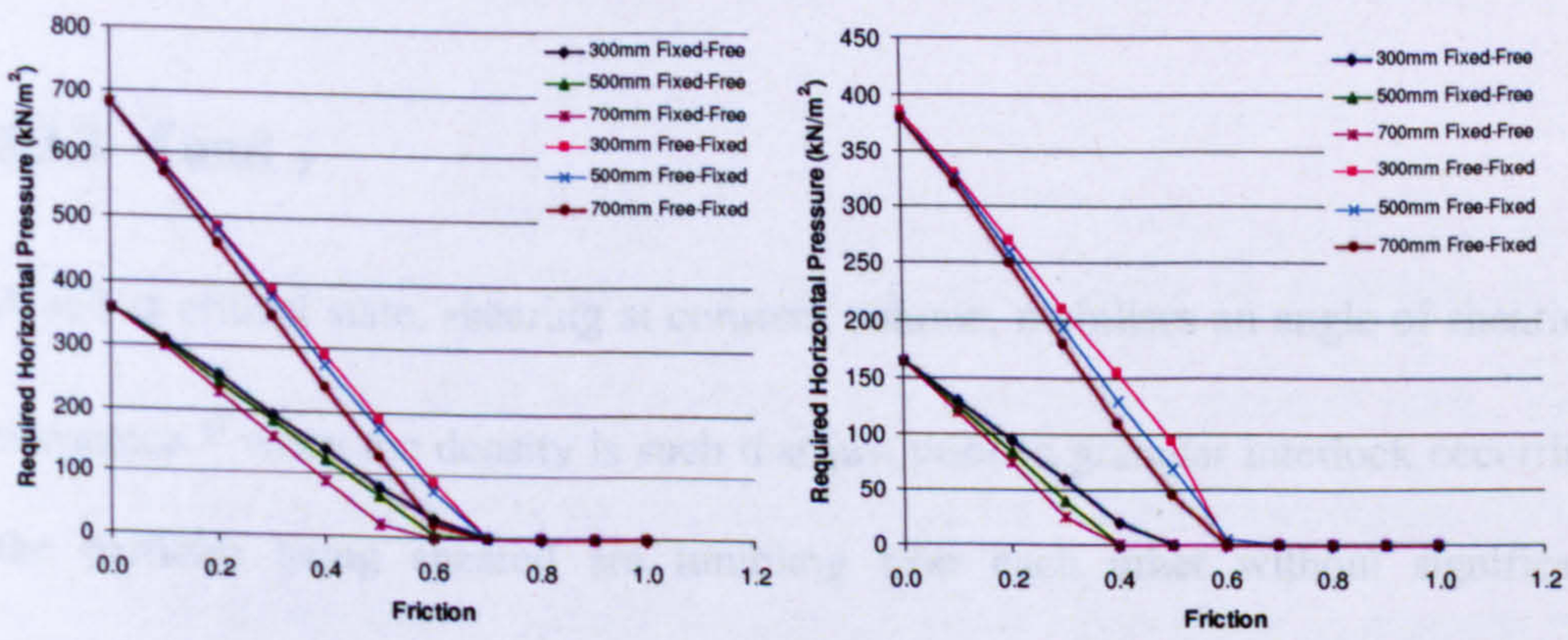

(a) Deep **(b) Shallow**

Figure 5-10 Parametric study showing influence of abutment width

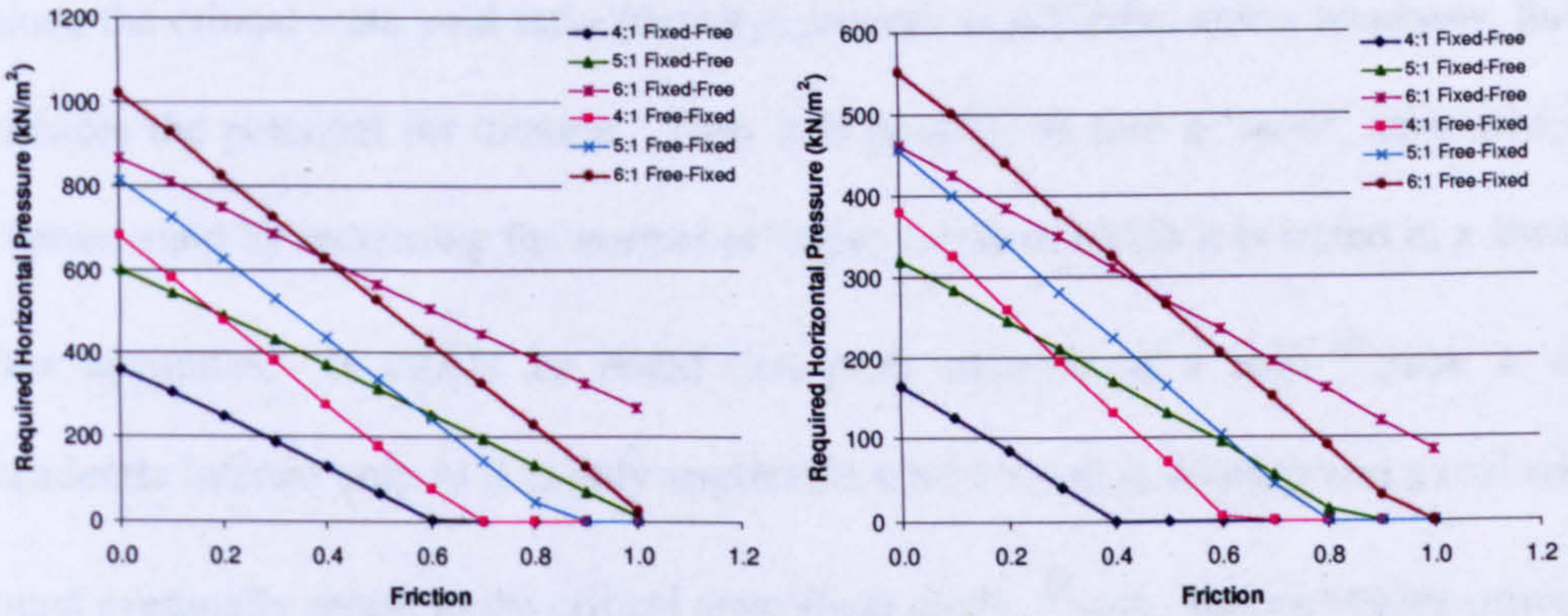

(a) Deep **(b) Shallow**

Figure 5-11 Parametric study showing influence of arch profile

It is evident that in most cases when the skewback base friction coefficient exceeds 0.6~0.7 no horizontal pressure had to be applied in order to develop a 4 hinge failure mechanism. Furthermore, it is evident that deeper fill and higher soil friction angles have little influence on the magnitude of the required restraining pressure. However, unsurprisingly, shallow arches were found to be very sensitive to friction coefficient, and required high restraining pressures in order to ensure 4 hinge failure mechanisms were developed.

5.3.3 ϕ' and γ

A soil at critical state, shearing at constant volume, mobilises an angle of shearing resistance ϕ' when the density is such that just prior to granular interlock occurring the particles being sheared are tumbling over each other without significant interference. Once interlocking has occurred, an additional shear force (dilation, ψ) is required to maintain motion. It is interesting to note that the peak shear strength is independent of initial packing arrangement and density. However,

since the critical state void ratio (density) reduces as effective stress increases, this reduces the potential for dilation. Thus it is possible to turn a 'loose' sand into a 'dense' sand by increasing the normal effective stress at which it is tested in a shear box apparatus. It should be noted that peak strength of a soil, ϕ' peak is of academic interest only as it is only applicable whilst a soil is dilating and a real soil must eventually return to the critical state shear angle, ϕ' crit. Bolton (1986) proves that for plane strain conditions, strength and dilation are related by the expression:

$$\phi'\text{peak} = \phi'\text{crit} + 0.8\psi_{max}$$

Thus for a Leighton Buzzard sand where:

$\phi' = 44°$, $\psi' = 6°$, $\gamma = 16.5$ kN/m^3 and

$$\frac{\partial \phi'}{\partial \gamma} \approx 4°/\text{kN/m}^3 \text{ and } \frac{\partial \psi'}{\partial \gamma} \approx 1°/\text{kN/m}^3 \quad \text{.....(5-1 \& 5-2)}$$

At $\gamma = 15.5$ kN/m^3, ϕ' would be 40° and $\psi' = 5°$. Likewise at $\gamma = 17.5$ kN/m^3, ϕ' would be 48° and $\psi' = 7°$.

5.3.4 K_p

The required restraint to prevent sliding can alternatively be expressed as an equivalent K_P value, where K_P is a multiplier of a hydrostatic pressure value. Thus Table 5-2 shows the equivalent K_P values for the zero skewback-abutment friction case when the normalised backfill density was present (this is just an example; full results are given in the Appendix). Also shown is the required multiplier of K_p required to attain rigid abutment equivalence.

Reference	σ_h (kN/m^2)	z (m)	γ (kN/m^3)	K_e [=$\sigma_h/\gamma z$]	ϕ' (°)	Required Multiplier of K_p
Deep ϕ'=30°-D2	415	1.81	16	14.3	30	4.8
Deep ϕ'=30°-D3	620	1.81	16	21.4	30	7.1
Deep ϕ'=40°-D2	360	1.81	16	12.4	40	2.7
Deep ϕ'=40°-D3	680	1.81	16	23.5	40	5.1
Deep ϕ'=50°-D2	250	1.81	16	8.6	50	1.1
Deep ϕ'=50°-D3	770	1.81	16	26.6	50	3.5
Shallow ϕ'=30°-S2	215	1.51	16	8.9	30	3.0
Shallow ϕ'=30°-S3	360	1.51	16	14.9	30	5.0
Shallow ϕ'=40°-S2	165	1.51	16	6.8	40	1.5
Shallow ϕ'=40°-S3	380	1.51	16	15.7	40	3.4
Shallow ϕ'=50°-S2	55	1.51	16	2.3	50	**0.3**
Shallow ϕ'=50°-S3	415	1.51	16	17.2	50	2.3

Table 5-2 Forces and K_P multiple for normalised backfill density

As the numbers in the table show, even in the case where shallow fill is present, (apart from when Shallow ϕ'=50° in test S2), a multiplier of the full passive pressure is needed to be mobilised from between a factor of 1.1 to 7.1. The average of the factors is 3.3. The discrepancy of 0.3 is attributed to a quirk of having a low calculated horizontal pressure since z and γ must remain constant. The zero friction case is of particular interest because, as mentioned earlier, it allows

skewback forces to be isolated, and also because it is possible to approximately model this scenario in the laboratory.

5.3.5 Conclusions

A summary of the main conclusions from each study is given in this section.

Soil Friction

Almost all of the arches failed with the loaded side abutment failing before the unloaded side abutment, as shown in Figure 5-12. (The ones that did not fail in this way had deep fill and/or properties of $\mu \geq 0.6$ and $\phi' = 30°$). This means that in nearly all cases the mobilised soil pressure necessary for stability on the loaded side was greater than that required on the unloaded side (though note that in the simplistic models used, passive pressures were not applied to the loaded side - despite the fact that the arch was moving into the soil in this region.

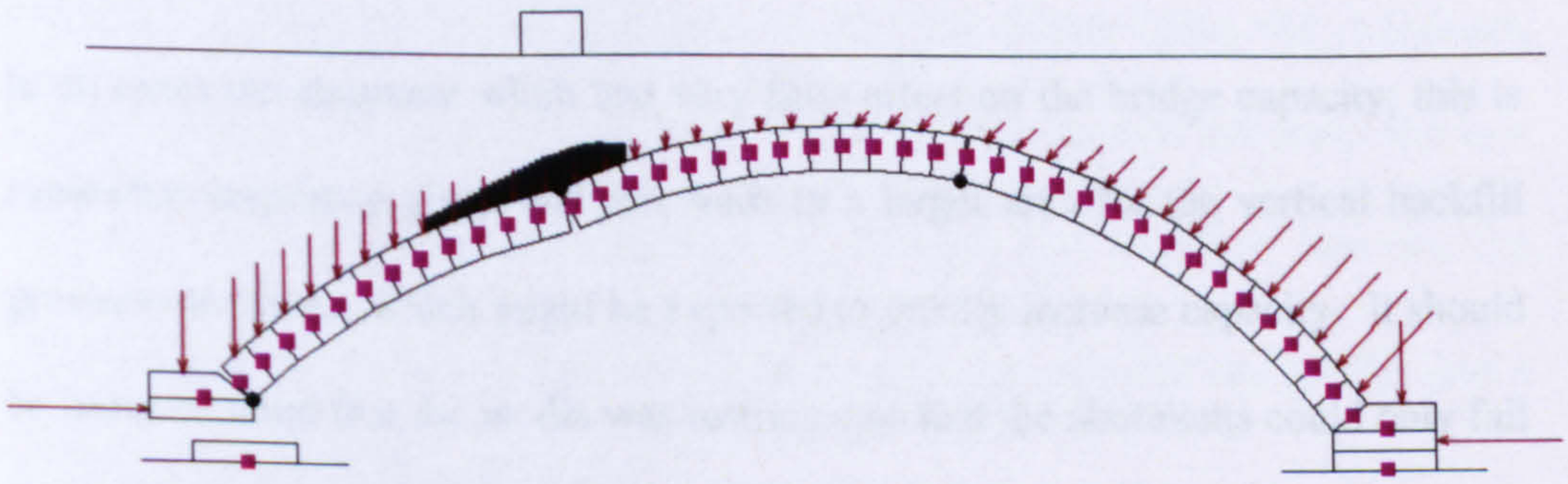

Figure 5-12 Sliding failure (Separation accompanies sliding due to saw-tooth friction model)

Additionally, the soil friction angle was found to have a large effect on the required skewback coefficient of friction whereas the influence of the backfill unit weight on this was smaller. Both backfill and soil friction angle were found to have a linear relationship with the friction value.

Once the skewback coefficient of friction exceeded 0.7, for deep arches a four hinge mechanism always formed.

In almost all cases a higher soil resistance value was required than that which could be explained by a fully mobilised basic Rankine triangular pressure distribution ($\sigma_h=K_p\gamma z$). [Note also that others have found that only approx. 33% ($^1/_3K_p$) of the full theoretical passive pressure is ever mobilised in arch bridges (e.g. Burroughs *et al.* 2002).]

Abutment Width

In all cases the abutment width had very little effect on the bridge capacity; this is somewhat surprising given that this leads to a larger area for the vertical backfill pressures to act on, which might be expected to greatly increase capacity. It should be borne in mind that the model was restricted so that the abutments could only fail by sliding at the skewback-abutment interface, and that no rotation was allowed at this point. However, given that once again for μ values >0.6 friction had negligible

influence and obviously at μ=0 no difference in the results were found for either depth of fill.

Arch Profile

As expected the arch profile was found to have a profound effect on the likelihood of sliding failure. The μ value always had an influence and when μ>0.5 the side which slides was found to change from the loaded to unloaded side. (In practice the value of μ is usually greater than 0.5). To determine the effect of this flip, simulations were run comparing no sliding to sliding capacities. The results of which showed that when sliding occurred on the unloaded side there was a 2% reduction in capacity, however, when the slide occurred on the loaded side there was an average 50% reduction in capacity which decreased with greater fill depth.

5.3.6 Summary

Based upon these studies the highest risk case for sliding being the significant failure mechanism would be an arch with a flat profile, shallow fill depth and low soil friction angle. However, should the friction (μ) interface between the abutment and the skewback have a coefficient of friction >0.6 for any profile, then a sliding failure is unlikely to occur.

5.4 Experiments

To better understand the true mode of response of masonry arch abutments, and to identify the range of applicability of current analysis models a series of tests on small and large scale models was commissioned by Essex County Council, to be undertaken by the University of Sheffield. Two test rigs were commissioned, the first being a 1/8th scale model constructed at the University of Sheffield and the second being a full scale model designed by the University of Sheffield but installed at the University of Salford for logistical reasons. The thinking was that issues could be examined quite rapidly using the smaller test rig and then corroborated and studied further using the larger rig. Both of the test rigs were designed with transparent side walls and were filled with backfill material with good contrast so that modern digital imaging techniques could be applied, permitting soil mass movements to be quantified at any point. Also in a break with tradition, the skewbacks were allowed to move relative to the abutments as required.

5.4.1 Small Test Apparatus

The tests were conducted using the same test rig, materials and in a similar manner to those covered in Chapter 4 of this thesis and more details can be found there.

For these experiments two depths of fill and four skewback abutment fixity conditions were investigated (refer to Table 5-3).

Bridge Test No.	Depth of Fill above crown extrados (mm)	Abutment Conditions (LHS:RHS)
1	38 (Deep)	Fixed : Fixed
2	38	Fixed : Free
3	38	Free : Fixed
4	38	Free: Free
5	2 (Shallow)	Fixed : Fixed
6	2	Fixed : Free
7	2	Free : Fixed
8	2	Free: Free

Table 5-3 Conditions of skewback fixity investigated

The interface between the skewbacks and the abutments were either free or fixed, (refer to Figure 5-13).

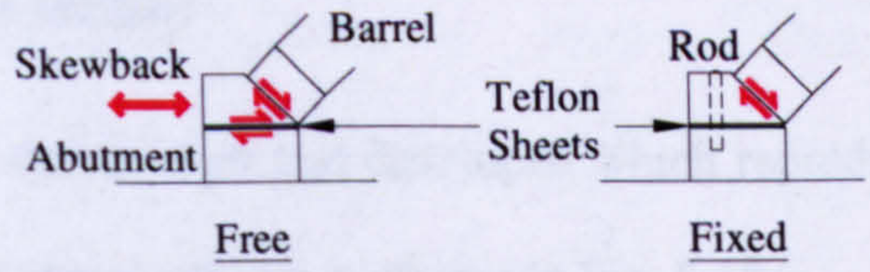

Figure 5-13 Abutment-skewback conditions

Fixed:

- Skewback was fixed to abutment with a metal rod to the abutment.

Free:

- Skewback was separated from the abutment by a low friction Teflon-Teflon contact surface.

Thus the four abutment conditions were as follows; fixed-fixed, fixed-free, free-fixed and free-free. The depth of fill at the crown for deep filled arches was 38mm

and 2mm for shallow filled arches. Figure 5-14 shows a photograph of a deep filled arch awaiting testing.

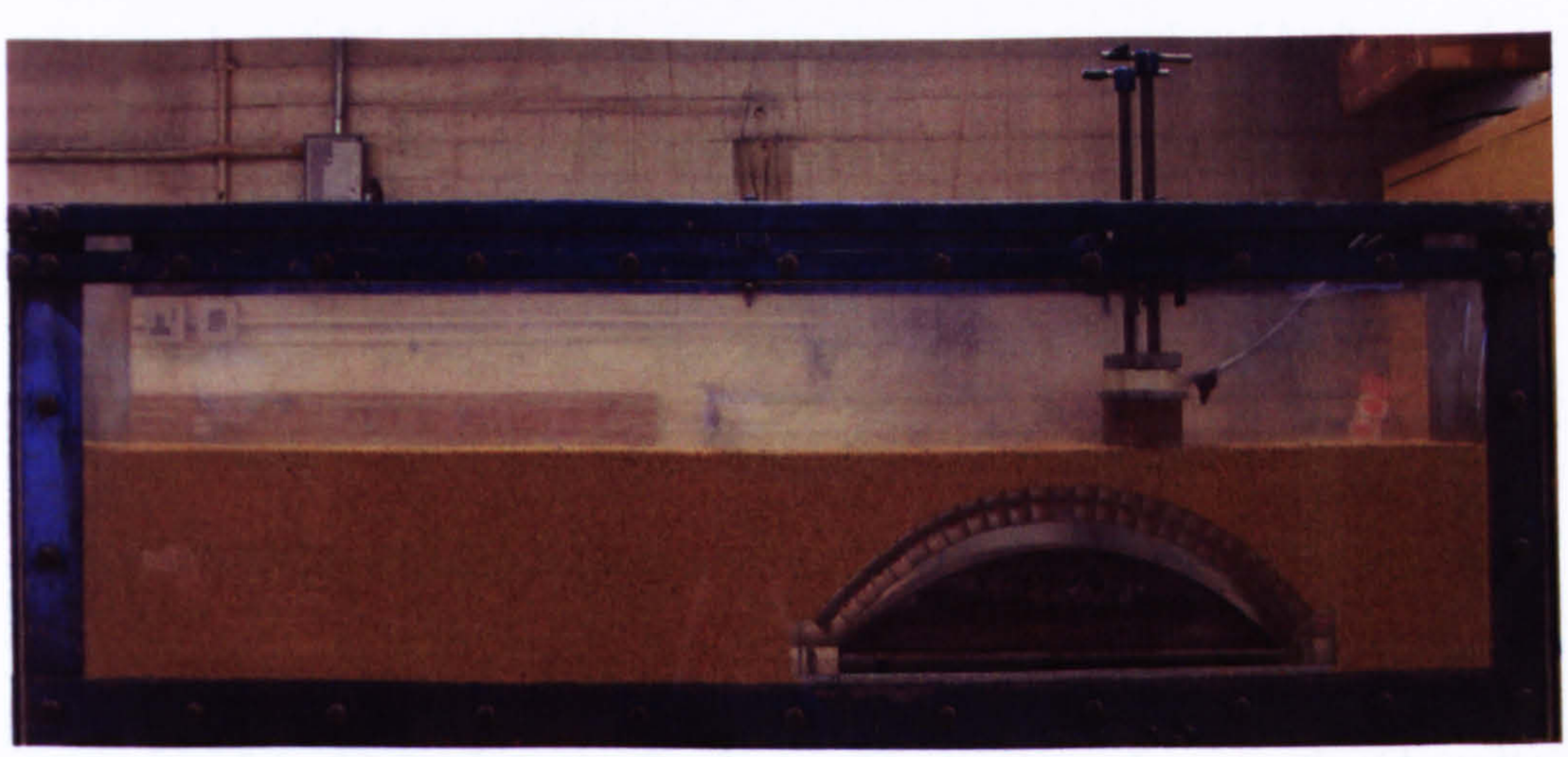

Figure 5-14 Photograph of a deep filled arch test

5.4.2 Sidewall Friction

An additional test was devised and developed which reproduced the fill's contact with the wall under test conditions as shown in Fig. 5-15.

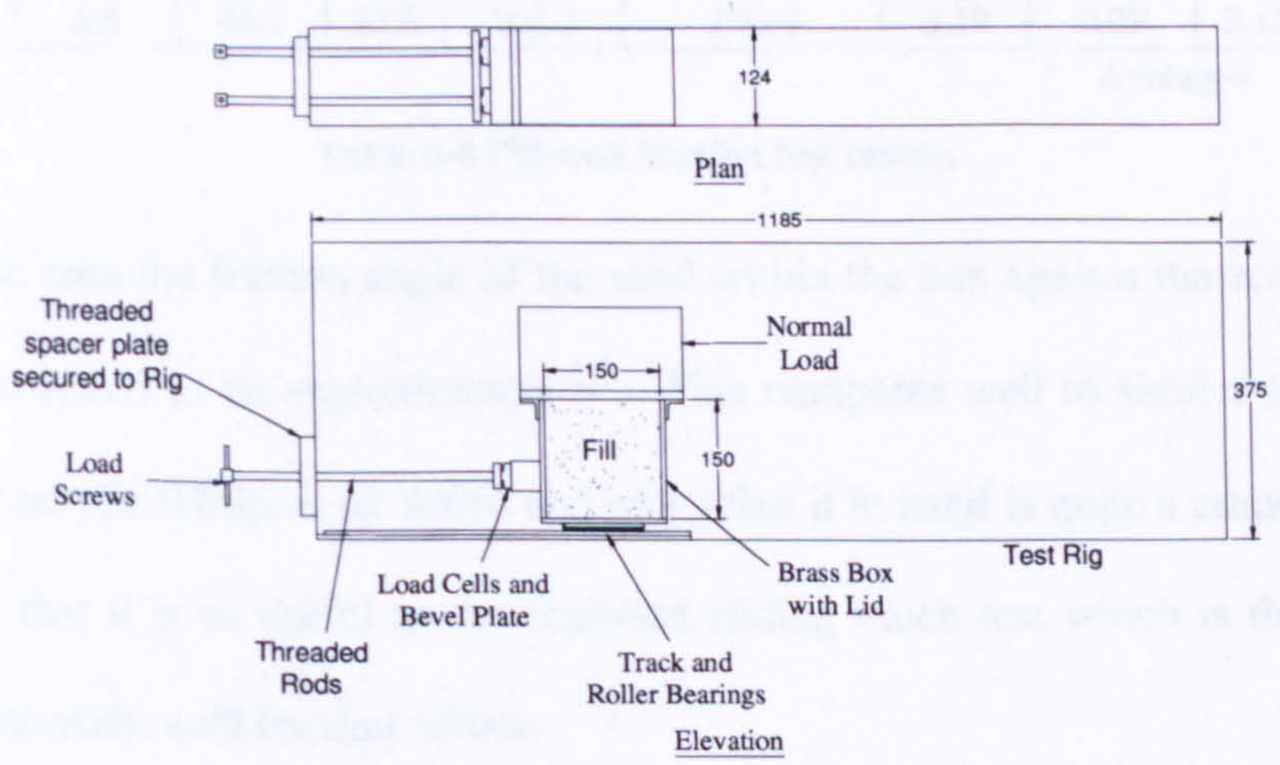

Figure 5-15 Wall friction test apparatus and set-up

Using a brass box on roller bearings, filled by a similar method to that used in the main experiments and a applying a vertical load on top, it was possible, by measuring horizontal movement, to ascertain the resistance produced by having the sand in contact with the sidewall acrylic. This displacement controlled experiment relied on horizontal loading which was applied via the bevel plate connected to a simple hand screw arrangement. The intensity of this load was recorded by two electrical resistance-strain-gauge type load cells. Each full turn of a load screw corresponded with a horizontal displacement of 1.6mm. By comparing an empty box test with a filled box under different applied vertical loads, an approximate estimation of the friction between the sand within the box and the acrylic side walls could be made using the equation $F=\mu R$. The results are shown in Table 5-4.

Normal Load (N)	Horizontal Load			Self Weight (N)	Vertical Load (N)	μ			
	Empty (N)	Filled (N)	E-F (N)			Filled	Empty	F-E	Angle (°)
0.0	4.1	18.6	14.5	102.3	102.3	0.14	0.04	0.10	5.8
19.6	4.3	26.4	22.1	102.3	122.0	0.18	0.04	0.14	7.9
39.2	4.8	33.9	29.1	102.3	141.6	0.21	0.05	0.16	9.0
58.9	6.1	39.6	33.6	102.3	161.2	0.21	0.06	0.15	8.5
78.5	6.9	45.6	38.7	102.3	180.8	0.21	0.07	0.15	8.3
98.1	8.5	46.1	37.6	102.3	200.4	0.19	0.08	0.10	6.0
								Average=	7.6

Table 5-4 Fill-wall friction test results

As can be seen the friction angle of the sand within the box against the acrylic side walls was found to be approximately 8°. This compares well to similar tests with sand and acrylic (Hulet *et al.* 2005) and given that it in itself is quite a crude method, it shows that it is as useful as the standard sliding block test which is the typical way to ascertain wall friction values.

5.4.3 Test Results

The experimental results obtained with the soil-arch test rig for different skewback-abutment conditions are summarised in Table 5-5.

For deep filled arches the different abutment fixity conditions appeared not to influence results significantly, and failure was via a four hinge mechanism. It is perhaps surprising that the 'Free-Free' and 'Fixed-Fixed' tests had similar peak loads; the numerical discrepancy can probably be attributed to test variability (although for repeat tests, variability was surprisingly low).

In the shallow filled arches the use of artificially low friction at the interface between the abutment and skewbacks led to three hinges plus sliding failure mechanisms, though again the effect on the overall load carrying capacity was essentially negligible.

	Scenario	Failure Mechanism	Peak Load (N)			% Difference
			Test 1	Test 2	Test 3	
D1	Deep: Fixed-Fixed	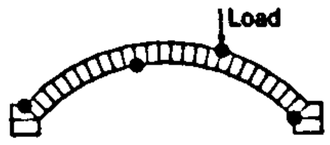	173	172	173	0
D2	Deep: Fixed-Free	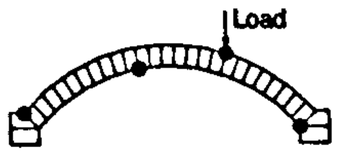	165	162	167	-5%
D3	Deep: Free-Fixed	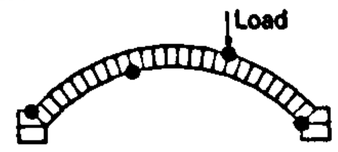	153	152	150	-12%
D4	Deep: Free-Free	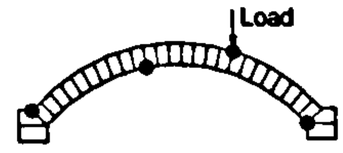	181	183	182	+5%
S1	Shallow: Fixed-Fixed	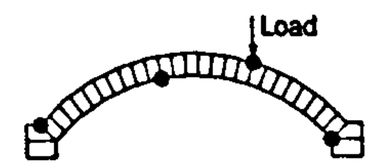	95	96	95	0
S2	Shallow: Fixed-Free	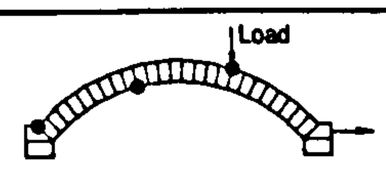	83	84	79	-14%
S3	Shallow: Free-Fixed	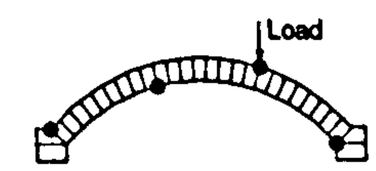	77	74	72	-22%
S4	Shallow: Free-Free	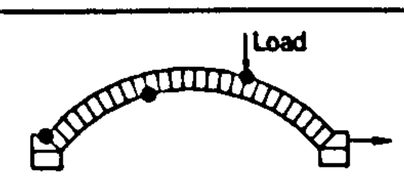	93	94	91	-3%

KEY: Hinge, Sliding

Table 5-5 Peak load and failure mechanism attained for different skewback fixity

5.4.4 Plate Bearing Test

To see how the backfill would fail without any buried arch present a plate bearing test was done (Figure 5-16). In an ideal environment the plotted velocities would be symmetrical about the centre of the load plate; however, a minor experimental inaccuracy has shown the fill prefers to go in the direction shown.

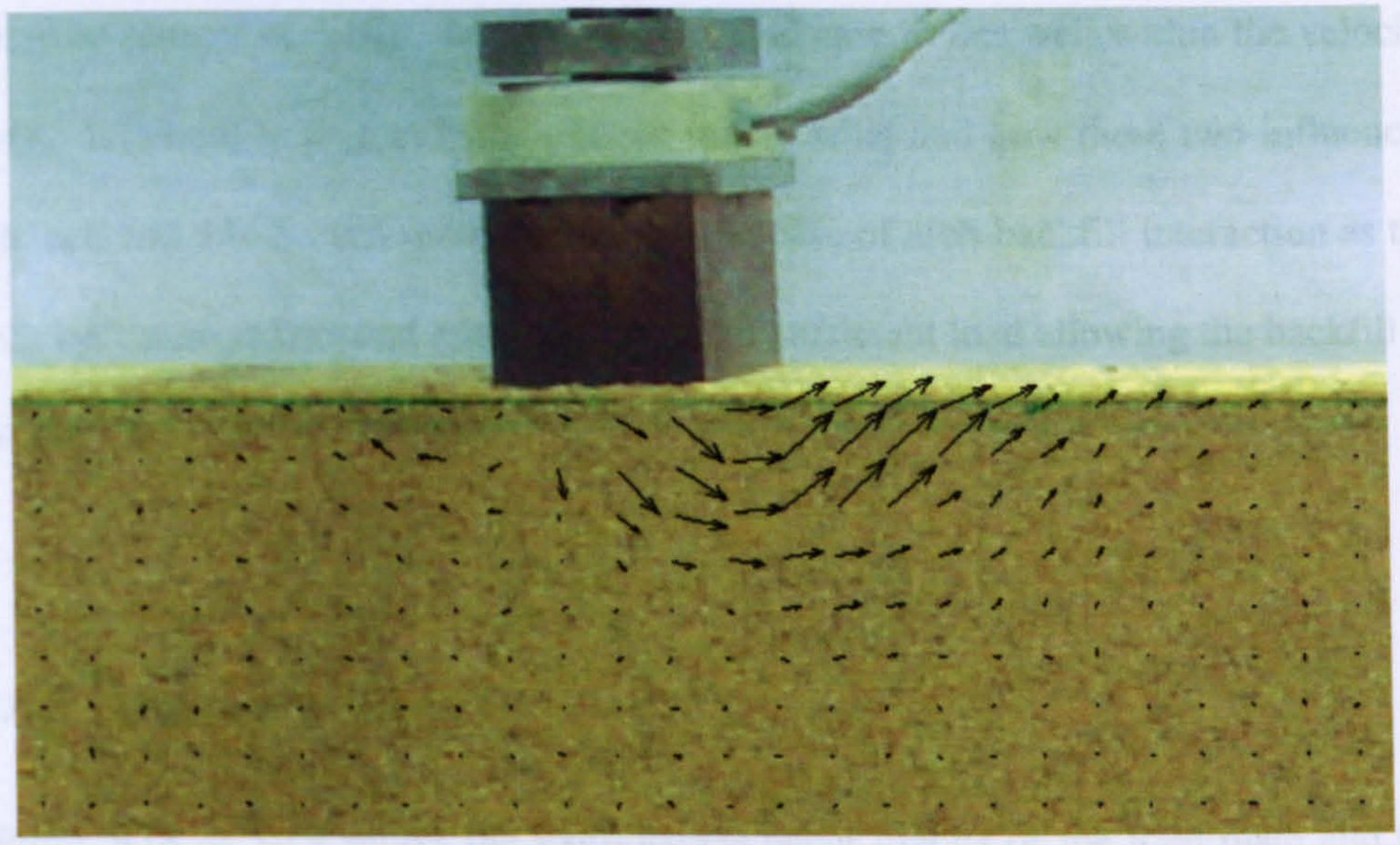

Figure 5-16 Plate bearing test

As can be seen in Figure 5-16 it resembles the upper bound assumed slip failure mechanism for a shallow foundation (Figure 5-17).

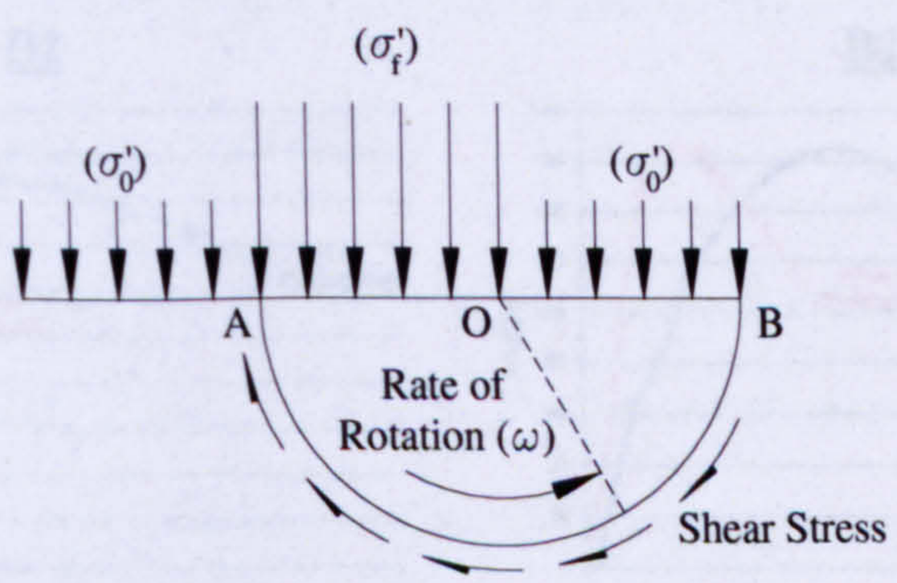

Figure 5-17 Assumed slip circle failure mechanism for a shallow foundation

It is easy to see in regards to the deep and shallow depths of fill used in these experiments that the load plate would have more influence on the shallow arch than the deeper filled one. This analogy isn't entirely accurate as when the arch is present in both the shallow and deep filled tests a hard boundary is present, in the case of the deep fill outside the (above) velocity zones but not outside the predicted

pressure zone of the plate. In the shallow filled case, it lies well within the velocity zone. It is hard to predict using current theory what and how these two influences interact, and this is even more difficult in the case of arch-backfill interaction as the arch isn't always firm and moves away under sufficient load allowing the backfill to follow.

5.4.5 Analysis of Results

Figure 5-18 & 5-19 shows the load-displacement graphs of the load plate and the voussoir directly beneath the load, for the deep and shallow filled arch tests. The greatest variability was during loading when the backfill compressed under the load plate and near the end of the test when gross deformation of the arch was present.

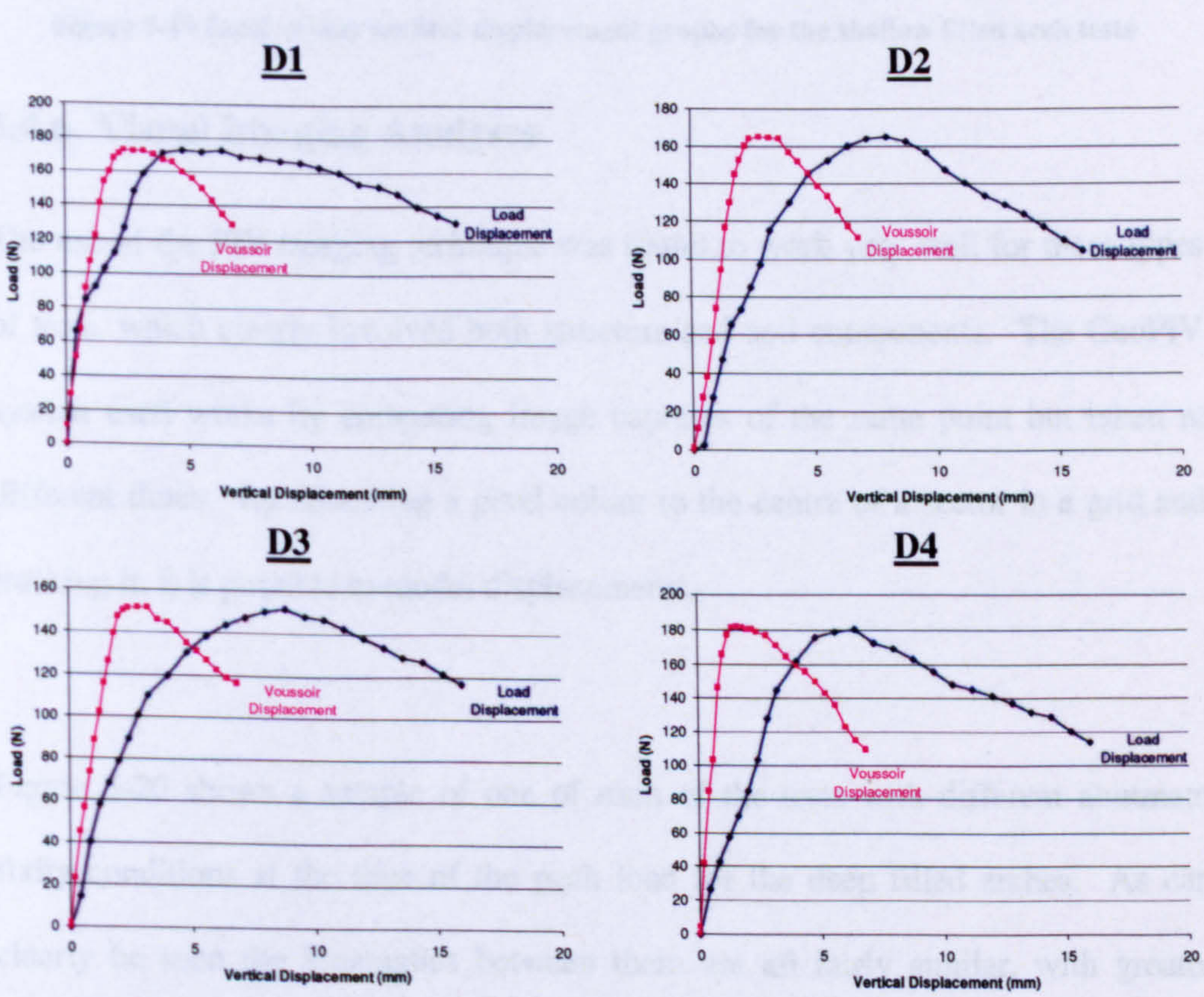

Figure 5-18 Load versus vertical displacement graphs for the deep filled arch tests

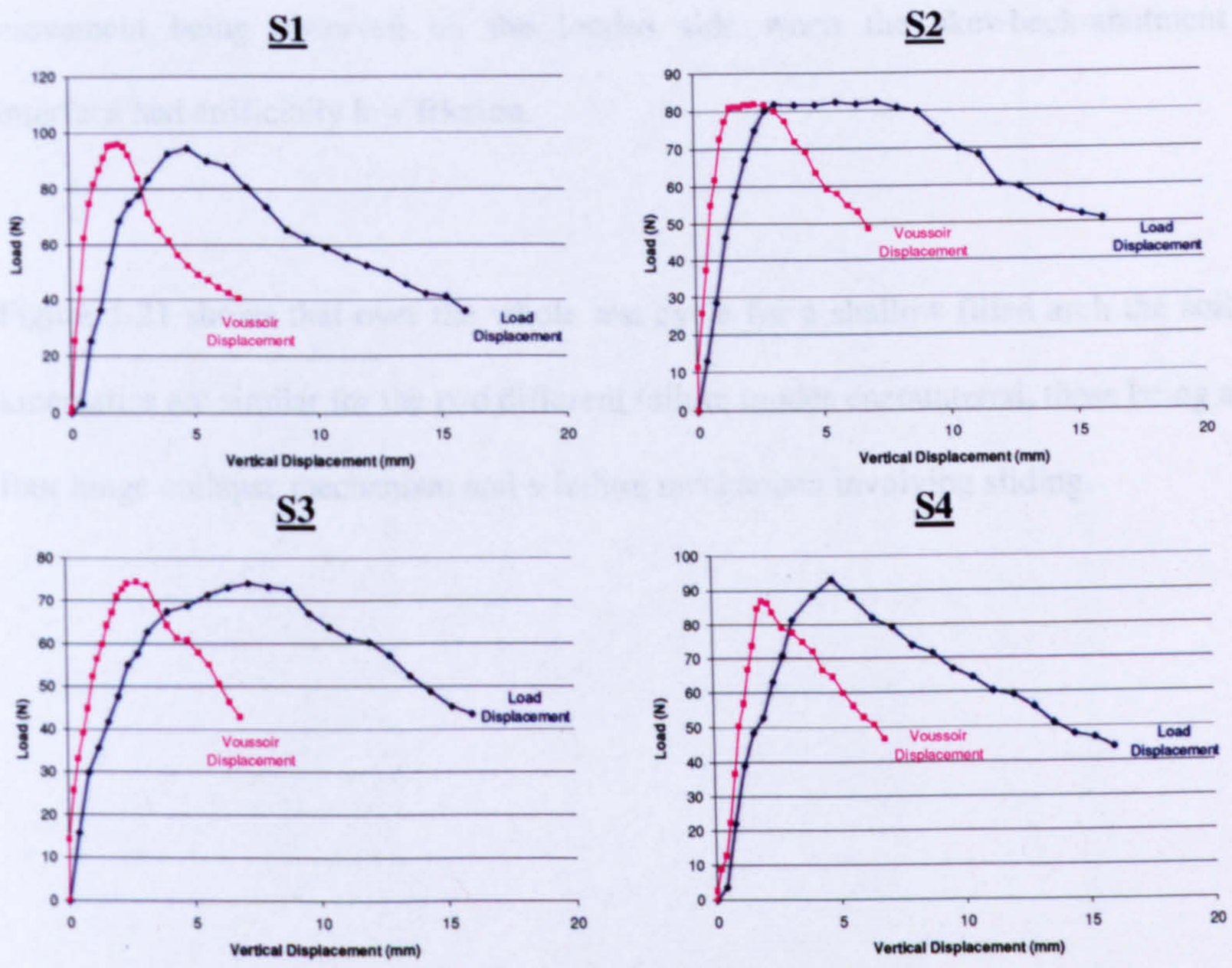

Figure 5-19 Load versus vertical displacement graphs for the shallow filled arch tests

5.4.6 Visual Imaging Analyses

The use of the PIV imaging technique was found to work very well for these types of tests, which clearly involved both structure and soil components. The GeoPIV system used works by comparing image captures of the same point but taken at different times. By allocating a pixel colour to the centre of a sector in a grid and tracking it, it is possible to model displacements.

Figure 5-20 shows a sample of one of each of the tests with different abutment fixity conditions at the time of the peak load for the deep filled arches. As can clearly be seen the kinematics between them are all fairly similar, with greater

movement being observed on the loaded side when the skewback-abutment interface had artificially low friction.

Figure 5-21 shows that over the whole test cycle for a shallow filled arch the soil kinematics are similar for the two different failure modes encountered, these being a four hinge collapse mechanism and a failure mechanism involving sliding.

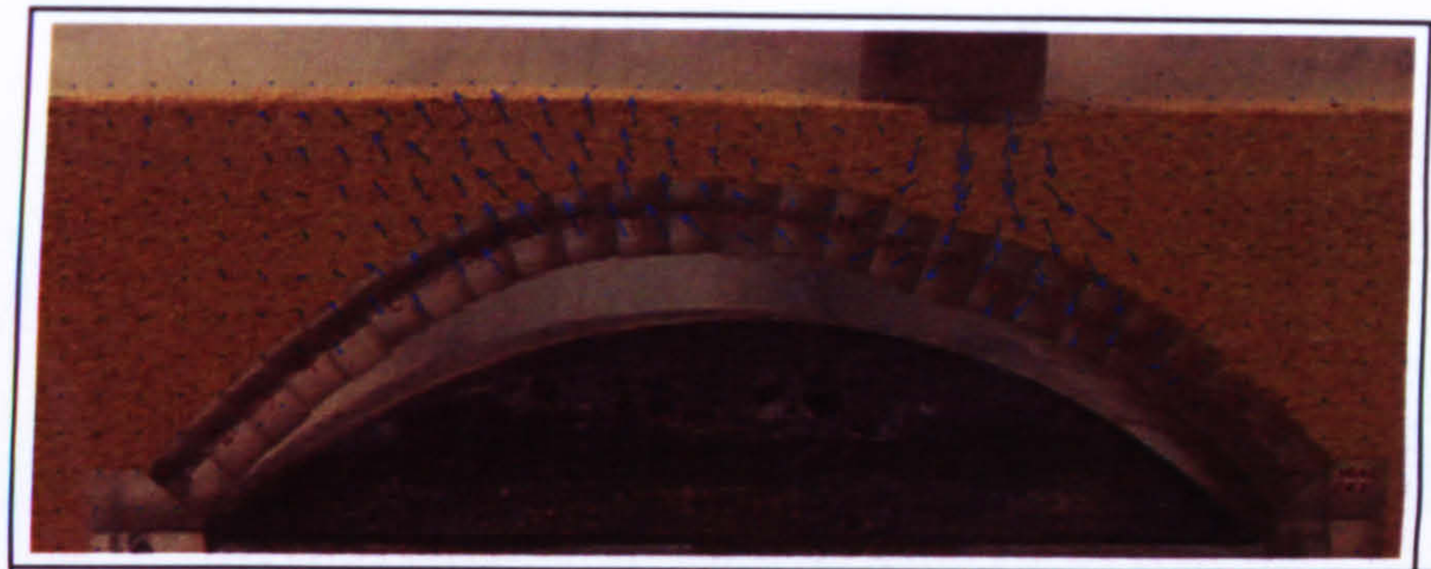

Fixed-Fixed-Deep
(Peak Load =173N)

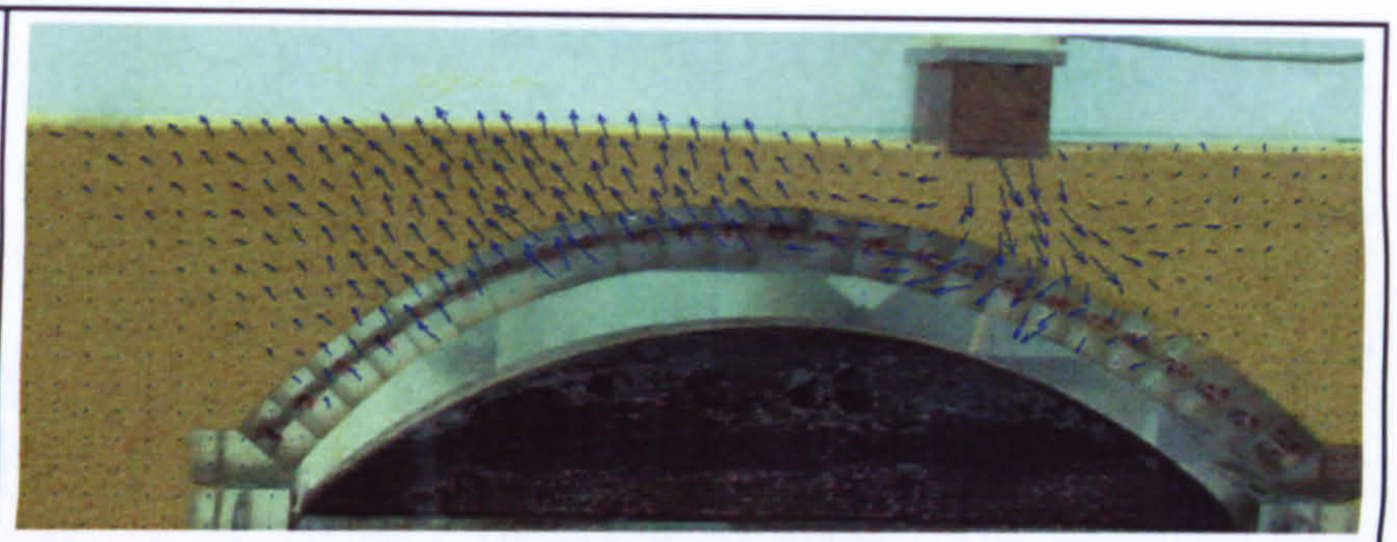

Fixed-Free-Deep
(Peak Load = 165N)

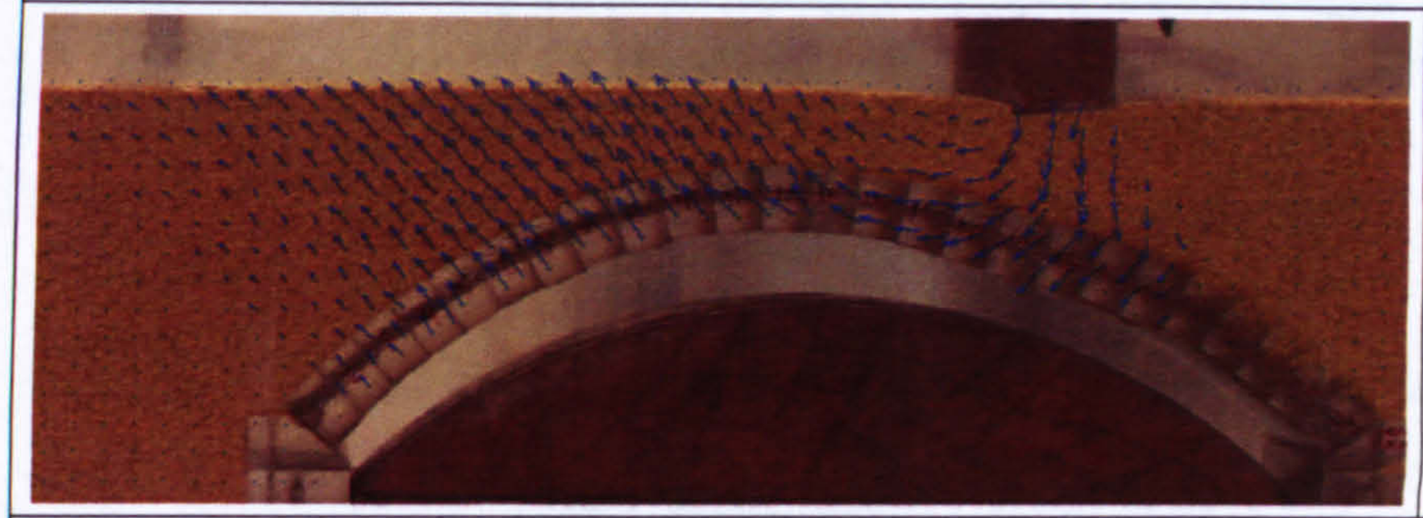

Free-Fixed-Deep
(Peak Load = 152N)

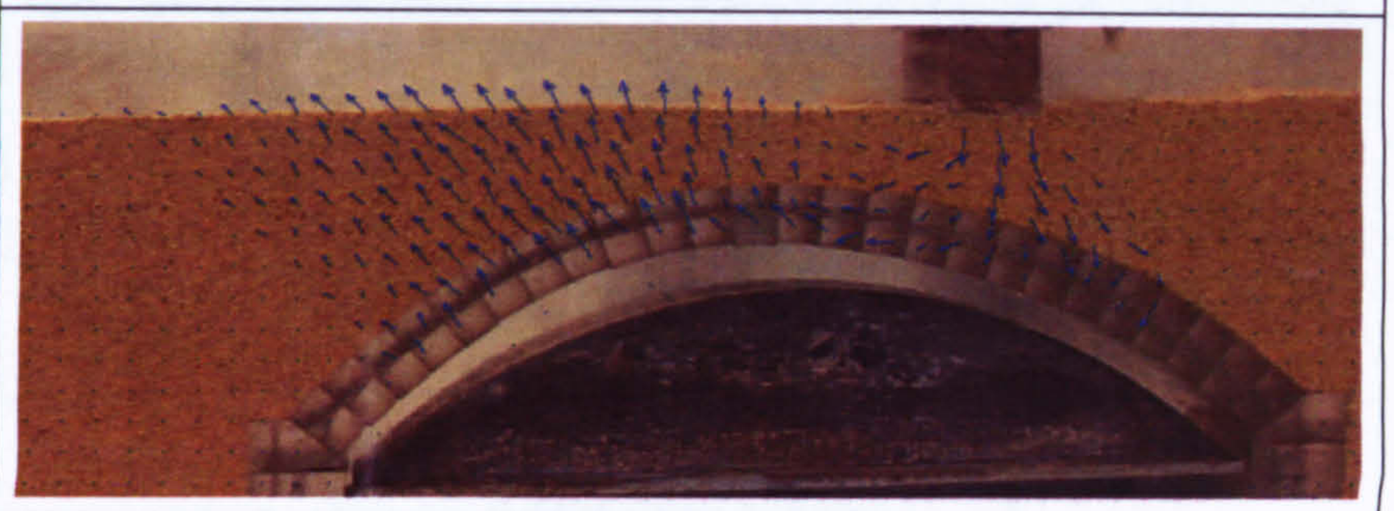

Free-Free-Deep
(Peak Load = 182N)

Figure 5-20 Typical PIV of test cycle for deep filled arches (Arrow magnification= 25)

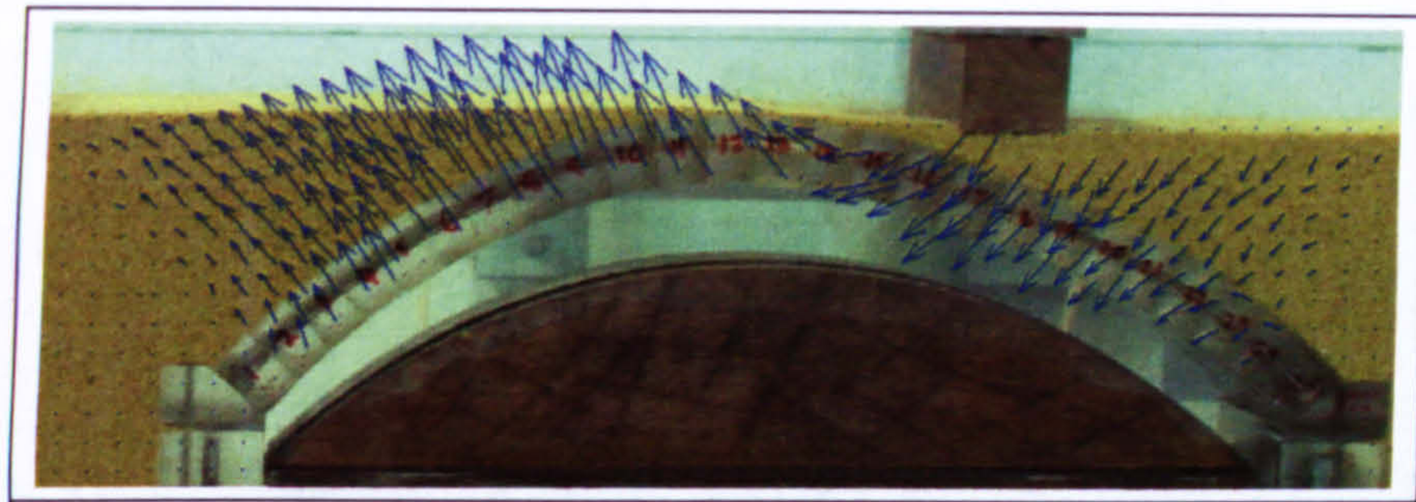

Fixed-Fixed-Shallow
(Peak Load = 95N)

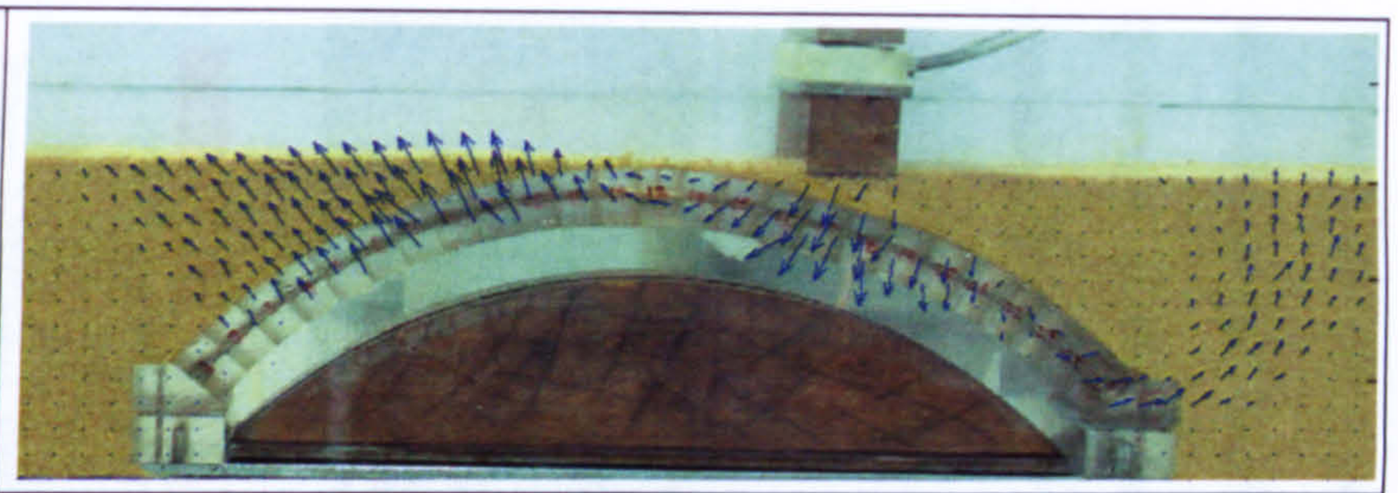

Fixed-Free-Shallow
(Peak Load = 82N)

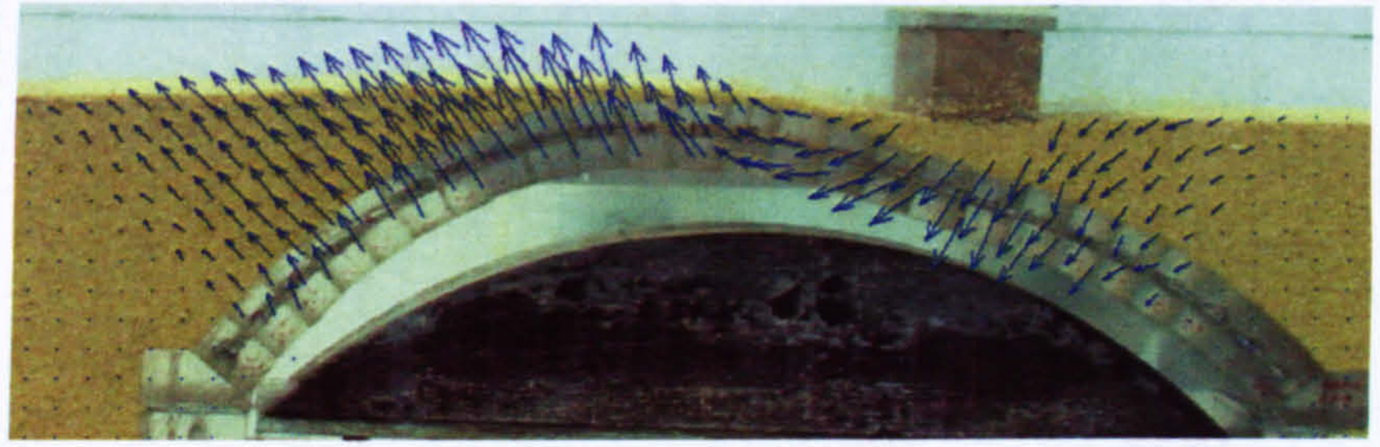

Free-Fixed-Shallow
(Peak Load = 74N)

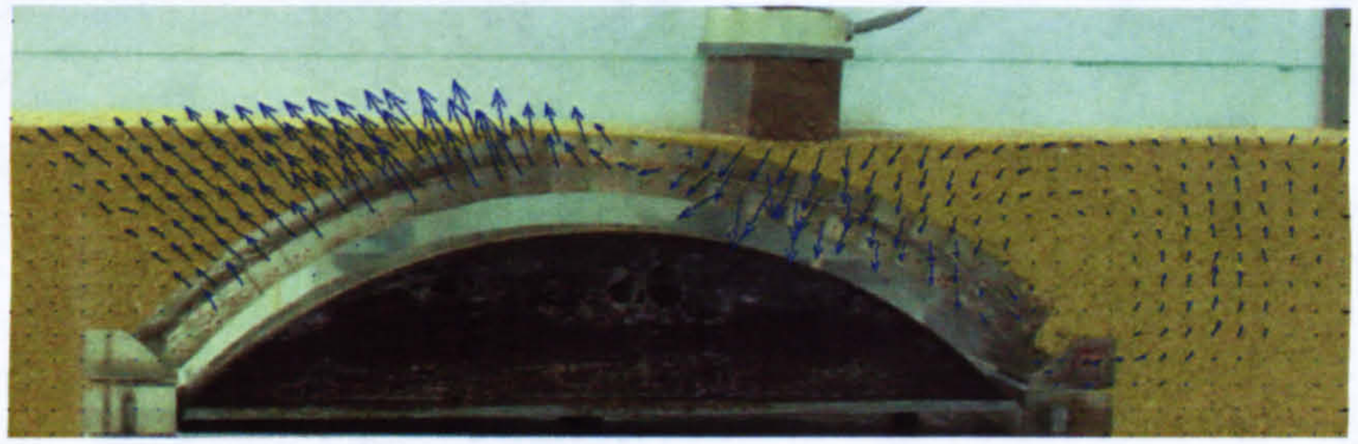

Free-Free-Shallow
(Peak Load = 93N)

Figure 5-21 Typical PIV of test cycle for shallow filled arches (Arrow magnification= 25)

Where sliding failures occurred as part of the failure mechanism the digital imaging technique showed that the backfill behaved similarly to when a vertical soil anchor positioned at depth was pulled out. Strain analyses undertaken using the quantitative abilities of GeoPIV showed that only a fraction of the full passive pressure was developed in these cases, generally ~20% to ~60%, (refer to Figures 5-22 & 5-23).

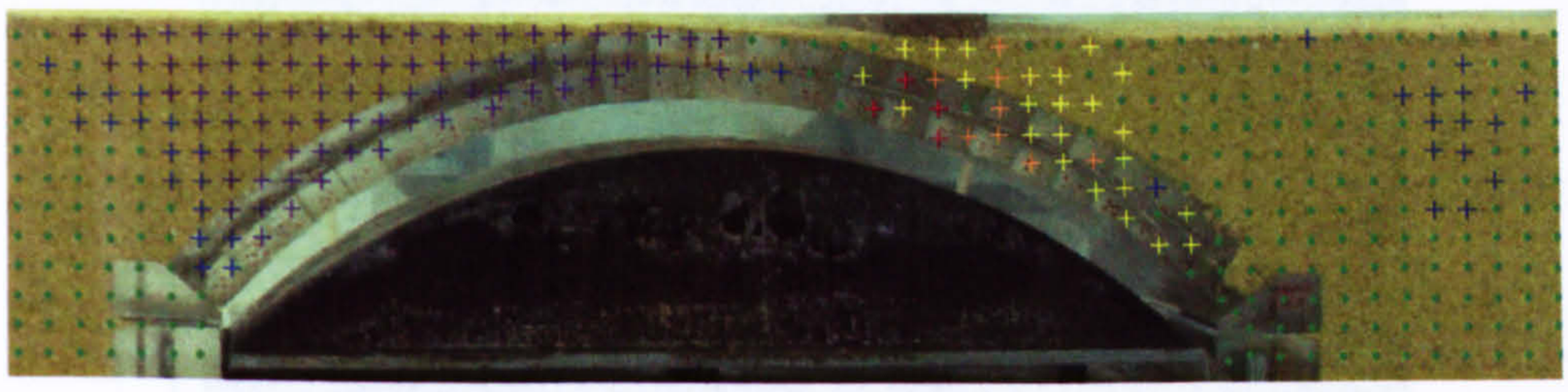

Figure 5-22 GeoPIV strain analysis for shallow filled arch test with the Free-Free scenario

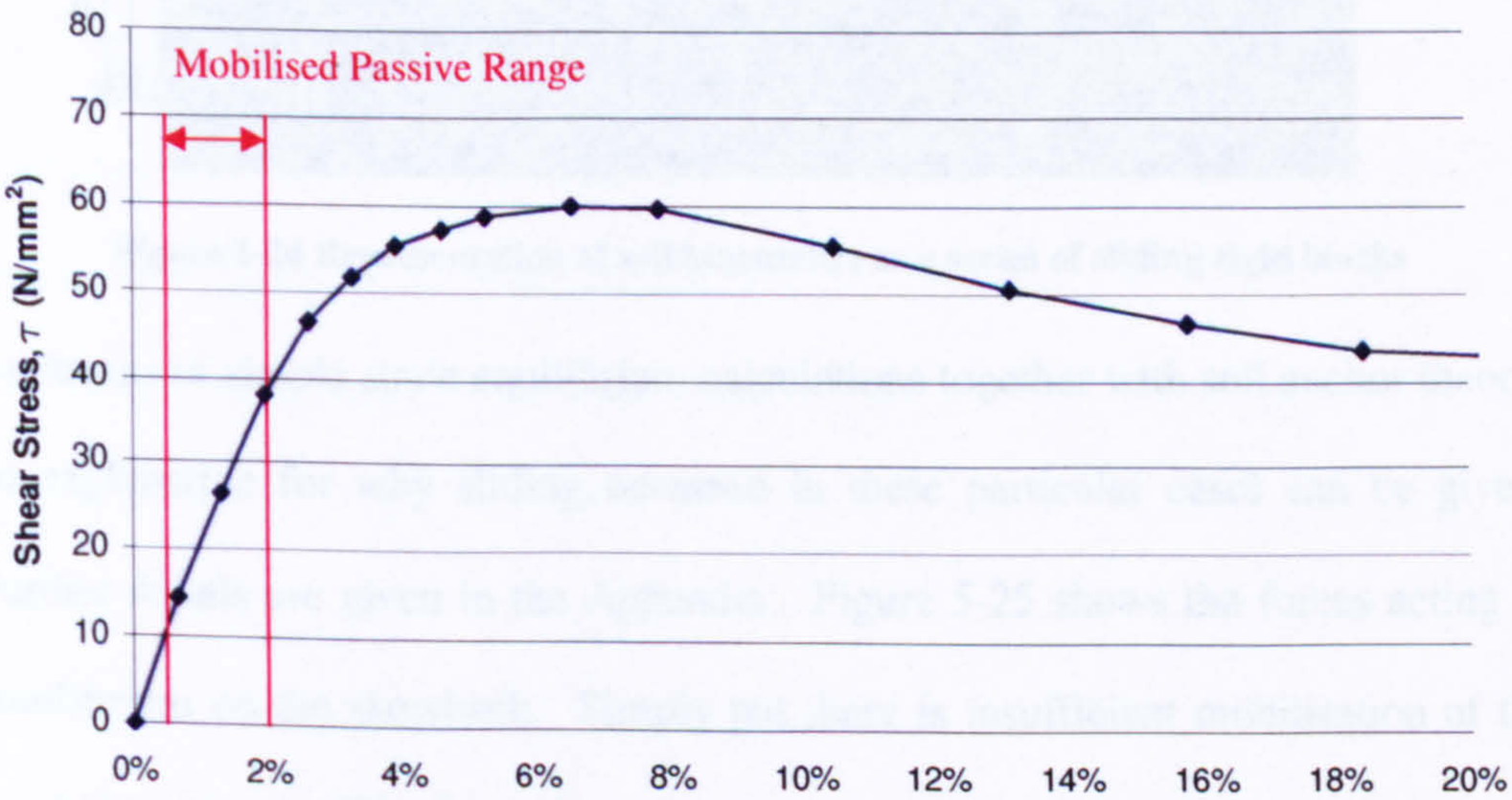

Figure 5-23 Mobilised passive pressures from Direct Shear Box Test (100mm)

5.5 Analysis

The soil kinematics observed following a GeoPIV analysis of the shallow filled arch experiments are similar to those expected when a buried vertical anchor plate is pulled out, (see Figure 5-24). Using this assumption an analytical approach is investigated in this section in order to numerically model such a failure.

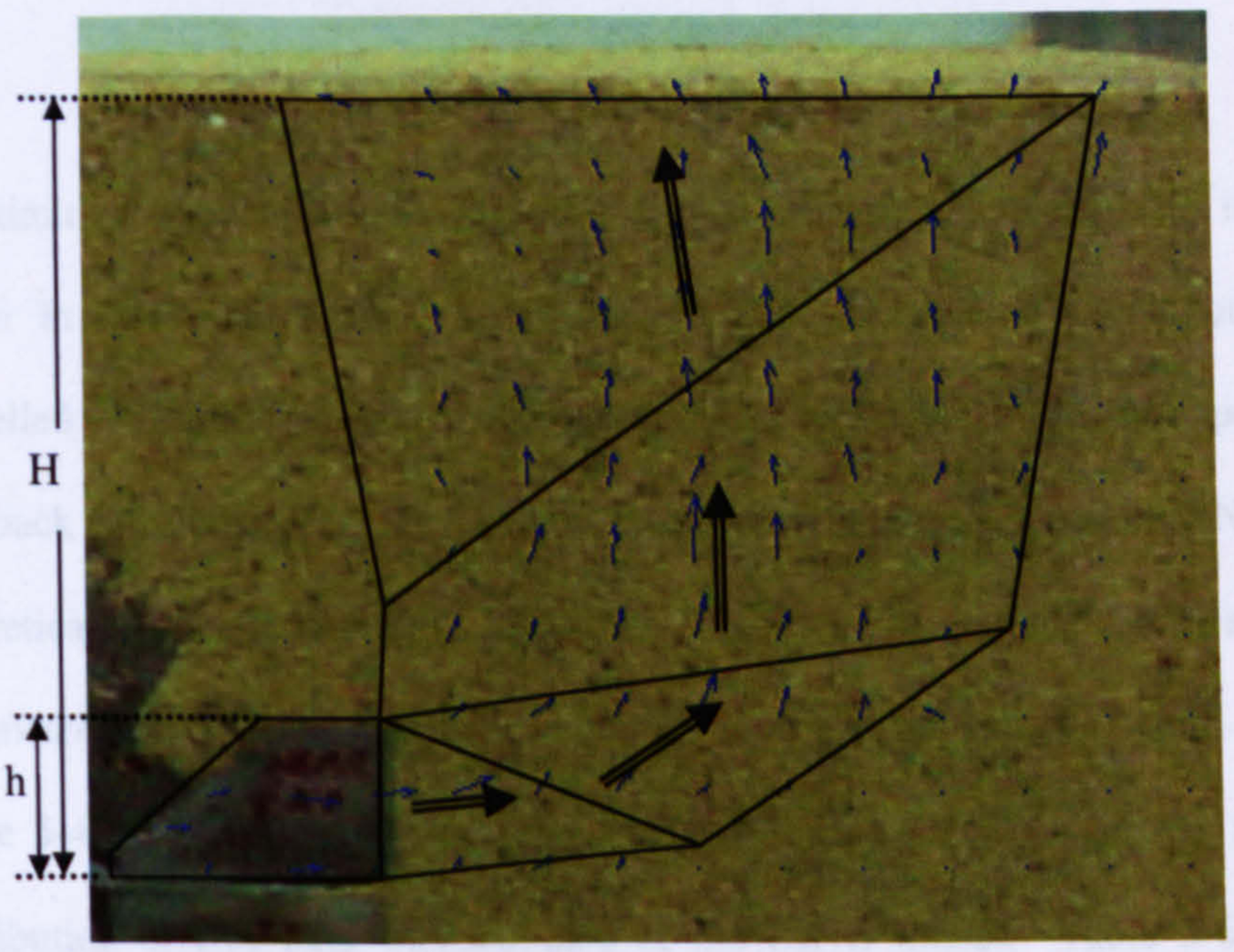

Figure 5-24 Representation of soil kinematics as a series of sliding rigid blocks

By means of simple static equilibrium calculations together with soil anchor theory, an explanation for why sliding occurred in these particular cases can be given, Further details are given in the Appendix. Figure 5-25 shows the forces acting in equilibrium on the skewback. Simply put there is insufficient mobilisation of the passive pressure within the soil to counter the horizontal thrust from the arch at low friction.

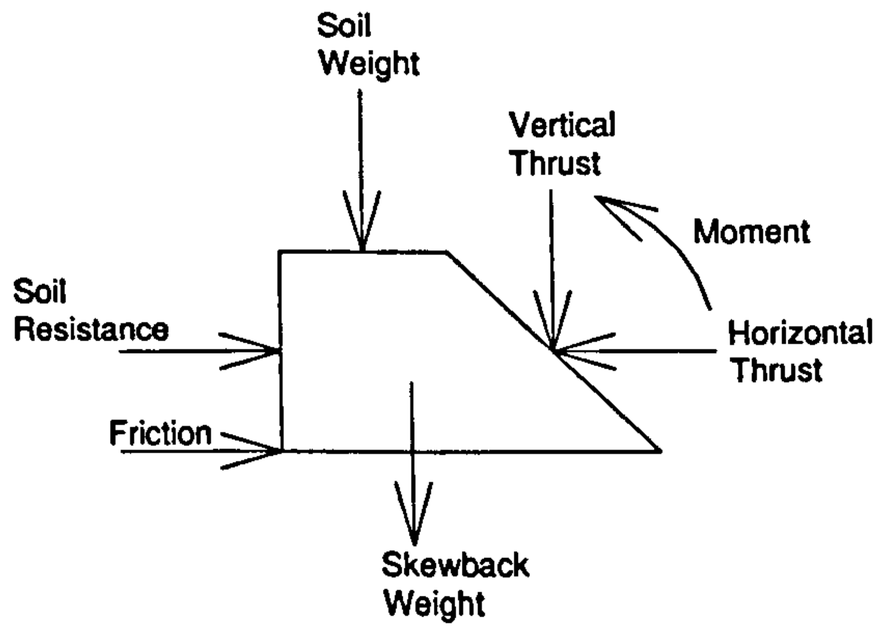

Figure 5-25 Forces acting on a skewback

The limiting trapdoor / horizontal soil anchor pressure was calculated using the solver in Microsoft Excel. The force required to produce a computationally modelled arch failure that replicated the failure present in the test rig experiments, was back calculated using RING. This was then manually replaced in RING by the theoretically determined soil pressure. The RING models used additional parameters from the experimental and mechanical data given in Figure 5-13 and Table 5-4. In line with the findings of the previous Chapter 4 of this thesis, no distribution of live load was included in the RING model. Table 5-6 shows a comparison between the experimental test rig results and the RING simulations carried out using the pressures calculated according to horizontal trapdoor / anchor theory.

Test No	Experimental	Basic RING Model	
D1	173	185.0	+7%
D2	165	184.8	+12%
D3	152	66.0	-67%
D4	182	65.7	-64%
S1	95	97.5	+3%
S2	82	97.1	+18%
S3	74	41.0	-45%
S4	93	40.6	-56%

Table 5-6 Comparison of RING results with normal then modified soil pressures

It can be seen that current theoretical soil models over predict by up to 18% for the tests where the non loaded side is free to slide and where a failure is by formation of a four hinge mechanism, giving unsafe results. Conversely, the models under predict for the live loaded side failures by up to 67% and expected sliding failures where in the tests there were none.

Soil Anchor Theory

There are several methods with which to design vertical anchors usually based upon a modified bearing capacity for deep anchors and passive earth pressure for shallow; a deep anchor being H/h>7. Also the resistance of shallow anchors where H/h<4 depends upon anchor roughness and weight, though perhaps fortunately at the intermediate zone 4<H/h<7 then computations in which the anchor wall is assumed to be smooth give good correlation to measured experimental values (Dickin & Leung 1984). Given that in all the tests presented within this thesis are within this intermediate zone (5.2<H/h<6.8) only solutions for this area are considered here.

A soil anchor may fail in two ways, either rotation (Figure 5-26) or translation (Figure 5-27). Now rotational failures tend to only occur in deep anchors and the kinematic pattern given on the GeoPIV image above correlates well with the pattern for a translation failure given for the Ovesen approach in the paper by Dickin & Leung (1984).

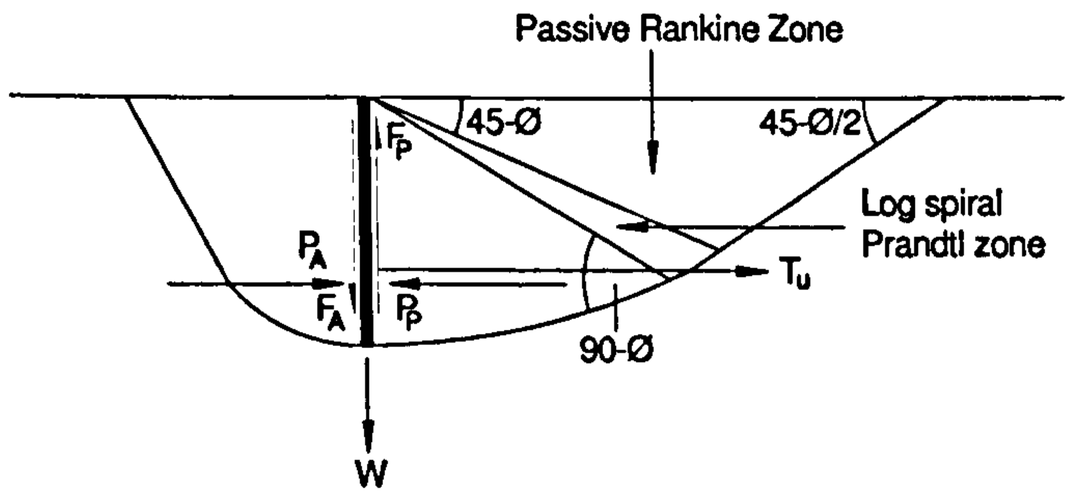

Figure 5-26 Translational failure of a vertical anchor plate (Ovesen)

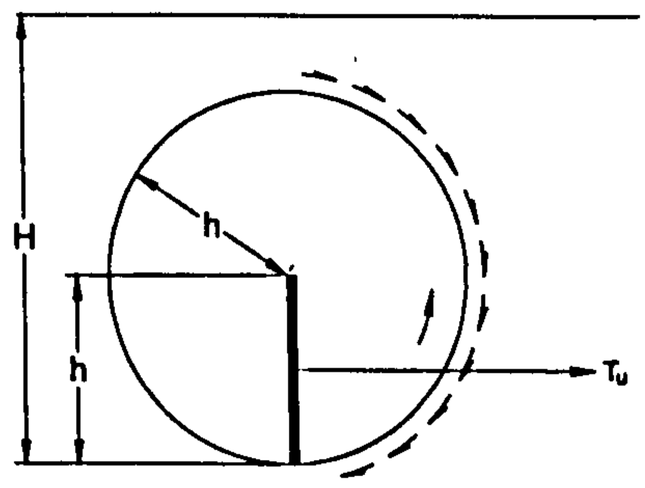

Figure 5-27 Rotational failure of a vertical anchor plate (Biarez)

One of the findings within the paper by Dickin is that comparison between experiments and design methods in dense sand tend to be inaccurate and that the use of mobilised soil friction angle rather than peak gives a good correlation. So in effect it means that current theoretical approaches do not work too well when compared with experimental test data. As part of the analysis in this PhD the mobilised soil friction angle has been determined by independent means so that this

angle can be used rather than assuming the peak passive soil friction angle for the fill material. Work done by Neeley referred to in the Dickin paper showed that a conservative surcharge method utilising a log spiral slip plane may be used to represent the failure exhibited by a vertical anchor but this takes no account of soil shear action above the height h. It is using a similar approach to this that is made use of in this analysis.

By turning the kinematics into a two stage problem to be solved using a computer a model can be made to replicate the experimentally observed soil kinematics. The first stage involves treating the back of the skewback as a smooth retaining wall which is solved using the two-triangle method described by Chen (1975). The next step uses a trapdoor solution proposed by Murray & Geddes (1987).

Two Triangle Method

This method consists of two rigid sliding blocks described by the parameters ρ, η and Ω; refer to Figure 5-28 for the corresponding velocity fields for the passive state.

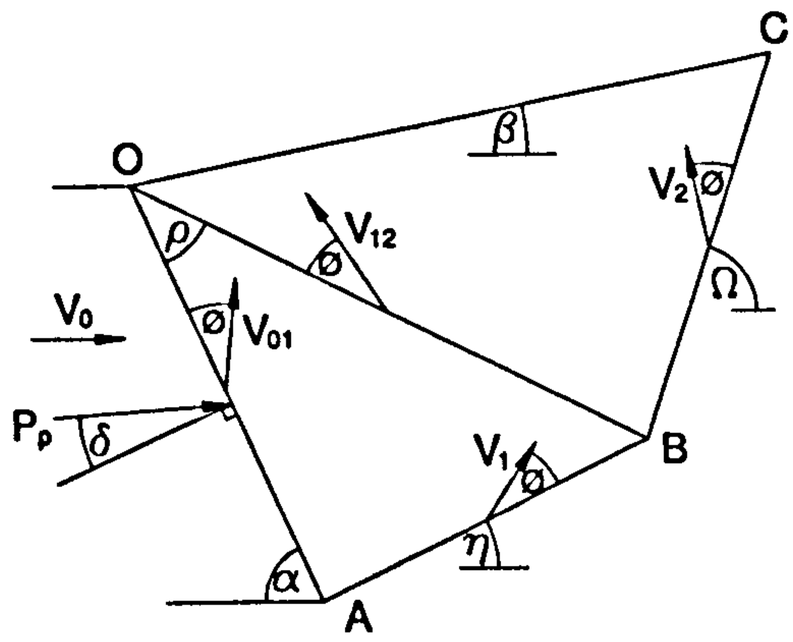

Figure 5-28: Passive state two triangle mechanism

Since the sand used in the experiments is taken as having weight, being cohesionless, and for ease having no surcharge loading. The wall is taken as being perfectly smooth. The external work is simply the area of the considered region multiplied by the vertical component of that region's velocity.

For region OAB: $$\frac{-{}^1/_2.\gamma.H^2.V_1.\mathrm{Sin}\rho.\mathrm{Sin}(\alpha+\eta).\mathrm{Sin}(\eta+\phi)}{\mathrm{Sin}^2\alpha.\mathrm{Sin}(\alpha+\eta-\rho)}$$

.....(5-3)

For region OBC: $$\frac{-{}^1/_2.\gamma.H^2.V_2.\mathrm{Sin}^2(\alpha+\eta).\mathrm{Sin}(\alpha-\rho+\beta).\mathrm{Sin}(\alpha-\rho+\Omega).\mathrm{Sin}(\Omega+\varphi)}{\mathrm{Sin}^2\alpha.\mathrm{Sin}(\alpha+\eta-\rho).\ \mathrm{Sin}(\Omega-\beta)}$$

.....(5-4)

This method relies on movement of the wall whose external work contribution can be determined by the equation:

Moving wall load: $P_{pn}.V_0.[\mathrm{Sin}\alpha+\mathrm{Tan}\delta.\mathrm{Cos}\alpha]$

.....(5-5)

The two triangle method relies on an equilibrium work balance equation where the rate of external work done equals the internal energy dissipated. Since the wall is taken to be smooth ($\delta<\phi$) the dissipation by sliding friction is given by:

Sliding friction: $P_{pn}.\,Tan\delta.V_{01}$

.....(5-6)

By using the compatible velocity diagrams to express all the mechanism velocities in terms of V_0 yields the following:

$$V_1 = \frac{V_0.Sin\alpha}{Sin(\eta+\phi+\alpha)} \qquad .....(5\text{-}7)$$

$$V_{01} = \frac{V_0.Sin(\eta+\varphi)}{Sin(\eta+\phi+\alpha)} \qquad .....(5\text{-}8)$$

$$V_2 = \frac{V_0.Sin\alpha.Sin(\alpha-\rho+\eta+2\,\phi)}{Sin(\eta+\phi+\alpha).Sin(\alpha-\rho+\Omega+2\,\phi)} \qquad .....(5\text{-}9)$$

$$V_{12} = \frac{V_0.Sin\alpha.\,Sin(\Omega-\eta)}{Sin(\eta+\phi+\alpha).Sin(\alpha-\rho+\Omega+2\,\phi)} \qquad .....(5\text{-}10)$$

By equating external work done to internal energy dissipated a value for $K_{p\gamma}$ can be established.

$$K_{p\gamma} = \frac{(A+B).Sec\delta}{Sin\alpha+Tan\delta.Cos\alpha-\dfrac{Tan\delta.Sin(\eta+\varphi)}{Sin(\rho+\phi+\alpha)}} \qquad .....(5\text{-}11)$$

Where,

$$A = \frac{\text{Sin}\rho.\text{Sin}(\alpha+\eta).\text{Sin}(\eta+\phi)}{\text{Sin}\alpha.\text{Sin}(\alpha+\eta-\rho).\text{Sin}(\eta+\phi+\alpha)} \qquad \text{.....(5-12)}$$

$$B = \frac{\text{Sin}^2(\alpha+\eta).\text{Sin}(\alpha-\rho+\beta).\text{Sin}(\alpha-\rho+\Omega).\text{Sin}(\Omega+\phi).\text{Sin}(\alpha+\eta-\rho+2\phi)}{\text{Sin}\alpha.\text{Sin}^2(\alpha+\eta-\rho).\text{Sin}(\Omega-\beta).\text{Sin}(\alpha+\eta+\phi).\text{Sin}(\alpha-\rho+\Omega+2\phi)} \qquad \text{.....(5-13)}$$

Thus by minimising $K_{p\gamma}$ with respect to ρ, η and Ω an upper-bound solution can be obtained.

Using superposition adding in a term for a uniform surcharge (q) requires the addition of a further external work parameter for a weightless soil which is given by the term:

$$\text{Surcharge} = \frac{-q.H.V_2.\text{Sin}(\alpha+\eta).\text{Sin}(\alpha-\rho+\Omega).\text{Sin}(\Omega+\phi)}{\text{Sin}\alpha.\text{Sin}(\alpha+\eta-\rho).\text{Sin}(\Omega-\beta)} \qquad \text{.....(5-14)}$$

Solving for K_{pq} gives:

$$K_{pq} = \frac{(C).\text{Sec}\delta}{\text{Sin}\alpha+\text{Tan}\delta.\text{Cos}\alpha - \dfrac{\text{Tan}\delta.\text{Sin}(\eta+\phi)}{\text{Sin}(\eta+\phi+\alpha)}} \qquad \text{.....(5-15)}$$

Where,

$$C = \frac{\text{Sin}(\alpha+\eta).\text{Sin}(\alpha-\rho+\Omega).\text{Sin}(\Omega+\phi).\text{Sin}(\alpha+\eta-\rho+2\phi)}{\text{Sin}(\alpha+\eta-\rho).\text{Sin}(\Omega-\beta).\text{Sin}(\eta+\phi+\alpha).\text{Sin}(\alpha-\rho+\Omega+2\phi)} \qquad \text{.....(5-16)}$$

Again it is necessary to minimise K_{pq} with respect to ρ, η and Ω to obtain an upper-bound solution.

Trapdoor Theory

The next stage of the process considers the failure of a trapdoor type mechanism being pulled vertically staying with an upper-bound approach using Figure 5-29.

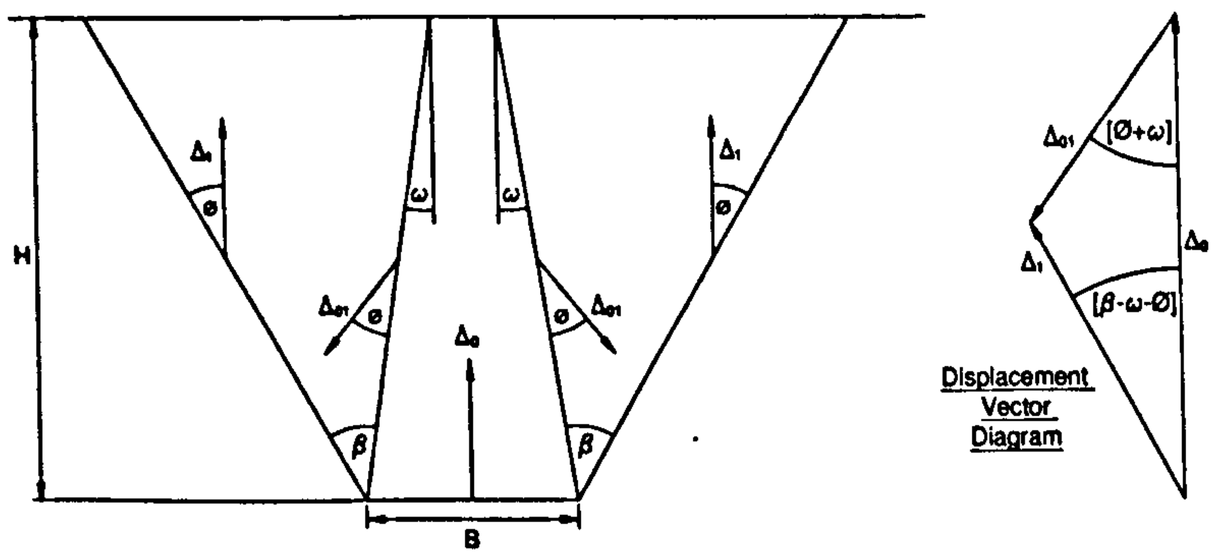

Figure 5-29: Passive state trapdoor mechanism

No energy is dissipated on any displacement continuity in a cohesionless soil. Therefore the work balance equation is given by:

$$\frac{P}{\gamma.B.H} = 1 + \frac{H}{B}\,\frac{Tan(\phi+\omega).Tan(\beta-\omega)-Tan\omega.Tan(\beta-\omega-\phi)}{Tan(\phi+\omega)+Tan(\beta-\omega-\phi)} \qquad .....(5\text{-}17)$$

Which, since a minimum value of β is required can be given by $\beta=\omega+\phi$, reduces to:

$$\frac{P}{\gamma.B.H} = 1 + \frac{H}{B}\,Tan\,\phi \qquad .....(5\text{-}18)$$

When it came to using the two-triangle method coupled with the trapdoor / anchor theory the horizontal pressures calculated were insufficient for the RING model to make a stable structure in the low friction cases. It was found that in most cases at least twice (and in some cases more) the calculated horizontal pressure was required to produce a numerically similar result to that attained in the experiments. It is not readily apparent why the passive pressures, proven to be mobilised during the experiment, are theoretically insufficient to obtain numerical agreement.

One difficulty for current analysis packages is that passive pressures usually have to be entered before the arch has failed in order to satisfy the solution algorithms used; however in reality, until the failure response of the arch is known, no passive pressures are generated either fully or partially. Another difficulty is that soil friction angles (and for clay, cohesion) can vary during the experimental tests, making the assumption that these are constant in any subsequent analysis inaccurate.

What is apparent though is that current relatively simplistic soil models are incapable of providing numerical predictions which are in agreement with the experiments, and that in an assessment where sliding is deemed likely, it is probable that the analysis will give an over-conservative result. To this end investigations into using and calibrating holistic models (e.g. as shown in Figure 5-30) should be undertaken, i.e. modelling both arch and backfill directly (rather than merely modelling the expected *effects* of backfill).

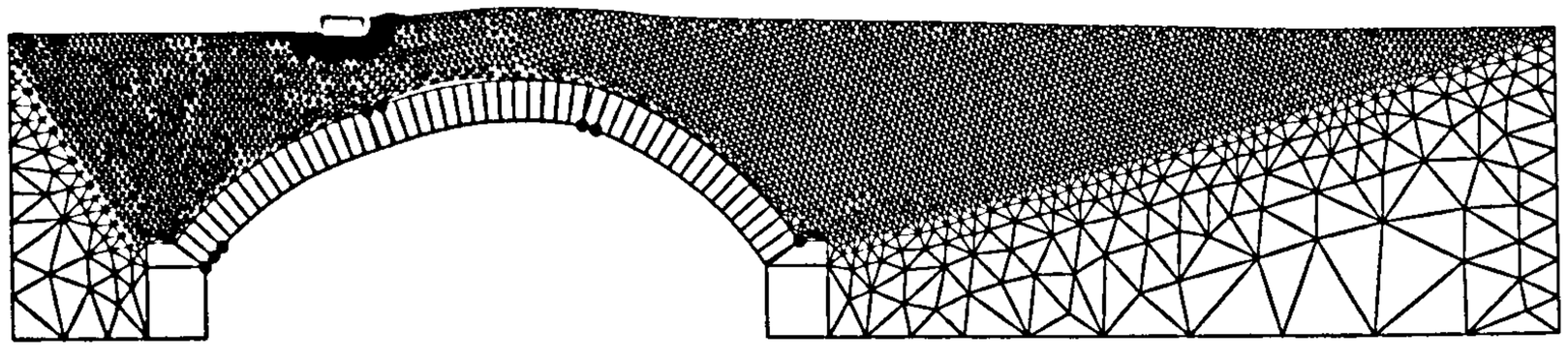

Figure 5-30 Advanced 2D soil structure interaction model, currently in development at the University of Sheffield (Gilbert *et al.* 2007)

5.6 Discussion of Results

The fact that even in a 'worst case scenario' where friction equals zero, there was no difference in the experimentally obtained peak load capacity of bridges with fixed or free abutment-skewback interfaces implies that for the majority of cases abutments can safely be assumed to be rigid, and whether the precise response of fill behind abutments is worth exploring further becomes something of a moot point. Also now knowing the kinematics of the soil proves that the horizontal component of the backfill passive pressure actually does contribute more than the vertical component of the backfill or dead weight to the stability of an arch. However, the ability of computational software to predict this is limited to scenarios where sliding occurs on the unloaded side of the arch. The bridges most at risk from a sliding failure are ones with a flat profile, low soil strength and shallow depth of fill.

The occurrence of skewback-abutment sliding at the side of the bridge where the load was applied gives cause for further thought, so too does the fact that only part of the full passive resistance available is mobilised during the translational failure mechanism observed. The sliding skewback acts like a vertical soil anchor at depth

rather than a retaining wall, at variance to the assumptions made by most existing arch analysis programs.

The current simple soil model incorporated in RING 1.5 has been found to be unable to reliably model situations where a skewback slides over the abutments.

5.7 Recommendations

Since more suitable computational assessment methods have still to be developed, a short term strategy for dealing with the issue of sliding is needed for bridges deemed to be a risk from this type of failure (e.g. those with flat profiles, low soil friction angles and shallow fill depths). It is therefore recommended that for these bridges the following method be adopted:

Step 1: Routine assessment.

Step 2: Assessment allowing skewbacks to slide. Unless other factors help determine this (i.e. demolition of an adjacent span or when significantly weaker fill is present behind one abutment) both sides should be investigated for sliding. It is technically possible to get a failure where sliding happens on both sides at the same time though in reality this is unlikely to happen, (see Figure 5-31).

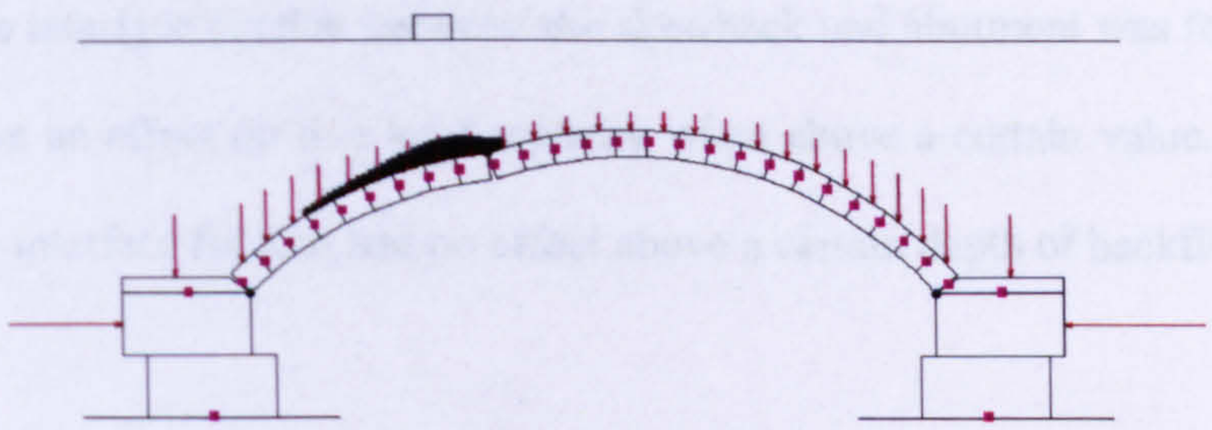

Figure 5-31 A theoretically possible but in reality unlikely failure mechanism involving sliding on both abutments

Step 3: Take the lowest value obtained by steps 1 and 2 as the predicted failure load of the bridge.

If sliding is deemed likely due to a failure at the skewback-abutment joint, it may be possible to reinforce this using remedial techniques (though more research in this field would be advisable).

5.8 Conclusions

1 Maintaining a symmetric profile for the arch during collapse allowed the live load carrying capacity to be largely unaffected despite having a sliding component present in the mechanism.

2 An asymmetric arch exhibited a lower live load carrying capacity than a symmetrically failing one due to the inability of enough passive resistance being mobilised by the system alone on one side of the arch.

3 The interface friction between the skewback and abutment was found not to have an effect on live load capacity when above a certain value. Likewise the interface friction had no effect above a certain depth of backfill.

4 The processing of the digital images indicated that a sliding skewback was kinematically similar to a buried soil anchor rather than a retaining wall a previously academic thinking suggested.

5 Development of the new proposed model based upon trapdoor and anchor theory presented shows promise and it is envisioned that numerical as well as kinematic agreement could be achieved with further development.

Chapter 6

Discussion

6.1 Introduction

This chapter discusses some of the findings given in the previous chapters. Three questions were posed in the introduction and here each it taken and examined in more detail drawing together this research, current literature information and relevant theory.

6.2 Effect of Load Distribution

Q1: What effect does the fill between the live load applied at the road surface and the extrados of a single span masonry arch barrel have on the load carrying capacity of the bridge, and why?

The experiments detailed in Chapter 4 indicate that the distribution can be zero in certain instances based upon fill type, depth and density. This is based upon the displacement rates of the load plate and the arch voussoirs during the tests, the peak load versus displacement graphs and the numerical simulations of the experiments within the computational software package RING 1.5.

The available literature (as covered in Chapter 2) provides guidance to use a 2 vertical in 1 horizontal distribution spread based upon work conducted in the 1950s. More recent examination of the actual live load distribution in an arch bridge specific environment within the laboratory gives evidence to suggest that no live load distribution occurs between the road level and the arch extrados. It is postulated in the (arch bridge related) literature in that what has been perceived as live load spreading is actually due to the arch redistributing the stresses internally without any significant contribution from the backfill material.

Somewhat contradictory, geotechnical theory suggests that at some depth/type/density of fill, load spreading must occur due to the increase in effective stresses and exploration of using settlement and strip footing foundation calculations has revealed that this must also be true.

Figure 6-1 shows what the potential live load distribution that satisfies the theory, the simulations and the experiments together with what others have observed as detailed in the literature. It also satisfies the original assumptions used as the reasoning behind the current assessment codes for the 2 vertical in 1 horizontal, in simplistic terms, once a certain depth of fill has been reached.

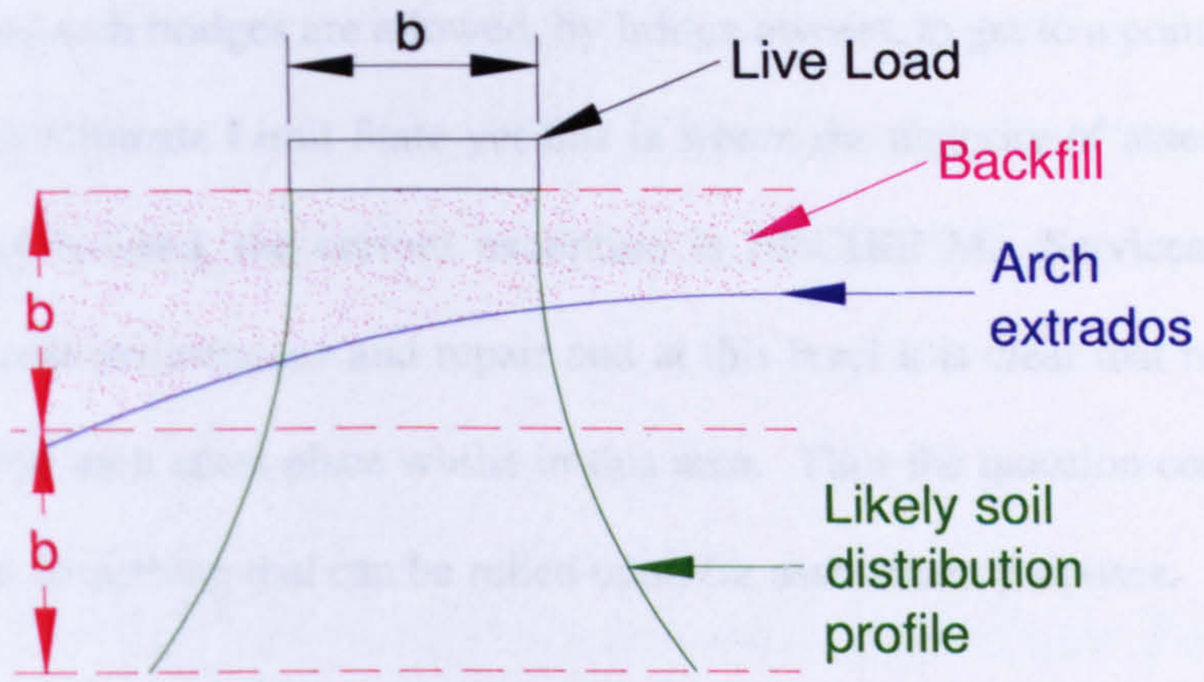

Figure 6-1: Probable shape of live load distribution

One observation obtained from this research is that for deeper depths of fill above the arch extrados the soil is likely to fail before the arch exhibiting a bearing capacity type failure. This coupled with the potential for greater distribution at depth may explain as to why an increase in fill depth over arch bridges, from an industrial point of view, increases the longevity under serviceability conditions.

6.3 Effect of Passive Soil Resistance

Q2: What contribution does the passive restraint of the backfill have on the load carrying capacity of the masonry arch bridge, and why?

Passive restraint provided by an arch's backfill is not a new concept in the research world of masonry arches; in particular this concept is responsible where significant quality backing is present. At present in academia there seems to be consensus on the degree to which it is mobilised under laboratory conditions and how much benefit is obtained by including it within assessment tools. In industry the contribution of backing appears to be well understood, however, the influence of backfill is not appreciated from this passive restraint point of view. The point of contention is that

not many real arch bridges are allowed, by bridge owners, to get to a point where they would fail at Ultimate Limit State yet this is where the majority of assessment tools are currently focused, the current exception is ARCHIE M. Serviceability issues drive industrial maintenance and repair and at this level it is clear that no significant rotation of the arch takes place whilst in this area. Thus the question comes up as to whether it is something that can be relied upon for assessment purposes.

The experiments conducted within this research have similar findings to tests done by other academics. The simplistic soil models used by the majority of currently available assessment tools have shown to be inadequate at quantifying their influence on load carrying capacity; primarily it seems due to the way the problems are formulated requiring equilibrium conditions to be in place prior to solving of the algorithms. With more sophisticated yet easy and cheap to operate soil models still some time away from being deliverable, the new model proposed by this research offers a logical 'next step' as it can be easily attached to existing assessment methods.

The model uses observations of the conducted experiments to inform what and how relevant geotechnical theory from parallel fields can be adapted to back fit. At present this sliding block model has demonstrated that it can produce kinematic similarities with the experiments, however, it could not be refined enough within the current research time to obtain numerical similarity, though it is the author's belief that further endeavours should be attempted given the model's promise. The current discrepancy in results is due to insufficient theoretical pressure being mobilised to restrain the arch when using the experimentally observed $^1/_3K_p$. Generally, to obtain numerical agreement between the model and the experiments, a multiple, greater than

$^1/_3$, is required. Technically, theory indicates that full K_p should be mobilised when the fill is in motion, however, experiments show that only about $^1/_3K_p$ ever does in reality. It is thought that this mismatch that lies at the heart of the proposed model's discrepancy.

6.4 Effect of Skewback/Abutment Interface Friction

Q3: Does having the skewbacks securely fixed to the abutments in a single span masonry arch bridge, affect bridge load carrying capacity? If so, what is the most likely reason for this?

Many if not all of the arch tests conducted in the laboratory outlined in the literature have utilised skewbacks fixed to the abutments. Indeed, even the assessment guidelines state that this should be assumed since most assessment techniques are all based upon this assumption, the exception being RING 1.5, although even this was calibrated against fixed abutment laboratory tests. In reality, where arch bridges have skewbacks it is very rare to encounter a bridge where skewback sliding is an issue without some other factor occurring, such as abutment rotation. It could not be found in the literature where anyone had put this assumption of fixed skewbacks to fixed abutments under scrutiny.

The parametric studies, unsurprisingly, showed that for most cases sliding would never be an issue due to geometry and the likely friction interface coefficient value. However, for shallow fill flat arches a much higher friction coefficient would be required to prevent sliding. It is accepted in real bridges that many arch bridges have

'low cover' indicating shallow fill, this is a historical driven issue based upon embankment failures. Fortunately, most arch bridges are not of the profile identified herein where sliding would need to be considered as an issue, though they do occur.

The experiments showed that even where sliding maybe an issue, provided symmetrical conditions are present at the interfaces between the skewbacks and abutments, sliding forming part of the mechanism has no significant influence on load capacity because the line of thrust can be accommodated within the deforming structure. Asymmetric conditions, which are more likely in real bridges, pose issues though and reduce the live load capacity as expected due to the line of thrust not being able to be accommodated. Figure 6-2 shows this in ARCHIE M. The current analytical models failed to replicate experimental behaviour in cases where asymmetry occurs.

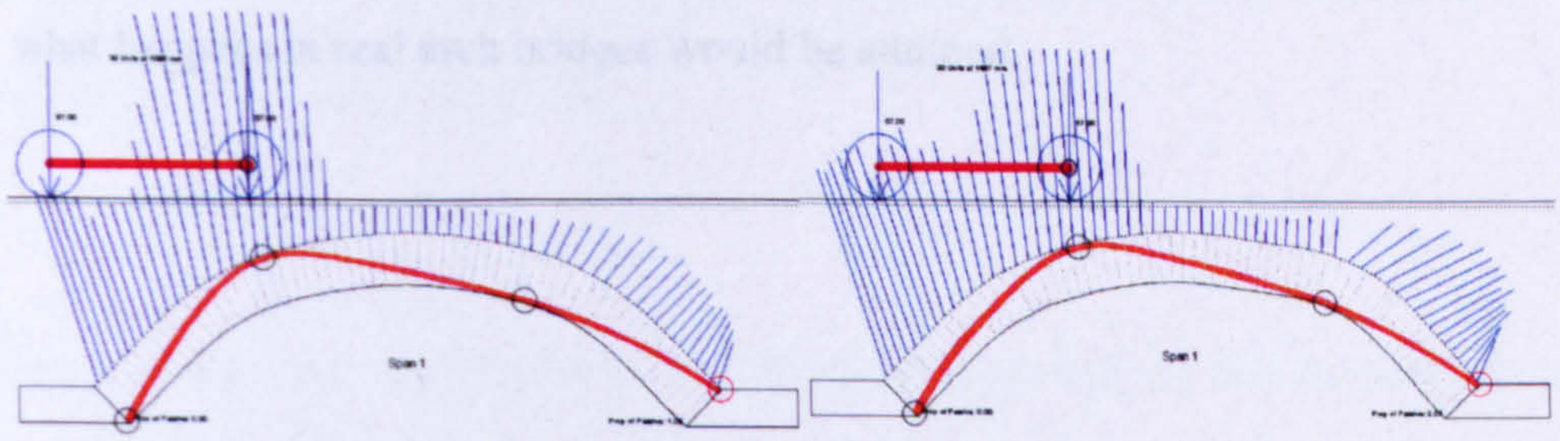

Figure 6-2: Symmetric and asymmetric arches (passive factor 1.06 and 2.07 respectively)

The evidence in this research suggests that the current soil models in the assessment tools, largely based upon a triangular Rankine type distribution, do not represent what actually occurs as the kinematics obtained show that the response of a sliding skewback has more in common with a buried soil anchor than a retaining wall. Once again a numerical model based on the theory has been postulated using trapdoor and inclined soil anchor theory. Like the sliding block model developed to represent

passive restraint, insufficient passive pressure is theoretically mobilised when back calculating using the experimentally obtained $^1/_3K_p$. It seems more than coincidence that in two independently developed models dealing with different geotechnical aspects that the same underlying cause is causing the discrepancy. Thus it is postulated that alternative theory regarding passive pressure mobilisation, based upon internal soil friction angle, needs to be scrutinised to explain why experimentally only $^1/_3K_p$ is ever achieved when theoretically it requires more to stabilise the systems investigated.

6.5 Comment

Provided the discrepancies can be overcome, the benefit of incorporating the two postulated sliding block models into existing assessment tools is easy to appreciate, and together with the new live load distribution model a more representative model of what happens in real arch bridges would be attained.

Chapter 7

Conclusions and Recommendations

7.1 Summary

Masonry arch bridges are an important part of the UK infrastructure and perform well, when maintained in a good state, more than 150 years after many were originally constructed, despite having to carry heavier loads and accommodate a much increased frequency of these heavier loads.

Bridge owners, namely local councils, The Highways Agency and Network Rail, have come to appreciate the longevity and minimal maintenance required to sustain their masonry arch bridge stock. Undertaking new research in this area is one way they are looking to ensure that many of the arches they have last for another 150 years.

Over the last ten years many masonry arch bridges have shown that they are reaching the peak of their load carrying capacity with increased rates of deterioration. It is

believed that maintaining and preserving the existing stock of arch bridges is the only viable and affordable long term solution to the UK's transport needs. To this end, more targeted research into understanding how arch bridges behave has been instigated to improve currently used assessment methods.

The research undertaken as part of this PhD examined areas not previously investigated as well as examining commonly covered areas in a new way in order to shed new insights into still unresolved issues.

Live load distribution through the backfill and the contribution of mobilised passive pressure were re-examined experimentally and theoretically within this research. In addition, following intrusive investigations undertaken by Essex County Council on their road bridges, the effects of having fixed abutments within test models (often used in research) were examined.

Investigations into how the live load is distributed through the backfill from road level to the arch extrados showed that current code of practice guidelines were shown to be in error. This research showed that whilst kinematic distribution occurs, the nature of the arch rotating away from the fill under loading negates any potential settlement type distribution, though some local bearing capacity failure can take place. This provides additional proof that the current 2 vertical in 1 horizontal distribution guidance is in need of refinement for different backfill types and different fill depth. The case for

using no distribution angle was established, and a case for load focussing taking place in some circumstances was also investigated with inconclusive results.

Experiments into the passive resistance mobilised under rotation or sliding of the arch as it undergoes failure has proven that only about one third of the full theoretical passive pressure is attained, which is consistent with other laboratory tests previously conducted in this area. Production of a theoretical sliding block model was attempted to be an improvement over the simplistic triangular pressure distribution used by current assessment tools. Whilst kinematic similarity was obtained by the analytical model, difficulty was encountered in attaining numerical agreement between the theoretical and experimental results, though initial findings are encouraging that this could be overcome with refinement.

Regarding the issue of abutment fixity, experiments proved that symmetrical conditions (either both skewbacks fixed to the abutments or both skewbacks free to move over the abutments) showed similar load carrying capacities, whilst asymmetric sliding of skewbacks over abutments decreased the live load carrying capacity of masonry arch bridges. The use of digital imaging techniques also showed that a sliding skewback exhibited similar kinematics to a buried soil anchor and a new sliding block model based upon this assumption has been put forward. This model could be incorporated into current assessment techniques where sliding is deemed to be part of a possible failure mechanism where low cover and a shallow span:rise profile is present on an arch bridge.

The research contained within this PhD has added to the understanding of the behaviour of masonry arch bridges and provided good experimental results that could be used for calibration of numerical assessment models in the future. Additions to existing assessment methods in the areas of live load distribution, passive pressure restraint and abutment fixity have been proposed as an intermediate step before computational holistic models are available.

Despite the last 30 years of new research and over 70 years since being devised MEXE is still the primary assessment method used by industry based upon unit percentage costs despite its known shortcomings, although many other and more scientifically robust methods have been available for many years. It is hoped that providing a step change improvement to existing packages, such as RING, that industry will begin to realise that a better value for money option now exists. Else the question will once again arise: "why bother with research into masonry arch bridges if the people who are responsible in dealing with them on a day to day basis, take little or no notice of the findings?"

7.2 Conclusions

This section draws together the main conclusions from this research and highlights the relevant sections within this thesis pertaining to each.

1 Live load dispersal is not 2 in 1. (Section 4.3.5)

The results obtained from the experiments and analytical models indicate that the current code of practice recommendation of using a 2 vertical in 1 horizontal live load distribution through the backfill for all scenarios can be unsafe.

2 Live load dispersion can be zero degrees. (Section 4.3.5)

The true dispersal angle has shown to be as low as zero in some instances depending upon type of backfill material, internal angle of soil friction, dilatency, void ratio and depth of fill.

Although live load focussing appears to occur it cannot be proven. (Section 4.3.5)
Back calculating an equivalent distribution angle for theory to match experiments resulted in the perception that the load could focus rather than disperse in some cases. However, further investigation using energy considerations and examining the influence of the side walls are needed to ascertain as to whether focussing actually takes place.

3 Some local bearing failure may take place prior to arch displacements. (Section 5.3.7)

For deeper filled arches, kinematics showed that a local bearing failure beneath the load would sometimes occur prior to the arch failing. It was found that a settlement type distribution occurring prior to arch rotation occurred kinematically, however, its influence numerically was minimal as the arch rotated away from beneath the fill at this point.

4 Smith model proposed. (Section 4.4.6)

Rather than utilising a Boussinesq or a 2 in 1 distribution for live load, the distribution model devised by Smith (2005) for strip footings provided good correlation between theory and experiments.

It has long been held by academics and industry that the vagueness of BD21/01 based upon work by Davey (1957) and Chettoe and Henderson (1953) is misleading. New work done herein confirms recently discussed works by Harvey (2006) that load distribution does not occur at 2 in 1 and in some instances may not happen at all. The Smith model offers a quantifiable alternative to Boussinesq and the 2 in 1.

5 *Passive pressure is mobilised as arch rotates. (Section 4.3.5)*

As previous research has shown passive pressure was mobilised during collapse, however, only as the arch rotated and it is unclear whether such a rotation would be classed as "failed" at full scale due to the size of the displacements involved.

6 *About one third of full theoretical value of passive resistance is experimentally mobilised. (Section 4.3.5)*

Similarly to previous research, only about one third of the full theoretical value of passive pressure was ever mobilised during the experiments.

7 *New sliding block model is kinematically similar. (Section 4.5)*

By using digital imaging techniques, a sliding block model was back developed using modern geotechnical theory based upon the observed kinematics during the experiments.

8 *New sliding block model is numerically dissimilar. (Section 4.5.8)*

This numerical model, although kinematically similar, could not attain numerically agreement with the experimental results within the research time and is currently approximately a factor of 2 away from what is required. However, it is envisioned that further refinement would overcome this shortcoming.

The idea that passive pressure contributes to the live load capacity of a masonry arch bridge is not a new idea, and experiments have shown that about one third of the full theoretical passive pressure is ever developed during collapse. What is less clear until now is why and how this happens in arches. It is clear that passive pressure is useful to stabilise an arch undergoing displacement, however, it is still unclear whether a real arch would be deemed unsafe at the required displacement values. The new proposed model offers a real alternative to current methods once it has been corrected.

9 *Symmetrical abutment fixity conditions have similar live load carrying capacities. (Section 5.3.2)*

Maintaining a symmetric profile for the arch during collapse allowed the live load carrying capacity to be largely unaffected despite having a sliding component present in the mechanism.

10 *Asymmetrical abutment fixity conditions have a lower live load carrying capacity than symmetrical. (Section 5.3.2)*

An asymmetric arch exhibited a lower live load carrying capacity than a symmetrically failing one due to the inability of enough passive resistance being mobilised by the system alone on one side of the arch.

This new research finding is useful as most if not all previous research on arch bridges conducted in a laboratory has used fixed arch abutments despite evidence gathered in the field suggesting that this might not always be the case in real structures.

11 *Above a certain value of interface friction between skewback and abutment, interface friction has no influence on load carrying capacity. (Section 5.3.3)*

The interface friction between the skewback and abutment was found not to have an effect on live load capacity when above a certain value.

12 Above a certain value of backfill depth, interface friction has no influence on load carrying capacity. (Section 5.3.3)

Likewise the interface friction had no effect above a certain depth of backfill. This provides confirmation that for most arch bridges the condition of this interface is not an issue to consider. However, where low cover and a shallow profile exist, sliding is a real possibility and therefore this interface must be carefully examined during inspection work to take account of sliding forming part of the potential failure mechanism.

13 A sliding skewback exhibits kinematics similar to a buried soil anchor. (Section 5.5)

The processing of the digital images indicated that a sliding skewback was kinematically similar to a buried soil anchor rather than a retaining wall a previously academic thinking suggested.

14 A sliding block model has been proposed though needs refinement to be numerically accurate. (Section 5.5)

Given that holistic models for basement of masonry arch bridges are still some time away and the industrial requirement for an immediate improvement to MEXE, development of this new proposed model offers a realistic way forward once it has been refined.

7.3 Recommendation for Future Work

The research work can be extended and modified and particular suggestions are listed as follows:

1) Alternative materials to sand such as limestone or clay could be tested both in the small scale model and in the large test rigs. Sand used in this study, although useful for research purposes is not generally found to any great extent in real arch bridges. However, clay is quite commonly used as backfill and limestone is a logical choice to use as backfill for any new arch bridges. In this sense, this would be a good starting point for further research.

2) The effect of introducing different soil reinforcement techniques could be investigated. Since passive soil resistance has been proven to contribute to the strength of arch bridges, the insertion of vertical piles into the soil around the bridge could be considered, as shown in Figure 7-1.

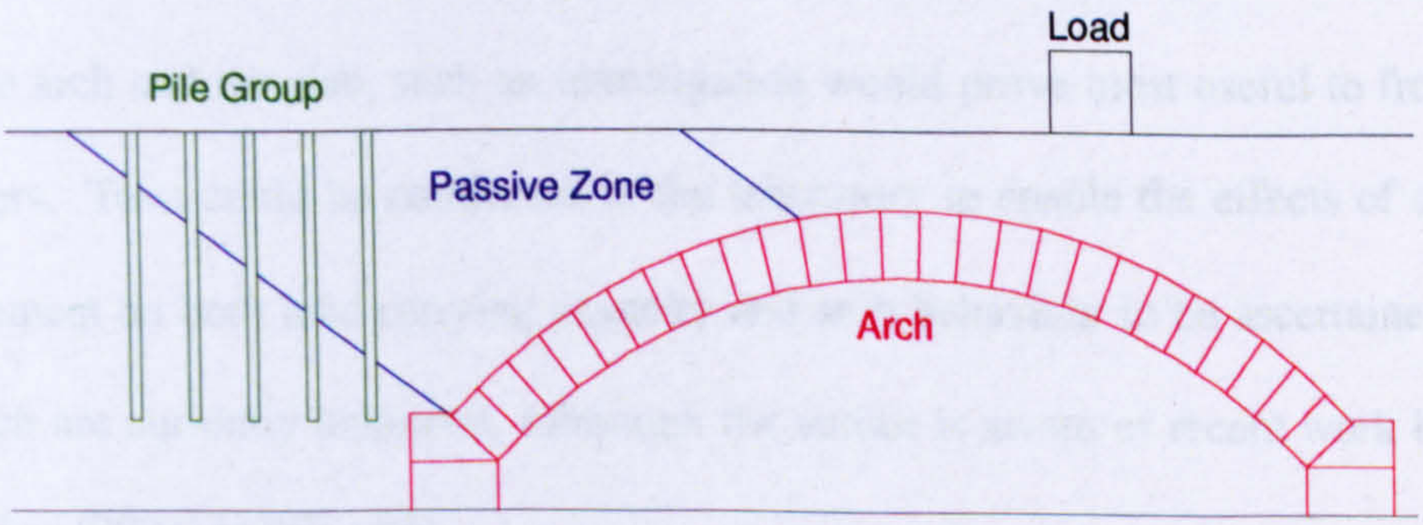

Figure 7-1: Possible soil reinforcement technique.

Such techniques, if successful could be implemented in the field at minimal cost compared to bridge replacement or other potential remedial measures likely to be considered for bridge strengthening.

3) The influence of concrete slabs on arch bridge behaviour could be investigated. Several real bridges in Essex have been found to have lean and/or reinforced concrete slabs spanning part-way across the arch in the fill, see Figure 7-2.

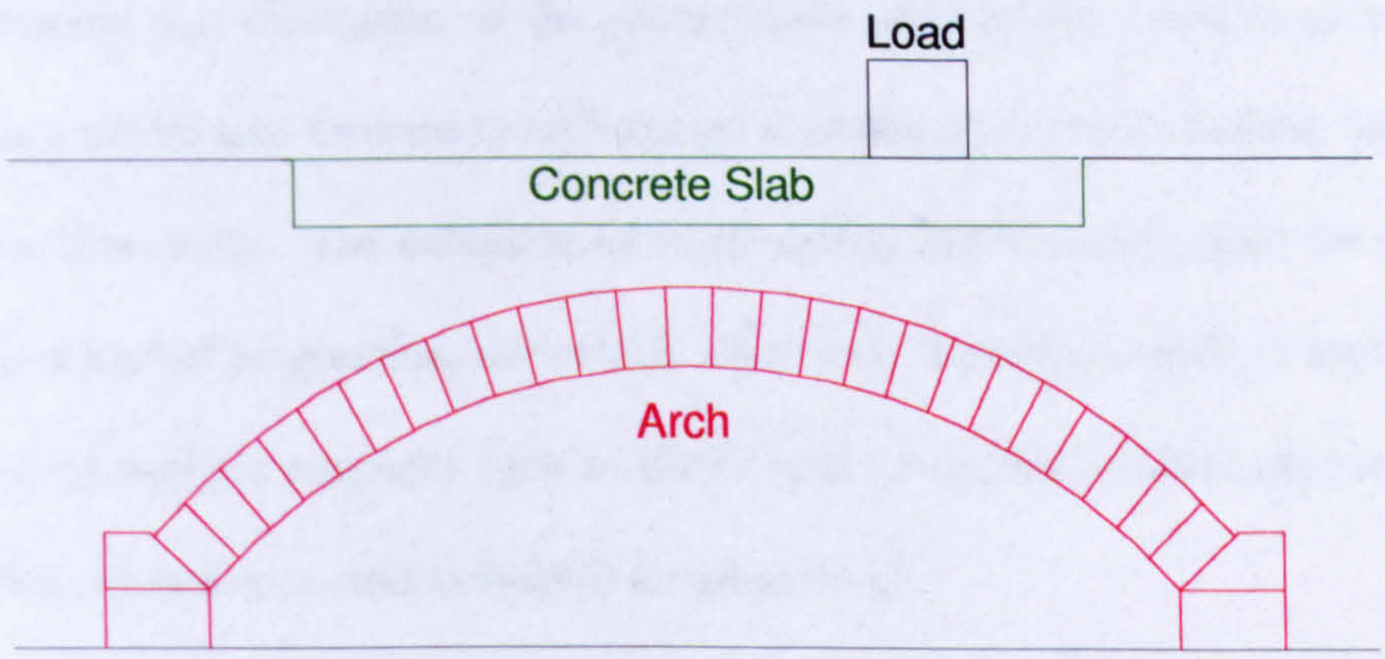

Figure 7-2: Slab inundation in Essex bridges.

These slabs have been assessed as being incapable of carrying the full live load by themselves and since there is no current simple means of doing a holistic analysis of both the arch and the slab, such an investigation would prove most useful to front line engineers. Tests could be conducted in the laboratory to enable the effects of such an arrangement on both load carrying capacity and arch behaviour to be ascertained, both of which are currently unknown, (although the author is aware of recent work by Miri & Hughes (2004) in this area).

4) It is clear that investigations of dynamic effects would be very useful. Dynamic tests could quite easily be incorporated into the small and large test rigs with relatively minimal effort. These dynamic tests together with PIV could show real time soil and arch flow from a moving wheel load crossing the bridge at different frequencies. Again this is data which is lacking at present, and which could be obtained using the current apparatus at Sheffield and Salford Universities.

5) Refinement and calibration of the geotechnical soil-structure models given herein would be a useful step forward in arch bridge assessment as usable holistic models are still some time away. The extension of rigid sliding block models from the arch into the fill is a logical progression, one which when fully developed could be incorporated into existing analysis programs such as RING with a minimal of effort (due to the way the current version uses object oriented programming).

References

Albano, B., '*Details of the construction of a stone bridge erected over the Doria Riparia, near Turin*', Proceedings of the Institution of Civil Engineers, Vol. 1, 1836, pp.183-197.

Alexander, T., Thomson, A.W., '*The scientific design of masonry arches with numerous examples*', Macmillan and Co Limited, London, 1927.

Atkins, A.G., Beard, W., Tourret, R., '*GWR goods wagons*', Tourret Publishing, Oxon, 1998.

Bernardini, A., Modena, C., Valluzzi, M.R., '*Load transfer mechanisms in masonry: friction along a crack within a brick*', Materials and Structures Journal, RILEM, Vol. 31, No. 205, 1998, pp. 42 – 48.

Bolton, M.D., '*The strength and dilatancy of sands*', Géotechnique, Vol. 36, Issue 1, 1986, pp. 65-78.

Boussinesq, J., '*Application des potentials à l'étude de l'équilibre et du movement des solides élastiques*', Gauthier-Villars, Paris, 1883.

Boyer, M.N., '*The Bridgebuilding Brotherhoods*' Speculum, Vol. 39, No. 4, 1964, pp. 635-650.

Brencich, A., DeFrancesco, U., Gambarotta, L., '*Non Linear Elasto Plastic Collapse Analysis of Multispan Masonry Arch Bridges*', Presses de l'Ecole Nationale des Ponts et Chausses, 2001, pp. 513-522.

Bridle, R.J., Hughes, T.G., '*An Energy Method for Arch Bridge Analysis*', Proceedings of the Institution of Civil Engineers, Vol. 89, Part 2, 1990, pp. 375-385.

Bruce, G.B., '*Description of the Royal Border Bridge over the River Tweed*', Proceedings of the Institution of Civil Engineers, Vol. 10, 1851, pp. 219-244.

Bruff, P., '*Description of the Chapple Viaduct upon the Colchester and Stour valley extension*', Proceedings of the Institution of Civil Engineers, Vol. 9, 1850, pp. 287-292.

BSI, '*Accuracy (trueness and precision) of measurement methods and results*', BS ISO 5275, 1994.

BSI, '*Code of practice for foundations*', British Standards Institute, BS 8004, 1986.

Buckton, E.J., Fereday, H.J., '*The demolition of Waterloo Bridge*', Proceedings of the Institution of Civil Engineers, Vol. 3, 1936, pp. 472-481.

Burroughs, P., Hughes, T.G., Hee, S., Davies, M.C.R., '*Passive pressure development in masonry arch bridges*', Proceedings of the Institution of Civil Engineers - Structures and Buildings, Vol. 152, Issue 4, 2002, pp. 331-339.

Burroughs, P.O., Baralos, P., Hughes, T.G., Davies, M.C.R., '*Soil effects and the service loading of masonry arch bridges*', Proceedings of the 12th International Brick/Block Masonry Conference, Madrid, 2000.

Cavicchi, A., Gambarotta, L., '*Upper Bound Limit Analysis of Multispan Masonry Bridges Including Arch-Fill Interaction*', ARCH '04 Advances in Assessment, Structural Design and Construction, 2004, pp. 302-311.

CfIT, '*Permitting 44 tonne lorries for general use in the UK*', Commission for Integrated Transport, Interim report, London, 2000.

CfIT, '*Permitting 44 tonne lorries for general use in the UK*', Commission for Integrated Transport- Rail Freight Working Group, Final report, London, 2002.

Chatterjee, S., '*Assessment of old bridges*', Journal of the Institution of Highways and Transportation, 1985, pp. 18-22.

Chen, W.F., '*Limit analysis and soil plasticity*', Developments in Geotechnical Engineering, Elsevier Scientific Publishing Company, 1975.

Chettoe, C.S., Henderson, W., '*Masonry Arch Bridges: A Study*', Proceedings of the Institution of Civil Engineers, 1957, pp. 723-774.

Choo, B.S., Coutie, M.G., Gong, N.G., '*Analysis of Masonry Arch Bridges by a Finite Element Method*', Proceedings of the Forth Rail Bridge Centenary International Conference, Edinburgh, 1990, pp. 381-392.

Crisfield, M.A., Packham, A.J., '*A mechanism program for computing the strength of masonry arch bridges*', TRRL, Vol. 124, 1987.

Cudworth, W., '*The Hownes Gill Viaduct on the Stockton and Darlington railway*', Proceedings of the Institution of Civil Engineers, Vol. 22, 1862, pp. 44-57.

Davey, N., '*Tests on Road Bridges*', Department of Scientific and Industrial Research-Building Research Station, 1953.

DEFRA, '*The government's response to the royal commission on environmental pollution 20th report*', Department for Environment, Food & Rural Affairs, London, 1998.

Dickin, E.A., Leung, C.F., '*Evaluation of design methods for vertical anchor plates*', ASCE Journal of Geotechnical Engineering, Vol. 111, Issue 4, 1985, pp. 500-520.

DoT, '*Reinforced earth retaining walls and bridge abutments for embankments*', Department of Transport, Technical Memorandum (Bridges) BE 3/78, 1978.

Drescher, A., Detournay, E., '*Limit load translational failure mechanisms for associative and non-associative materials*', Géotechnique, Vol. 43, Issue 3, 1993 pp. 443-456.

Fairfield, C.A., '*Soil-structure interaction in arch bridges*', PhD Thesis, University of Edinburgh, 1994.

Fairfield, C.A., Ponniah, D.A., '*The effect of fill on buried model arches*', Proceedings of the Institution of Civil Engineers, Structures and Buildings, Vol. 104, 1994, pp. 471-482.

Fang, Y.S., Chen, T.J., Holtz, R.D., Lee, W.F., '*Reduction of boundary friction in model tests*', Geotechnical Testing Journal, ASTM, Vol. 27, Issue 1, 2004, pp. 3-12.

Gachet, P., Klubertanz, G., Vulliet, L., Laloui, L., '*Interfacial Behaviour of Unsaturated Soil with Small-Scale Models and Use of Image Processing Techniques*', ASTM Geotechnical Testing Journal, Vol. 26, Issue 1, 2003.

Gaudard, J., '*Description of several bridges erected in Switzerland; with remarks on bridges of large spans, and on the stability of arches*', Proceedings of the Institution of Civil Engineers, Vol. 58, Issue 4, 1879, pp. 310-336.

Gibson, R.E, '*Some results concerning displacements and stresses in a non-homogeneous elastic half-space*', Géotechnique, Vol. 17, No. 1, 1967, pp. 58-67.

Gilbert, M., '*RING: A 2D rigid-block analysis program for masonry arch bridges*', University of Sheffield, 2001.

Gilbert, M., Melbourne, C., '*Rigid Block Analysis of Masonry Structures*', The Structural Engineer, 1994, Vol. 72, Issue 21, pp. 356-361.

Gilbert, M., Smith, C.C., Wang, J., Callaway, P.A., Melbourne, C., '*Small and large-scale experimental studies of soil-arch interaction in masonry bridges*', Arch Bridges V, Madeira, 2007.

Harvey, W.J. '*Some problems with arch bridge assessment and potential solutions*', The Structural Engineer, 2006, pp. 45-50.

Harvey, W.J., '*Application of the Mechanism Analysis to Masonry Arches*', The Structural Engineer, 1991.

Harvey, W.J., '*Inspection, assessment & repair of masonry arch bridges (course notes)*', Wolfson Bridge Research Unit, Institution of Structural Engineers, London, 1992.

Harvey, W.J., '*New bridges for old*', The Structural Engineer, Vol. 68, Issue 25, 1990, pp. 31-35.

Harvey, W.J., Tomor, A., Smith, F., '*A three dimensional model for Masonry Arch bridge behaviour*', Structural Engineering International, Volume 15, Number 2, 2005, pp. 4-7.

Hauck, G.F.W., '*Structural design of the Pont du Gard*', ASCE Journal of Structural Engineering, Vol. 112, Issue 1, 1986, pp. 105-119.

Hawkshaw, J., '*Description of Lockwood Viaduct*', Proceedings of the Institution of Civil Engineers, Vol. 10, 1851, pp. 296-302.

Hayes, J., '*The strengthening and reconstruction of Weak bridges under the road and rail traffic act, 1933*', Institution of the Civil Engineers, Student's Paper No. 953, 1938, pp. 15-40.

Head, K H., '*Manual of Soil Laboratory Testing*', Volume X, Pentech Press Ltd, Plymouth, 1982.

Heyman, J., '*The estimation of the strength of masonry arches*', Proceedings of the Institution of Civil Engineers, Vol. 69, Part 2, 1980, pp. 921-937.

Heyman, J., Padfield, C.J., '*Two masonry bridge: I. Clare College Bridge*', Proceedings of the Institution of Civil Engineers, 1972, pp. 305-318.

Highways Agency, '*Manual of contract documents for highway works, Volume 1 specification for highway works, Series 800 road pavements – unbound cement and other hydraulically bound mixtures*', London, 2005, pp. 9-10.

Highways Agency, '*The assessment of highway bridges and structures*', Design manual for roads and bridges, BA16/97, London, 2001.

Highways Agency, '*The assessment of highway bridges and structures*', Design manual for roads and bridges, BD 21/01, Vol. 3, Section 4, Part 3, London, 2001.

Highways Agency, '*Unreinforced masonry arch bridges*', Design manual for roads and bridges, BD 91/04, Vol. 2, Section 2, Part 14, London, 2004.

Hooke, R. '*A description of helioscopes, and some other instruments*', Royal Society, London, 1676.

Hopkins, H.J., '*A Span of bridges: an illustrated history*', David and Charles Limited, Newton Abbot, 1970, pp. 10.

Hughes T.G., Discussion on; Proc. Instn Civ. Engnrs, Structs & Bldgs, 94(4) 1994, 358-371. *Ibid.* with authors' reply & closure, 122(2) 1997, 247-250.

Hughes, T.G., Discussion on; Proceedings of the Institution of Civil Engineers, Structures and Buildings, Vol. 128, 1998, pp. 81-90. *Ibid.* with authors' reply & closure, Vol. 152, Issue 4, 2002, pp. 407-408.

Hughes, T.G., Discussion on; Proceedings of the Institution of Civil Engineers, Structures and Buildings, Vol. 104, 1994, pp. 471-482. *Ibid.* with authors' reply & closure, Vol. 122, Issue 2, 1997, pp. 247-250.

Hughes, T.G., Kitching, N., '*Small scale testing of masonry*', Proceedings of the 12th International Brick/Block Masonry Conference, Madrid, 2000.

Hulet, K.M, Smith, C.C., Gilbert, M., '*The influence of flooding on the load carrying capacity of masonry arch bridges*', Department of Civil and Structural Engineering, University of Sheffield, 2005.

Jâky, J., '*A nyugalmi nyomâs tényezöje*'. *The coefficient of earth pressure at-rest*, Journal of the Union of Hungarian Engineers and Architects, 1944, 355-358.

Ketcham, S.A., Black, P.B., '*Initial results from a small-scale frost heave experiments in a centrifuge*', Cold Regions Research and Engineering Laboratory (CRREL), CRREL Report 95- 9, 1995.

Laurie, K.S., '*The Jubilee Bridge over the River Hooghly*', Proceedings of the Institution of Civil Engineers, Vol. 158, Part 4, 1904, pp. 374-379.

Livesley, R., '*Limit analysis of structures formed from rigid blocks*', International Journal for Numerical Methods in Engineering, Vol. 12, 1978, pp. 1853-1871.

MacFarlane, A., Ricketts, N., '*Evaluation of existing software for the assessment of masonry arch bridges*', TRL Limited, Project Report PR/IS/18/01, 2001.

Mackay, T. '*The life of Sir John Fowler*', John Murray, Albemarle Street, 1900, pp. 88-91.

Mallinson, R., '*Soil structure interaction in masonry arch bridges*', BEng dissertation, University of Edinburgh, 1990.

Mann, P., Gunn, M., '*Computer modelling of the construction and load testing of a masonry arch bridge*', Arch Bridges: Proceedings of the First International Conference on Arch Bridges, Bolton, UK 3-6 September, 1995, pp. 277-286.

Margary, P.J., '*Reconstruction of the St. Pinnock and Moorswater viaducts on the Cornwall railway*', Proceedings of the Institution of Civil Engineers, Vol. 69, Part 3, 1882, pp. 312-317.

Melbourne, C., '*A new arch construction technique*', Structural Engineering Review, Chapman & Hall Ltd, Vol. 1, 1988, pp. 91-95.

Melbourne, C., '*An overview of experimental arch bridge research in UK*', ARCH '01, Proc of 3rd International Arch Bridges Conference, 19-21 September, Paris, 2001, pp. 343-350.

Melbourne, C., Gilbert, M., '*The behaviour of multi-ring brickwork arch bridges*', The Structural Engineer, Vol. 73, Issue 3, 1995, pp. 39-47.

Melbourne, C., Gilbert, M., Wagstaff, M., '*The collapse behaviour of multi-span brickwork arch bridges*', The Structural Engineer, Vol. 75, Issue 17, 1997, pp. 297-305.

Milwich, M., Speck, T., Speck, O., Stegmaier, T., Planck, T., '*Biomimetics and technical textiles: solving engineering problems with the help of nature's wisdom*', American Journal of Botany, Vol. 93, Issue 10, 2006, pp. 1455–1465.

Miri, M., Hughes, T.G., '*Increased load capacity of arch bridges using slab reinforced concrete*', Proceedings of the 4th Arch bridge Conference, 2004, pp. 460-478.

Morley, A., '*Theory of Structures*', 5th Edition, Longmans, 1950.

Morris, E.H., '*The reconditioning of a defective arch in Stockport viaduct*', Journal of the ICE, Vol. 31, No. 1, 1948, pp. 82-90.

Mullet, P., Rance, J., '*Applied discrete element technology: the assessment and strengthening of masonry arches*', NAFEMS, Benchmark, 2003, pp. 17-24.

Murray, E.J., Geddes, J.D., '*Uplift of anchor plates in sand*', ASCE Journal of Geotechnical Engineering, Vol. 113, Issue 3, 1987, pp. 202-215.

Network Rail, '*Assessment of structures*', London, RT/CE/S/035, Issue 2, 2004.

Network Rail, '*Examination of bridges and culverts*', London, RT/CE/S/017, Issue 2, 2004.

Network Rail, '*Route availability heavy axle weight vehicles*', Network Rail London North Eastern Territory, Issue 11, London, 2006.

Ng, K.H., Fairfield, C.A., '*Modifying the mechanism method of masonry arch bridge analysis*', Elsevier, Construction and Building Materials, Vol. 18, 2004, pp. 91-97.

Ochsendorf, J.A., '*The Masonry Arch on Spreading Supports*', The Structural Engineer, Vol. 84, Issue 2, 2006, pp. 29-35.

O'Connor, C., '*Roman bridges*', Cambridge University Press, 1993, pp. 163-188.

Orduna, A., Lourenco, P.B., '*A limit analysis approach for masonry structures*', ARCH '01, Proc of 3rd International Arch Bridges Conference, 19-21 September, Paris, 2001, pp. 451-457.

Packham, A.J., '*The effects of 25.5 tonne axle load freight wagons on bridges*', British Rail research, Report Ref: TR CES 006, 1989.

Page, J., '*Load tests to collapse on two arch bridges at Preston, Shropshire and Prestwood, Staffordshire*', TRRL Research Report 110, 1987.

Page, J., '*Load tests to collapse on two arch bridges at Strathmashie and Barlae*', TRRL Research Report 201, 1989.

Page, J., '*Load tests to collapse on two arch bridges at Torksey and Shinafoot*', TRRL Research Report 159, 1988.

Page, J., '*Masonry arch bridges (state of the art review)*', The Stationery Office Books, 1993.

Pippard, A.J.S., Tranter, E., Chitty, L., '*The mechanics of the voussoir arch*', Journal of the Institution of Civil Engineers, Vol. 4, No. 2, 1936, pp. 281-306.

Ponniah, D.A, Fairfield, C.A., Prentice, D.J., '*Fill stresses in a new brick arch bridge subject to heavy axle-load tests*', Proceedings of the Institution of Civil Engineers, Structures and Buildings, Vol. 123, Issue 2, 1997, pp. 173-185.

Ponniah, D.A., Prentice, D.J., '*Load-carrying capacity of masonry arch bridges estimated from multi-span model tests*', Proceedings of the Institution of Civil Engineers, Structures and Buildings, Vol. 128, 1998, pp. 81-90.

Poulos H.G., Davis E.H., '*Elastic solutions for soil and rock mechanics*', Wiley & Sons, New York, U.S.A., 1974.

Railtrack, '*Railtrack Line Code of Practice: The Assessment of Underbridge Capacity*', London, RT/CE/C/015, Issue 1, 1995.

Railtrack, '*Railtrack Line Code of Practice: The Structural Assessment of Underbridges*', London, RT/CE/C/025, Issue 1, 2001.

Roca, P., Molins, C., '*Advances in Assessment, Structural Design and Construction*', ARCH '04, Barcelona, 2004, pp. 365-374.

Rowe, P.W., Barden, L., '*Importance of free ends on triaxial testing*', Journal of the Soil Mechanics and Foundations Division, ASCE, Vol. 90, No. SM1, 1964, pp. 1-77.

Royles, R., Hendry, A.W. '*Model Tests on masonry arches*', Proceedings of the Institution of Civil Engineers, Vol. 2, Issue 91,1991, pp. 299-321.

Shave, J., Denton, S.R., Charlton, M., '*A review of bridge assessment failures on the motorway and trunk road network*', Parsons Brinckerhoff Ltd, Manchester, 2003.

Sicilia, C., Pande, G., Hughes, T.G., '*A homogenisation-based FE model for the analysis of masonry arch bridges*', ARCH '01, Proc of 3rd International Arch Bridges Conference, 19-21 September, Paris, 2001, pp. 465-470.

Smith, C.C., '*Complete limiting stress solutions for the bearing capacity of strip footings on a Mohr-Coulomb soil*', Géotechnique, Vol. 55, Issue 8, 2005, pp. 607-612.

Smith, F.W., Harvey, W.J., Vardy, A.E., '*Three-hinge analysis of masonry arches*', The Structural Engineer, Vol. 68, Issue 11, 1990, pp. 203-213.

Smith, J.D., '*Egton Bridge*', North Yorkshire County Council, 1994.

Smith, N.A.F., '*The roman bridge-builder: some aspects of his work*', The Structural Engineer, Vol. 71, Issue 9, 1993, pp. 160-165.

Smith, T. M., '*Account of the Pont-y-tu-Prydd, over the River Tafe, near Newbridge in the county of Glamorgan*', Proceedings of the Institution of Civil Engineers, Vol. 5, 1846, pp. 474-477.

Sowden, A.M., '*The Maintenance of Brick and Stone Masonry Structures*', Spon Press, 1990.

Taylor, R.N., '*Geotechnical centrifuge technology*', Blackie Academic and Professional, Chapman and Hall, 1995.

Toms, A.H., '*Repairs to railway viaduct over London Road, Brighton, after damage by enemy action in May 1943*', Journal of the ICE, Vol. 24, No. 8, 1945, pp. 353-367.

UIC, '*Assessment, reliability and maintenance of masonry arch bridges*', International Union of Railways, Final Report, 2004.

Ward, A.W., '*The reconstruction of the English bridge over the river Severn at Shrewsbury*', ICE Selected Engineering Paper 66, 1928, pp. 2-14.

Westergaard, H., '*A problem of elasticity suggested by a problem in soil mechanics: A soft material reinforced by numerous strong horizontal sheets*', Contribution of Solids, Stephen Timoshenko 60th Anniversary Volume, Macmillan, New York, 1938, pp. 268-277.

White, D.J., Take, W.A., Bolton, M.D., '*Measuring soil deformation in geotechnical models using digital images and PIV analysis*', 10th International Conference on Computer Methods and Advances in Geomechanics, Tuscon, USA, 2001, pp. 997-1002.

Yan, Y., Loo, Y.C., Best, R., '*Behaviour of Stanwell Park viaduct, a multi-span brick masonry arch system on tall piers*', Proceedings of the 8th International Brick/Block Masonry Conference Dublin, Ireland, 19-21 September 1988, pp. 1759-1767.

Zekkos, D., Manousakis, J., Athanasopoulos, A., '*Geotechnical engineering practice in the Mycenaean civilization (1600-1100 BC)*', 2nd International Conference on Ancient Greek Technology, Athens, 17-21 October 2005.

Appendix A

Arch Bridges in the Literature

Introduction

Table A-1 provides basic pertinent details and references to many arch bridges examined as part of the Literature Review of this thesis. This does not purport to be an exhaustive list and there were many instances where bridges had been tested or examined but the reference lacked the key details relating to span and rise.

Name	Span mm	Rise mm	S/R	Profile	Reference	Date	Situation
	1219	305	4	Segmental	A study of the voussoir arch	1951	Lab Tests
	500	250	2	Semi-Circular	Burroughs et al	2000	Lab Tests
	500	125	4	Elliptical	Burroughs et al	2000	Lab Tests
	700	175	4	Segmental	Fairfield & Ponniah	1994	Lab Tests
	3000	750	4	Segmental	Gilbert et al	2007	Lab Tests
	380	85	4	Segmental	Gilbert et al	2007	Lab Tests
Dundee	4000	2000	2	Semi-Circular	Harvey	1989	Lab Tests
	22980	4600	5	Segmental	Howe	1897	Lab Tests
	779	175	4	Not given	Konno et al	1983	Lab Tests
	8065	2000	4	Not given	Mann & Gunn	Not Known	Lab Tests

Name	Span mm	Rise mm	S/R	Profile	Reference	Date	Situation
Bolton	6000	1000	6	Segmental	Melbourne	1989	Lab Tests
	3000	750	4	Segmental	Melbourne & Gilbert	1992	Lab Tests
	5000	1250	4	Segmental	Melbourne & Gilbert	1992	Lab Tests
	3000	750	4	Segmental	Melbourne & Wagstaff	1992	Lab Tests
	1000	500	2	Semi-Circular	Melbourne et al	1989	Lab Tests
	5000	1250	4	Segmental	Molins et al	2001	Lab Tests
	5000	1250	4	Segmental	Mullet & Rance	2003	Lab Tests
	3050	860	4	Segmental	Pippard	1951	Lab Tests
	3050	760	4	Segmental	Pippard	1951	Lab Tests
	8000	2000	4	Segmental	Ponniah et al	1997	Lab Tests
Bargower	2080	1040	2	Semi-Circular	Royles & Hendry	1991	Lab Tests
Bridgemill	1000	158	6	Parabolic	Royles & Hendry	1991	Lab Tests
Carron	2480	750	3	Segmental	Royles & Hendry	1991	Lab Tests
	2084	1042	2	Semi-Circular	Royles & Hendry	1991	Lab Tests
	2480	750	3	Segmental	Royles & Hendry	1991	Lab Tests
	1000	158	6	Segmental	Royles & Hendry	1991	Lab Tests
	4000	1000	4	Segmental	Towler	1981	Lab Tests
Cabra	10420	2650	4	Segmental	Boothby et al	2001	Real
Griffith	9450	2700	4	Segmental	Boothby et al	2001	Real
Sarah	31800	6580	5	Segmental	Boothby et al	2001	Real
Cantalupo	18500	9250	2	Semi-Circular	Brencich et al	2003	Real
Waterloo	36576	10668	3	Elliptical	Buckton & Fereday	1836	Real
Abbotsworthy	8534	2591	3	Elliptical	Chettoe and Henderson	1957	Real
Blackwell	20726	6248	3	Elliptical	Chettoe and Henderson	1957	Real
Blackwell	23774	6858	3	Elliptical	Chettoe and Henderson	1957	Real
Blythe End	9296	2591	4	Segmental	Chettoe and Henderson	1957	Real
Byfield	7772	1372	6	Segmental	Chettoe and Henderson	1957	Real
Cold Blow	15951	3861	4	Segmental	Chettoe and Henderson	1957	Real
Crawley Down	15545	3962	4	Segmental	Chettoe and Henderson	1957	Real
Crawley Down	15545	3658	4	Segmental	Chettoe and Henderson	1957	Real
Hazelden	18288	6096	3	Segmental	Chettoe and Henderson	1957	Real
Itchen Abbas	8534	2591	3	Elliptical	Chettoe and Henderson	1957	Real
Radford River	12802	2515	5	Elliptical	Chettoe and Henderson	1957	Real
Rudswick	8534	2134	4	Segmental	Chettoe and Henderson	1957	Real
Sutton Scotney	7722	1575	5	Segmental	Chettoe and Henderson	1957	Real
Tuffley	7315	2134	3	Elliptical	Chettoe and Henderson	1957	Real
Tuffley	8534	2286	4	Elliptical	Chettoe and Henderson	1957	Real
Westwell	7925	1626	5	Segmental	Chettoe and Henderson	1957	Real
Wetherby	10973	2286	5	Segmental	Chettoe and Henderson	1957	Real
Yarm	10973	5131	2	Semi-Circular	Chettoe and Henderson	1957	Real
Yarm	18288	5334	3	Segmental	Chettoe and Henderson	1957	Real
Alcaster Road	6452	1930	3	Segmental	Davey	1953	Real

Name	Span mm	Rise mm	S/R	Profile	Reference	Date	Situation
Beeding	12344	4051	3	Elliptical	Davey	1953	Real
Broadmeadow Lane	6629	1829	4	Segmental	Davey	1953	Real
Croft	6452	2057	3	Elliptical	Davey	1953	Real
Dartmouth Street	10566	3962	3	Elliptical	Davey	1953	Real
Dolywern Bridge	12395	3023	4	Elliptical	Davey	1953	Real
Egg Bridge	7341	1626	5	Segmental	Davey	1953	Real
Hythe Road	9271	2870	3	Elliptical	Davey	1953	Real
Kennington Bridge	11176	2819	4	Elliptical	Davey	1953	Real
Lenham	8839	2057	4	Segmental	Davey	1953	Real
Lenham	8230	1905	4	Segmental	Davey	1953	Real
Lenham	8230	1905	4	Segmental	Davey	1953	Real
Lifford Lane	7125	2127	3	Segmental	Davey	1953	Real
Ludgate Hill	6350	1581	4	Elliptical	Davey	1953	Real
Mill Bridge	7925	1372	6	Segmental	Davey	1953	Real
Pont Bell Bridge	12268	2781	4	Elliptical	Davey	1953	Real
Powdermills	13741	4013	3	Elliptical	Davey	1953	Real
Stearden	9220	2515	4	Elliptical	Davey	1953	Real
The Lodge	4369	1372	3	Elliptical	Davey	1953	Real
Warstok Road	6629	1943	3	Segmental	Davey	1953	Real
Yarldey Wood Road	6502	1975	3	Segmental	Davey	1953	Real
Bargower	10365	5180	2	Semi-Circular	Hendry et al	1985	Real
Bridgemill	18288	2845	6	Parabolic	Hendry et al	1985	Real
Clare Bridge	6720	2320	3	Not given	Heyman	1980	Real
Ponte Mosca	45000	5500	8	Not given	Heyman	1980	Real
Tetson	7200	2660	3	Not given	Heyman et al	1980	Real
Barlae	9860	1690	6	Segmental	Page	1989	Real
Preston	5180	1640	3	Elliptical	Page	1987	Real
Prestwood	6550	1430	5	Segmental	Page	1987	Real
Shinafoot	6160	1190	5	Segmental	Page	1988	Real
Strathmashie	9420	2990	3	Segmental	Page	1989	Real
Torksey	4900	1150	4	Segmental	Page	1988	Real
Dean Salisbury	3660	1830	2	Semi-Circular	Page	1993	Real
Dean Salisbury	3660	1830	2	Semi-Circular	Page	1993	Real
Romsey Dunbridge	3660	1830	2	Semi-Circular	Page	1993	Real
Romsey Dunbridge	3660	1830	2	Semi-Circular	Page	1993	Real
Romsey Dunbridge	1960	910	2	Semi-Circular	Page	1993	Real
Romsey Dunbridge	7120	2060	3	Segmental	Page	1993	Real
Westwell	11130	1630	7	Segmental	Page	1993	Real

Table A-1 Arch bridges in the literature

Appendix B

Large-Scale Test Rig

Introduction

A full scale (1:1) test rig was designed and procured by the author at the University of Sheffield as part of this PhD project. This large test rig was constructed in partnership with Salford University who would carry out the test programme under guidance from Sheffield. This rig was built at Salford University and was funded by Essex County Council. Details of the tender drawings and the design calculations are available from the author.

Design Considerations

To fill the gap in the information surrounding masonry arch bridges and quantifying the effect and behaviour of the backfill it was necessary to design and build a full scale purpose built test rig which was large enough to enclose a brickwork arch and surrounding fill material. In addition, it was to be designed to specific requirements to enable useful analytical data to be produced.

The first constraint was that in order to monitor soil kinematics, via the taking of digital images, large sections of the external walls would have to be full transparent. After some investigation glass was deemed to be both expensive and relatively problematic whereas clear cast acrylic was fairly cheap and could be drilled and cut on site with minimum effort. Although the resultant 50mm thick clear cast acrylic required to keep deflection under control had to be cast specially it was still cheaper and easier to use than the glass equivalent. The difference between using clear cast acrylic and glass is that glass was the first material choice as it had a proven track record with use in plane strain model test rigs and has a lower friction coefficient than acrylic.

The contained arch had already been decided to match those of the Bolton tests (Melbourne et al 1995) and therefore the rig had to be large enough for a 3 m span 4:1 (span:rise) segmental arch or a 3 m semicircular arch, so that the soil failure mechanism would not be unduly affected by surface boundaries. This influenced the choice of dimensions used in the arch rig design.

As previously mentioned it was desirable to attain plane strain conditions which meant that high stiffness walls had to be provided. The total limit of lateral deflection was calculated to be <1 mm over the given height. This meant that the clear cast acrylic and the steel frame were designed to the deflection limit produced by a 50 kPa internal stress which was obtained from the Bolton test data.

Another side effect of plane strain conditions that had to be taken into account at the design stage was the effect of side wall friction. Alternative methods of achieving this were investigated using the small scale test rig, with the use of a thin layer of latex greased with silicon sealant being chosen as this provided the lowest coefficient of friction when used with limestone backfill. The use of the latex reduced visibility of the fill material through the clear cast acrylic so that measures had to be taken to ensure the images captured had sufficient visible texture to be successfully analysed using the GeoPIV software.

Tests on the small test rig had revealed the damaging effects of compacting limestone against clear cast acrylic. Therefore, a sacrificial 4 mm layer of acrylic would be employed along all the internal side walls, which also allowed for the non-transparent sides to be made of plywood which was less expensive than constructing the entire rig with 50 mm acrylic walls. Between successive tests this 4 mm layer could be relatively easily and cheaply replaced with minimum labour.

Filling and compaction of the backfill also had to be allowed for in the design of the test rig. Filling was to be done by use of a large hopper suspended from a crane above the test rig whilst compaction provided its own difficulties which are discussed below.

Compaction of clay was carried out in 100 mm layers using a 10 kN vibrating compaction plate suspended from a crane; this was to stop the plate digging in. In sensitive areas such as beneath the applied load hand tampers were used. Compaction

was carried out until there was no further discernable reduction in layer thickness rather than specifying the number of passes. Moisture content samples and pocket penetrometer tests were conducted throughout filling together with small holes being dug in several layers after compaction to check air voids removal.

Compaction of the limestone was undertaken in 150 mm layers using a small 10 kN vibrating compaction plate since the desired internal area of the rig provided insufficient room for anything larger to be handled (see Figure B-1). Supporting tests of the limestone fill, such as shear box etc, were undertaken as part of the experiment. The limestone itself was the same as that used in the small scale rig tests even to being sourced from the same supplier.

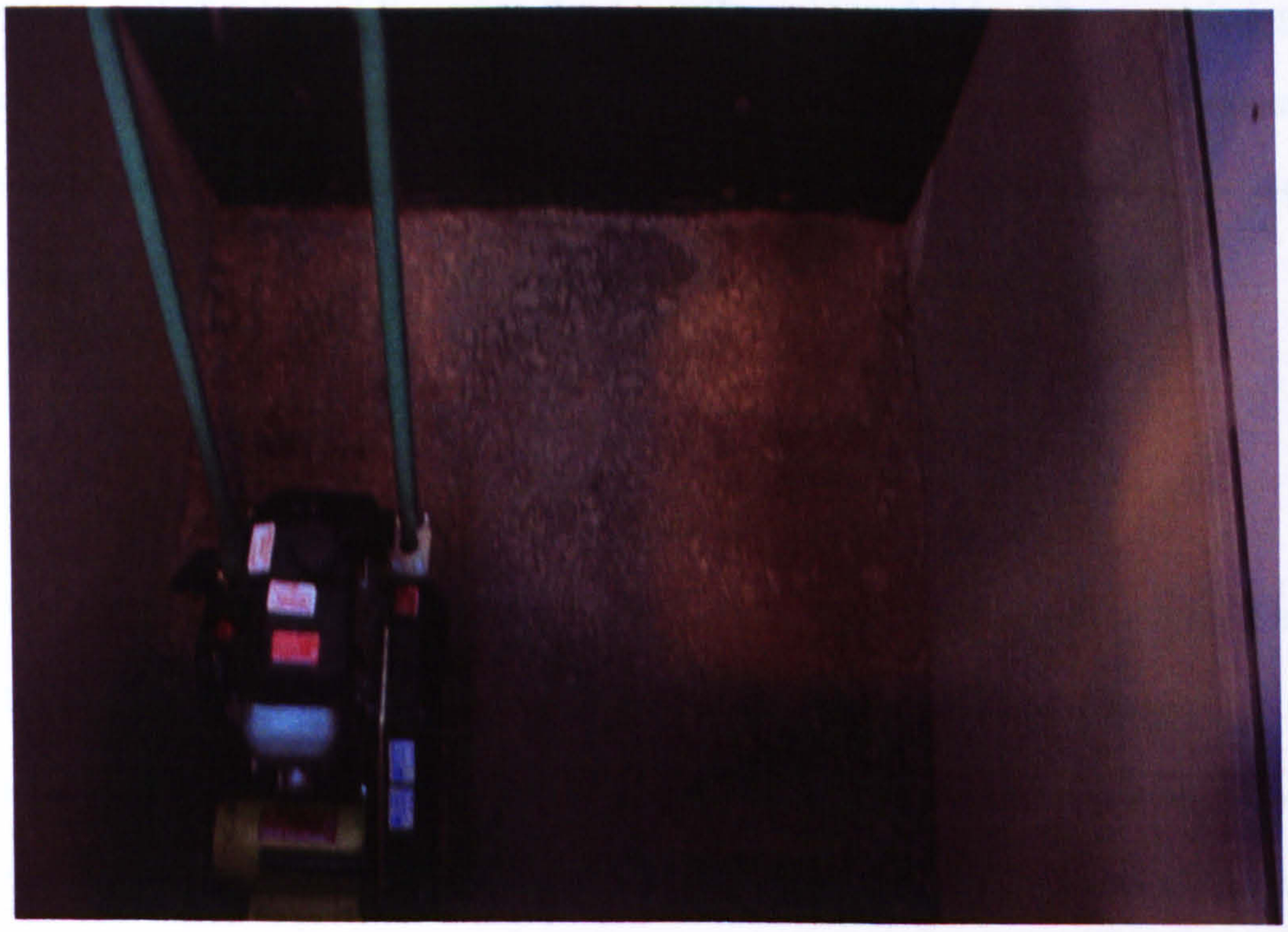

Figure B-1 Whacker plate space restriction

One of the aims of this research was to determine abutment fixity conditions since theoretically it is possible that a sliding failure can occur, however, it is not seen that often in real life. No other model tests (to the author's knowledge) have looked specifically at this area and in the design of the skewbacks and abutments a method was devised whereby none, one or both skewbacks could be allowed to slide independently of the corresponding abutments. This was achieved by having two piece abutments, one skewback which supported the arch and one abutment piece. Together with an arrangement of Macalloy bars the skewbacks could in effect be fixed or allowed to slide over the abutment.

Live loading was initially going to be by 'flying carpet' method, which involves reacting off of a strong I-Beam into the strong floor via vertical bars, however during the proving test it transpired that the vertical bars were too slender for constant vertical loading. Therefore, a 'goal post' method was adopted which involves replacing the vertical slender rods with a more substantial load bearing frame.

Procurement and Construction

The full scale test rig and associated components was commissioned and built at Salford University. The commissioning process took longer than expected for a number of reasons, including: problems obtaining clear cast acrylic sheeting of the required quality. Further delays were caused by manpower shortages and unforeseen problems involving a change of laboratory at Salford University. This meant that it was not possible for the author to continue the investigations utilising the full scale rig due to time constraints.

Apart from the aforementioned issues, the only real physical problem encountered during construction that was not anticipated was the sealing of the interface between the 50 mm acrylic and the steel columns, which was necessary to enable an even load spread between the fill and the steel frame, as the surface float of acrylic is not perfectly level. 'No More Nails' proved to be unsuitable and the backup of using araldite meant that it would no longer be possible to remove the 50 mm acrylic sheets without damage as the use of solvents discolours the acrylic.

Figure B-2 shows basic dimensions of the test rig at Salford University.

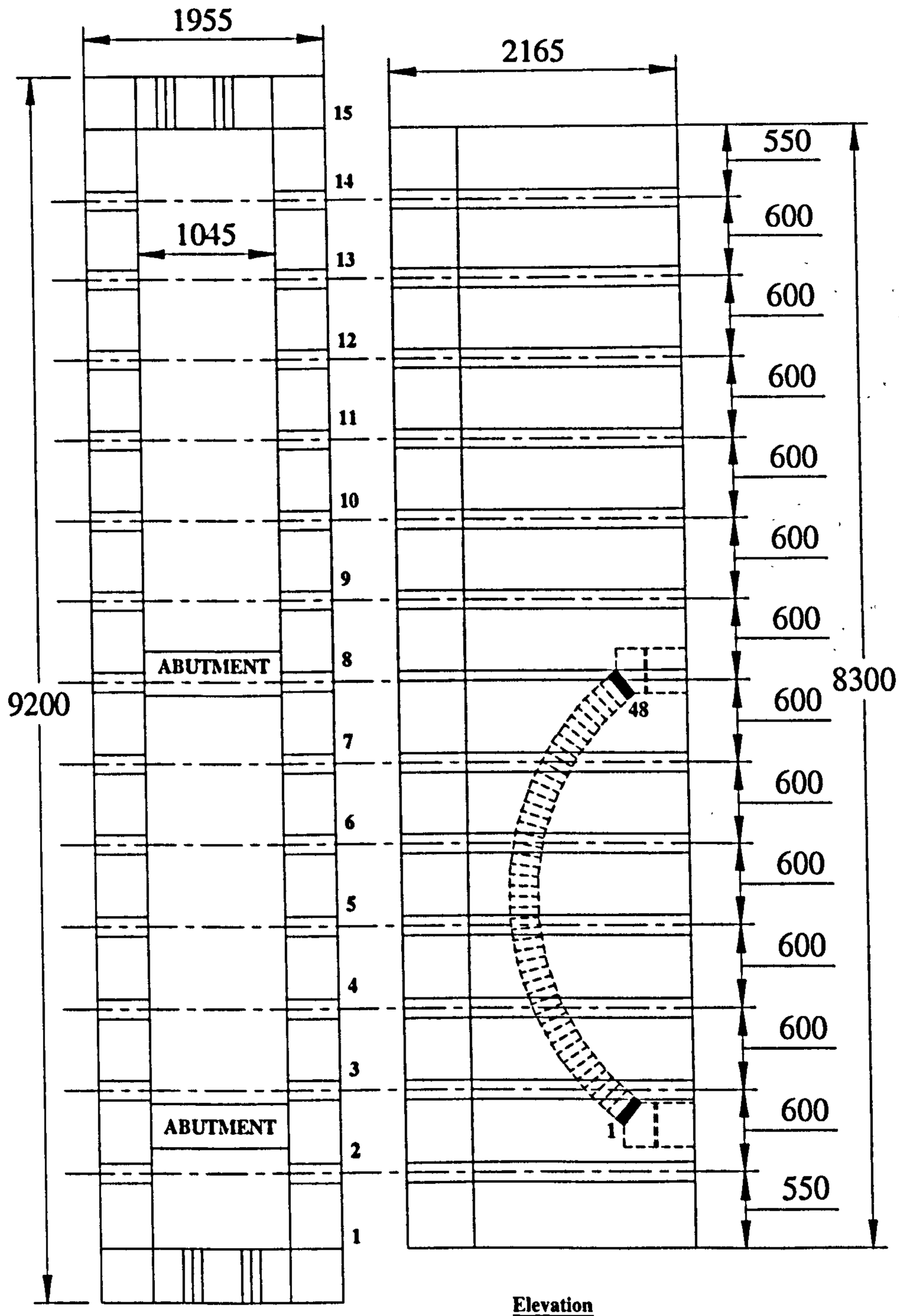

Figure B-2 Full scale arch test rig (all dimensions in mm)

Load Tests

As well as a proving test, two bridges have been tested to date, mainly to test out the performance of the test rig setup, procedure and design and construction.

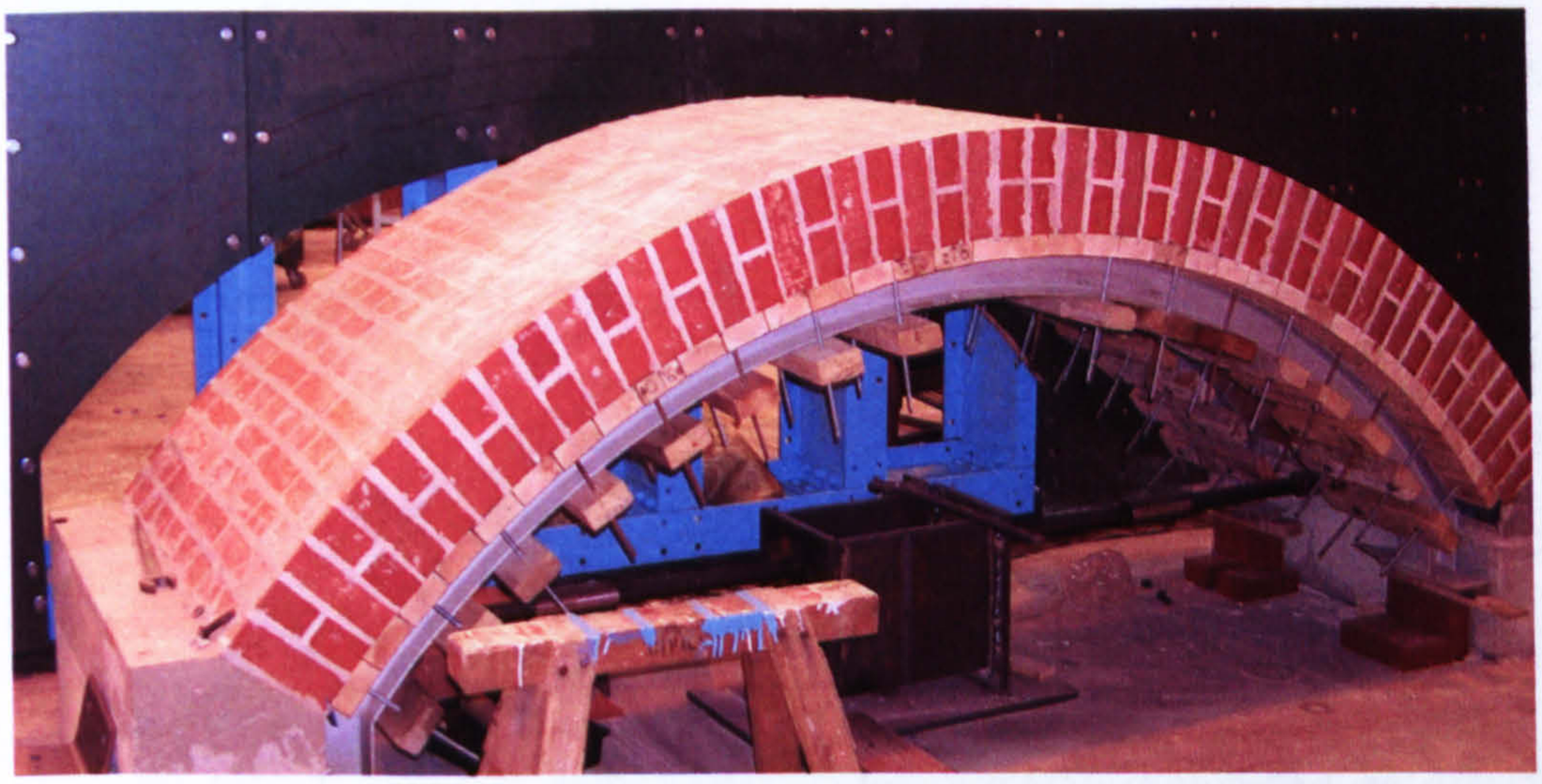

Figure B-3 The brickwork arch

The brick arch (Figure B-3) comprised stretcher bonded brickwork with headers interconnecting the two layers to prevent ring separation contributing to the failure. The arch itself comprised the following nominal dimensions: span = 3 m; rise = 0.75 m; barrel thickness = 0.215 m; depth of fill above crown = 0.3 m. These values were chosen so that a direct comparison with the 3 m span bridges tested at Bolton in the 1990s could be made.

The abutments were bolted to the structural strong floor of the laboratory and the skewback mortared onto the top of the abutment. The skewback had the option of being tied to a central fixed pillar using a large diameter threaded steel rod, though for the first two bridge tests the lock nut at the end of this rod was slackened off to permit the skewback to slide freely if the resistance along the skewback-abutment interface was overcome (see Figure B-4).

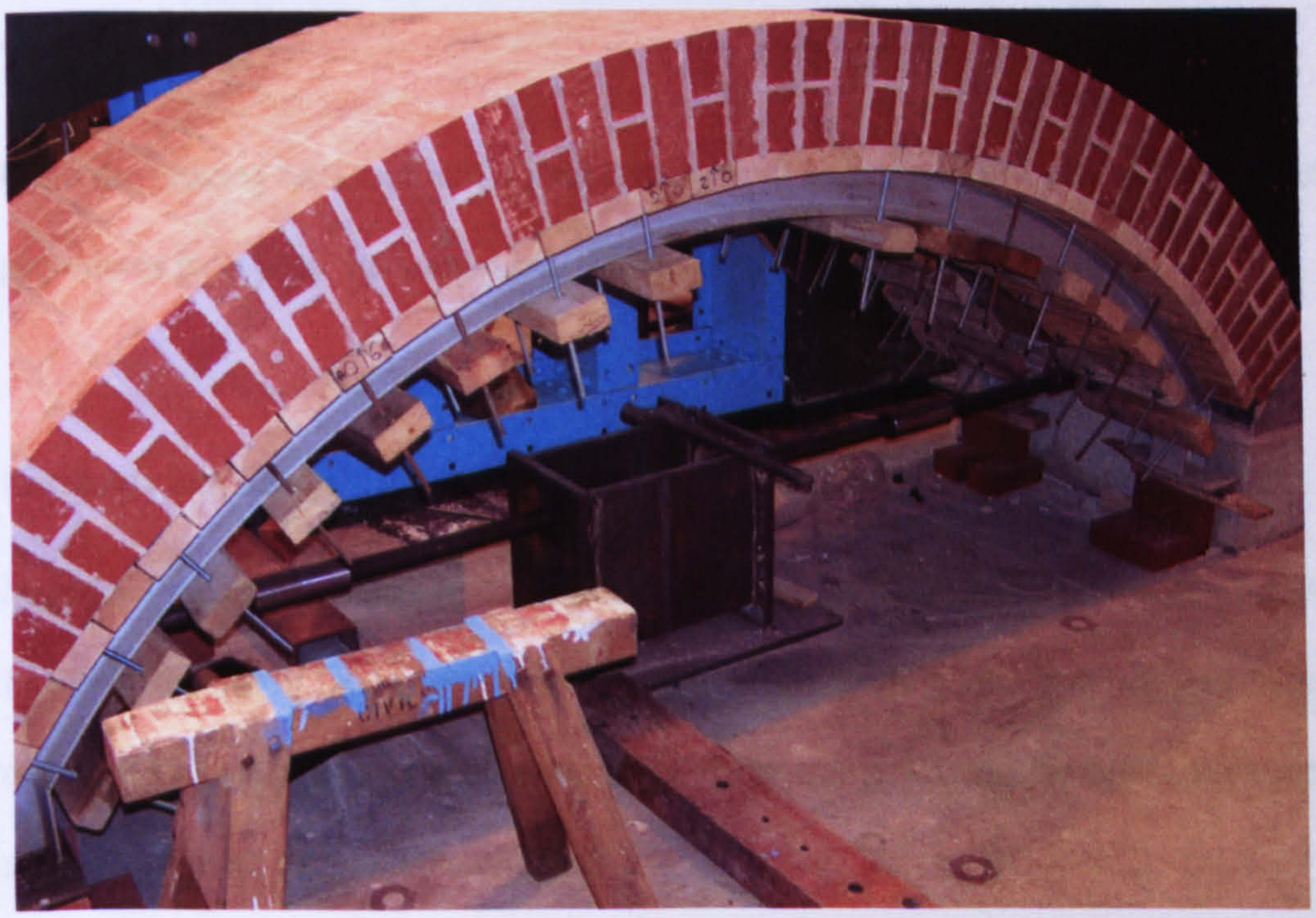

Figure B-4 Skewback fixity arrangement

Since the first test bridge was designed to be as similar as possible to those conducted at Bolton, a similar SHW Type 1 sub base material of crushed limestone fill material was used to maintain the comparison. However, in these tests the skewbacks were allowed to move relative to the abutments to give an indication as to whether sliding would actually occur at full scale. The bridge was loaded to about 80 kN on 24th March 2005, although this was not the peak load, the test had to be cut short and demobilised without further monitoring due to time constraints.

A second bridge of identical set up to the first but backfilled with clay instead of limestone was tested to failure on 11th April 2005. A layer of crushed limestone was used above the crown to prevent a local failure of the soil in the vicinity of the applied load in an imitation of road sub-base material normally present in real road bridges. This bridge had a peak failure load of around 125 kN.

Test Findings

From the proving tests and initial load tests several amendments to the test setup and procedures have been recommended. These are discussed in this section.

Procedure and Set-up

In general the testing frame & integrated hydraulic actuators / load cells worked well, however, the use of the same external scaffold frame to simultaneously support many displacement gauges was problematic since if the frame was inadvertently knocked, readings from all gauges were affected.

Both the acrylic and steel performed as anticipated with few instances where tearing of the latex occurred and only very small lateral movements (<1 mm) of the frame which indicate plane strain conditions were largely intact. One small issue of water ingress was identified, most likely from condensation between the sacrificial acrylic and the greased latex, prior to testing with the limestone fill, see Figure B-5. However, this is thought to have a negligible effect since it was only in small patchy areas.

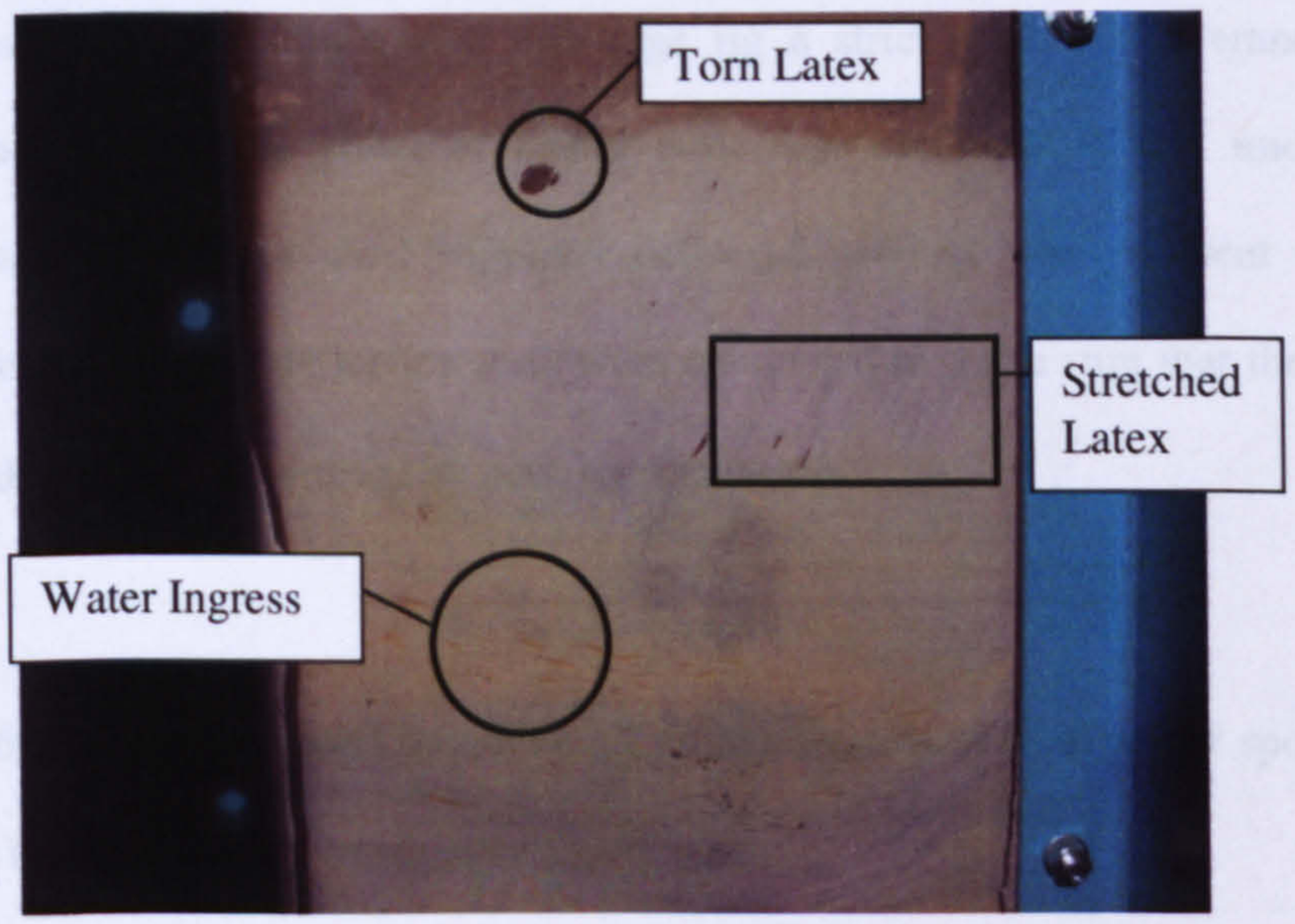

Figure B-5 Small problems with the use of the Greased Latex in the Limestone proving test

Visual Imaging

The tests proved that the digital imaging set-up and procedure worked well at large scale. The resultant images captured were able to be processed using GeoPIV, (see Figure B-6).

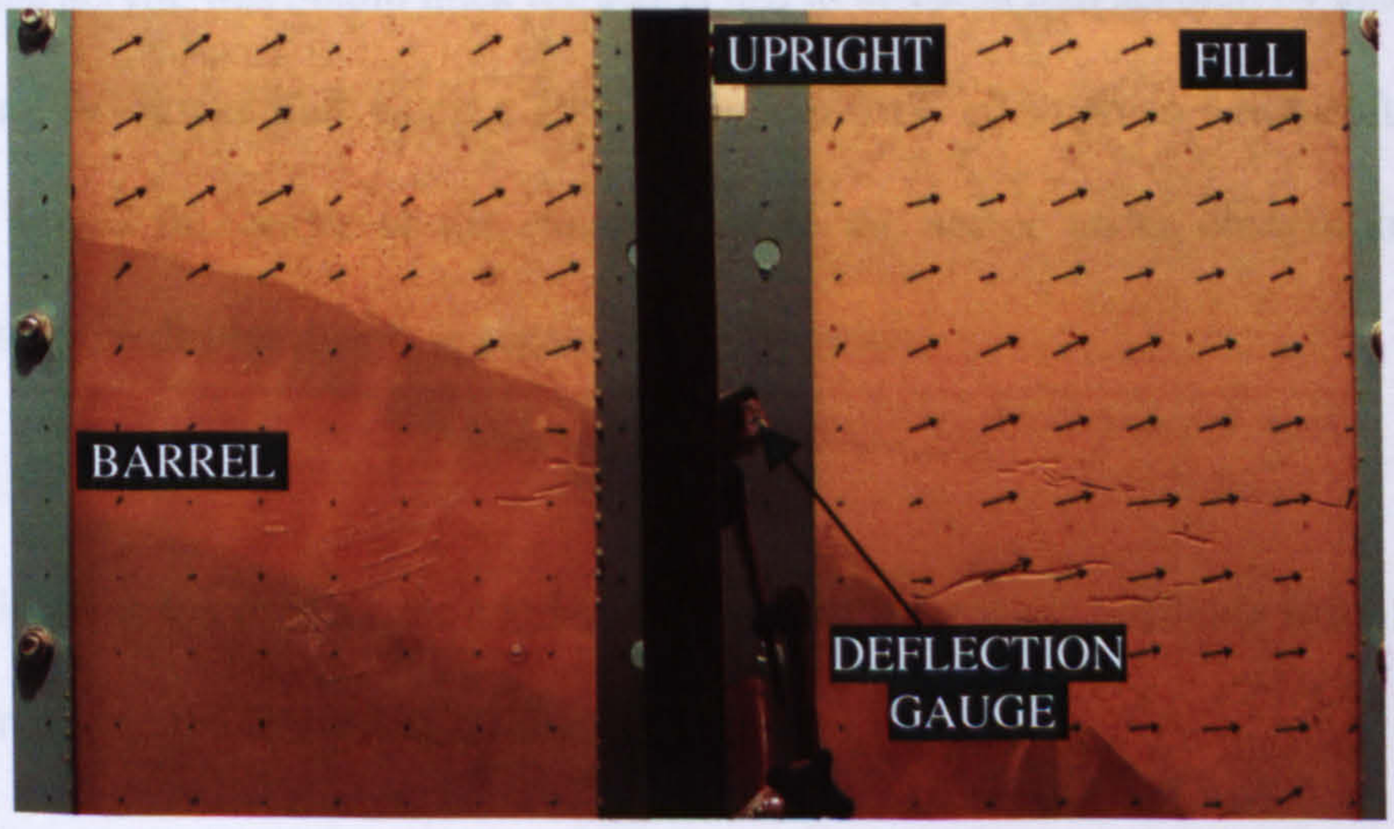

Figure B-6 GeoPIV of a section of the Limestone test

Notes on the Tests

During design and construction of the large rig a strict ±0.2 mm tolerance was adopted to minimise the effect of lateral deflection once testing was underway, unfortunately the chosen steel suppliers delivered product was different to that designed and additional deflection tests were conducted to make sure that the future tests would not be compromised by poor workmanship.

To avoid the problems caused by ambient lighting a series of high power spot lights were used to illuminate the area under observation.

In the cases where foreign particles were included to improve visual contrast, this comprised very thin layers of graphite shavings immediately adjacent to the acrylic sidewalls and had no discernable effect on the physical properties of the fill material being tested.

Since the acrylic was 50mm thick refraction had to be taken into account by amending the GeoPIV output files using a simple trigonometric equation in Microsoft Excel which linked the centre of the camera lens to the sector under observation thus correcting the displacements in regard to the distortion.

More information on the tests conducted using the large rig is available from Salford University and the University of Sheffield.

Appendix C

Parametric Studies and Calculation Information

Influence Values

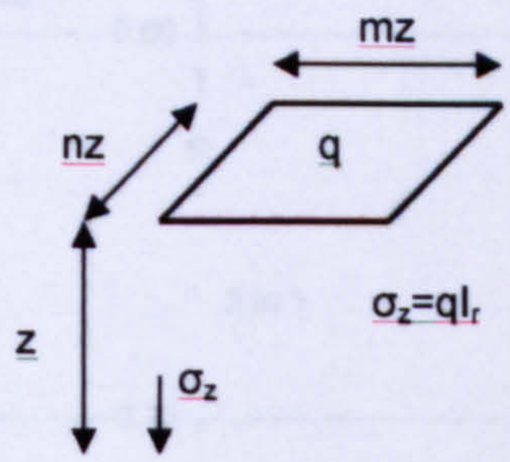

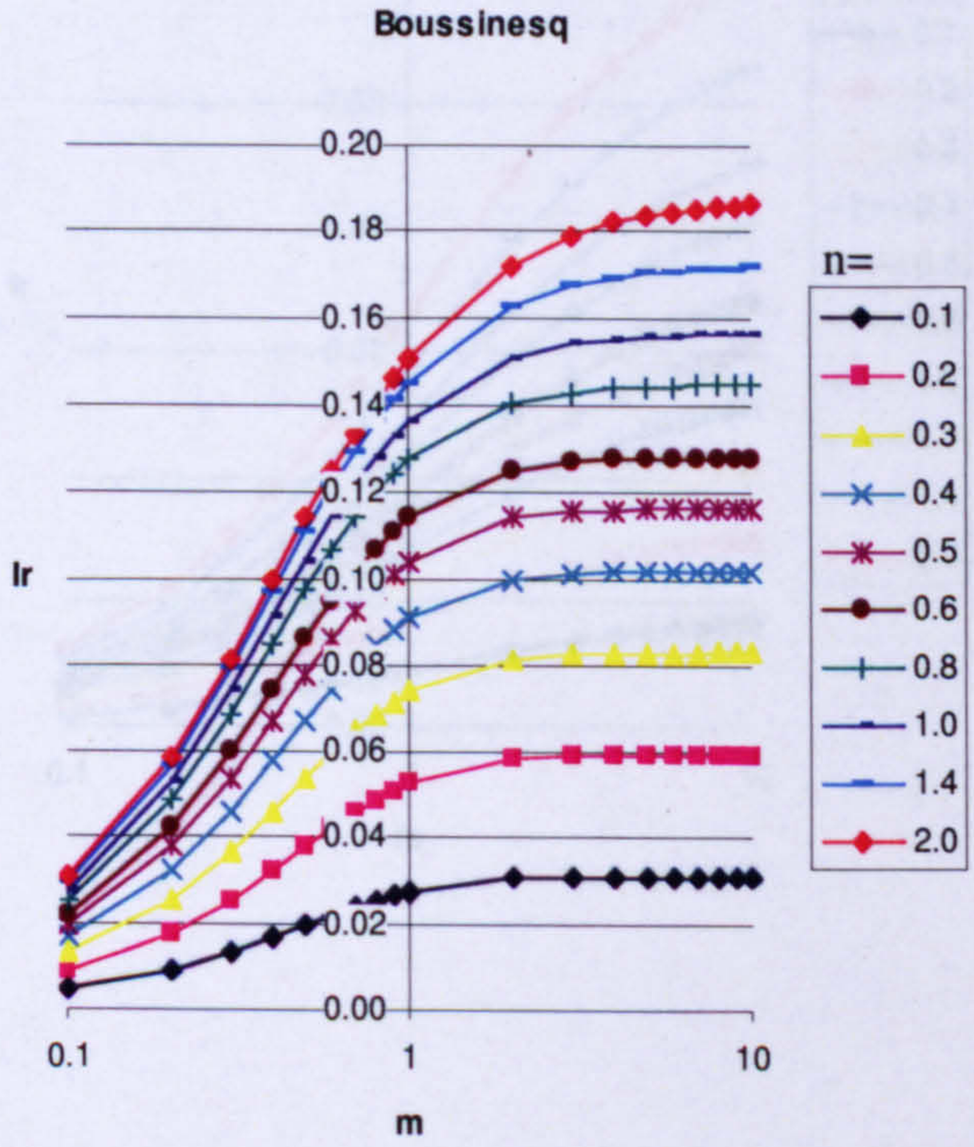

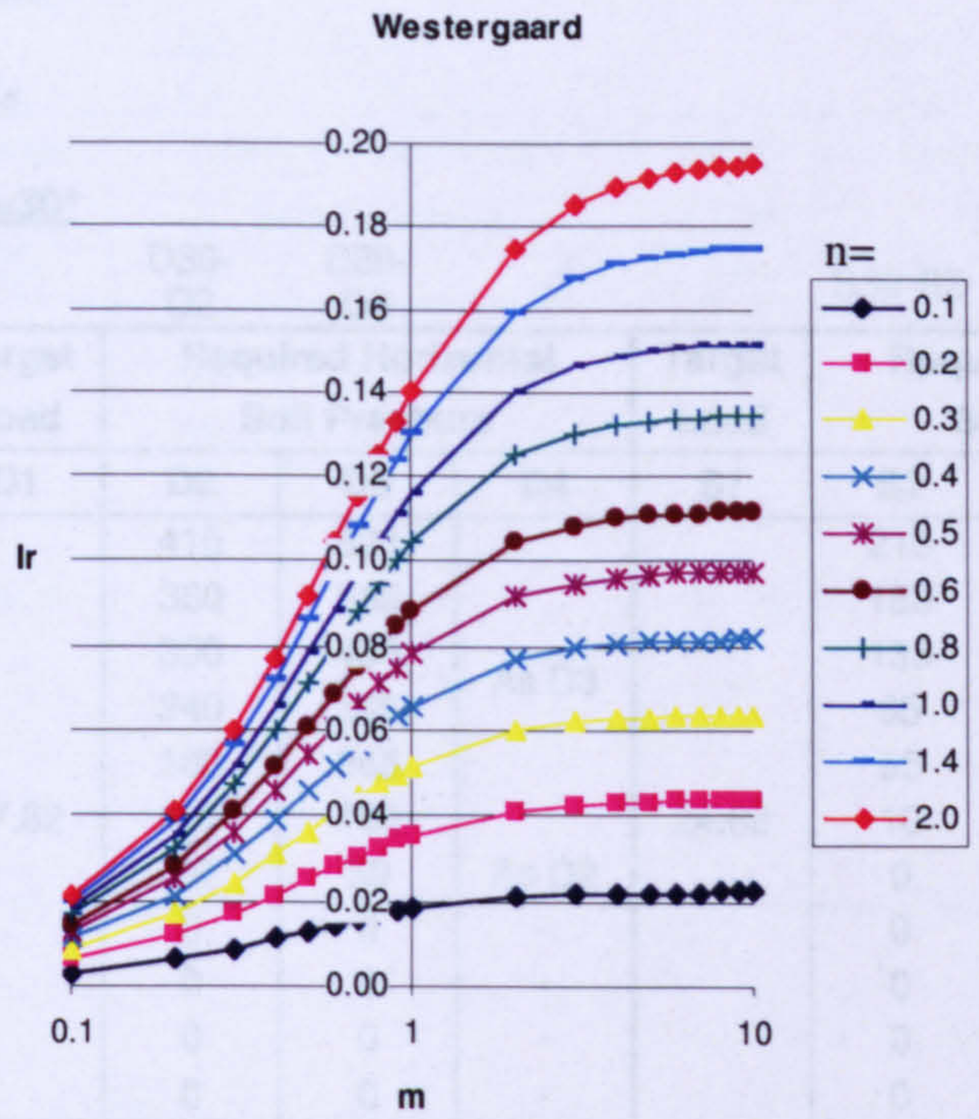
Westergaard
0.20
0.18
0.16
0.14
0.12
0.10
0.08
0.06
0.04
0.02
0.00
Ir
0.1
1
10
m
n=
0.1
0.2
0.3
0.4
0.5
0.6
0.8
1.0
1.4
2.0

2 in 1

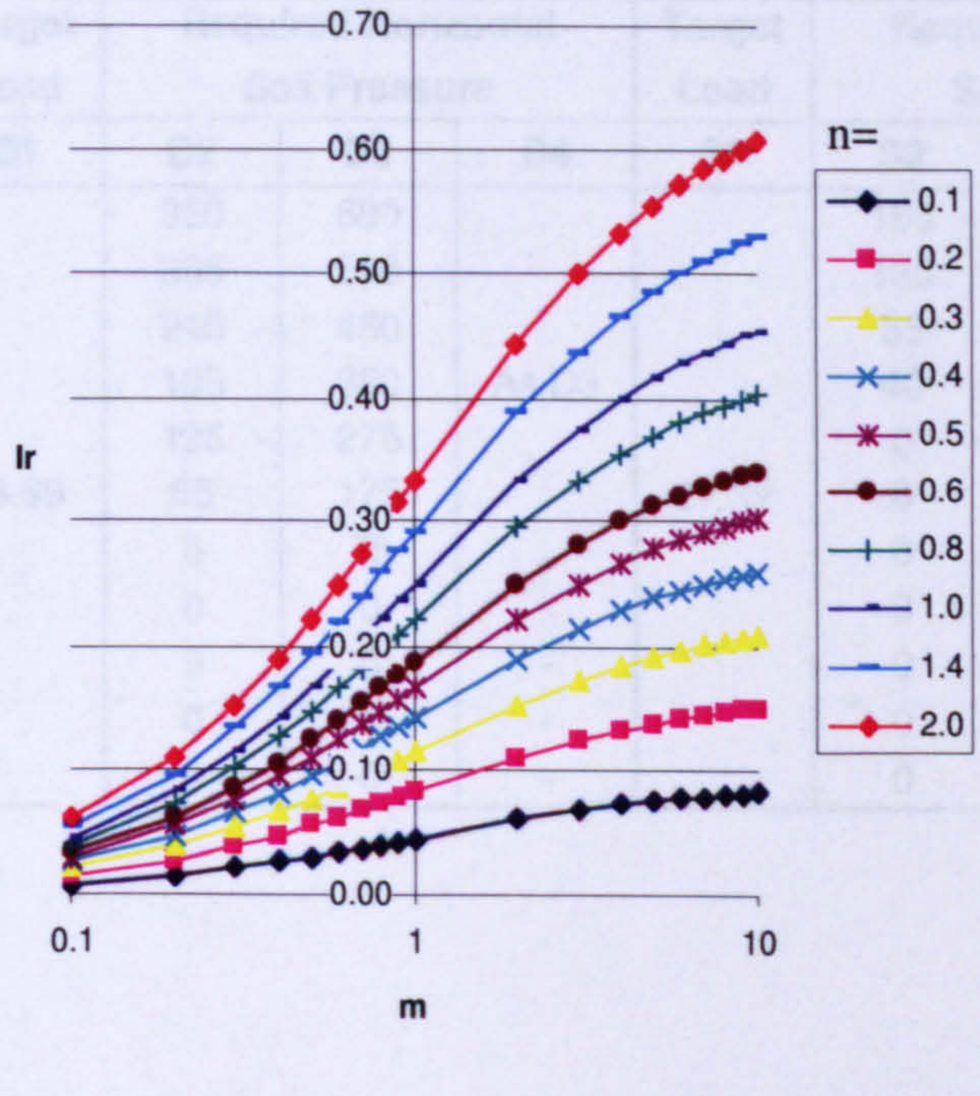
0.70
0.60
0.50
0.40
0.30
0.20
0.10
0.00
Ir
0.1
1
10
m
n=
0.1
0.2
0.3
0.4
0.5
0.6
0.8
1.0
1.4
2.0

Parametric Studies

Soil Friction Angle

γ=16kN/m^3 φ'=30°

Friction Value	Target Load	Required Horizontal Soil Pressure			Target Load	Required Horizontal Soil Pressure		
		D30-D2	D30-D3			S30-S2	S30-S3	
	D1	D2	D3	D4	S1	S2	S3	S4
0.0		415	620			215	360	
0.1		360	530			180	300	
0.2		300	435	As D3		135	240	As S3
0.3		240	340			95	180	
0.4		180	245			55	120	
0.5	47.82	120	150		24.88	10	60	
0.6		60	50	As D2		0	0	-
0.7		0	0	-		0	0	-
0.8		0	0	-		0	0	-
0.9		0	0	-		0	0	-
1.0		0	0	-		0	0	-

γ=16kN/m^3 φ'=40°

Friction Value	Target Load	Required Horizontal Soil Pressure			Target Load	Required Horizontal Soil Pressure		
		D40-D2	D40-D3			S40-S2	S40-S3	
	D1	D2	D3	D4	S1	S2	S3	S4
0.0		360	680			165	380	
0.1		305	580			125	325	
0.2		245	480			85	260	
0.3		185	380	As D3		40	195	As S3
0.4		125	275			0	130	
0.5	54.99	65	175		27.32	0	70	
0.6		5	75			0	5	
0.7		0	0	-		0	0	-
0.8		0	0	-		0	0	-
0.9		0	0	-		0	0	-
1.0		0	0	-		0	0	-

γ=16kN/m^3 φ'=50°

Friction Value	Target Load	D50-D2 Required Horizontal Soil Pressure	D50-D3 Required Horizontal Soil Pressure		Target Load	S50-S2 Required Horizontal Soil Pressure	S50-S3 Required Horizontal Soil Pressure	
	D1	D2	D3	D4	S1	S2	S3	S4
0.0		250	770			55	415	
0.1		195	665			15	355	
0.2		135	555			0	285	
0.3		75	440	As D3		0	220	As S3
0.4		15	330			0	150	
0.5	64.9	0	220		30.78	0	85	
0.6		0	105			0	20	
0.7		0	0	-		0	0	-
0.8		0	0	-		0	0	-
0.9		0	0	-		0	0	-
1.0		0	0	-		0	0	-

Backfill Density

γ=18kN/m^3 φ'=30°

Friction Value	Target Load	D18-D2 Required Horizontal Soil Pressure	D18-D3 Required Horizontal Soil Pressure		Target Load	S18-S2 Required Horizontal Soil Pressure	S18-S3 Required Horizontal Soil Pressure	
	D1	D2	D3	D4	S1	S2	S3	S4
0.0		440	675			215	380	
0.1		380	575			175	315	
0.2		315	470			130	250	As S3
0.3		250	365	As D3		85	185	
0.4		185	260			40	120	
0.5	52.11	120	160		26.11	0	55	
0.6		55	55			0	0	-
0.7		0	0	-		0	0	-
0.8		0	0	-		0	0	-
0.9		0	0	-		0	0	-
1.0		0	0	-		0	0	-

γ=16kN/m^3 φ'=30°

Friction Value	Target Load	D16-D2 / D16-D3 Required Horizontal Soil Pressure			Target Load	S16-S2 / S16-S3 Required Horizontal Soil Pressure		
	D1	D2	D3	D4	S1	S2	S3	S4
0.0		415	620			215	360	
0.1		360	530			180	300	
0.2		300	435	As D3		135	240	As S3
0.3		240	340			95	180	
0.4		180	245			55	120	
0.5	47.82	120	150		24.88	10	60	
0.6		60	50	As D2		0	0	-
0.7		0	0	-		0	0	-
0.8		0	0	-		0	0	-
0.9		0	0	-		0	0	-
1.0		0	0	-		0	0	-

γ=14kN/m^3 φ'=30°

Friction Value	Target Load	D14-D2 / D14-D3 Required Horizontal Soil Pressure			Target Load	S14-S2 / S14-S3 Required Horizontal Soil Pressure		
	D1	D2	D3	D4	S1	S2	S3	S4
0.0		385	565			215	340	
0.1		335	485			180	285	
0.2		280	395	As D3		140	230	As S3
0.3		225	310			100	175	
0.4		170	225			65	115	
0.5		120	135		23.52	25	60	
0.6		65	50	As D2		0	0	-
0.7		10	0			0	0	-
0.8		0	0	-		0	0	-
0.9		0	0	-		0	0	-
1.0		0	0	-		0	0	-

Abutment Width

γ=16kN/m^3 φ'=40°

Friction Value	Target Load	Required Horizontal Soil Pressure			Target Load	Required Horizontal Soil Pressure		
		D400-D2	D400-D3			S300-S2	S300-S3	
	D1	D2	D3	D4	S1	S2	S3	S4
0.0		360	680			165	385	
0.1		310	585			130	330	
0.2		255	485			95	270	
0.3		195	390	As D3		60	210	As S3
0.4		140	290			20	155	
0.5	54.99	80	190		27.32	0	95	
0.6		30	90			0	0	
0.7		0	0	-		0	0	-
0.8		0	0	-		0	0	-
0.9		0	0	-		0	0	-
1.0		0	0	-		0	0	-

γ=16kN/m^3 φ'=40°

Friction Value	Target Load	Required Horizontal Soil Pressure			Target Load	Required Horizontal Soil Pressure		
		D500-D2	D500-D3			S500-S2	S500-S3	
	D1	D2	D3	D4	S1	S2	S3	S4
0.0		360	680			165	380	
0.1		305	580			125	325	
0.2		245	480			85	260	
0.3		185	380	As D3		40	195	As S3
0.4		125	275			0	130	
0.5	54.99	65	175		27.32	0	70	
0.6		5	75			0	5	
0.7		0	0	-		0	0	-
0.8		0	0	-		0	0	-
0.9		0	0	-		0	0	-
1.0		0	0	-		0	0	-

γ=16kN/m^3 φ'=40°

Friction Value	Target Load	Required Horizontal Soil Pressure (D800-D2, D800-D3)			Target Load	Required Horizontal Soil Pressure (S700-S2, S700-S3)		
	D1	D2	D3	D4	S1	S2	S3	S4
0.0		360	680			165	380	
0.1		300	570			120	320	
0.2		230	460			75	250	As D3
0.3		160	350	As D3		25	180	
0.4		90	240			0	110	
0.5	54.99	20	130		27.32	0	45	
0.6		0	20			0	0	-
0.7		0	0	-		0	0	-
0.8		0	0	-		0	0	-
0.9		0	0	-		0	0	-
1.0		0	0	-		0	0	-

Arch Profile

γ=16kN/m^3 φ'=40°

Friction Value	Target Load	Required Horizontal Soil Pressure (D4:1-D2, D4:1-D3)			Target Load	Required Horizontal Soil Pressure (S4:1-S2, S4:1-S3)		
	D1	D2	D3	D4	S1	S2	S3	S4
0.0		360	680			165	380	
0.1		305	580			125	325	
0.2		245	480			85	260	
0.3		185	380	As D3		40	195	As S3
0.4		125	275			0	130	
0.5	54.99	65	175		27.32	0	70	
0.6		5	75			0	5	
0.7		0	0	-		0	0	-
0.8		0	0	-		0	0	-
0.9		0	0	-		0	0	-
1.0		0	0	-		0	0	-

γ=16kN/m^3 φ'=40°

Friction Value	Target Load	Required Horizontal Soil Pressure			Target Load	Required Horizontal Soil Pressure		
		D5:1-D2	D5:1-D3			S5:1-S2	S5:1-S3	
	D1	D2	D3	D4	S1	S2	S3	S4
0.0		600	815			320	455	
0.1		545	725			285	400	
0.2		490	625	As D3		245	340	
0.3		430	530			210	280	As S3
0.4		370	435			170	225	
0.5	56.28	310	335		28.38	130	165	
0.6		250	240			95	105	
0.7		190	140			55	45	As S2
0.8		130	45	As D2		15	0	
0.9		70	0			0	0	-
1.0		10	0			0	0	-

γ=16kN/m^3 φ'=40°

Friction Value	Target Load	Required Horizontal Soil Pressure			Target Load	Required Horizontal Soil Pressure		
		D6:1-D2	D6:1-D3			S6:1-S2	S6:1-S3	
	D1	D2	D3	D4	S1	S2	S3	S4
0.0		865	1020			460	550	
0.1		810	925			425	500	
0.2		750	825	As D3		385	440	As S3
0.3		685	725			350	380	
0.4		625	625			310	325	
0.5	64.26	565	525		31.54	270	265	
0.6		505	425			235	205	
0.7		445	325	As D2		195	150	As S2
0.8		385	225			160	90	
0.9		325	125			120	30	
1.0		265	25			85	0	